



APPENDIX A - Empirical Subsidence Prediction Model Details

**DGS MODIFIED ACARP, 2003 EMPIRICAL SUBSIDENCE AND HEIGHT OF
FRACTURING PREDICTION MODEL**

A1 Introduction

This appendix provides a description of how subsidence and sub-surface fracturing develops above longwall panels and provides a summary of the empirical subsidence prediction models used in this study.

The **ACARP, 2003** model was originally developed by Strata Engineering (Australia) Pty Ltd under ACARP funding with the goal of providing the industry with a robust and reliable technique to utilise the significant amount of geological and testing information already gathered by mining companies.

Over the past six years the **ACARP, 2003** model has been used successfully by the model's author, Steven Ditton, at several longwall mines in the Newcastle, Hunter Valley, Western and Southern Coalfields of NSW and the Bowen Basin, Queensland.

Subsidence prediction work for Stage 1 of the Moolarben Coal Project in 2006 resulted in further external scrutinization of the model and the robustness of the methodology by an Independent Hearing and Assessment Panel (IHAP), which was set up to assess Environmental Impact Assessments for new coal mining projects by NSW Department of Planning (DoP).

The outcomes of the IHAP for Moolarben resulted in several refinements to the model, as requested by the independent subsidence expert, Emeritus Professor J M Galvin, UNSW School of Mining and Director of Galvin and Associates Pty Ltd.

The refinements generally included several technical adjustments and clarification of the terminology used to enable a better understanding of the model by the wider technical community.

Over the past 7 years, Ditton Geotechnical Services Pty Ltd (DgS) has modified the **ACARP, 2003** model to be able to use it to calibrate an influence function model (SDPS[®]) that was developed by the Polytechnical Institute for the US Coalfields. The SDPS[®] program allows a wider range of topographic and complex mining layouts (including longwall and pillar extraction panels) to be assessed.

This appendix summarises the **ACARP, 2003** model in its current format and explains the refinements made to the original model. Details of the SDPS[®] model itself are provided at the back of this appendix.

A2 Description of Subsidence Development Mechanisms above Longwalls

After the extraction of a single longwall panel, the immediate mine roof usually collapses into the void left in the seam. The overlying strata or overburden then sags down onto the collapsed material, resulting in settlement of the surface.

The maximum subsidence occurs in the middle of the extracted panel and is dependent on the mining height, panel width, cover depth, overburden strata strength and stiffness and bulking characteristics of the collapsed strata. For the case of single seam mining, maximum panel subsidence has not exceeded 60% of the mining height (T) in over 95% of the published cases for the Newcastle, and Southern Coalfields (refer **ACARP, 2003** and **Holla and Barclay, 2000**). For the 5% of cases, which did exceed 58%T, the maximum subsidence did not exceed 65%T (i.e. 2.7 m for a 4.2m mining height). The actual subsidence may also be lower than this value due to the spanning or bridging capability of the strata above the collapsed ground (or the goaf).

The combination of the above factors determines whether a single longwall panel will be *sub-critical*, *critical*, or *supercritical* in terms of maximum subsidence.

Sub-critical subsidence refers to panels that are narrow and deep enough for the overburden to bridge or 'arch' across the extracted panel regardless of geology. It is therefore termed 'deep arching' in the context of the subsidence model.

Beyond the *sub-critical* range, the overburden becomes *critical*, and is unable to develop deep arching behaviour. Spanning of the overburden is dependent on 'shallow beam' bending or Voussoir arching behaviour and the presence of massive, competent strata. Cracking or breakdown of the overburden strata may therefore start to develop above *critical* panel geometries as the spanning mechanism transitions from 'deep arching' to 'shallow beam' behaviour.

Supercritical panels refer to panel geometries that cause complete collapse of the overburden. In the case of super-critical panels, maximum panel subsidence does not usually continue to increase significantly with increasing panel width.

In the Newcastle Coalfields, *sub-critical* or (deep arching) behaviour generally occurs when the panel width (W) is <0.7 times the cover depth (H) and supercritical when $W/H > 1.4$. Critical behaviour usually occurs between W/H ratios of 0.7 and 1.4. In the deeper areas of the Southern Coalfield, critical subsidence behaviour may start to occur when $W/H > 0.5$. As the cover depth averages at about 250 m in the Newcastle Coalfield and 450 m in the Southern Coalfield and both areas have massive strata units in the overburden, this indicates that the cover depth is likely to be a key factor when assessing subsidence.

The transition point from sub-critical to critical behaviour in a particular coalfield is also influenced by the 'bridging' capability of the strata if it can develop a spanning Voussoir Arch. In the Newcastle Coalfield, the commencement of critical panel behaviour can effectively increase up to W/H ratios of 0.9.

The maximum subsidence for sub-critical and critical panel widths is generally < 60% of the longwall extraction height (T) and could range between 5% and 40% T, depending on the thickness of massive sandstone or conglomerate strata.

The surface effect of extracting several adjacent longwall panels is dependent on the stiffness of the overburden and the chain pillars left between the panels. Invariably, 'extra' subsidence occurs above a previously extracted panel and is caused primarily by the compression of the chain pillars and adjacent strata between the extracted longwall panels.

A longwall chain pillar undergoes the majority of life-cycle compression when subject to double abutment loading (i.e. the formation of goaf on both sides of it, after two adjacent panels have been extracted). Surface survey data indicates that an extracted panel can affect the chain pillars between three or four previously extracted panels. The stiffness of the overburden and chain pillar system will determine the extent of load transfer to the preceding chain pillars. If the chain pillars go into yield, the load on the pillars will be mitigated to some extent by load transfer to adjacent fallen roof material or goaf.

The surface subsidence usually extends outside the limits of extraction for a certain distance (i.e. the angle of draw). The angle of draw distance is usually less than or equal to 0.5 to 0.7 times the depth of cover (or angles of draw to the vertical of 26.5° to 35°) in the NSW and QLD Coalfields.

A3 ACARP Project Overview

The original **ACARP, 2003** model was originally developed for the Newcastle Coalfield to deal with the issue of making reliable subsidence predictions over longwall panels by using both geometrical and geological information.

The project was initially focused on the behaviour of massive sandstone and conglomerate strata in the Newcastle Coalfield, but has now been successfully used in other coalfields since development over the past six years. This has occurred naturally due to the expansion of the model's database with data from other coalfields and has resulted in generic refinements to the model to deal with the wider range of geometrical and geological conditions.

In regards to geometry, the subsidence above a series of longwalls is strongly influenced by the panel width, the cover depth, the extraction height and the stiffness of the interpanel pillars (i.e. the chain pillars) and immediate roof and floor strata.

In regards to geology, the presence of massive strata units, such as conglomerate and sandstone channels above longwall panels, has resulted in reduced subsidence compared to that measured over longwall panels with similar geometry and thinner strata units.

Geological structure, such as faults and dykes, can cause increases in subsidence due to their potential to adversely affect the spanning capability of the overburden.

During the original development of the model, a database of maximum single and multi longwall panel subsidence and associated massive strata units was compiled for the

Newcastle Coalfield. The database draws on subsidence data from over fifty longwall panels and covers a panel width to cover depth (W/H) ratio from 0.2 to 2.0 (cover depth ranges between 70 m and 351 m), as shown in **Figure A1**.

The original project database includes single seam longwall mining data from eleven collieries within the Newcastle Coalfield, as presented in **Table A1**.

Table A1 - Empirical Database Sources from Newcastle Coalfield

Colliery	Colliery	Colliery
Cooranbong	Lambton	Wyee
New Wallsend No. 2 (Gretley)	Teralba	
Moonee	Burwood	
Stockton Borehole	West Wallsend	
Newstan	John Darling	

The wide range of single longwall panel W/H ratios in the database was considered unique compared to the other Australian coalfields and enabled the study to focus on overburden and chain pillar behaviour effects separately.

Pillar extraction or multiple seam data was not used to produce the subsidence prediction curves, as it invariably makes the assessment of geological influences more difficult. Other NSW and QLD longwall and high pillar extraction mine data that have been added to the model database over the past seven years as shown in **Table A2**.

Table A2 - Empirical Longwall Database from Other Mines

Coalfield	Colliery	Colliery
Newcastle	West Wallsend	Newstan
	Mandalong	Chain Valley
Hunter Valley	United	Wollemi
	Austar	North Wambo
Southern	Berrima	Appin
	Elouera	Dendrobium
	Metropolitan	
Western	Springvale	Angus Place
	Ulan	
Queensland	Cook	Oaky Creek
	Moranbah North	

In summary, the key features of the **ACARP, 2003** model are that it:

- Is derived from a comprehensive database of measured subsidence, strain, tilt and curvature above longwalls in the Newcastle, Hunter Valley, Western and Southern Coalfields.

- Has been validated with measured subsidence profile data.
- Adds to the **DMR, 1987** model for the Newcastle Coalfield, as it addresses multiple panels and contains a significantly larger data base.
- Includes the effects of massive sandstone/conglomerate lithology on subsidence.
- Allows reliable predictions of maximum single panel subsidence, chain pillar subsidence, tilt, curvature, strain and the angle of draw within a 95% Confidence Limit.
- Enables 'greenfield' sites (i.e. where there is no subsidence data) to be assessed rapidly and accurately.
- Provides maximum subsidence predictions based on Upper 95% Confidence Limits (or 5% Probability of Exceedence limits), which in practice have rarely been exceeded.
- The confidence limits have been derived by the application of central limit theory and the likely normal distribution of residuals about lines of best fit or regression lines determined for the model database.
- Utilises historical information directly - predictions are based on actual data.
- Enables prediction of secondary tilt, curvature and strain magnitudes. Effects such as 'skewing' due to rapid surface terrain variations, surface 'hump' or step development and cracking can result in tilt, curvature and strain magnitudes significantly greater than predicted 'smooth' profile values.

This issue has been addressed empirically by linking measured impact parameters with key mining geometry variables. Strain concentration factors and database confidence limits have been developed to estimate the likely range of subsidence impact parameters.

- Is amenable to subsidence contouring and allows the impacts on surface features to be assessed, including post-mining topography levels for watercourse impact assessment.
- Predictions of subsidence at specific locations can be done to provide an indication of likely subsidence magnitude; however, depending on the sensitivity of the feature, it may be prudent to adopt maximum predicted subsidence for a given panel.
- Incorporates an empirical model of sub-surface fracturing and far-field displacements.

Note: Recent far-field horizontal displacement model work in the Newcastle Coalfield indicates the empirical model is conservative.

The following key input parameters are required to make subsidence predictions using the model:

- Panel Width (W)
- Cover Depth (H)
- Seam Working Height (T)
- Overburden lithology details, specifically the thickness and location of massive strata units (t, y).
- Chain Pillar Height (h), Width (w_{cp}) and Length (l) [solid dimensions]
- Roadway width (r)

The statistical inferences and estimates of the model uncertainty associated with the prediction methodology are presented in the following sections.

A4 Single Panel Subsidence Predictions

A4.1 Geometrical Factors

The major finding of the **ACARP, 2003** project in regards to mining geometry was that the historical relationship between subsidence and panel width to cover depth ratio (W/H) is not a constant for the range of cover depths (H) involved.

Figure A2.1 shows the range of maximum subsidence that can occur above longwall panels with similar mining geometries and a range of cover depths. The apparent differences between the DMR's Southern NSW and Newcastle Coalfield curves and laminated overburden theory (**Heasley, 2000**) also support the above finding.

For an overburden consisting of sedimentary rock layers or plates, **Heasley, 2000** applied laminated beam theory by **Salamon, 1989** to form the basis of the pseudo-numerical subsidence prediction program LAMODEL ("LAYERed MODEL" of overburden) that has been found to have reasonable success in the US Coalfields.

According to LAMODEL theory, the maximum seam roof convergence (C_{max}) above a longwall panel of mining height (T), width (W) and cover depth (H), with an idealised overburden of uniform lamination thickness (t), Youngs Modulus (E), unit weight (γ) and Poisson's Ratio (ν) is:

$$C_{max} = [\sqrt{12(1-\nu^2)}]/t (\gamma H/E) (W^2/4) \text{ or } T \text{ (whichever gives the lower value)}$$

Several points can be made about this equation:

- The γH term represents the vertical stress acting on the plates at seam level and assumes spanning strata (i.e. sub-critical to critical panels).
- For completely collapsed strata, C_{\max} may be assumed to equal T at seam level.
- The surface subsidence may then be estimated as the minimum of $0.5C_{\max}$ and $0.6T$ for sub-critical/critical and supercritical panel geometries.
- In terms of traditional empirical models of estimating subsidence, the above equation indicates that the maximum single panel subsidence is a function of W^2/t and $\gamma H/E$ for sub-critical W/H ratios < 0.7 or T for super-critical W/H ratios > 1.4 . The influence of the panel width and mining height will therefore change with W/H .

Clamped elastic beam theory indicates that strata beam deflections, that are located at a distance y above the mine workings, are a function of $\gamma(H-y)/E$ and W^4/t^3 before cracking at the abutments and mid-span. The deflection of the beam will generate higher tensile stresses in the top of the beam at the abutments than in the bottom of the beam at mid-span. The cracking results in a transition from continuous elastic beam behaviour to a cracked beam of separate blocks or ‘voussoirs’ under simply supported loading conditions.

The Voussoir beam supports the load through the formation of a compressive arch, which develops as the individual blocks or Voussoirs rotate towards the goaf below it (i.e. the voussoirs cannot sustain tensile stresses, however, the deformed beam will span if the blocks have sufficient strength, stiffness and geometry. The elastic and Voussoir beam cases are shown in **Figure A2.2**.

If the rotated blocks are able to support the load, then the deflection of the cracked Voussoir beam is a function of $\gamma(H-y)/E$ and W^2/t , which is consistent with the laminated beam model theory; see **Figure A2.3**.

The **ACARP, 2003** model surmised that single panel subsidence normalised by mining height T , was a function of W/H , $\gamma H/E$ or H , W/t and y/H in accordance with Buckingham’s Pi theory.

The first three parameters above are related to panel geometry (i.e. the panel width, W , cover depth, H , and mining height, T , whilst the last two parameters (strata unit thickness, t , and distance, y , to the unit above the workings) infer geological influences of massive strata units.

Based on the above equations, surface subsidence is expected to increase with increasing cover depth (H) for the same W/H ratio, and is primarily a function of the increasing panel width (W) as $S_{\max} = f(W^2/H)$ according to beam theory. For constant single panel width (W), subsidence will therefore decrease with increasing cover depth (H). The subsidence data was subsequently separated into three cover depth categories of $H = 100, 200$ and 300 m ± 50 m and is presented in **Figures A3 to A5**.

The influence of overburden lithology was found to be readily apparent once the database was filtered using the above cover depth ranges.

A4.2 Geological Factors

Once the first stage in the development of the subsidence prediction model had addressed the influence of cover depth the effect of “significant” overburden lithology above single longwall / miniwall panels could be addressed. **Figure A6** illustrates a physical model, showing the subsidence reducing effects of a massive strata unit.

Borehole data was used to derive the thickness and location of massive strata units considered to be critically important for surface subsidence prediction, for a given panel width and depth. The methodology takes into account the maximum massive strata unit thickness (t) at each location and the height to the base of the unit above the longwall panel (y).

The subsidence above a panel, given cover depth (H) and panel width (W) decreases significantly when a massive strata unit is thicker than a certain minimum limit value. The thickness is also reduced when the unit is closer to the surface. The strata unit is considered to have a 'high' subsidence reduction potential (SRP) when it exceeds a minimum thickness for a given y/H ratio, as shown in **Figures A7.1** to **A7.3** for each cover depth category.

For a thin strata unit located relatively close to a panel, the 'Subsidence Reduction Potential (SRP)' will be 'low'. However, there is also an intermediate zone, where a single strata unit (or several thinner units) below the 'high' subsidence reduction thickness can result in a 'moderate' reduction in subsidence. A second limit line can therefore be drawn, which represents the threshold between 'moderate' and 'low' SRP.

It is considered that the 'high' SRP limit line represents the point between elastic and yielding behaviour of a spanning beam. The 'moderate' SRP limit line represents the point between yielding behaviour and collapse or failure of a spanning beam (which has been yielding).

The limit lines have been determined for the strata units located at various heights (y) above the workings in each depth category, as shown in **Figures A8** to **A10**.

A4.3 Summary of Model Concepts

The **ACARP, 2003** model introduces several new parameters, to improve the definition of various types of overburden behaviour and the associated mechanics.

As outlined in **Section A4.2**, the 'Subsidence Reduction Potential' (SRP) of massive or thickly bedded geological units above single longwall panels for the Newcastle Coalfield has been introduced to describe the influence that a geological unit may have on subsidence magnitudes. The massive geological units are defined in terms of 'high', 'moderate' or 'low' SRP.

Massive unit thickness, panel width, depth of cover and height of unit above the workings are considered to be key parameters for assessing overburden stiffness and spanning capability over a given panel width, controlling surface subsidence. A conceptual model for overburden behaviour is illustrated in **Figure A11**.

Variation in subsidence along the length of a panel may therefore be due to the geometry and / or SRP variation of geological units within the overburden.

For W/H ratios <0.7 , the overburden spans across the extracted panel like a ‘deep’ beam or linear arch, whereby the mechanics of load transfer to the abutments is governed by axial compression along an approximately parabolic shaped line of thrust, see **Figure A12**.

For W/H ratios >0.7 the overburden geometry no longer allows axially compressive structural behaviour to dominate, as the natural line of thrust now lies outside of the overburden. Bending action due to subsequent block rotation occurs. Provided that the abutments are able to resist this rotation, flatter lines of thrust still develop within the overburden, but the structural action is now dominated by bending action. This type of overburden behaviour has been defined as ‘shallow’ beam behaviour, which in structural terms is fundamentally less stiff than ‘deep’ beam behaviour. This results in a significant increase in subsidence or sag across an extracted longwall panel (all other factors being equal), as shown **Figure A12**.

“Voussoir beam” or “fractured linear arch” theory can be used to explain both types of overburden behaviour, as deep seated or flatter arches develop in the strata in an attempt to balance the disturbing forces.

The database also indicates the presence of a ‘Geometrical Transition Zone’, whereby subsidence increases significantly, regardless of the SRP of the geological units, as shown in **Figure A13**. This behaviour occurs when panel width to cover height ratio (W/H) ranges from 0.6 to 0.9. This phenomenon can be simply explained as a point of significant shift in structural behaviour and the commencement of overburden breakdown.

The model therefore allows the user to determine the range of expected subsidence magnitudes and the location of geology related SRP and/or ‘geometrical transition zones’ along a panel. Identification of the transition zones is an important factor in assessing potential damage risks of differential subsidence to important infrastructure, buildings and natural surface features, such as rivers, lakes and cliff lines etc.

The ‘strata unit location factor’ (y/H) was developed to assist in assessing the behaviour of massive strata units above the workings. The y/H factor is a simple way to include the influence of the unit location above the workings in terms of the effective span of the unit and the stresses acting upon it.

The key elements of this factor and their influence on the behaviour of the strata unit are:

- y , the height of the beam above the workings, which determines the effective span of the beam, and
- H , cover depth over the workings, which exerts a strong influence on the stress environment and, hence, the propensity for buckling or compressive failure of the beam.

Essentially beam failure due to the action of increasing horizontal stress (i.e. crushing or buckling) appears more likely as y decreases and H increases. The ratio of y/H may therefore be used to differentiate between the SRP of a beam of similar thickness, but at varying heights above the workings. The model also demonstrates that as the depth of cover increases, a thicker beam is required to produce the same SRP above a given panel width. This phenomenon may also be simply due to greater vertical load acting upon the massive strata 'beam'.

A5 Multiple Longwall Panel Subsidence Prediction

A5.1 General

The effect of extracting several adjacent longwall panels is governed by the stiffness of the overburden and the chain pillars left between the panels. Invariably, 'extra' subsidence occurs above a previously extracted panel and is caused primarily by cracking of the overburden and the compression of the chain pillars and adjacent strata between the extracted longwall panels.

A conceptual model of subsidence mechanisms above adjacent longwall panels in a single seam is shown in **Figure A14**.

A5.2 Predicting Subsidence above Chain Pillars (ACARP, 2003 Model)

A chain pillar undergoes the majority of life-cycle compression when subject to double abutment loading (i.e. the formation of goaf on either side, after two adjacent panels have been extracted). Surface survey data indicates that an extracted panel can affect the chain pillars of up to three or four previously extracted panels. The stiffness of the overburden and chain pillar system will determine the extent of load transfer to preceding chain pillars.

Multiple-panel effects have therefore been included in the model by adding empirical estimates of surface subsidence over chain pillars to the maximum subsidence predictions for single panels.

The empirical model presented in **ACARP, 2003** for estimating the subsidence above a chain pillar, was based on the regression equation presented in **Figure A15**. The model compares the ratio of chain pillar subsidence (S_p) over the extraction height (T), to the width of the chain pillar divided by the cover depth multiplied by the total extracted width ($1000w/W'H$).

A regression analysis on the data indicates a strong exponential relationship for $1000wcp/W'H$ values up to 0.543. For values > 0.543 , the relationship becomes constant.

$$S_p/T = 7.4044e^{-10.329F} (R^2 = 0.92) \text{ for } F < 0.543, \text{ and}$$

$$S_p/T = 0.023 \text{ for } F > 0.543$$

where

$$F = 1000w/W'H$$

W' = The total extracted width which includes the width of the panels extracted on both sides of the subject chain pillar, and the width of the chain pillar itself (i.e. $W' = W_i + w_i + W_{i+1}$).

Note that the final subsidence for a longwall panel with several subsequent extracted panels was then determined empirically by adding 50% of the predicted chain pillar subsidence (S_p) to the single panel S_{max} estimate.

This approach however, did not include an abutment angle to estimate pillar loads, which are likely to vary significantly between sub-critical and supercritical panel layouts.

*The chain pillar model has now been amended to include better predictions of chain pillar load that are consistent with ALTS methodology (refer **ACARP, 1998a**) and has resulted in the modified version presented in Section A5.2.*

A5.2 Predicting Subsidence above Chain Pillars (DgS, 2008 Model)

After the **ACARP, 2003** model was published; further studies on chain pillar subsidence measurements were undertaken at several mine sites in the Western (Springvale, Angus Place and Ulan) and Southern Coalfields (Appin and Elouera). The measured subsidence above the chain pillars was significantly greater than the Newcastle Coalfield pillars and considered to be linked to the stress acting on the pillars and the longwall mining height.

Maximum subsidence above the chain pillars invariably occurred after the pillars were subject to double abutment loading conditions (i.e. goaf on both sides).

The **ACARP, 2003** model for estimating chain pillar subsidence was subsequently superseded by the pillar stress v. strain type approach presented in **Figure A16**. The chain pillar stress was estimated by assuming a design abutment angle of 21° for the pillar load, according to the methodology presented in **ACARP, 1998a** for sub-critical and supercritical longwall panels.

Prediction of subsidence above the chain pillars (S_p) was determined based on the following regression equation using the mining height, T and pillar stress, σ :

$$S_p/T = 0.238469/(1+e^{-[(\sigma-25.5107)/7.74168]}) \quad (R^2 = 0.833)$$

The uncertainty of the predictions was estimated by calculating the variance of the residuals about the regression lines and calculating 90% Confidence Limits for the database as follows:

$$90\% \text{ CL } S_p \text{ error} = 0.048T$$

It was also considered necessary to test if the above stress v. strain type approach was adequate for reliable predictions, by comparing the subsidence outcomes with the pillar Factor of Safety; see **Figure A17**.

The strength of the chain pillars was estimated using the rectangular pillar strength formulae presented in **ACARP, 1998b**. The FoS was derived by dividing the pillar strength by the pillar load (i.e. stress).

Generally it has been found that significant surface subsidence above the chain pillar (i.e. 10 - 30% of pillar height) starts to occur when the pillar FoS is < 2 . For FoS values greater than 2, subsidence above the pillars is virtually independent of FoS and the pillars generally perform elastically under load.

The database indicates that when the FoS is < 2 , the stiffness of the pillar starts to decrease, due to the development of load induced fracturing within the pillar and surrounding strata. FoS values of < 2 represent pillar stresses that exceed 50% of the pillar strength. Laboratory testing of coal and sandstone samples also show sample 'softening' as the ultimate load carrying capacity of the sample is approached.

For pillars with FoS values < 1 , the subsidence above the chain pillars tend to a maximum limit of approximately 25 to 30% of the mining height. This type of behaviour is expected for chain pillars that have width to height ratios $w/h > 5$, which is the point where 'strain hardening' deformation starts to develop with increased confinement of the 'pillar core'.

A5.3 Calculation of First and Final Subsidence for Multiple Longwall Panels

Multiple panel predictions can be made by adding the predicted single panel subsidence to a proportion of the chain pillar subsidence (including the residual subsidence) to estimate first and final subsidence above a given longwall panel.

The definition of first and final S_{\max} is as follows:

First S_{\max} = the first maximum subsidence after the extraction of a longwall panel, including the effects of previously extracted longwall panels adjacent to the subject panel.

Final S_{\max} = the final maximum subsidence over an extracted longwall panel, after at least three more panels have been extracted, or when mining is completed.

In the Newcastle Coalfield, First and Final S_{\max} values for a panel are predicted by adding 50% and 100% of the predicted subsidence over the chain pillars respectively (i.e. between the previous and current panel) less the goaf edge subsidence (see **Section A5**).

Residual subsidence above chain pillars and longwall blocks tends to occur after extraction due to (i) increased overburden loading on pillars and (ii) on-going goaf consolidation or creep effects. Based on the final chain pillar subsidence measurements presented in **Figure A16**, the residual movements can increase subsidence by a further 10 to 30%.

An example of measured multiple longwall subsidence behaviour is presented in **Figure A18**.

Final subsidence is normally estimated by assuming a further 20% of the chain pillar subsidence will occur. However, this may be increased or decreased, depending on local experience.

The prediction of first and final subsidence originally presented in **ACARP, 2003** involved the use of several empirical coefficients, which have proven to be difficult to apply in practice. The interested reader may refer to this methodology, however, the above method is considered easier to apply and likely to result in a similar outcome.

In summary, the mean values of the First S_{\max} and Final S_{\max} are calculated as:

$$\text{First } S_{\max} = \text{Single } S_{\max} + 0.5(S_{p(i-1)} - S_{goe(i-1)})$$

$$\text{Final } S_{\max} = \text{First } S_{\max} + 1.0(\text{Final } S_{p(i)} - \text{First } S_{goe(i)})$$

The U95% Confidence Limits or Credible Worst Case Values are then:

$$\text{U95\% First } S_{\max} = \text{mean First } S_{\max} + 1.64 (\text{U95\% } S_{\max} \text{ error} + \text{U95\% } S_p \text{ error})^{1/2}.$$

$$\text{U95\% Final } S_{\max} = \text{mean Final } S_{\max} + 1.64 (\text{U95\% } S_{\max} \text{ error} + \text{U95\% } S_p \text{ error})^{1/2}.$$

It should also be understood that the terms 'mean' and 'Upper 95% Confidence Limit' used in the model generally infer that the predicted maximum values will be exceeded by 50% and 5% respectively of the panels mined with similar geometry and geology etc.

Using lower probability of exceedence values (e.g. U99%CL) may be justified for particularly sensitive features, however, the magnitude of the maximum values does not usually increase significantly above the U95%CL values.

When local subsidence data is available for multiple longwall panels, the relationship between the multiple and single panel subsidence predictions can be determined as follows:

$$\text{First } S_{\max} = \text{Single } S_{\max} + 0.5b(S_{p(i-1)} - S_{goe(i-1)})$$

$$\text{Final } S_{\max} = \text{First } S_{\max} + b(\text{Final } S_{p(i)} - \text{First } S_{goe(i)})$$

The 'b' factor may be estimated from measured subsidence profiles, and allows the load transfer effect between the goaf and the chain pillars to be included in the model if necessary.

It has been observed at deeper NSW Coalfield Mines (i.e. the Western and Southern Coalfields) where the proportion of subsidence over the chain pillars to be added to the single panel subsidence decreased when the cover depth exceeded 350 m.

A6 Subsidence Profile and Impact Parameter Predictions

Part of the **ACARP, 2003** project included the development of several models to predict the maximum panel deformation parameters and surface profiles associated with subsidence. The following models were developed:

- panel goaf edge or rib subsidence,
- angle of draw,
- maximum transverse and longitudinal tilt, curvature and strain,
- the locations of the above parameters over the longwall panel for the purposes of subsidence profile development, and
- heights of continuous and discontinuous fracturing above the longwall, based on measured surface tensile strains and fracture limit horizons over extracted panels (see **Section A7** for details).

A conceptual model of surface deformation profiles that develop above longwall panels is given in **Figure A19**.

All of the above subsidence parameters have been statistically linked to key geometrical parameters such as the cover depth (H), panel width (W), working height (T) and chain pillar width (w_{cp}) and shown in **Figures A20 to A27**.

A summary of all the empirical model relationships between the key subsidence profile parameters that were developed in **ACARP, 2003** and DgS are presented in **Table A3**.

Table A3 - Summary of Subsidence Impact Parameter Prediction Models Developed from ACARP, 2003

Parameter	Regression Equation and +/- 90% Confidence Limits or Upper95% CL	Coefficient of Determination (R ²)	Figure No.
Subsidence Reduction Potential (SRP) of Strata Unit in Overburden with thickness t, panel width, W and location factor, y/H above workings for Cover Depth Category	<p>High SRP t for a given panel W plots above line for given strata unit y/H.</p> <p>Moderate SRP t plots between High SRP line and next y/H line below it.</p> <p>Low SRP t plots below Moderate SRP limit line.</p>	N/A - curve location determined by successful re-prediction of >90% of cases I databases	<p>Figure A8 for H<150m;</p> <p>Figure A9 for H< 250m;</p> <p>Figure A10 for H< 350m</p>
Single Maximum Longwall Panel Subsidence (Single S _{max}) for Assessed Strata Unit SRP of Low, Moderate or High	<p>Upper and Lower bound prediction lines for a given SRP are used to estimate range of S_{max}/T for a given Panel W/H.</p> <p>Average of limit lines value is mean Single S_{max} value +/- 0.03T for W/H < 0.6; +/- 0.1T for 0.6<W/H<0.9; +/-0.05T for W/H>0.9</p>	N/A - curve location determined by successful re-prediction of >90% of cases I databases	<p>Figure A3 for H<150m;</p> <p>Figure A4 for H< 250m;</p> <p>Figure A5 for H< 350m</p>
Chain Pillar Subsidence, S _p (m)	$\text{Mean } S_p/T = 0.238469 / (1 + e^{-\frac{(\sigma_{DAL} - 25.5107)/7.74168}{T}})$ <p>+/- 0.048T</p>	R ² = 0.833	Figure A16
Goaf Edge Subsidence	$\text{Mean } S_{goe}/S_{max} = 0.0722(W/H)^{-2.557}$ $\text{U95\%CL } S_{goe}/S_{max} = 0.0719(W/H)^{-1.9465}$	R ² = 0.82	Figure A20
Angle of Draw	$\text{Mean AoD} = 7.646 \ln(S_{goe}) + 32.259$ $\text{U95\%CL} = \text{Mean AoD} + 8.7^\circ$	R ² = 0.56	Figure A21
Maximum Tilt T _{max} (mm/m)	$T_{max} = 1.1925(S_{max}/W')^{1.3955}$ <p>+/- 0.4T_{max} (W' = lesser of W and 1.4H)</p>	R ² = 0.94	Figure A22
Maximum Convex Curvature C _{max} (km ⁻¹)	$\text{Mean } C_{max} = 15.60(S_{max}/W'^2)$ <p>+/- 0.5Mean</p>	R ² = 0.79	Figure A23
Maximum Concave Curvature C _{min} (km ⁻¹)	$\text{Mean } C_{min} = 19.79(S_{max}/W'^2)$ <p>+/- 0.5Mean</p>	R ² = 0.79	Figure A24
Maximum Tensile Strain E _{max} (mm/m)	$\text{Mean 'smooth' } E_{max} = 5.2C_{max} \text{ +/- 0.5 Mean}$ $\text{Mean 'Cracked' } E_{max} = 14.4C_{max}$	R ² = 0.72 R ² = 0.32	Figure A25
Maximum Compressive E _{min} (mm/m)	$\text{Mean } E_{min} = 5.2(C_{min}) \text{ +/- 0.5 Mean}$ $\text{Mean 'Cracked' } E_{min} = 14.4C_{min}$	R ² = 0.72 R ² = 0.32	Figure A25
Critical Panel Width	W _{crit} = 1.4H where H = cover depth	N/A	ACARP, 2003

Table A3 (Continued) - Summary of Subsidence Impact Parameter Prediction Models Developed from ACARP, 2003

Subsidence at Inflexion Point or Maximum Tilt S_{Tmax}	Mean $S_{Tmax}/S_{max} = -0.0925(W/H)+0.7356$ +/- 0.2	$R^2 = 0.5$	ACARP, 2003
Distance to Inflexion Point, d/H	$d/H = 0.2425Ln(W/H) + 0.3097$	$R^2 = 0.73$	Figure A27
Distance to Peak Tensile Strain (mm/m)	$d_t/H = 0.1643Ln(W/H) + 0.2203$ for $W/H > 0.6$; $d_t/H = 0.2425Ln(W/H) + 0.2387$ for $W/H < 0.6$;	$R^2 = 0.28$	Figure A27
Distance to Peak Compressive Strain (mm/m)	$d_c/H = 0.3409Ln(W/H) + 0.3996$ for $W/H > 0.6$; $d_c/H = 0.2425Ln(W/H) + 0.3767$ for $W/H < 0.6$	$R^2 = 0.59$	Figure A27

* - If H within 25 m of depth category boundary, then average result with overlying or underlying depth category value.

- Centreline profile parameters are not presented here (refer to **ACARP, 2003**).

A7 Subsidence Profile Predictions above Longwall Panels

Predicted 'smooth' subsidence profiles above single and multiple longwall panels have been determined based on cubic spline curve interpolation through seven key points along the subsidence trough (i.e. maximum in-panel subsidence, inflexion point, maximum tensile and compressive strain, goaf edge subsidence, subsidence over chain pillars and 20 mm subsidence or angle of draw limit).

The locations of these points have been determined empirically, based on regression relationships between the variables and the geometry of the panels (see **Table A3**). Both transverse and longitudinal profiles have been derived in this manner.

First and second derivatives of the fitted spline curves provide 'smooth' or continuous subsidence profiles and values for tilt and curvature. Horizontal displacement and strain profiles were derived by multiplying the tilt and curvature profiles by an empirically derived constant associated with the bending surface beam thickness (based on the linear regression relationship between the variables, as discussed in **ACARP, 2003**).

An allowance for the possible horizontal shift in the location of the inflexion point (within the 95% Confidence Limits of the database) has also been considered, for predictions of subsidence at features located over the goaf or extracted area.

A8 Subsidence Contour Predictions above Longwall Panels

Subsidence contours can be derived with geostatistical kriging techniques over a 10 m square grid using Surfer 10® software and the empirically derived subsidence profiles along cross lines, centre lines and corner lines around the ends of the longwall panels. Vertical ‘slices’ may taken through the contours to (i) determine subsidence profiles along creeks or infrastructure, and (ii) assess the likely impacts on the relevant surface features.

A8.1 Subsidence Contours

Subsidence contour predictions have been made in this study using SPDS®, which is an influence function based model that firstly calculates seam convergence and pillar displacements empirically around the workings. The influence of an extracted element of coal is transmitted to the surface via a 3-D influence function, which also takes varying topography into account.

The model is usually calibrated to measured maximum subsidence values by adjusting key parameters such as influence angles and inflexion point location from extracted panel sides.

A8.2 Tilt and Curvature Contours

The predicted principal tilt and curvature contours were derived using the calculus module of the Surfer10® program and the predicted subsidence contours from the SPDS® runs. The subsidence contours were based on a 10 m grid.

Principal tilts (i.e. surface gradient or slope) were calculated by taking the first derivative of the subsidence contours in x and y directions as follows:

$$T_p = [(\partial s/\partial x)^2 + (\partial s/\partial y)^2]^{0.5}$$

where ∂s = subsidence increment over distances ∂x and ∂y along x and y axes.

Principal curvatures (i.e. rate of change in slope or surface bending) were calculated by taking the second derivative of the subsidence contours in x and y directions as follows:

$$C_p = [(\partial^2 s/\partial x^2)(\partial s/\partial x)^2 + 2(\partial^2 s/\partial x \partial y)(\partial s/\partial x)(\partial s/\partial y) + (\partial^2 s/\partial y^2)(\partial s/\partial y)^2]/pq^{2/3}$$

where $p = (\partial s/\partial x)^2 + (\partial s/\partial y)^2$ and $q = 1+p$

A8.3 Strain

Before predictions of strain can be made, the relationship between the measured curvatures and strain must be understood. As discussed in **NERDDP, 1993b** and **ACARP, 2003**, structural and geometrical analysis theories indicate that strain is linearly proportional to the curvature of an elastic, isotropic bending ‘beam’; see **Figure A28**. This proportionality actually represents the depth to the neutral axis of the beam, or in other words, half the beam

thickness. **NERDDP, 1993b** studies returned strain over curvature ratios ranging between 6 and 11 m for NSW and Queensland Coalfields. Near surface lithology strata unit thickness and jointing therefore dictate the magnitude of the proportionality constant between curvature and strain.

ACARP, 2003 continued with this approach and introduced the concept of secondary curvature and strain concentration factors due to cracking. The peak strain / curvature ratio for 'smooth' subsidence profiles in the Newcastle Coalfield was assessed to equal 5.2 m (mean) and 7.8 m (U95%CL) with the possibility that surface cracking could increase the 'smooth-profile' strains to 10 or 15 times the curvature. The above values may also be affected by the thickness of near surface geology.

Reference to **DMR, 1987** also suggests a curvature to strain multiplier of 10 for high pillar extraction and longwall panels in the Newcastle Coalfield.

Attempts by others to reduce the variability in strain and curvature data by introducing additional parameters, such as the radius of influence, r , by **Karmis et al, 1987** and cover depth, H , by **Holla and Barclay, 2000**, appear to have achieved moderate success in the coalfields in which they were applied. However, when these models were applied to the Newcastle Coalfield data presented in **ACARP, 2003**, the results did not appear to improve things unfortunately; see **Figures A29.1** and **A29.2**.

It is therefore considered that the variability in behaviour is probably due to other parameters, which are very difficult to measure (such as the thickness and flexural, buckling and shear strengths of the near surface strata).

Provided that the likelihood of cracking can be ascertained from the strain predictions, then appropriate subsidence management plans can still be implemented.

A9 Prediction Of Subsidence Impact Parameters And Uncertainty Using Regression Analysis Techniques

A9.1 Regression Analysis

Key impact parameters have been predicted using normalised longwall subsidence data from the Newcastle Coalfield. This approach allows a reasonable assessment of the uncertainty involved using statistical regression techniques. A linear or non-linear regression line has been fitted to the database for each impact parameter, normalised to easily measured parameters, such as maximum subsidence, panel width and cover depth. The quality or significance of the regression line is influenced by the following parameters:

- (i) the size of the database,
- (ii) the presence of outliers, and
- (iii) the physical relationship between the key parameters.

The regression curves were reviewed carefully, as such curves can be (i) affected by outliers, and (ii) misleading, in that by adopting a mathematical relationship which gives the best fit (i.e. R^2) the curves are controlled by the database and may not reflect the true underlying physical dependencies or mechanisms that the data represents.

These issues are inherent in all prediction modelling techniques because, for example, all models must be calibrated to field observations to validate their use for prediction or back analysis purposes.

The regression techniques presented in the **ACARP, 2003** was done by firstly assessing conceptual models of the mechanics and key parameter dependencies (based on established solid mechanics and structural analysis theories), before generating the regression equations.

Several outliers in the model databases were excluded in the final regression equations, but only when a reasonable explanation could be given for each anomaly (i.e. multiple seam subsidence, geological faults / dykes and surface cracking effects).

The regression equations in **ACARP, 2003** have R^2 (i.e. Coefficients of Determination) values generally greater than 50%; indicating that the relationships between the variables are significant. For cases where the R^2 values are $< 50\%$, the regression lines are almost horizontal (i.e. the parameter doesn't change significantly over the range of the database), and the use of the regression line will be close to the mean of the database anyway.

A9.2 Prediction Model Uncertainty

The level of uncertainty in the model predictions has been assessed using statistical analysis of the residuals or differences between the measured data and regression lines (i.e. lines of best fit). The *Standard Error* of the prediction has been derived from the residuals, which has then been multiplied by the appropriate 'z' or 't' statistic for the assumed normal probability distribution to define Upper (and Lower) Confidence Limits.

The residual population errors for the single panel subsidence model are shown in **Figure A30**.

The empirical database therefore allows an assessment of variance and standard error such that the required subsidence parameter's mean and upper 95% Confidence Limit (Credible Worst Case) values can be determined for a given mining geometry and geology.

Provided there are (i) more than 10 data points in the data sets covering the range of the prediction cases, and (ii) the impact parameter and independent variables have an established physical relationship based on solid or structural mechanics theories, then it is considered unlikely that the regression lines will be significantly biased away from the underlying physical relationship between the variables by any limitations of the data set.

On-going review of each of the regression equations over the past six years by DgS has not required significant adjustment of the equations to include new measured data points. The

regression equations derived are also amenable to spreadsheet calculation and program automation.

It is also important to make the distinction between the terms *confidence limit* and *confidence interval*. The Credible Worst Case terminology used in the model is **not** the upper limit of the 95% Confidence **Interval** - which would encompass 95% of the data. Since the lower 95% Confidence Limit is rarely used in practice, it was considered appropriate to adopt the 5% Probability of Exceedence values instead (this by definition represents the upper limit of the **90% Confidence Interval**).

Further, the term *Upper 95% Confidence Limit* used in the **ACARP, 2003** model is considered acceptable in the context of 'one-tailed' probability distribution limits (i.e. the Lower 95% Confidence Limit is generally of little practical interest).

A10 Subsidence Model Validation Studies

A10.1 Model Development

The **ACARP, 2003** model was developed so that it could re-predict > 90% of the database on which it is based. Validation studies also included comparison of measured and predicted subsidence, tilt and strain profiles above several longwall panel crosslines and centrelines. Examples of predicted and measured profiles above multiple panels for the Newcastle Coalfield are shown in **Figures A31 to A34** using the **ACARP, 2003** model. Subsequent predictions v. measured subsidence profiles are presented in **Figures A35 to A38** using the updated version of the model discussed herein.

DgS is usually required to review predicted v. measured subsidence profiles after the completion of a longwall panel and report the results to mines and government departments. Over the past nine years, the model has usually over predicted measured subsidence, with the data falling somewhere between the mean and U95%CL values. Prediction exceedances have occurred less than 5% of the time and where the assessment of the overburden SRP was found to be incorrect.

The predictions of curvature and strain, however, are generally problematic due to the common effects of discontinuous or cracking behaviour (i.e. lithological variation and cracking), resulting in measured strains that can be two to four times greater than predicted 'smooth' profile strains. This issue is discussed further in **Section A10.2**.

A10.2 Field Testing of Strain Predictions

Strain and curvature concentrations can increase 'smooth' profile strains by 2 to 4 times in the Newcastle Coalfield, when the panel width to cover depth ratio (W/H) exceeds 0.8 or radius of curvature is less than 2 km, see **ACARP, 2003**.

Where cracking occurs, measured strains will be highly dependent on the bay-length. Rock exposures with widely spaced or adversely orientated jointing can also result in much larger crack widths than for a location with deep soil profiles.

For example, a measured strain of 3 to 6 mm/m along a cross line above a longwall panel in the Newcastle Coalfield caused several cracks in soil that ranged in width from 10 mm to 30 mm and a single 100 mm wide crack in a sandstone rock exposure with medium strength and widely spaced jointing, see **Figure A39**.

At the moment, it is not possible to predict the magnitude of strains from ‘smooth profile’ models confidently, however, it is possible to make reasonable predictions that strains > 2 mm/m will cause cracking within the tensile strain zones. Shearing and buckling is also likely to occur within the compressive zones above a longwall with shallow surface rock.

Overall, strains and cracking can be managed effectively by assuming cracks will occur within the limits of a longwall panel and may need to be repaired after each panel is completed.

A11 Sub-Surface Fracturing Model

A11.1 Sub-Surface Fracturing Zones

The caving and subsidence development processes above a longwall panel usually result in sub-surface fracturing and shearing of sedimentary strata in the overburden, according to **Peng and Chiang, 1984** (see **Figure A40a**) and **Whittaker and Reddish, 1989** (see **Figure A40b**). The height of fracturing (HoF) is dependent on mining geometry and overburden geology.

International and Australian research on longwall mining interaction with groundwater systems indicates that the overburden may be divided into essentially four or five zones of surface and subsurface fracturing. The zones are defined in **Table A4** (in descending order):

Table A4 - Sub-Surface Fracture Zone Summary

Zone Type	Zone	Fracture and Groundwater Response Description	Typical Vertical Strain (mm/m)
Surface Cracking Zone (un-constrained)	D	Vertical cracking due to horizontal strains extending to maximum depths of 10 - 15 m. Surface waters may be diverted below affected area and resurface downstream where interaction with B & C Zones occur.	<3
Elastic Deformation Zone (dilated bedding & constrained)	C	Generally unaffected by strains with some bedding parting dilation. Horizontal strains constrained by overlying/underlying strata. Groundwater levels may be lowered temporarily due to new storage volume in voids between beds, but likely to recover at a rate dependant on climate. Elastic Zone may not be present if B or A Zones extend up to Surface Zone.	<3
Discontinuous Fracture Zone (dilated bedding & constrained)	B	Minor vertical cracking due to bending that do not extend through strata units. Increased bedding parting dilation and similar groundwater response to Zone C. Some groundwater leakage may occur to B Zone, however, losses likely to be recharged by surface hydro-geological system.	<8
Continuous Fracture Zone (unconstrained)	A	Major vertical cracking due to bending that pass through strata units and allow a direct hydraulic connection to workings below. Full depressurisation of groundwater occurs in the Zone that may recover in the long term once mining is completed.	>8
Caved (included in the A-Zone)	A	Caved strata up to 3 to 5 x Mining Height above the workings. Collapsed roof bulks in volume to provide some support to overlying strata.	>80

The characteristics of each HoF zone are further described below:

Starting from the seam level, the **Caved Zone** (included in the **A-Zone**) refers to the immediate mine workings roof above the extracted panel, which has collapsed into the void left after the coal seam has been extracted. The Caved Zone usually extends for 3 to 5 times the mining height, T, above the roof of the mine workings due to bulking factors of 1.3 to 1.5, and sometimes from 10 to 15T if the strata have low bulking properties (e.g. bulking factors of 1.10 to 1.15). Thinly bedded and laminated strata are likely to have lower bulking factors than thickly bedded or massive units within the Caved Zone.

The **Continuous Fracture Zone (A-Zone)** has been affected by a high degree of bending deformation, resulting in significant fracturing and bedding parting separation and shearing of the rock mass. Vertical tensile strains range from -10 to 140 mm/m with strata dilation in excess of 1 m. Compressive strains tend to develop at horizontal bedding separations after initial fracturing and overlying strata deflections occur resulting in re-compaction of the goaf and disturbed strata.

Continuous sub-surface fracturing refers to the zone of cracking above a longwall panel that is likely to result in a direct flow-path or hydraulic connection to the workings. All groundwater (or surface waters) within this Zone would be expected to drain vertically into the mine workings goaf.

The **Strata Dilation Zone (B-Zone)** refers to the section of overburden immediately above the A-Zone that has also been deformed by bending action, but to a lesser degree than the A-Zone. The B-Zone will have bedding parting separations and discontinuous fractures through bending strata units due to vertical strains ranging from -2 to 8 mm/m and strata dilation from 30 mm to 400 mm, depending on the panel width. An increase to horizontal rock mass permeability (hydraulic conductivity) is expected in the B-Zone with groundwater flowing horizontally into dilated strata.

Only minor vertical permeability increases are expected in the B-Zone due to alternating horizontal tensile and compression zones associated with Voussoir Beam action above the A-Zone. It is noted in **Whittaker and Reddish, 1989**, that some groundwater leakage from the B-Zone to the A-Zone is possible due to limited crack or joint interaction between the zones.

Overall, the majority of the B-Zone is considered to be a 'constrained' and 'dilated' zone with low connectivity potential to the mine workings. The B-Zone therefore represents a sub-surface fracturing zone that causes temporary groundwater system disturbance.

The **Elastic Deformation Zone (C-Zone)** is located above the B Zone and is the zone where the strata may have suffered minor bending and disturbance. Impacts include horizontal shearing and minor bed separations or dilation of up to 30 mm due to vertical tensile strains between 1 and 2 mm/m. The bedding separations may result in minor increases to horizontal hydraulic conductivity and negligible changes to vertical hydraulic conductivity. Groundwater system disturbance is expected to be negligible in this zone.

The development of the Elastic Deformation Zone (C-Zone) will depend on the mining geometry and the presence of spanning strata. The C-Zone is probably only likely to develop above critical to sub-critical mining geometries (i.e. $W/H < 1.4$) but may also be present above super-critical panels also if favourable geological conditions exist.

The strata in the B and C-Zones are also likely to be in compression due to natural arch formation (above sub-critical and critical panels). The arch will also act as barrier to vertical drainage of groundwater despite the presence of naturally occurring vertical joints in the rock mass. Low permeability strata such as claystone, tuff and mudstone will also limit rock mass 'gaps' and further retard vertical flow rates through these zones.

In the absence of significant geological structure (i.e. faults and dykes), the overall effect on the surface groundwater system due to leakage through the B and C-Zones will be minimal, with re-charging of groundwater losses likely to occur from the surface hydrological system. The presence of significant geological structure may increase the drainage rates through these strata zones however. Monitoring of mine groundwater makes v. rainfall - runoff data will determine the rate of leakage that is occurring through these zones.

The **Surface Cracking Zone (D-Zone)** includes the vertical cracking due to horizontal tensile and compressive strains caused by mine subsidence deformation. The D-Zone may extend to depths ranging from 5 m to 20 m (typically < 15 m) in the Newcastle Coalfield, and is dependent on near-surface geology and surface topography.

For mine design purposes, typical D-Zone depths in relatively flat terrain may be assumed to range from 10 m to 12 m (i.e. < 15 m). *Note: Forster and Enever, 1992 adopted a D-Zone thickness of < 15 m based on data from Wye and Cooranbong Collieries, and included it in the minimum cover depth formula of $45T + 10$ m for designing supercritical panels below tidal waters of Lake Macquarie in the Newcastle Coalfields.*

A11.2 Impact on Rock Mass Permeability

In regards to changes to rock mass permeability, **Forster, 1995** indicates that horizontal permeabilities in the fractured zones above longwall mines could increase by 2 to 4 orders of magnitude (e.g. pre-mining $k_h = 10^{-9}$ to 10^{-10} m/s; post-mining $k_h = 10^{-7}$ to 10^{-6} m/s).

Vertical permeability's could not be measured directly from the boreholes but could be inferred by assuming complete pressure loss in the 'A Zone', where direct hydraulic connection to the workings occurs. Only a slight increase in the 'B zone' or indirect / discontinuous fracturing develops (mainly due to increase in storage capacity) from bedding parting separation. It is possible that minor vertical flows will occur from B zone into A zone (and workings) as well.

Discontinuous fracturing would be expected to increase rock mass storage capacity and horizontal permeability without direct hydraulic connection to the workings. Rock mass permeability is unlikely to increase significantly outside the limits of extraction.

A11.3 Mine Design Criteria for Sub-Surface Fracture Height Control

When designing mining layouts for sub-surface fracture control, the A-Zone is the most significant in regards to groundwater and surface water interaction as it represents the region of broken ground whereby a hydraulic connection to the mine workings will most certainly occur.

The B-Zone is probably just as important as it represents the transition zone between the continuously fractured ground and elastic deformation or surface zones. The B-Zone also includes strata which are confined and where bedding parting separations (i.e. dilations) occur in the sagging rock mass above the caved and broken strata units in the A-Zone.

The C-Zone has been deformed as well, but not to the same extent as the B-Zone.

Note: It is difficult to define the boundary between the B and C-Zones without vertical strain measurements from extensometers. Both zones are considered to be 'constrained' and 'dilated' and will act as an effective barrier between the A-Zone and near surface groundwater and surface watercourses.

The formation and thickness of the HoF Zones will firstly be dependent on the 'criticality' of the proposed longwall panel. The same terms used for subsidence prediction are also referred to below and are based on the ratio between panel width (W) and the cover depth (H):

- Subcritical refers to panels with $W/H < 0.7$;
- Critical refers to panels with $W/H > 0.7$ and < 1.4 ; and
- Supercritical refers to panels with $W/H > 1.4$.

Several case studies have been referred to below which consider super-critical and sub-critical panel geometries separately due to their fundamental differences in spanning behaviour.

Conceptual models of the A and B-Zones above supercritical panels are presented in **Whittaker & Reddish, 1998** and are based on physical modelling results. **Forster and Enever, 1992** indicated similar strata zoning from field monitoring (**Figure A40c**) above supercritical, total pillar extraction panels in the Lake Macquarie Area of the Newcastle Coalfield.

A conceptual model that includes the B and C-Zones was presented in **ACARP, 2007 (Figure A40d)** for sub-critical mining geometries in the Western Coalfield. A similar sub-surface fracture zoning is also suggested by **Mark, 2007 (Figure A40e)** for the US Coalfields and **Kendorski, 1993** for the UK Coalfields (**Figure A40f**).

From the above conceptual height of fracturing models, several simple empirical models have been developed over the years to estimate the thicknesses of the A, B and C-Zones for the purpose of avoiding groundwater and surface water connectivity with underground mines.

The suite of HoF prediction models that probably represent the state-of-the-art are summarised in the following sections.

A11.3.1 Wardell, 1975, Reynolds, 1977 and Singh and Kendorski, 1981

Wardell, 1975 recommended a minimum rock cover depth of 50T - Surface Zone thickness above total extraction or longwall panels when mining under tidal waters in the Newcastle Coalfield. The minimum cover depth (H) was based on a maximum horizontal tensile strain limit of 7.5 mm/m and the Newcastle Holla curves. It is noted that a maximum horizontal tensile strain of 10 mm/m has been specified in the UK when mining below permanent waters.

Wardell has also recommended a minimum cover depth of 60T (which included a Surface Zone thickness ranging from 12 m to 15 m) for mining below stored waters with longwalls in the Southern Coalfield.

The Wardell Guidelines recommended that panel widths should be limited to $<0.4H$ to maximize the thickness of the Constrained Zone (i.e. B and C-Zones) beneath tidal waters. **Reynolds, 1977** recommended $0.33H$ for maximum panel widths at depths more than 120 m below the reservoirs in the Southern Coalfield.

The height of continuous fracturing was not estimated in the Wardell Guidelines, but probably assumed to be significantly lower than 50T - the 15 m thick surface cracking zone. **Holla, 1991** noted that the 60T value is dependent on the S_{max} and K ratio (and hence W/H ratio) and should not be applied blindly to all mining geometries.

Singh and Kendorski, 1981 adopted a general height of A-Zone Fracturing of $56T^{0.5}$ based on a review of international case studies with a minimum Constrained plus Surface Zone thickness of 45 m for mudstone and 57 m for sandstone strata conditions when mining below tidal waters. The model recognizes that fracturing may extend further through massive strata than thinly bedded units due to their propensity to carry greater load.

A11.3.2 Whittaker and Reddish Physical Model, 1989

It is considered that the published physical modeling work in **Whittaker and Reddish, 1989** provides valuable insight into the mechanics of sub-surface fracturing over longwall panels. The outcomes included specific guidelines (over and above such work as the Wardell, 1975 Guidelines) for the prevention of inundation of mine workings beneath surface and sub-surface water bodies.

The **Whittaker and Reddish, 1989** height of fracturing model was developed in response to the water ingress problems associated with early longwall extraction at the Wistow Mine in Selby, UK. The longwall panel was located at 350 m depth and experienced groundwater inflows of 121 to 136 litres/sec when sub-surface fracturing intersected a limestone aquifer 77 m above the seam.

The physical model is a scaled down version of the real-world, and therefore requires compatible material strength properties (i.e. plaster) to generate fracturing from the laboratory-sized void widths and mining heights being simulated. The pattern of cracking and heights of fracturing observed should therefore not be dismissed because of the materials used to create the model.

The Whittaker and Reddish model identifies two distinct zones of fracturing above super-critical width extractions (continuous A-Zone and discontinuous B-Zone fracturing) and indicates the height of each is a function of maximum tensile strain at the surface. As such, its use is also based upon being able to make credible subsidence and strain predictions. The mechanical concepts of the model are shown in **Figure A40b**.

The definition of the ‘continuous’ height of fracturing refers to the height in which a zone of direct hydraulic connection for groundwater inflows to the mine workings develops (i.e. the A-Zone).

The definition of the extent of ‘discontinuous’ height of fracturing refers to the height at which the horizontal permeability increases as a result of strata de-lamination and incomplete fracturing through the strata beds (i.e. the B-Zone). Minor occurrences of direct connection of fractures to the workings is considered possible, but will depend on the geology (e.g. the presence of persistent vertical structure such as faults and dykes).

The outcomes of the modeling work resulted in two logarithmic type curves that relate the surface horizontal strain to the measured A and B fracture heights normalized to the cover depth (see **Figure A40b**).

The physical modeling work that was completed to derive the prediction curves is summarised below:

- The physical model was constructed from multiple 1.25 cm thick layers of coloured sand and plaster with sawdust bond breakers placed between each successive layer. Based on a real world/model ratio of 92, the model layers represented 1.15 m thick layers in the real world. The model was initially devoid of vertical joints or cracks.
- The scale and mechanical properties of the model satisfied dimensional analysis and similitude laws. *Note: This aspect of mechanical models is very important, as overburden strength properties will not fracture if they are too high for the model’s mining geometry.*
- The plaster layers for the model were equivalent to a rock mass with a density of 2.35 t/m³, a UCS of 10.94 MPa and Youngs Modulus, E, of 984 MPa.
- The model was used to simulate the overburden behaviour of a panel with a W/H ratio of 1.31 and a progressively increasing working height range that commenced at 1.2 m and finished at 10.8 m. The advancing longwall face was simulated by removing timber blocks at the base of the model in 1.2 m to 2.0 m lift stages.

- The extent or heights of ‘continuous’ and ‘discontinuous’ fracturing above the longwall ‘face’ were measured and plotted with the associated peak tensile strain predictions at the surface. The subsidence and strains were measured from a grid and calculated using the method provided in the **UK Subsidence Engineers Handbook, 1975**.
- The fracturing path progressed up at an inward angle of approximately 18° to 19° from the solid rib and increased towards the centre of the panel higher up into the strata. Continuous fracturing occurred in the cantilever bending zone close to the rib-side only, as fracturing in the overburden above the middle portion of the panel tended to ‘close’ and did not appear to represent an area where groundwater inflows into the workings would eventuate.
- Surface cracks extended down from the surface for a depth up to 7.5 m.
- Other similar models were also prepared and used to demonstrate the “ability of strong overburden at the surface to cause bridging of the strata in this manner is dependent upon the strength and general competence of the rocks near to the surface, in addition to the width of the extracted region.”
- Any groundwater inflow conditions were therefore considered to be “mainly associated with the longwall rib-side fracture zone [or tensile strain zone]” above longwall panels.

The findings above are considered reasonable for super-critical longwall geometries where panel widths are greater than the critical width (i.e. 1.2 - 1.4H) and the height of fracturing is likely to be controlled primarily by the mining height and strata properties.

Using the analytical model equations derived in **Section A11.4.2**, the progression of the height of continuous fracturing was back analysed by DgS using the maximum compressive beam stress for spanning strata units under full loading conditions (Equation 1) and goaf supported strata units (Equation 2):

$$\sigma_c = 0.75\gamma(H - A)(W - 2A\tan\theta)^2/t_i^2 \quad (\text{Lower Beam}) \quad (1)$$

$$\sigma_c = 4\Delta E t_i / (W - 2A\tan\theta)^2 \quad (\text{Upper Beams}) \quad (2)$$

It was noted that the goaf did not ‘bulk’ in the model, resulting in no reduction in subsidence between the seam and surface (i.e. $S_{\max} = T$) and measured surface strain/curvature ratio indicated $\Delta = 0.5T$ over the effective span, $W_i = W - 2y\tan\theta$ above the goaf.

The results of the model are summarized in **Table A5** below:

Table A5 - Physical Model Results Summary for the Height of Continuous Fracturing Development above a Supercritical Longwall Panel

Lift No	Mining Height T (m)	S _{max} (m)	E _{max} (mm/m)	A (m)	Effective Beam Span W _i (m)	Measured Beam Curvature in Spanning Strata (km ⁻¹)	Measured Effective Beam Thickness t _i (m)	Stress in Lowest Beam after Lift & Prior to Collapse (MPa)	Stress in Spanning Unit above Goaf (MPa)	Predicted Minimum Beam Thickness Required to Span Goaf (m)
1	1.2	1.2	7.6	23.96	137.55	0.51	105 (47.9)	12.0	4.82	56.7
2	2.4	2.4	15.3	43.26	120.77	0.66	81 (38.6)	12.5	7.81	43.6
3	4.2	4.2	26.8	67.38	107.25	1.46	62 (24.1)	17.3	6.55	26.6
4	6.0	6.0	38.2	85.60	90.36	2.94	38 (18.2) (9.1)	13.8	10.10	10.8
5	8.4	8.4	53.5	99.57	77.60	5.58	19.4 (14) (7)	19.2	7.45	5.6
6	10.8	10.8	68.8	105.0	67.81	9.39	5.4 (2.7)	12.5	-	3.0

W_i = Effective Span above mine workings at A-Zone Limit Horizon ($W - 2A \tan \theta$).

(9.1) - Bedding thickness halved as bedding sheared under load > it's shear strength during test.

Bold - stress limited to UCS based on full cover load (Equation 1).

italics - stress limited to UCS based on deflecting strata curvature (Equation 2).

UCS = 10.94 MPa; E = 984 MPa; $\theta = 19.3^\circ$.

The measured strata unit thickness (t_i) required to span the goaf voids and limit the height of continuous fracturing (A) after each successive lift were back-analysed using the measured A-Zone heights and Equation (2); see **Figure A40g**. The minimum beam thickness required to span the goaf was also estimated based on the two analytical model Equations (1) and (2) and compared to the measured beam thickness at the A-Horizon in **Figure A40h**.

Several further salient points are apparent from the results as follows:

- After extraction of the panel, all of the spanning units deflected under gravity loading until the tensile, shear and compressive stresses in some of the rock mass bedding units were exceeded.
- It was apparent from the modelling data that the overburden above each mining stage resulted in the beam shearing into two or three separate beams, with the lower beam collapsing and the upper beam(s) left to span the void. It is noted that the maximum shear stress acting on the initial beam would have developed on the bedding surface near the middle of the beam section, so it would be expected to shear or slip there first.
- If the strata unit separated from the overlying rock mass, it either collapsed into the void below (if the stress exceeded the UCS of the beam) or it was thick enough to span under its own self weight. The sagging beam units were also supported by the underlying goaf to some degree.

- The rock mass units caved up into the overburden at an angle of break (θ) and effectively reduced the span of overlying units to $W_i = W - 2y \tan(\theta)$. The potential load acting on the strata units also decreased linearly with the reduction in overlying cover.
- The height of continuous fracturing (i.e. the A-Zone) was defined as the point where the overlying strata were spanning the cracked and collapsed strata below it.
- The A-Zone height increased after the mining height T was increased, with no change to panel width or cover depth.
- The strata units continued to deflect after each incremental increase in mining height, with the lower units collapsing when the UCS of the beam was exceeded. In some of the lifts, it is apparent that the spanning strata units sheared into units that were approximately half the thickness of the original spanning beam. The beam stress was also subsequently decreased if shearing occurred. Estimates of shear stress at mid-beam thickness exceeded the shear strength of the strata unit (or bedding plane surface) in these instances, assuming a friction angle of 20° along the bedding planes.
- The spanning strata lost stiffness when their thickness was decreased, resulting in further deflection (and stress acting in the beam).
- Collapsed strata units provided support to the sagging strata above and ultimately controlled the deflection of the overlying units.
- The A/T ratio ranged from 20 to 10 as the mining height increased from 1.2 m to 10.8 m. For real world mining heights of 2.4 m to 6 m, the A/T ranged from 18 to 14.

Further discussion on the analytical height of fracturing models for real world conditions is presented in **Section A11.4.2**.

A11.3.3 Forster and Enever, 1992

A comprehensive monitoring program above two supercritical pillar extraction and one longwall panel in the Great Northern Seam was presented in **Forster and Enever, 1992**.

The outcomes of the work was to recommend a reduction in the minimum rock cover limit required to extract coal beneath Lake Macquarie to $45T + 10$ m, and was based on borehole piezometric and rock mass permeability testing before and after total extraction mining. The 10 m was not added to account for the surface cracking zone, but to allow for localized depressions that could reduce the rock cover thickness to $< 45T$. The surface cracking zone of < 15 m was therefore included in the $45T + 10$ m criterion.

The height of continuous fracture zone was assessed to have ranged between $21T$ and $33T$ above the mine workings. The thickness of the Constrained Zone was defined as being dependent on the cover depth, but should be $> 12T + 10$ m below tidal waters.

The thickness of the 'Constrained Zone' above the 'Fractured Zone' was also considered to have greater importance in regards to providing a groundwater drainage path barrier than the tensile strain limit of 7.5 mm/m set by **Wardell, 1975**. It was considered that the thickness of the Constrained Zone and the presence of low permeability lithologies, such as mudstone and claystone, were more likely to influence the performance of the strata barrier above the A-Zone than putting a limit on surface strain. The strain limit criterion has subsequently been left out of sub-aqueous mine design criteria in NSW Coalfields.

A11.3.4 ACARP, 2006

This report reviews the impacts of shallow longwall mining on the groundwater systems based on fieldwork conducted in the Hunter Valley, NSW (Beltana Mine) and Bowen Basin, Queensland (Gregory Crinum Mine).

The **ACARP, 2006** report suggests that continuous cracking is likely to occur through the strata beams within the Fractured Zone defined by an "angle of break" of 12° to the vertical and extending inwardly from the rib-sides. International research suggests a range between 10° and 15°.

A complementary set of fractures would also be expected to develop further inside the panel on the undersides of the bending units where full subsidence develops in the strata. The angle to full subsidence ranges from 25° to the vertical according to **ACARP, 2006** and from 32° to 45° in **Li and Cairns, 2000**.

Back analysis of the angles of break suggest that surface to seam cracking could theoretically reach the surface above panels that are wide enough to prevent the opposing cantilevering abutments to interact together and limit fracturing. For a panel width of 200 m, this would occur where cover depths are < 370 m to 470 m (due to angles of break of 12° to 15°). It is also noted that the inferred height of fracturing is very sensitive to the assumed angle of break.

Note: The panel geometry discussed is actually still in the sub-critical range (i.e. $W/H < 0.7$) and it is considered by DgS that theoretical fracturing to the surface can only occur in the critical to supercritical panel width range.

ACARP, 2006 also notes an absence of surface to seam fracturing connection or groundwater inflows in the literature, where sub-aqueous mining has occurred below a depth of cover of 120 m to 160 m (for assumed critical to super-critical panel widths). The reason for this phenomenon is considered to be related to the observation that cracked and rotated blocks may still interact and provide low permeability regions in the zones of compressive strain above and below tensile cracking in the deflected beams. It was assessed that the reduction in effective span due to the cantilever effect over the ribs and increase in support that develops to overlying strata units may also allow strata units as thin as 10 m or so span across the fractured zone.

The report concluded that the height of continuous fracturing is therefore likely to be controlled by either spanning strata units or units that are not spanning which are thick enough to stop fracturing occurring right through the unit.

In the case of the non-spanning strata mechanism, **ACARP, 2006** did not have the resources available to fully evaluate what the minimum strata thickness range is likely to be in order to limit the continuous fracturing height.

Note: A similar conclusion was reached by DgS after a case by case review by DgS of supercritical longwall geometries in the NSW Coalfields in this study. It is also considered likely that this phenomenon would require the compressive stress in the deformed rock mass units to exceed their unconfined compressive strength for complete break-through to occur. However, it is also apparent that the presence of thin strata units that deform predominately in shear along slipping bedding partings, can also limit vertical cracking developing to the surface cracking zones.

A11.3.5 MSEC, 2011 and SCT, 2001

The MSEC and SCT models are based on several published case-studies for mining impacts in the NSW Coalfields and their own internal analytical and numerical modeling results. The ‘heights of fracturing’ are predicted based on longwall and total pillar extraction panel widths and indicate maximum values ranging from 1W to 1.5W (SCT) and 1.374 (W-30) (MSEC). The database of ‘observed heights of fracturing’ and the above panel width models are presented in **Figure A40i**.

Based on a review by DgS of the database from which the MSEC and SCT models are derived, and extensometer and vertical strain measurements at other mines, it is apparent that the models include cases of both A and B-Zone fracture heights (see **Figure A40j** and **Section 11.4** for further details). DgS concludes that the MSEC and SCT ‘height of fracturing’ models are probably conservative.

It is also apparent that there are three reported cases in the database which indicate ‘fracturing through to the surface’ has occurred (LW1 at Invincible, LW11 at Angus Place and LWE1 at South Bulga). A review of the extensometer data published by **Holla, 1991** for the Invincible case study, DgS concurs with the assessment that continuous fracturing has probably extended to the surface cracking zone (or to within 10 m below the surface). No data is available for the latter two cases, however, based on the above discussion, it is considered possible that surface to seam connectivity of the B-Zone (and not the A-Zone) occurred at these sites (further discussion on these sites are included in the following sections).

A11.3.6 Bulli Seam PAC, 2010

The NSW Government Planning and Assessment Commission (PAC) for the Bulli Seam Project Application in 2010 identified several apparent deficiencies in the commonly used ‘height of sub-surface fracturing’ models as follows:

- It is apparent that the prediction models based on panel width only indicated significantly greater sub-surface fracture heights than the models based on mining height.
- The panel width only-based models did not distinguish between continuous and discontinuous fracture heights.
- The authors and reviewers of the prediction models all recognize the deficiencies in the height of fracturing models that are based solely on panel width or mining height. They also indicate that more thorough analysis is probably required to determine a 'more definitive' function that relates the height of connective cracking to the mining geometry.

Based on the PAC report and review of available published data the following comments are made by DgS:

- The data on which the Panel Width-Only models are based are likely to include both A and B type fracturing zones (hence the review of MSEC and SCT database presented in **Figures A40i & A40j**).
- The Panel Width only models appear to have been developed mainly from data obtained at deep, sub-critical mines of the Southern and Western Coalfields.
- The height of fracturing is considered unlikely to extend further up into the strata once the critical panel width is reached (for a given mining height) and no further deformation of the overburden can occur.
- The behaviour of the overburden is more likely to be influenced by panel width for sub-critical panels and mining height for supercritical panels.

A11.3.7 State of the Art Summary and Gap Analysis for Alternative Models

In summary, the literature review outcomes indicate the following:

- The A-Zone is assessed to range from 21T to 33T above supercritical panels and up to 43T above critical and sub-critical panels. The B and C-Zone thicknesses will generally depend on the cover depth less the A-Zone Horizon estimate.
- The models that are based on the longwall panel widths only indicate maximum 'heights of fracturing' that range from 1.0W to 1.5W (SCT) and 1.374(W-30). These models however, probably include both A and B-Zone fracture heights in some instances and are therefore likely to be conservative.
- It is apparent that the published height of fracturing models based on mining height alone varies significantly for supercritical, critical and sub-critical mining geometries. The A-Zone could (and does) extend higher up into the overburden above sub-critical

panel geometries as the fracturing due to strata deformation is also influenced by the panel width.

- It is also reasonable to assume that the maximum height of the A-Zone will probably occur above the centre of a sub-critical longwall panel with a naturally spanning catenary arch.
- Surface drilling investigations above subsided longwall panels in NSW and QLD have found the maximum height of fracturing is in fact ‘dome-shaped’ and develops somewhere between the point of maximum tensile strain and the centre of the panels.
- In order to distinguish between A and B-Zones it is considered best-practice to install borehole extensometers and multiple-piezometers (deep and shallow) above longwall panels and measure the various fracture and dilated zones based on anchor displacements, vertical strain and the short to medium term impacts to established groundwater regimes.
- When longwall mining beneath lakes and sensitive groundwater aquifers, it is essential that the mining geometry be controlled to provide an effective B/C-Zone or Constrained Zone thickness to minimise the potential for connective cracking to develop up to the feature. The presence of geological structure should also be considered as it may act as a potential groundwater conduit between the A and B-Zones.
- Based on **Forster and Enever, 1992**, the minimum Constrained Zone (B/C Zone) thickness above the Fractured A-Zone should be $>12T + 10$ m and include the surface cracking zone thickness of <15 m beneath Lake Macquarie. The minimum B/C Zone thickness does not include weathered material and/or alluvial sediments.
- For cases where permanent water bodies do not exist, but surface to seam hydraulic connection is not desirable, it is recommended that the continuous height of fracturing zone should not encroach within the surface cracking zone (ie. A minimum of 10 m to 12 m below the surface should be assumed generally, but may need to be increased up to 20 m for steep topography affects).
- As mentioned earlier, the height of A-Zone fracturing is strongly dependant on the presence of the bridging capability of massive conglomerate or sandstone units above a given panel. Therefore, estimating the height of A and B-Zone fracturing also requires a review of the overburden lithology and the presence of geological structure.
- It is also apparent from a case by case review, that the height of fracturing may be controlled by strata that is not actually spanning, but may be thick enough or flexible enough to stop fracturing occurring right through the strata unit. For this scenario, it is considered the height of fracturing will be controlled by (i) the thickness and/or flexibility of the strata unit relative to the panel width and its location above the workings, (ii) the thickness of compressible goaf material that will induce curvature in

the overlying strata units as the goaf is compressed, and (iii) the presence of confined, semi-impermeable strata units such as mudstone and claystone in the B and C-Zones that will swell in the presence of groundwater and effectively seal off small width cracks.

- For the case of sub-critical panels, the maximum non-spanning strata height and load acting on the goaf may be limited by the ‘natural’ or catenary arch that can form across the mined void width. It is noted that the A-Zone has not intersected the surface above any of the 13 sub-critical longwall panels in the NSW Coalfields.
- For super-critical panels however, the height of fracturing could theoretically reach the surface and the maximum load acting on the goaf will probably equal the cover depth. It is noted that the A-Zone has not intersected the surface above critical and supercritical panels at 17 out of 20 longwalls (85%) in NSW and Queensland Coalfields.
- Near surface geology will affect the potential for surface cracking to intersect the sub-surface fractures above supercritical longwall panels. Based on physical modelling results and mine site case studies, thinner and weaker strata units may actually reduce the likelihood of cracking zone interconnection compared to thicker and stronger units.
- Subsidence effect data (i.e. Horizontal strain/curvature ratios or K Factors) also suggest that the near surface strata will behave like a beam with a thickness equal to twice this ratio or the observed cracking depths (i.e. the depth to the neutral axis of bending). For the Newcastle Coalfield, the effective beam thickness ranges from 10 m to 30 m (i.e. K Factors of 5 to 15). The Western and Southern Coalfields have effective beam thickness ranges from 30 m to 60 m (i.e. K Factors of 15 to 30).

Based on the HoF prediction model review, it was considered necessary in this study to:

- (i) review and expand the database of continuous and discontinuous cracking to include a representative range of mining geometries on which to base the empirical models on;
- (ii) update and re-evaluate the **ACARP, 2003** models;
- (iii) attempt to develop further subsurface fracturing models that included the panel width, mining height, cover depth and lithology (effective strata unit thicknesses and their properties).
- (iv) provide a clearer definition of the surface cracking depth (D-Zone).

A11.4 Expansion of the Database and Review of Sub-Surface Fracturing Prediction Models Presented in ACARP, 2003

A recent review of the **ACARP, 2003** database and the inclusion of new HoF data has recently been undertaken by DgS in 2012 and 2013 for various projects in the Newcastle/Lake Macquarie and Hunter Valley Coalfields. The up-dated database is presented in **Table A6.1** and includes a greater number of cases where A and B-Zone fracture heights have been determined from borehole extensometer and piezometric data collected over a reasonable period of time (i.e. > 12 months after mining impacts). Surface and groundwater interaction may also be established by other means in the absence of piezometers and extensometer results (e.g. mine water make increases several days or weeks (instead of months) after rainfall events, would indicate direct hydraulic connection to the surface).

The measured coalfield data base presented in **ACARP, 2003** was based mainly on a dataset of post-mining drilling data to estimate heights of fracturing for the A and B-Zones (except for the **Forster and Enever, 1992** data). The updated model database now includes further extensometer and/or piezometric data from the Southern, Western and Hunter Valley Coalfields in NSW, including Newcastle (West Wallsend, Mandalong, Wyee, Cooranbong, Teralba), Lower Hunter Valley (Abel, Austar, Ellalong); the Upper Hunter Valley (Homestead, Ashton, South Bulga), Southern Coalfield (Berrima, Metropolitan, Kemira, Belambi West, West Cliff, Tahmoor, Dendrobium, Appin) and the Western Coalfield (Springvale, Invincible). Two cases for Queensland (Oak Creek and Crinum) were also included in the database.

Based on a review of published extensometer results presented in **Holla, 1991, Frith, 2006, MSEC, 2011** and **ACARP, 2007**, it is assessed that there are six cases in the database presented in **MSEC, 2011** that appear to include the A and B-Zones and four cases whereby the 'height of fracturing' are claimed to have reached the surface at distances above the workings of 21T (Homestead Mine, LWs 9/9A), 39T (Invincible Colliery, LW1), 57T (South Bulga, LWE1) and 106T (Angus Place, LW11).

In order to use the height of fracturing data presented in **MSEC, 2011** with the **ACARP, 2003** data, it was necessary to identify the likely A-Zone cases and B-Zone cases based on the following fracture zoning criteria:

- (i) A-Zones are likely to have vertical strains > 20 mm/m and large strata dilations > 200 mm; and
- (ii) B-Zones are likely to have vertical strains of < 8 mm/m and strata dilations < 200 mm, based on measured values for cases with piezometer-established B-Zone strains measured at other mines.

Note: it does not necessarily follow that uniform vertical strains throughout the strata mean the height of continuous fracturing is likely to have reached the surface. The uniform strains may also be due to strata bedding dilations if strains are < 8 mm/m. Rock mechanics theory also indicates that a vertical tensile strain of 8 - 9 mm/m will induce a horizontal tensile strain of 2 - 3 mm/m in the rock mass due to

Poisson's ratio effect. The theoretical strain to fracture a joint-free sample of rock is 0.3 to 0.6 mm/m. It has been observed in the field that existing joints and bedding in the rock mass allow it to 'absorb' higher levels of tensile strain before developing fresh cracks at around 2 - 3 mm/m. The use of the proposed vertical strain of 8 mm/m is therefore considered to be a reasonable indicator that fresh cracking is likely to occur in the rock mass.

The following cases were changed from A to B-Zone fracturing horizons or reinterpreted by DgS based on the above criteria:

- Tahmoor LW3 (extensometer interpretation by **Holla & Buizen, 1991**)
- Westcliff / Endeavour Drift BH3 (post-mining bore interpretation by **MSEC, 2006**)
- Angus Place LW11 (fractures to surface interpreted by **Kay, 1990**)
- Springvale LW411 (extensometer & piezometer interpretation by **CSIRO, 2007**)
- Springvale LW409 (piezometer interpretation by **CSIRO, 2007**)
- Ellalong LW2 (extensometer interpretation by **Holla, 1986**)

The height of continuous fracturing for LW11 at South Bulga (**SCT, 2000**) has been assumed to extend to within 10 m of the surface and into the surface cracking zone as the extensometer or piezometric data is not available to review at this stage.

The assessment in **Kay, 1990** that the height of fracturing above LW11 at Angus Place extended to the surface was well above previous ranges (106T) measured at the mine to-date. Further discussions by the mine with the author recently indicates that a 100 m high cliff face probably affected the overburdens spanning capability, resulting in a greater than normal level of subsidence and near surface cracking. Although the surface flows in the creeks may have been re-routed into near surface cracks at the time, it is not likely that a surface to seam connection occurred.

It has also been decided to remove two case study points (Central and Southern German Creek Mines) from the original **ACARP, 2003** data base as they appear to be much lower than other cases with similar geology and geometry and were based on drilling data only.

The results of the database review and re-assignment of A- to B-Zones are shown in **Figure A40j** with the reinterpreted values summarised in **Table 6.1**. A summary of several representative extensometer results that were used to review the published heights of fracturing data presented in **Table A6.1** are provided in **Table A6.2**.

The expanded database presented in **Table A6.1** has subsequently been used to (i) update the strain and curvature index-based models presented in **ACARP, 2003** and (ii) develop more technically concise models that allow variations in geology and geometry to be assessed in each coalfield. The results are presented in the following sections.

Table A6.1 - Updated HoF Model Database for Australian Coalfields

Site	Panels	Mine	Seam	W (m)	H (m)	W/H	T (m)	A (m)	B (m)	A/T	ACARP 2003 Model Predictions				
											t^ (m)	y^ (m)	Unit SRP*	U95% CL S _{max} (m)	U95% CL E _{max} (mm/m)
1	MW508	Bellambi W.	Bulli	110	421	0.26	2.50	92	-	37	100	90	High	0.30	2
2	LW10	Metropolitan	Bulli	140	460	0.30	3.40	130	-	38	100	130	High	0.29	3
3	LW1-4	South Coast	Bulli	110	325	0.34	2.50	85	-	34	100	85	High	0.24	3
4	LW6	Kemira	Wong.	117	335	0.35	2.75	98	-	36	100	98	High	0.16	2
5	LW20	Metropolitan	Bulli	163	450	0.36	3.40	100	-	29	100	100	High	0.34	2
6	LWA1	Austar	Greta	159	417	0.38	6.00	87	277	15	100	80	High	0.56	4
7	LW514	Bellambi W.	Bulli	150	400	0.38	2.70	90	-	33	100	90	High	0.29	2
8	LW28	Appin	Bulli	200	500	0.40	2.30	90	-	39	120	90	High	0.27	1
9	LW2	Ellalong	Greta	150	368	0.41	3.50	113	210	32	100	113	High	0.40	3
10	LW3	Tahmoor	Bulli	180	424	0.42	2.18	-	204	-	100	100	High	0.29	2
11	LW9	Teralba	YW	150	350	0.43	2.70	110	150	41	34	110	High	0.32	2
12	TE	West Cliff	Bulli	200	446	0.45	2.50	101	245	40	100	101	High	0.30	1
13	TE	Berrima	Wong.	120	176	0.68	2.3	76	112	33	100	76	High	0.50	3
14	LW409	Springvale	Lithgow	265	385	0.69	3.25	133	254	41	55	133	High	0.6	3
15	LW9	Mandalong	WW	160	220	0.73	4.50	-	-	-	30	160	High	0.5	3
16	LW11	Angus Place	Lithgow	211	263	0.80	2.47	-	253	-	100	253	High	0.5	3
17	411	Springvale	Lithgow	315	368	0.86	3.25	139	288	43	55	139	High	0.68	5
18	LW5	Mandalong	WW	160	179	0.89	3.70	118	154	32	25	83	Mod	1.38	3
19	LW5	Dendrobium	Wong.	245	255	0.96	3.75	123	-	33	80	123	High	1.25	5
20	LW1	Wyee	Fassifern	216	206	1.05	3.44	126	-	37	30	126	High	1.09	5
21	LW1	Invincible	Lithgow	145	116	1.25	2.70	106	111	39	15	106	Low	1.62	16
22	TE1	Abel	U. Don.	120	95	1.26	2.55	45	75	20	15	41	Low	1.51	22
23	LWs	Ashton	Pikes Gully	216	154	1.40	2.55	82	130	32	30	82	Low	1.5	15
24	LW40	WWC	WBH	179	113	1.58	3.80	80	108	21	20	80	Low	2.28	21
25	LWE1	Sth Bulga	Whybrow	259	155	1.67	2.55	145	150	57	20	145	Low	1.53	8
26	LW41	WWC	WBH	179	105	1.70	3.80	72	100	19	20	72	Low	2.28	24
27	LW9	Crinum	Lillyvale	280	155	1.81	3.50	85	150	24	35	105	High	1.82	8
28	LW39	WWC	WBH	179	97	1.84	3.90	68	92	17	20	68	Low	2.18	25
29	TE-3D	Wyee North	GN	355	185	1.92	1.90	63	143	33	50	63	High	1.14	4
30	TE-355	Wyee North	GN	355	180	1.97	1.90	40	-	21	50	40	High	1.14	4
31	Panel2	Abel	U. Don	150	76	1.97	1.88	45	71	24	15	33	Low	1.13	23
32	TE-Nth B	Cooranbong	G.N	150	75	2.00	2.80	58	70	21	20	58	Low	1.68	33
33	LW1	Oaky Ck	German Ck.	205	95	2.16	3.20	55	90	17	30	55	Low	1.92	25
34	LW9/9a	Homestead	Whybrow	200	80	2.50	3.40	75	75	23	15	65	Low	1.98	29

- = not available; **bold** - surface to seam fracturing assessed by others; *italics* - Continuous Fracture Zone heights (A-Zone) was originally reported by others and included the Discontinuous Fracture and Dilated Zone (B-Zone). A and B- Zone height of the B-Zone heights were re-assessed by DgS based on a review of available measured vertical strains and piezometric data (see **Figure A40i and A40j**); No shade - Sub-critical panels (W/H<0.7); Light grey shade - Critical panels (0.7<W/H<1.4); Grey shade - Supercritical panels (W/H>1.4).
 * - SRP = Subsidence Reduction Potential for strata unit with thickness t and distance y above the workings. The SRP may be due to spanning or bulking behavior over the range of W/H and is also considered to be an indicator of whether a strata unit will limit the height of continuous fracturing; ^ - likely values assessed from borehole and subsidence data; Wong. = Wongawilli; YW= Young Wallsend; WW = West Wallarah; U. Don = Upper Donaldson; WBH = West Borehole; GN - Great Northern.

Table A6.2 - Summary of Measured A, B, C & D Zone Strains in Extensometers*

Parameter	Underground Coal Mines									
	Angus Place [§]		West Wallsend				Abel [^]			
Panel No.	LW11		LW39		LW40		Panel 1		Panel 2	
Cover Depth H (m)	211		97		113		95		76	
Panel Width W (m)	263		179		179		120		150	
W/H	0.8		1.84		1.58		1.26		2.0	
Mining Height, T	2.5		3.8		3.9		2.1		2.1	
Fracture Zone	Dilatation (mm)	Strains [#] (mm/m)	Dilatation (mm)	Strains [#] (mm/m)	Dilatation (mm)	Strains [#] (mm/m)	Dilatation (mm)	Strains [#] (mm/m)	Dilatation (mm)	Strains [#] (mm/m)
<i>D-Zone</i>	-	3 - 5	-	25	-	24	-	24	-	23
<i>C-Zone</i>	-	-	-	-	-	-	-	-	-	-
B-Zone	~60 - 120	5 - 6	8 - 17	1 - 2	25 - 50	5 - 8	14 - 19	1 - 2	<20	-1 - 0
A-Zone	~1000	100	234 - 957	115 - 139	390 - 769	39 - 77	279 - 1289	28 - 129	158 - 185	16 - 19
Parameter	Mandalong		Austar		Ellalong		Invincible		Tahmoor	
Panel No.	LW5		LWA1		LW2		LW1		LW3	
Cover Depth H (m)	179		453		368		116		424	
Panel Width W (m)	160		159		150		145		180	
W/H	0.89		0.35		0.41		1.25		0.42	
Mining Height, T	3.7		6.0		3.5		1.26		2.2	
Fracture Zone	Dilatation (mm)	Strains [#] (mm/m)	Dilatation (mm)	Strains [#] (mm/m)						
<i>D-Zone</i>	-	5	-	3	3	3	10	10	1	1
<i>C-Zone</i>	<20	<1	<10	<1	<1	<1	-	-	<1	<1
B-Zone	19 - 29	2 - 5	24 - 133	1 - 7	1 - 5	1 - 5	<5	<5	1 - 4	1 - 4
A-Zone	73 - 672	80	222 - 1177	11 - 59	>10	>10	10 - 75	10 - 75	N/A	N/A

* - A, B & C-Zone strains are vertical and approximately 3 to 4 times the horizontal strain due to Poisson's ratio effect; *italics* - D-Zone strains are horizontal.

- tensile strains are positive. Negative strains or compression develops after full subsidence occurs and goaf compresses under load from sagging overburden strata; ^ - Effective mining height for total pillar extraction (Te = 0.85T); § - Strain data not available and quoted from published literature.

Table A6.2 (Cont...) - Summary of Measured A, B, C & D Zone Strains in Extensometers*

Parameter	Underground Coal Mine			
	Springvale			
Panel No.	LW411		LW412	
Cover Depth H (m)	368		400	
Panel Width W (m)	315		315	
W/H	0.90		0.79	
Mining Height, T	3.25		3.25	
Fracture Zone	Dilation (mm)	Strains [#] (mm/m)	Dilation (mm)	Strains [#] (mm/m)
<i>D-Zone</i>	-	3	-	3
C-Zone	<42	<5	<33	<5
B-Zone	39 - 410	4 - 10 (17)	2 - 505	4 - 8 (25)
A-Zone	194 - 1441	14 - 42	174 - 1571	5 - 42

* - A, B & C-Zone strains are vertical and approximately 3 to 4 times the horizontal strain due to Poisson's ratio effect; *italics* - D-Zone strains are horizontal.

- tensile strains are positive. Negative strains or compression develops after full subsidence occurs.

^ - Effective mining height for total pillar extraction ($T_e = 0.85T$).

bold - measure strain near the top of the B-Zone where a bedding separation occurred. Piezometer data indicates the height of continuous fracturing is further below this point.

A11.4.1 Updated Tensile Strain Model

The physical model presented in **Whittaker and Reddish, 1989** related the ratio of the height of continuous and discontinuous fracturing (A and B) above longwall panels over cover depth (H) with the maximum tensile strain (E_{max}) at the surface due to mine subsidence. Actual drilling data over extracted longwall panel goaf was subsequently used to define a real-world relationship between these variables at several Australian Coalfield mines in **ACARP, 2003**.

The additional data presented in **Table A6.1** has been added to the original database and the regression equations have been revised below:

$$\{A\text{-Line}\} \text{ Mean } A/H = 0.180 \ln(E_{max}) + 0.1405, \quad R^2 = 0.70$$

$$U95\%CL \text{ } A/H^* = 0.180 \ln(E_{max}) + 0.3742.$$

$$\{B\text{-Line}\} \text{ Mean } B/H = 0.146 \ln(E_{max}) + 0.5315, \quad R^2 = 0.47$$

$$U95\%CL \text{ } B/H^* = 0.146 \ln(E_{max}) + 0.8426.$$

* - Maximum A/H and B/H = 1.

where

A, B = height above workings to A and B-Zone horizons,
H = cover depth,

E_{\max} = the maximum predicted tensile strain for a ‘smooth’ subsidence profile.

The new tensile strain model is presented in **Figure A41a** and has a much stronger fit to the new database for the A-Zone than the **ACARP, 2003** model, with only a slight improvement for the B-Zone horizon. The R^2 value for the logarithmic regression curve fitted to the revised A-Zone data was previously 0.44 and is now 0.70. The R^2 value for the B-Zone was previously 0.46 and is now 0.47.

The measured database model still appears to indicate a similar height of fracturing trend to the **Whittaker and Reddish, 1989** physical model. However, as was concluded in **ACARP, 2003**, the predicted heights of ‘continuous’ and ‘discontinuous’ fracturing in the real world were again higher for a given tensile strain at the surface, and probably due to the influence of jointing in the rock mass (compared to none in the physical model).

The real world database indicates that the tensile strain probably needs to be >32 mm/m for surface to seam connection to occur, and is approximately 50% of the physical model value of 60 mm/m. It should also be noted that if connective cracking is likely to extend into the Surface Cracking Zone (a depth of 10~15 m below the surface), then the maximum tensile strain for surface to seam connection reduces to 25 mm/m. It is assessed however, that the predicted strains are also dependent on surface crack width development and should therefore not be used to assess surface to seam connectivity directly without considering the near surface B and C-Zone lithologies.

Considering the potential difficulties with predicting strains after the onset of cracking, it is still assessed that it is unlikely that the tensile strain-based model will be reliable. **ACARP, 2003** attempted to modify the strain-based model to a curvature-based approach. The resulting regression equations however, did not improve the correlation between the adopted variables (i.e. both methods had R^2 values of 0.44). The curvature-based model of height of sub-surface fracture prediction was subsequently revised with the expanded model database in **Section A11.4.2** to see if the regression equations could be improved upon.

A11.4.2 Updated Overburden Curvature Index Model

The Overburden Curvature Index or S_{\max}/W'^2 term was introduced in **ACARP, 2003** in an attempt to provide a readily measurable field parameter that would not be compromised as much by surface strain concentration effects (i.e. cracking). The logarithmic regression lines were re-derived using the expanded database to give new predictions of the mean and U95%CL values for both A and B-Zones as follows:

$$\{\text{A-Line}\} \text{ Mean A/H} = 0.198 \ln(S_{\max}/W'^2) + 1.1518, \quad R^2 = 0.66$$

$$\text{U95\%CL A/H}^* = 0.198 \ln(S_{\max}/W'^2) + 1.3915.$$

$$\{\text{B-Line}\} \text{ Mean B/H} = 0.152 \ln(S_{\max}/W'^2) + 1.3265, \quad R^2 = 0.52;$$

$$\text{U95\%CL B/H}^* = 0.152 \ln(S_{\max}/W'^2) + 1.5928.$$

* - Maximum A/H and B/H = 1.

where

A, B = height above workings to A and B Horizons,
 H = cover depth (m).
 S_{\max}/W'^2 = Overburden Curvature Index,
 W' = lesser of W and 1.4H

Note: It is reasonable to assume the effective mining width (W') and height of fracturing (A/B) will be limited beyond the point where the maximum subsidence or strata deformation has been reached above supercritical mining geometries (i.e. W/H > 1.4).

The revised regression results are shown in **Figure A41b**.

Despite the apparent improvement in the regression equations, the same apparent differences still remain between the Australian height of fracturing database and the UK physical modelling results. One obvious difference is that the UK physical model represents a supercritical case study where the panel width and cover depth was constant (i.e. W/H = 1.34). The Australian database however, has a significant range of sub-critical, critical and super-critical panel geometries and further investigation of this difference is therefore required (see **Section A11.4.4**).

A11.4.3 Influence of Lithology on Sub-Surface Fracture Heights

An assessment was made in **ACARP, 2003** on whether massive lithology had the potential to control or limit the height of fracturing above a longwall panel. The expanded model database presented in **Table A6.1** still indicates that it does, with the A-Horizon likely to have coincided with the base of the massive strata units in 17 out of 21 cases with 'Moderate' to 'High' SRP strata units.

The potential for massive strata units to mitigate the height of continuous fracturing above the workings should therefore not be ignored where subsidence magnitudes and HoF are clearly being controlled by spanning strata.

Overall, the HoF results suggest that the presence of massive sandstone or conglomerate lithology can control the height of hydraulic fracturing due to their spanning capability or thickness generally. However, as has been observed at Mandalong and Springvale Mines, the presence of geological structure (faults, dykes, seam rolls and shear zone or joint swarms) has resulted in a weakening of the overburden by the tectonic activity and there has been increased subsidence due to the breakdown of massive sandstone / conglomerate into several thinner units and (ii) increased shearing and tensile stress acting on the discontinuities has resulted in groundwater conduits developing deeper into the overburden.

It is therefore usually recommended that a mine undertake a sub-surface fracture-monitoring program which includes a combination of borehole extensometer and piezometer measurements during extraction in non-sensitive areas of the mining lease. Mitigation strategies for longwall mining are generally limited to (i) reducing the extraction height, (ii) decreasing the panel width and (iii) panel location adjustment. On-going monitoring of

surface alluvium and near surface rock mass aquifers is also undertaken with standpipe piezometers to check the post-mining integrity of ground water dependent ecosystems (GDE) and surface water systems generally.

A11.4.4 Height of Fracturing Angle Model, DgS 2012

Due to the currently held belief in the Australian mining industry that the sub-surface fracture heights are strongly influenced by panel width and mining height, an alternative model was developed by DgS in 2012 using a different approach to analysing the UK model data presented in **ACARP, 2003**.

Predictions of the heights of continuous and discontinuous fracturing (the A and B-Zone horizons) were re-analysed using the panel width, the mining height and a simple parabolic profile formula to estimate A and B-Zone fracture heights from a calibrated abutment angle at seam level (θ_A and θ_B) as follows:

- Continuous Fracture Zone Height, $A = W'/(4\tan(\theta_A))$
- Discontinuous Fracture Zone Height, $B = W'/(4\tan(\theta_B))$

where,

W' = Effective Panel width or minimum of W and $1.4H$.

θ_A = abutment angle to estimate height of A-Zone

θ_B = abutment angle to estimate height of B-Zone

When the UK model's fracture height data is plotted as a height of fracturing angle (estimated from an assumed parabolic fracturing profile between rib abutments), a strong correlation is apparent between the mining height for a given panel width and cover depth ($W/H = 1.34$); see **Figures A41c** and **A41d** for A and B-Zone Horizons respectively.

The regression analysis indicates the following fracture height angles (in degrees) apply for estimating A and B-Zone fracture heights in the real world:

$$\theta_A = 41.617T^{-0.467} \text{ (mean)} \quad \text{and} \quad 25.083T^{-0.401} \text{ (lower 95\%CL)}$$

$$\theta_B = 21.806T^{-0.233} \text{ (mean)} \quad \text{and} \quad 17.295T^{-0.238} \text{ (lower 95\%CL)}$$

Real world fracture height data measured with piezometers and borehole extensometers indicates a similar trend as the physical model results, although there is more scatter in the data that is probably due to both mining geometry (W/H) and geological variability.

The UK physical model assessed mining heights of 1.2 m to 10.8 m, and generated fracture height angles at the abutments ranging from 55° to 18° for the A-Zone and from 37° to 18° for

the B-Zone horizon. The fracture height angle tends to follow a decaying power law as the mining height increases.

For real-world mining heights of 1.9 m to 6.0 m (median of 3.0 m), the calibrated fracture height angles range from 34° to 18° for the A-Zone, and from 22° to 13° for the B-Zone. One A-Zone case had a fracture height angle of 58° due to the apparent ‘truncating’ effect of a 40 m thick conglomerate strata unit 40 m to 60 m above a supercritical panel in the Great Northern Seam (Wyee Colliery’s North-3D Panel).

As was found in the strain and curvature-based model’s, the presence of pre-existing jointing in the rock mass is likely to have contributed to greater fracture heights determined from the field data compared to the laboratory model.

The effect of massive strata units is apparent in the database (see **Figure A41c**) and further measurements are necessary to develop a more discerning prediction model that allows ‘Low’ and ‘High’ SRP strata to be assessed separately using this model. The height of fracturing model proposed at the time was considered likely to be conservative for greenfields sites if based on the lower bound fracture height angles and to give upper bound fracture height predictions.

Further review of sub-critical, critical and supercritical panel case studies in 2013 has found that the A and B-Zone fracture height angle model could also be further divided into sub-critical, critical and supercritical panel geometries (see **Figure A41e** and **A41f**) as follows:

$$\theta_A = 32.448T^{-0.241} \text{ for the mean fracture height angle.}$$

Upper 95% Confidence limits for the A-Zone were estimated by reducing the mean angle by 5°, 7° and 10° for supercritical, critical and sub-critical longwalls respectively.

$$\begin{aligned} \theta_B &= 31.5T^{-0.373} \text{ for the mean fracture height angle for supercritical panels} \\ &= 25.4T^{-0.373} \text{ for the mean fracture height angle for critical/sub-critical panels} \end{aligned}$$

Upper 95% Confidence limits for the B-Zone were estimated by reducing the mean angle by 3.5°, 7° and 7° for supercritical, critical and sub-critical longwalls respectively.

The review outcomes suggest that heights of subsurface fracturing appear to increase above sub-critical panels for a given mining height, but are also likely to be due to the panel width and changes in macro-scale structural behaviour of the overburden as well.

Whilst the trend from sub-critical to supercritical panel geometries appears reasonably consistent across the abutment angle model database (with a few cases where thick strata has clearly limited the fracture heights) it is noted that the predicted heights of fracturing are highly sensitive to the selected value of theta. It was therefore considered that a new modelling approach based on Dimensional Analysis and Buckingham’s Pi-Theorem would be

needed to reasonably establish definitive relationships between the key variables over a broader range of mining geometries and geological conditions.

A11.5 Alternative Sub-surface Fracture Model Development

Starting with the influence of mining height (T) on the height of A-Zone fracturing, if we firstly consider a supercritical panel of a given width (W) and cover depth (H), **Whittaker and Reddish, 1989** and **Singh & Kendorski, 1991** each demonstrated that the height of continuous fracturing (A) will increase with the square root of the mining height, $T^{-0.5}$, or a power rule of the form $A = aT^b$, as shown in **Figure A41g**. It is apparent that the database of real-world fracture heights with W/H range from 0.3 to 2.22 has greater scatter than the UK model curve for supercritical panel geometry, and therefore indicates that other factors such as the panel width and geology should probably be considered. The apparent under prediction of A-Zone fracture heights by the **Forster and Enever, 1992** model, also supports this view.

If the fracture heights are plotted against panel width (W) only, a similar ‘scattered’ outcome results as shown in **Figure A41h**. The conservative nature of the height of fracturing models presented by SCT and MSEC is also demonstrated in the figure and suggests that both A and B-Zones are included in their models.

A slightly improved regression analysis results if A is plotted against W/H in **Figure A41i** or when normalized to the panel width (A/W) and is plotted against T in **Figure A41j** for sub-critical, critical and super-critical panel geometries.

Based on these plots, it is clear that consideration needs to be given to the structural behavior of the overburden across the full range of mining geometries, its constituent strata units (or ‘beams’) and the influence of mining height, T on the development of fracture heights above longwall panels.

A11.5.1 Strata Behaviour Mechanisms that Influence Fracture Heights above Longwalls

Based on structural analysis theories, a conceptual model of the macro-scale and micro-scale mechanisms of sub-surface fracture height development are described below and shown graphically in **Figure A42a**:

Macro-Scale Mechanisms:

- For sub-critical panels, a natural catenary will probably form and transfer the weight of the top half to 2/3 of the overburden to the abutments. The strata below the arch will be subject to sagging or bending forces caused by the void formation. Depending on the span and thickness of individual strata units, the strata in the immediate roof will bend, separate, crack and ultimately cave into the extracted coal void (see *Micro-scale Mechanisms* below).
- Natural catenary arching action infers that the spanning overburden can remain entirely in compression and there is an absence of tensile and shear or ‘bending’

stresses. Subsidence data indicates that catenary arching stops occurring once W/H exceeds 0.7.

- Once W/H exceeds 0.7, the overburden will still attempt to span, however, the geometry of the arch will be too shallow for a catenary arch to develop, resulting in bending and cracking of the rock mass.
- The load will still be able to be carried over the void by the overburden, provided the rock mass has adequate strength and stiffness to resist the applied bending moments and shear and tensile stresses (along with increased compressive stresses from inward strata block rotation). This type of behaviour is known as Voussoir or 'cracked beam' behaviour, and is basically a flatter, but a less stiff version of a catenary arch.
- Shallow arching or Voussoir beam action will continue across the panel until it can no longer support the span or weight of the shallow arch. This is usually assumed to have occurred once W/H reaches 1.2 to 1.4H. The weight of the overburden will then be fully supported by the goaf beyond this point and subsidence will be a function of the mining height and cover depth or goaf load.
- The above macro-mechanisms will influence the behavior of the overburden strata units and subsequent development of the sub-surface fracture heights as follows:

Micro-scale Mechanisms:

- Soon after the coal seam is extracted from beneath the overburden, its constituent 'beams' in the immediate roof will generally deflect and behave elastically until the tensile and shear stresses within the rock mass units exceed the material and/or bedding parting strength of the units.
- The strata units will subsequently crack at the abutments and mid-span and the confinement will be partially lost. The cracked beam segments will then rotate inwardly and create a shallow compression arch within the beams (Voussoir action) that may or may not support the load.
- The cracks in the beams at this stage are likely to be discontinuous, with the beam continuing to behave pseudo-elastically with zones of compressive stress above and below the tensile cracks.
- The beam will continue to span and deflect under the applied loading until the compressive strength of the beam is reached, where the beam will then either collapse into the available void, or yield and load the previously failed strata units and goaf below it.
- Based on the physical model results presented in **Whittaker and Reddish, 1989**, the beams may also shear into two or three thinner units before the lower units ultimately crush if their UCSs are exceeded. Bending beam theory indicates that the maximum

shear stress will occur at mid-beam thickness. The beams are therefore likely to break down into half their thickness units each time shearing occurs along bedding partings.

- The goaf will compress and cause further overlying strata units to deflect, shear and crack. The goaf load will continue to increase as cracking continues up into the strata.
- The curvature induced in the beams will probably not cause complete fracture to develop through the beam until the compressive strength of the beam materials is reached. The induced curvature will therefore be a function of the stiffness of the goaf, the stiffness (and thickness) of the deflecting beam and the load acting on it.
- The goaf stiffness will initially be a function of the mining height and the bulking properties of the collapsed roof materials. The goaf stiffness will also increase as the load acting upon it increases (i.e. strain hardening behavior).
- The goaf load will be a function of the rock mass density and effective height of rock above it. The effective goaf load height is likely to be somewhere between the height to the underside of the spanning arch (above sub-critical and critical panels) and the full cover depth. Full load spanning of strata units above supercritical panel geometries are unlikely to occur and full cover depth load may be assumed to act upon the goaf.

A11.5.2 Analytical Height of Fracturing Model

An analytical model of how sub-surface fracturing develops in the overburden is described below in an attempt to define the likely relationships between the mining geometry and overburden as described in the previous section.

Initial Conditions - Elastic Beam Response to Longwall Mining

The maximum horizontal tensile stress before fracturing (σ_t) in a beam of thickness (t) with an effective span of W_i at a distance (y) above the workings will be:

$$\sigma_t = 6M/t^2 = 3\gamma(H-y)W_i^2/4t^2$$

where

$$M = \text{surcharge load} \times \text{span}^2 / 12 = \gamma D W_i^2 / 12 = \gamma(H-y) W_i^2 / 12$$

γ = unit weight of the rock mass

D = the depth to the base of the spanning beam (or H-y)

The equation shows that the tensile stress in a stack of beams will be greatest near the roof of the mine workings and then decrease linearly towards the surface. The effective span W_i of the beam will decrease as a function of the angle of break of the collapsing strata in the

Caving Zone. The angles of break (θ) are likely to range between 12° and 19° according to the literature and underground observations.

Elastic Beam Cracking and Voussoir Beam Development

The fracturing will continue to progress higher up into the strata until a beam of a certain critical thickness is reached that can either span the distance between the naturally occurring abutments or is thick enough not to fracture right through the beam after it has failed. It is also important to note that the angle of break is not the same as the height of fracturing angles (θ_A and θ_B) discussed in **Section A11.3.4**, as the latter angles were back-calculated from measured heights of continuous fracturing and assumed parabolic fracture limit profiles.

As discussed earlier, the cracking of the strata will lead to the development of Voussoir arching or ‘cracked beam’ behaviour. The stability of the Voussoir beam will depend upon the compressive stress (σ_c) developed in the beam of thickness (t) that is located a distance, y , above the workings with an effective span (W_i) as follows:

$$\sigma_c = \gamma(H' - y)W_i^2 / (4nt^2(1 - 0.667n))$$

where

n = the proportion of the beam t in compression and may be determined iteratively by minimizing σ_c as the arch shortens under load and develops a new equilibrium (and provided the stress remains in the elastic region or is less than the UCS). Voussoir analysis results based on the method presented in **Diedrichs and Kaiser, 1999**, indicate that ‘ n ’ can range from 0.5 and 0.75 in spanning beams, and will be closer to 0.5 when beam crush conditions are reached.

$W_i = W - 2y \tan \theta$ = effective span of the bending beam at distance, y above the mine workings.

H' = Effective Goaf Load Height, H' or Cover Depth, H .

Voussoir Beam Crushing and Height of Continuous Fracturing

It follows then, that the height of continuous fracturing, A , is likely to develop up to the point where the beam crushes or $\sigma_c = \text{UCS}$ and infers the following relationship exists at the point where the beam starts to yield or crush:

$$\begin{aligned} \text{UCS} &= \gamma(H' - A)(W - 2A \tan \theta)^2 / (4nt^2(1 - 0.667n)) \\ &= 0.75\gamma(H' - A)(W - 2A \tan \theta)^2 / t^2 \end{aligned} \quad (1)$$

where

θ = the angle of break that subtended to vertical from the rib side and ranges from 12° - 19° based on subsidence data and underground observations.

$H' - A$ = thickness of rock supported by the beam and may decrease to t (the beam thickness) if the strata beds shear and dilate during subsidence development.

$n = 0.5$ (conservative).

Equation (1) indicates that the height of A-Zone fracturing is likely to be a cubic function that is dependent on the following variables:

- Panel width, W
- Effective Goaf Load Height, H' or Cover Depth, H .
- Thickness, location and strength and stiffness of the strata units within the overburden (t , y , UCS, E)
- Angle of break, $\tan\theta$

Stresses in Overlying Beams Supported by Collapsed/Fractured Beams

It is noted that Equation (1) ignores the presence of collapsed and fractured material within the A-Zone itself. The formation of the goaf will provide support to overlying fractured units, but also influence the magnitude of curvature and bending stress in the overlying beams as the goaf is compacted and the beams deflect. The curvature of the overlying 'beams' (p_i) may be estimated as follows:

$$p_i = 8\Delta/(y+W_i)^2 = 8(S_{\max})/(y+W_i)^2 = 8(\epsilon_g 4T)/(y+W_i)^2 = 32(\sigma_g/E_g)T/(y+W_i)^2 \\ = 32(\gamma H'/E_g)T/(y+W_i)^2$$

where

Δ = mid-span deflection of beam with an effective span, $W_i = W - 2y\tan\theta$.

ϵ_g = vertical strain of goaf with thickness of $4T$ ($T+3T$) and a bulking factor of 1.3.

σ_g = maximum vertical stress acting on the goaf = $\gamma H'$.

H' = effective goaf load height = minimum of H and $W/(4\tan\theta)$.

E_g = stiffness of the goaf, which is likely to be a function of H , W , T and t .

From the estimated curvature of the strata units above the compacting goaf, the bending stress in the beam may be estimated as follows:

$$\sigma_c = 2M/(Znt) = 2p_i E' t^3/[12(nt^2(1-0.667n))] = 16(\gamma H)T t E'/(E_g(A+W_i^2)) \quad (2)$$

where

E' = rock mass Young's Modulus = 100 - 300UCS (depending on rock mass Geological Strength Index (**Hoek & Diederichs, 2006**));

$n = 0.5$ for beam at the yield point (i.e. $\sigma_c = \text{UCS}$)

As before, if σ_c exceeds the UCS, the cracking may extend right through the beam and the height of fracturing, A, may then continue to develop up to the next strata unit. The following relationship will therefore exist at the A horizon:

$$\sigma_c = \text{UCS} = 16(\gamma H') T t E' / E_g (W + A(1 - 2 \tan \theta))^2$$

Overall, the equations represent the physical relationships for either spanning strata (Equation (1)) or non-spanning strata (Equation (2)) that are of sufficient thickness to limit fracture continuation through it for a given UCS and mining geometry. As discussed in the following sections, the goaf modulus is likely to be dependent on the mining geometry (W, T and H').

The above equation indicates a complex system with a significant number of independent variables that will influence the height of fracturing outcomes.

Considering the complexity of the above equation and uncertainty in regards to assigning the rock mass and goaf properties, the physical relationship between the variables may also be assessed practically with Dimensional Analysis, a commonly used tool by hydraulics engineers (see **Section A11.5.3**).

A11.5.3 Dimensional Analysis and Buckingham's Pi Theory

According to **Vennard and Street, 1982**, Dimensional Analysis is “the mathematics of dimensions of quantities” built on Fourier’s 1882 “principle of dimensional homogeneity”. The underlying principle states that “an equation expressing a physical relationship between quantities must be dimensionally homogeneous” i.e. the dimensions of each side of the equation must be the same. It is a valuable means of determining physical relationships between variables in complex systems that defy analytical solution and must be solved by empirical means (i.e. observation, intuition or experiment).

Buckingham’s Pi-theory accomplishes this by the formation of dimensionless groups of independent variables that are measureable in the field. For the theory to work, the Pi-terms together must represent all of the three fundamental or primary dimensions of Mass (M), Distance (L) and Time (T), be independent of each other, and not break down into further dimensionless groups.

Buckingham’s Pi theory states that in order to determine the physical relationship between a set of ‘n’ independent parameters in a complex system, it follows that n-3 dimensionless parameters (known as Pi-terms) will be required to reasonably define the dependent variable.

The final equations obtained are in the form of:

$$\pi_1 = f(\pi_2, \pi_3 \dots \pi_{n-3}) \text{ or } f'(\pi_1, \pi_2 \dots \pi_{n-3}) = 0$$

From the previous analytical equations derived in **Section A11.5.2**, it is assessed that up to 10 variables may influence the height of Continuous Fracturing (A) and Discontinuous Fracturing (B) as follows:

$$A, B = f(W, H, T, t, \rho, \text{UCS}, E, E_g, \tan\theta)$$

The above variables may then be expressed as a combination of products and powers:

$$A, B = aW^b H^c T^d t^e \text{UCS}^f \rho^g E^h E_g^i \tan\theta^j$$

Seven dimensionless Pi-terms will therefore be necessary to describe the relationships between ten variables identified in a system driven by horizontal and vertical stress, panel width, cover depth, mining height, rock mass density, rock mass strength and stiffness, goaf stiffness, caving angle or angle of break and the location of competent or relatively thick strata units in the overburden.

Notes:

1. The y term may be ignored as it corresponds with the dependent variable (A or B).
2. The goaf modulus (E_g) and caving angle (θ) are considered to be dependent on the mining geometry and may therefore be precluded from the regression analysis.
3. The beam thickness, t refers to the thickness likely to exist just above the fracture height location (t is the most difficult of the parameters to assess, as the strata units may 'break down' into thinner units during subsidence development. The assignment of the appropriate t value therefore requires engineering judgment and analysis that includes a review of borehole logs and rock mass properties with extensometer and piezometer data (if available).

The first step in the analysis is to select a suitable set of recurring variables that cannot themselves be formed into a dimensionless group and can be used to represent one or more of the fundamental dimensions. The recurring variable set selected included the panel width, W , rock mass strength, UCS, and density, ρ , and were used to express the fundamental variables as follows:

$$\text{Length, } L: W; \quad \text{Mass, } M: \rho W^3; \quad \text{Time, } T: \rho^{0.5} W / \text{UCS}^{0.5}$$

The dimensionless π terms for the remaining independent variables were then assessed using the recurring variable set as follows:

$$\pi_1: A \cdot L^{-1} = A/W \quad (\text{Height of Fracturing Term})$$

$$\pi_2: H \cdot L^{-1} = H/W \quad (\text{Goaf Load Index Term})$$

$$\pi_3: T \cdot L^{-1} = T/W \quad (\text{Strata Curvature Index Term})$$

$$\pi_4: t \cdot L^{-1} = t/W \quad (\text{Strata Unit Thickness Term})$$

$$\pi_5: E \cdot M^{-1} L^1 T^2 = E/\text{UCS} \quad (\text{Strata Unit Stiffness Term})$$

which gives:

$$A/W = a (H/W)^b (T/W)^c (t/W)^d (E/\text{UCS})^e$$

The constants and powers for each Pi-term can now be determined using measured values in the field and non-linear regression techniques.

If we assume for the moment that the last π term representing the ratio of rock mass stiffness over strength for all cases in the database will be constant (E is typically 250 to 300 times the UCS), then the full equation of dimensionless π terms may be simplified as follows:

$$A/W = a (H/W)^b (T/W)^c (t/W)^d \text{ and } B/W = e (H'/W)^f (T/W)^g (t/W)^h$$

The form of the dimensionless π term equations will be explained in the following sections.

Note: Some of the published literature recommends that the super-critical panel width $W' = 1.4H$ should be used instead of the Panel Width, W , for estimating the height of fracturing above super-critical panels. This is because it was argued that the height of fracturing would probably not continue to develop higher into the strata once the overburden had reached the critical width and had already completely failed. The author agrees with this view and considers the height of continuous fracturing beyond this point would then be controlled by the mining height, cover depth (or goaf load) and geological conditions only.

A11.5.4 Pi-Term Model for Predicting Height of Continuous Fracturing (A) above Longwalls based Mining Geometry Only (i.e. Geometry Model)

For the purposes of demonstrating that height of fracturing prediction models need to consider the influence of geology, a regression analysis was completed without the strata unit thickness Pi-term (t'/W') included. Based on the empirical database presented in **Table A6.1**, the statistics software XLSTAT[®] was used to complete a multi-nonlinear regression analyses on the first three Pi-terms defined earlier as follows:

$$\underline{\text{Mean } A/W' = 2.215 (H/W')^{0.271} (T/W')^{0.372}} \quad R^2 = 0.61 \text{ \& r.m.s.e.} = 0.12W' \text{ (21\%)}$$

$$\underline{\text{U95\% } A/W' = \text{Mean } A/W' + a}$$

where $a = 0.16$ for subcritical panels; $0.16 - 0.085(W/H - 0.7)$ for critical panels; and 0.10 for supercritical panels.

W' = Effective Panel Width = minimum of W and $1.4H$.

T = Mining Height.

Re-arranging the above equation in terms of A gives:

$$\underline{A = 2.215W'^{0.357} H^{0.271} T^{0.372} \quad +/- aW'}$$

The regression results suggest that the height of continuous fracturing (A) will increase with effective panel width (W'), the cover depth or goaf load (H) and the mining height (T) all raised to powers ranging from 0.27 to 0.37.

The above equation(s) may be used to estimate A-Zone fracture heights in the absence of specific geological information (i.e. borehole data). The predicted v. measured outcomes using the “geometry” Pi-terms only model are presented in **Figures A42b to A42d**.

The plots indicate that the ‘geometry only’ Pi-term model is likely to provide reasonably conservative predictions, provided that the geology is not too dissimilar to the conditions that were present for the given mining geometry. For cases where the geology is significantly different above a proposed mining geometry, the above equation may underestimate or overestimate the fracture heights by a significant amount.

The development of a Pi-term model that considers the influence of overburden geology is subsequently addressed in **Section A11.5.5**.

A11.5.5 Pi-Term Model for Predicting Height of Continuous Fracturing (A) above Longwalls with the Geology Pi-Term Included

The presence of massive strata units such as sandstone, conglomerate and igneous rock that may span the fractured strata in the A-Zone is likely to limit the potential range of continuous fracture height development above the mine workings. Based on the analytical models (Equations (1) and (2)), the minimum thickness required to span the A-Zone or limit its development will depend on a number of factors, including span, thickness and rock mass axial and diametric strength. The minimum strata unit thickness required to span the A-Zone may be estimated using empirical and analytical methods, and are described in **Sections A11.5.6 and A11.5.7** respectively.

If no obvious strata unit thickness is present in the overburden, then it will be necessary to adopt an appropriate minimum value based on subsidence data and typical or atypical geological conditions. The minimum effective t' values are also defined in **Section A11.5.6**.

Based on the empirical database presented in **Table A6.1**, the statistics software XLSTAT[®] was used to complete a multi-nonlinear regression analyses on the first four Pi-terms defined earlier as follows:

$$\underline{\text{Mean } A/W'} = 1.52 (H/W')^{0.535} (T/W')^{0.464} (t'/W')^{-0.4} \quad R^2 = 0.81 \text{ \& rmse} = 0.09W' (15\%)$$

$$\underline{\text{U95\% } A/W'} = \text{Mean } A/W' + a$$

where $a = 0.15$ for subcritical panels; $0.15 - 0.0714(W/H - 0.7)$ for critical panels; and 0.10 for supercritical panels.

H = cover depth = the maximum potential goaf load height.

W' = effective panel width = minimum of W and $1.4H$.

T = mining height.

t' = effective strata unit thickness; see **Sections A11.5.6**.

Re-arranging the above equation in terms of A , gives:

$$\underline{A = 1.52W'^{0.4}H^{0.535}T^{0.464}t'^{-0.4} \quad +/- aW'}$$

The regression results indicate that the height of continuous fracturing (A) will increase with effective panel width (W'), the cover depth or goaf load (H) and mining height (T), all raised to powers ranging from to 0.4, 0.54 and 0.46 respectively and decrease with effective strata unit thickness (t') raised to the power of -0.4. The form of the power rule equation requires the powers to sum to unity to achieve dimensional consistency. The back-analysed powers are also similar in magnitude to the analytical models previously discussed.

A11.5.6 Effective Strata Unit Thickness Estimates for the Geology Pi-Term Model using Empirical Modelling Techniques

In order to calibrate the geological Pi-term model, it was necessary to use back-analysis techniques to estimate the likely strata unit thicknesses that existed immediately above the measured heights of continuous fracturing for a given mining geometry.

One of the difficulties in estimating the effective strata thickness from borehole data is the uncertainty in regards to the response of the 'bedded' strata under bending forces and whether they will break down into thinner units.

For example, a 33 to 40 m thick unit of Munmorah Conglomerate existed 80 m above LW5 at the Mandalong Mine and extensometer data measured the beam shearing into 15 m and 20 m thick units, which reduced the effective thickness of the conglomerate beam by approximately 50% (i.e. 15 m to 20 m). The height of continuous fracturing was estimated to occur at 118 m or near the top of the conglomerate, based on piezometer data.

Other longwalls with similar geometry at Mandalong did not break down into thinner units (based on measured subsidence data). The presence of a seam roll and thrust fault to the near the panel was identified in the mine workings and indicates that the strata may have been significantly 'worked' and weakened by tectonic activity prior to mining. It is suggested that assessments in greenfields sites should consider the outcome of massive units shearing into two beams for worst-case geological condition scenarios.

Initial values of t' were therefore estimated from borehole log and extensometer data to derive the general form of the equation presented in **Section A11.5.5**. The resulting regression equation indicated the strata unit thickness should be raised to a power of -0.4 to -0.5. A single iteration was then required to re-define the coefficients and remaining Pi-term powers. The results of the analysis are summarized in **Table A6.3a** and **Figure A42e**.

The results indicate that the back-analysed (or measured) t' values ranged between 18 m and 80 m (median of 46 m) for the *sub-critical* panels; from 8.5 m to 42 m (median of 25 m) for the *critical* panels and between 6 m and 34 m (median of 23 m) for the *supercritical* panel geometries. The measured t' values for the deeper panels appear to be generally thicker than the panels at lower depth of cover in areas with similar geological conditions (i.e. massive sandstones and conglomerate units capable of spanning the longwall voids were present in both cases). Further review of the geomechanical properties of the overburden is necessary to increase our understanding of this phenomenon.

Table A6.3a - Effective Strata Unit Thicknesses (t') Back Analysed from HoF Model Database for Australian Coalfields

Site	Panels	Mine	W (m)	H (m)	W/H	A (m)	Back Analysed t' (m)	Bore log t _{log} (m)	t _{max} 95% goaf span probability	Rock Mass Conditions (see TA6.3b)	t _{min} from subsidence data (m)	Effective Strata unit thickness* t' (m)
1	MW508	Bellambi W.	110	421	0.26	92	36.5	100	49	Normal	30	49
2	LW10	Metropolitan	140	460	0.30	130	31.5	100	49	Normal	30	49
3	LW1-4	South Coast	110	325	0.34	85	31.5	100	41	Normal	20	41
4	LW6	Kemira	117	335	0.35	98	27	100	40	Normal	20	40
5	LW20	Metropolitan	163	450	0.36	100	68	100	70	Normal	30	70
6	LWA1	Austar	159	417	0.38	87	160	100	78	Normal	30	78
7	LW514	Bellambi W.	150	400	0.38	90	54	100	64	Normal	30	64
8	LW28	Appin	200	500	0.40	90	80	120	103	Normal	40	103
9	LW2	Ellalong	150	368	0.41	113	37	100	49	Normal	30	49
10	LW3	Tahmoor	180	424	0.42	-	60	100	74	Normal	30	74
11	LW9	Teralba	150	350	0.43	<i>110</i>	27	34	48	Normal	30	30
12	TE	West Cliff	200	446	0.45	<i>101</i>	57	100	85	Normal	30	85
13	TE	Berima	120	176	0.68	76	18	100	29	Normal	20	29
14	LW409	Springvale	265	384	0.69	<i>133</i>	42	55	78	Normal	32	32
15	LW9(11)	Mandalong	160	220	0.73	-	30	30	25	Normal	20	25
16	LW11	Angus Place	211	263	0.80	-	30	100	26	Normal	10	26
17	411	Springvale	315	368	0.86	139	42	55	86	Normal	32	32
18	LW5	Mandalong	160	179	0.89	118	14.5	25	37	Normal	20	20
19	LW5	Dendrobium	245	255	0.96	123	32	80	55	Normal	20	55
20	LW1	Wye	216	206	1.05	126	18.2	30	39	Normal	20	20
21	LW1	Invincible	145	116	1.25	96	8.5	15	19	Adverse	10	10
22	TE 1	Abel	120	95	1.26	45	18	15	29	Normal	15	15
23	LWs	Ashton	216	154	1.40	82	25.5	30	44	Normal	15	15
24	LW40	WWD	179	113	1.58	80	21	20	25	Normal	20	20
25	LWE1	Sth Bulga	259	155	1.67	145	6.2	15	28	Adverse	10	10
26	LW41	WWD	179	105	1.70	72	23	20	24	Normal	20	20
27	LW9	Crinum	280	155	1.81	85	34	35	36	Normal	20	20
28	LW39	WWD	179	97	1.84	68	22.5	20	22	Normal	20	20
29	TE (3D)	Wye North	355	185	1.92	63	54	50	78	Normal	20	20
30	TE(LW4)	Wye North	355	180	1.97	40	>54	50	109	Normal	20	20
31	TE	Abel	150	76	1.97	45	15.5	15	26	Normal	15	15
32	TE(NthB)	Cooranbong	150	75	2.00	58	12.5	20	16	Normal	20	16
33	LW1	Oaky ck	205	95	2.16	55	29	30	25	Normal	15	25
34	LW9/9a	Homestead	200	80	2.50	70	11	15	16	Normal	15	15

W' = minimum (W, 1.4H); t_{min} - minimum beam thickness values at A-Horizon based on subsidence and borehole extensometer data; t' = effective beam thickness above A-Zone derived from back analysis techniques; * - t' is selected by consideration of t_{log}, t_{max} and t_{min} (see text below).

Bold - surface to seam fracturing reported by others; *italics* - Continuous Fracture Zone heights (A-Zone) was originally reported and included the Discontinuous Fracture and Dilated Zone (B-Zone). The A and B- Zone heights were re-assessed by DgS based on a review of available measured vertical strains and piezometric data (see **Figure A40i and A40j**).

In order to be able to make credible height of continuous fracturing predictions at a 'green fields' site based on borehole data alone, it was necessary to identify strata unit thicknesses that did and did not stop the height of fracturing.

To do this, the effective strata unit thicknesses from the database that appeared to have stopped the height of fracturing were normalized to the effective panel width (t'/W') and plotted against the unit's location factor (y/H); see **Figure A42f**. A similar exercise was completed for the strata units that did not stop the height of fracturing development, and are plotted on the above figure as well.

The two strata thickness categories were subsequently used in a logistic regression analysis to define the probabilistic power line equation below to indicate whether a strata unit is likely to span the goaf and limit the development of the height of fracturing at a given horizon above the workings:

$$P(i=1)=50\% \text{ for } t_{\max} = W'[0.035(y/H)^{-1.3}]$$

where

$i = 1$ for a spanning unit, and

$P(i=1)=50\%$ for t_{\max} refers to a 50% probability that a beam of a given thickness will span the fractured zone at a given location in the overburden.

A similar exercise was completed in order to define for the 95% probability of spanning equation:

$$P(i=1)=95\% \text{ for } t_{\max} = W'[0.12(y/H)^{-0.85}]$$

where

$i = 1$ for a spanning unit, and

$P(i=1)=95\%$ for t_{\max} refers to a 95% probability that a beam of a given thickness will span the fractured zone at a given location in the overburden.

The two above equations above are shown in **Figure A42f** with the database of 'goaf spanning' and 'non-goaf spanning' units.

For conservative or worst-case height of fracturing prediction, subsidence data was also reviewed to indicate the minimum effective beam thickness values (t_{\min}) when massive strata units are not obviously present to span and limit the height of the A-Zone.

For this scenario, it is considered that t_{\min} is likely to equal twice the measured peak surface strain to curvature ratios or twice the depth of observed cracking (whichever is the greater). For the Newcastle and Hunter Coalfields, a t_{\min} range from 15 m to 20 m is indicated from subsidence monitoring data, with a t' range from 30 m to 40 m indicated for the Western and Southern Coalfields.

The t_{\min} values for the likely cover depths are provided in **Table A6.3b**.

Table A6.3b - Minimum Effective Strata Thickness Based on Subsidence Data for Normal and Adverse Rock Mass Conditions in Australian Coalfields

Cover Depth H (m)	Minimum Effective t_{min}					
	Normal*					Adverse**
	Southern	Western	Newcastle/ Greta	Tomago/Hunter Valley/Narrabri	Bowen Basin	All Coalfields
>450	40	-	-	30	30	15
350 - 450	40	40	30	20	20	15
250 - 350	20	20	20	20	20	10
150 - 250	20	20	20	15	15	10
<150	20	15	20	15	15	10

* - Normal conditions refer to rock mass behaviour that is unlikely to be adversely affected by geological structure or atypical rock mass conditions (e.g. deep weathering or a lack of low permeability units in the B-Zone).

** - Adverse are likely to be affected by geological structure or atypical rock mass conditions (see definition above).

Validation of the model involved the application of the following algorithm to check that the predicted beam thickness values (t') from the available borehole data (t_{log}) were consistent with the back-analysed results and the maximum (t_{max}) and minimum thicknesses (t_{min}) derived from borehole and subsidence data that is required to span the goaf:

- If $t_{log} > t_{max}$ (for 95% spanning probability) then $t' = t_{max}$ (for 95% spanning probability) (so as not to bias the database above the required t' to span the goaf at a given horizon);
- If $t_{log} < t_{max}$ for 95% spanning probability then $t' = t_{min}$ based on subsidence data (see below).

A summary of the back analysis v. predicted effective strata unit thickness presented in **Table A6.3a** are compared graphically in **Figure A42g**. It is assessed that the proposed algorithm to estimate the likely strata unit thickness for the Pi-Term model is reasonable to give an R^2 value of 0.8 and root mean square area of 15%.

The predicted v. measured outcomes using the “Geology” Pi-term model are presented in **Figures A42h** to **A42j**. Further validation of the Geology Pi-term model outcomes are presented in **Sections A11.5.7** and **A11.5.8**.

A11.5.7 Analytical Models of Goaf Spanning Strata Unit Thickness

The minimum thicknesses of the strata units required to limit the height of continuous fracturing have also been estimated analytically for the following scenarios:

- (i) Strata units that can support the full overburden load.

- (ii) Single goaf spanning units, which are single strata units that have sheared / dilated away from the overlying rock mass but are able to support their own weight and span any partial voids immediately below.

For Scenario (i) the minimum strata unit thickness to fully support the overburden above it was assessed using Voussoir Beam theory presented in **Diedrichs and Kaiser, 1999**. For a factor of safety against crushing of 2:

$$t_{\min, \text{full}} = \sqrt{(1.5\gamma(H-y)(W-2y\tan\theta)^2/UCS)}$$

For Scenario (ii) the minimum strata unit thickness to support its self-weight only was also assessed using Voussoir Beam theory presented in **Diedrichs and Kaiser, 1999**. For a factor of safety against crushing of 2:

$$t_{\min, \text{single}} = 1.5\gamma(W-2y\tan\theta)^2/UCS$$

Note: The above equations were derived from Equation (1) and assume that the compression arch forms within 50% of the beam thickness (conservative).

Back analysis of the database indicated the angle of break increases with W/H and ranges from $\theta = 12^\circ$ for sub-critical panels and 19.3° for supercritical panels. The following equations give the best fit to the geology model presented in **Section A11.5**:

$\theta = 12^\circ$	or $W/H < 0.45$
$\theta = 9.63^\circ + 4.42(W/H) + 1.8(W/H)^2$	for $0.45 < W/H < 1.4$
$\theta = 19.3^\circ$	for $W/H > 1.4$

Published laboratory UCS testing data on sandstone / conglomerate / igneous core samples from each coalfield were adopted as shown in **Table A6.4**.

A summary of the analytical goaf spanning equation results and back analysed strata unit thicknesses and beam stresses are presented in **Table A6.4**. It is considered that the minimum beam stress will govern the loading/spanning scenario for a given mining geometry. The results again demonstrate the complexity of how the fracture zone heights develop and the difficulties involved with using analytical or numerical techniques v. empirical methods.

The analytical beam thicknesses estimated for the goaf spanning scenarios are also plotted in **Figure A42f**. It is apparent the minimum thicknesses determined for the full rock mass loading case scenario and single spanning unit scenario generally plot above and below the logistic regression line for a 50% Probability of Spanning respectively. This would suggest that the Scenario (i) model is more likely to reflect the loading behaviour of the rock mass compared to Scenario (ii) (assuming the rock mass properties adopted are reasonable).

The predicted v. observed A values for the proposed Geology Pi-term model are presented in **Figures A42f** and **Figure A42g** respectively. The residual errors reasonably follow a normal probability distribution about the regression curve according to Central Limit Theory in statistics (see **Figure A42h**).

Table A6.4 - Minimum Strata Unit Thicknesses Required for Spanning the Goaf based on Analytical Models of the Overburden

Site	Panels	Mine	W (m)	H (m)	W _i	UCS (MPa)	t (m)	y (m)	y/H	Back analysed t (m)	Full Load t _{min} (m)	Single Beam t _{min} (m)	Full Beam Load Stress (MPa)	Goaf Supported Beam Stress (MPa)
1	MW508	Bellambi W.	110	421	71	70	100	90	0.21	36.5	30	3	23	72
2	LW10	Metropolitan	140	460	85	70	100	130	0.28	31.5	36	4	45	49
3	LW1-4	South Coast	110	325	74	70	100	85	0.26	31.5	26	3	25	66
4	LW6	Kemira	117	335	75	70	100	98	0.29	27	27	3	35	52
5	LW20	Metropolitan	163	450	120	70	100	100	0.22	68	52	8	21	100
6	LWA1	Austar	159	417	122	70	100	80	0.19	160	51	8	18	208
7	LW514	Bellambi W.	150	400	112	70	100	90	0.23	54	46	7	25	75
8	LW28	Appin	200	500	162	70	120	90	0.18	80	76	14	31	61
9	LW2	Ellalong	150	368	102	70	100	113	0.31	37	38	6	36	59
10	LW3	Tahmoor	180	424	180	70	100	100	0.24	60	75	17	72	85
11	LW9	Teralba	150	350	103	70	34	110	0.31	27	37	6	66	34
12	TE	West Cliff	200	446	157	70	100	101	0.23	57	68	13	49	45
13	TE	Berima	120	176	84	70	100	76	0.43	18	19	4	40	34
14	LW409	Springvale	265	384	201	70	55	133	0.27	78	74	22	108	26
15	LW9(11)	Mandalong	160	220	160	67	30	160	0.73	30	29	14	-	-
16	LW11	Angus Place	211	263	211	70	100	253	0.96	30	15	24	-	-
17	411	Springvale	315	368	242	70	100	139	0.38	42	85	31	142	20
18	LW5	Mandalong	160	179	97	67	25	83	0.46	14.5	18	5	51	23
19	LW5	Dendrobium	245	255	177	70	80	123	0.48	32	47	17	75	28
20	LW1	Wye	216	206	143	70	30	126	0.61	18.2	30	11	92	18
21	LW1	Invincible	145	116	83	70	15	106	0.91	8.5	9	4	36	15
22	TE 1	Abel	120	95	91	30	15	41	0.43	18	23	10	24	20
23	LWs	Ashton	216	154	158	30	30	82	0.53	25.5	47	31	52	10
24	LW40	WWD	179	113	102	30	20	80	0.71	21	21	13	15	22
25	LWE1	Sth Bulga	259	155	115	30	20	145	0.94	6.2	13	17	65	2
26	LW41	WWD	179	105	97	30	20	72	0.69	23	20	12	11	28
27	LW9	Crinum	280	155	157	130	35	105	0.68	34	22	7	28	79
28	LW39	WWD	179	97	88	30	20	68	0.70	22.5	17	10	8	32
29	TE (3D)	Wye North	355	185	215	70	50	63	0.34	54	55	25	36	28
30	TE(LW4)	Wye North	355	180	224	70	50	40	0.22	<u>156</u>	61	27	37	34
31	TE	Abel	150	76	75	30	15	33	0.43	15.5	15	7	14	18
32	TE(NthB)	Cooranbong	150	75	64	67	20	58	0.77	12.5	8	2	8	47
33	LW1	Oaky ck	205	95	94	30	30	55	0.58	29	21	11	8	37
34	LW9/9a	Homestead	200	80	63	30	15	65	0.81	11	8	5	6	18

W' = minimum (W, 1.4H); t_{min} - minimum beam thickness values at A-Horizon based on subsidence and borehole extensometer data; t' = effective beam thickness above A-Zone derived from back analysis techniques;

Bold - surface to seam fracturing reported by others;

Underlined - Conservative estimate of t' returned.

italics - Continuous Fracture Zone heights (A-Zone) was originally reported and included the Discontinuous Fracture and Dilated Zone (B-Zone). The A and B- Zone heights were re-assessed by DgS based on a review of available measured vertical strains and piezometric data (see **Figure A40i** and **A40j**).

A11.5.8 Pi-Term Model for Predicting Heights of Discontinuous Fracturing (B) Above Longwalls using Geometry Pi-Terms Only (Geometry Model)

Based on the empirical database presented in **Table A6.1**, the statistics software XLSTAT[®] was used to complete a multi-nonlinear regression analysis as follows for estimating the height of the dilated B-Zone :

$$\underline{\text{Mean } B/W' = 1.621 (H'/W')^{0.55} (T/W')^{0.175}} \quad R^2 = 0.86 \text{ \& rsme} = 0.12W' \text{ (13\%)}$$

$$U95\% B/W' = \text{Mean } B/W' + b$$

where $b = 0.16$ for subcritical panels, $0.16-0.085(W/H-0.7)$ for critical panels and 0.10 for supercritical panels.

$$H' = \text{Goaf Load Height} = H$$

$$W' = \text{Effective Panel Width} = \text{minimum of } W \text{ and } 1.4H.$$

$$T = \text{Mining Height.}$$

Re-arranging the above equation in terms of B gives:

$$\underline{B = 1.621 W'^{0.275} H'^{0.55} T^{0.175} \text{ +/- } bW'}$$

The predicted v. observed B/W' and B' values are presented in **Figure A42k** and **Figure A42l** respectively. The residual errors follow a normal probability distribution about the regression curve as expected according to Central Limit Theory in statistics (see **Figure A42m**). The regression indicates a relatively weaker relationship exists between the height of B-Zone fracturing and the mining height compared to the A-Zone relationship.

A11.5.9 Pi-Term Model for Predicting Heights of Discontinuous Fracturing (B) Above Longwalls using the Geology Pi-Term

Based on the empirical database presented in **Table A6.1**, the statistics software XLSTAT[®] was used to complete a multi-nonlinear regression analysis as follows for estimating the height of the dilated B-Zone :

$$\underline{\text{Mean } B/W' = 1.873 (H'/W')^{0.635} (T/W')^{0.257} (t'/W')^{-0.097}} \quad R^2 = 0.86 \text{ \& rmse} = 0.13W' \text{ (15\%)}$$

$$\underline{U95\% B/W' = \text{Mean } B/W' + b}$$

where $b = 0.15$ for subcritical panels; $0.15-0.0714(W/H-0.7)$ for critical panels and 0.10 for supercritical panels.

$$H' = \text{Goaf Load Height} = H$$

$$W' = \text{Effective Panel Width} = \text{minimum of } W \text{ and } 1.4H.$$

T = Mining Height.

t' = Effective strata unit thickness; see **Section A11.5.6**.

Re-arranging the above equation in terms of B gives:

$$B = 1.873 W^{0.205} H^{0.635} T^{0.257} t'^{-0.097} \quad +/- \quad bW'$$

The predicted v. observed B/W' and B' values are presented in **Figure A42n** and **Figure A42o** respectively. The residual errors follow a normal probability distribution about the regression curve as expected according to Central Limit Theory in statistics (see **Figure A42p**). The regression indicates a relatively weaker relationship exists between the height of B-Zone fracturing, the mining height and strata unit thickness compared to the A-Zone relationship.

A11.5.10 Pi-Term Model Validation

Validation of the proposed Pi-Term model has been completed as follows:

- (i) A review of the range of independent variables within the database to check if the model is likely to be biased towards a particular parameter or mining geometry.
- (ii) Comparison of predicted v. measured A and B-Horizons for each model to check model reliability.
- (iii) Sensitivity analysis of the model to the assumed input parameters (based on method applied in **Hydrosimulations, 2013**).
- (iv) Comparison of model results with other models over a representative range of mining geometries and overburden geologies.

(i) Database Variable Review

In regards to the data base, the following parameters from **Table A6.1** were plotted against the W/H ratio in **Figures A43a to 43d** to test for sample bias:

- Panel Width (W)
- Cover Depth (H)
- Mining Height (T)
- Height of A-Zone Fracturing (A)
- Height of B-Zone Fracturing/Strata Dilation (B)

It is assessed that the database has sufficient coverage in regards to panel width, cover depth and mining height to reliably estimate HoF Zones above sub-critical to super-critical panels with W/H values ranging from 0.3 to 2.2.

(ii) Model Reliability

In regards to prediction model reliability, the minimum effective strata unit thickness assessed for each site has used to estimate the height of A and B-Zones and the residual areas subjected to a Normality test. The distributions of model residual errors should follow the Central Limit theorem for regression analysis. That is, a normal distribution of errors would be expected to occur about the regression line of 'best-fit'. If the regression lines are deemed to meet this requirement, the assessment of predicted confidence limits will then be possible. It would then be expected that < 5% of measured values would exceed the predicted U95%CL values on average.

The regression results for the A-Zone Geological model are summarised in **Table A6.5** and **Figure A42j**. The results demonstrate the model errors satisfy normality tests with 61% of the measured values below the predicted mean values and 97% of the measured values below the Upper 95%CL predictions. A slightly lower reliability outcome was achieved for the Geometry Model for the B-Zone with 55% of measured values below the mean and 90% below the U95%CL (see **Table A6.6**).

It is therefore considered that the reliability of the Pi-Term geology model is acceptable for worst-case estimates of A-Zone fracture heights at new or existing coal mines in Australia until local performance data either confirms or supersedes it.

The results for the B-Zone geology model checks also indicate the model errors satisfy normality tests as shown in **Figure A42p** and are summarised in **Table A6.7**. The proposed mean and U95%CL model satisfactorily over predicts 52% and 95% of the measured B-Zone data (i.e. within 5% of the expected values). A slightly lower reliability outcome was achieved for the Geometry Model for the B-Zone (see **Table A6.8**).

Overall, it is considered that the reliability of both the Pi-Term Models is acceptable for estimates of B-Zone discontinuous fracture height assessments at new or existing coal mines in the NSW Coalfields and should be confirmed or re-calibrated with local measurement data.

The above results indicate that the model is likely to provide reasonably conservative estimates of the height of continuous fracturing for the full range of mining geometries, based on the effective panel width, effective goaf load height (cover depth), mining height and effective strata unit thickness in the A or B-Zones.

Table A6.5 - Summary of Measured v. Predicted Height of Continuous Fracture A-Zones for the Geology Model

Site	Panel	Mine	Panel Width W (m)	Cover Depth H (m)	W/H	Mining Height T (m)	Predicted t' (m)	Predicted A (m)		Measured A (m)	Pass = 1; Fail = 0	
								mean	U95%CL		m	U95
1	MW508	Bellambi W	110	421	0.26	2.50	49	82	98	92	0	1
2	LW10	Metropolitan	140	460	0.30	3.40	49	109	130	130	0	1
3	LW1-4	South Coast	110	325	0.34	2.50	41	76	93	85	0	1
4	LW6	Kemira	117	335	0.35	2.75	40	84	102	98	0	1
5	LW20	Metropolitan	163	450	0.36	3.40	70	99	124	100	0	1
6	LWA1	Austar	159	417	0.38	6.00	78	118	142	87	1	1
7	LW514	Bellambi W	150	400	0.38	2.70	64	84	106	90	0	1
8	LW28	Appin	200	500	0.40	2.30	103	81	111	90	0	1
9	LW2	Ellalong	150	368	0.41	3.50	49	101	123	113	0	1
10	LW3	Tahmoor	180	424	0.42	2.18	74	80	107	-	-	-
11	LW9	Teralba	150	350	0.43	2.70	30	106	128	110	0	1
12	TE	West Cliff	200	446	0.45	2.50	85	86	116	101	0	1
13	TE-SW1	Berrima	120	176	0.68	2.3	29	63	81	76	0	1
14	LW409	Springvale	265	384	0.69	3.25	32	148	188	133	0	1
15	LW9	Mandalong	160	220	0.73	4.50	25	115	139	-	-	-
16	LW11	Angus Place	211	263	0.80	2.47	16	129	159	-	-	-
17	411	Springvale	315	368	0.86	3.25	32	156	199	139	0	1
18	LW5	Mandalong	160	179	0.89	3.70	20	103	125	118	0	1
19	LW5	Dendrobium	245	255	0.96	3.75	55	100	132	123	0	1
20	LW1	Wyee	216	206	1.05	3.44	20	121	148	126	0	1
21	<i>LW1</i>	<i>Invincible</i>	<i>145</i>	<i>116</i>	<i>1.25</i>	<i>2.70</i>	<i>15</i>	90	106	<i>96</i>	0	1
22	TE1	Abel	120	95	1.26	2.30	15	59	72	45	1	1
23	LWs	Ashton	216	154	1.40	2.55	15	101	123	82	1	1
24	LW40	WWD	179	113	1.58	3.80	20	81	97	80	1	1
25	<i>LWE1</i>	<i>South Bulga</i>	<i>259</i>	<i>155</i>	<i>1.67</i>	<i>2.55</i>	<i>15</i>	120	142	<i>145</i>	0	0
26	LW41	WWD	179	105	1.70	3.80	20	76	91	72	1	1
27	LW9	Crinum	280	155	1.81	3.50	20	105	127	85	1	1
28	LW39	WWD	179	97	1.84	3.90	20	71	85	68	1	1
29	TE-3D	Wyee North	355	185	1.92	1.90	20	60	86	63	0	1
30	TE-355	Wyee North	355	180	1.97	1.90	20	59	84	40	1	1
31	Panel2	Abel	150	76	1.97	1.88	15	45	56	45	1	1
32	TE - North B	Cooranbong	150	75	2.00	2.80	16	53	64	58	0	1
33	LW1	Oaky Ck	205	95	2.16	3.20	25	58	71	55	1	1
34	<i>LW9/9a</i>	<i>Homestead</i>	<i>200</i>	<i>80</i>	<i>2.50</i>	<i>3.30</i>	<i>15</i>	62	73	<i>70</i>	0	1
Percentage of Measured < Predicted Value											39	97

italics - Surface to seam connection reported by authors.

Table A6.6 - Summary of Measured v. Predicted Height of Continuous Fracture A-Zones for the Geometry Model

Site	Panel	Mine	Panel Width W (m)	Cover Depth H (m)	W/H	Mining Height T (m)	Predicted A (m)		Measured A (m)	Pass = 1; Fail = 0	
							mean	U95%CL		m	U95
1	MW508	Bellambi W	110	421	0.26	2.50	86	103	92	0	1
2	LW10	Metropolitan	140	460	0.30	3.40	107	130	130	0	1
3	LW1-4	South Coast	110	325	0.34	2.50	80	98	85	0	1
4	LW6	Kemira	117	335	0.35	2.75	85	104	98	0	1
5	LW20	Metropolitan	163	450	0.36	3.40	113	139	100	1	1
6	LWA1	Austar	159	417	0.38	6.00	135	161	87	1	1
7	LW514	Bellambi W	150	400	0.38	2.70	97	121	90	1	1
8	LW28	Appin	200	500	0.40	2.30	108	140	90	1	1
9	LW2	Ellalong	150	368	0.41	3.50	105	129	113	0	1
10	LW3	Tahmoor	180	424	0.42	2.18	97	126	-	-	-
11	LW9	Teralba	150	350	0.43	2.70	94	118	110	0	1
12	TE	West Cliff	200	446	0.45	2.50	108	140	101	1	1
13	TE	Berrima	120	176	0.68	2.3	68	87	76	0	1
14	LW409	Springvale	265	384	0.69	3.25	126	169	133	0	1
15	LW9	Mandalong	160	220	0.73	4.50	102	128	-	-	-
16	LW11	Angus Place	211	263	0.80	2.47	95	127	-	-	-
17	411	Springvale	315	368	0.86	3.25	133	179	139	0	1
18	LW5	Mandalong	160	179	0.89	3.70	90	113	118	0	0
19	LW5	Dendrobium	245	255	0.96	3.75	116	150	123	0	1
20	LW1	Wyee	216	206	1.05	3.44	101	129	126	0	1
21	<i>LW1</i>	<i>Invincible</i>	<i>145</i>	<i>116</i>	<i>1.25</i>	<i>2.70</i>	69	85	96	0	0
22	TE1	Abel	120	95	1.26	2.30	57	71	45	1	1
23	LWs	Ashton	216	154	1.40	2.55	84	105	82	1	1
24	LW40	WWD	179	113	1.58	3.80	80	105	80	0	1
25	<i>LWE1</i>	<i>South Bulga</i>	<i>259</i>	<i>155</i>	<i>1.67</i>	<i>2.55</i>	84	119	145	0	0
26	LW41	WWD	179	105	1.70	3.80	76	100	72	1	1
27	LW9	Crinum	280	155	1.81	3.50	95	129	85	1	1
28	LW39	WWD	179	97	1.84	3.90	73	95	68	1	1
29	TE-3D	Wyee North	355	185	1.92	1.90	84	126	63	1	1
30	TE-355	Wyee North	355	180	1.97	1.90	83	123	40	1	1
31	Panel2	Abel	150	76	1.97	1.88	48	65	45	1	1
32	TE-NthB	Cooranbong	150	75	2.00	2.80	55	72	58	0	1
33	LW1	Oaky Ck	205	95	2.16	3.20	67	88	55	1	1
34	<i>LW9/9a</i>	<i>Homestead</i>	<i>200</i>	<i>80</i>	<i>2.50</i>	<i>3.30</i>	61	79	70	0	1
Percentage of Measured < Predicted Value										45	90

italics - Surface to seam connection reported by authors.

Table A6.7 - Summary of Measured v. Predicted Height of Dilated B-Zones for the Geology Model

Site	Panel	Mine	Panel Width W (m)	Cover Depth H (m)	W/H	Mining Height T (m)	t' (m)	Predicted B (m)		Measured B (m)	Pass = 1; Fail = 0	
								mean	U95%CL		m	U95
1	MW508	Bellambi West	110	421	0.26	2.50	49	198	214	-	-	-
2	LW10	Metropolitan	140	460	0.30	3.40	49	238	259	-	-	-
3	LW1 to 4	South Coast	110	325	0.34	2.50	41	170	187	-	-	-
4	LW6	Kemira	117	335	0.35	2.75	40	181	198	-	-	-
5	LW20	Metropolitan	163	450	0.36	3.40	70	234	258	-	-	-
6	LWA1	Austar	159	417	0.38	6.00	78	254	278	277	0	1
7	LW514	Bellambi West	150	400	0.38	2.70	64	203	225	-	-	-
8	LW28	Appin	200	500	0.40	2.30	103	227	257	-	-	-
9	LW2	Ellalong	150	368	0.41	3.50	49	211	233	210	1	1
10	LW3	Tahmoor	180	424	0.42	2.18	74	204	231	204	0	1
11	LW9	Teralba	150	350	0.43	2.70	30	200	223	150	1	1
12	TE	West Cliff	200	446	0.45	2.50	85	220	250	245	0	1
13	TE SW1	Berrima	120	176	0.68	2.3	29	119	137	112	1	1
14	LW409	Springvale	265	384	0.69	3.25	32	249	289	254	0	1
15	LW9	Mandalong	160	220	0.73	4.50	25			-	-	-
16	LW11	Angus Place	211	263	0.80	2.47	16	177	208	253	0	0
17	411	Springvale	315	368	0.86	3.25	32	251	295	288	0	1
18	LW5	Mandalong	160	179	0.89	3.70	20	150	171	154	0	1
19	LW5	Dendrobium	245	255	0.96	3.75	55	186	218	-	-	-
20	LW1	Wye	216	206	1.05	3.44	20	171	198	-	-	-
21	LW1	Invincible	145	116	1.25	2.70	10	110	116	111	0	1
22	TE1	Abel	120	95	1.26	2.30	15	86	95	75	1	1
23	LWs	Ashton	216	154	1.40	2.55	15	135	154	130	1	1
24	LW40	WWD	179	113	1.58	3.80	20	112	113	108	1	1
25	LWE1	South Bulga	259	155	1.67	2.55	10	141	155	150	0	1
26	LW41	WWD	179	105	1.70	3.80	20	100	105	100	1	1
27	LW9	Crinum	280	155	1.81	3.50	20	143	155	150	0	1
28	LW39	WWD	179	97	1.84	3.90	20	92	97	92	0	1
29	TE-3D	Wye North	355	185	1.92	1.90	60	128	154	143	0	1
30	TE-355	Wye North (LW4)	355	180	1.97	1.90	60	125	150	-	-	-
31	Panel2	Abel	150	76	1.97	1.88	15	69	76	71	0	1
32	TE-North B	Cooranbong	150	75	2.00	2.80	16	70	75	70	1	1
33	LW1	Oaky Ck	205	95	2.16	3.20	25	91	95	90	1	1
34	LW9/9a	Homestead	200	80	2.50	3.30	15	75	80	75	1	1
Percentage of Measured < Predicted Value											43	96

Table A6.8 - Summary of Measured v. Predicted Height of Dilated B-Zones for the Geometry Model

Site	Panel	Mine	Panel Width W (m)	Cover Depth H (m)	W/H	Mining Height T (m)	Predicted B (m)		Measured B (m)	Pass = 1; Fail = 0	
							mean	U95%CL		m	U95
1	MW508	Bellambi West	110	421	0.26	2.50	192	210	-	-	-
2	LW10	Metropolitan	140	460	0.30	3.40	228	250	-	-	-
3	LW1 to 4	South Coast	110	325	0.34	2.50	167	184	-	-	-
4	LW6	Kemira	117	335	0.35	2.75	175	194	-	-	-
5	LW20	Metropolitan	163	450	0.36	3.40	235	261	-	-	-
6	LWA1	Austar	159	417	0.38	6.00	247	272	277	0	0
7	LW514	Bellambi West	150	400	0.38	2.70	206	230	-	-	-
8	LW28	Appin	200	500	0.40	2.30	246	278	-	-	-
9	LW2	Ellalong	150	368	0.41	3.50	206	230	210	0	1
10	LW3	Tahmoor	180	424	0.42	2.18	216	245	204	1	1
11	LW9	Teralba	150	350	0.43	2.70	192	216	150	1	1
12	TE	West Cliff	200	446	0.45	2.50	234	266	245	0	1
13	TE SW1	Berrima	120	176	0.68	2.3	120	139	112	1	1
14	LW409	Springvale	265	384	0.69	3.25	244	286	254	0	1
15	LW9	Mandalong	160	220	0.73	4.50	165	191	-	-	-
16	LW11	Angus Place	211	263	0.80	2.47	177	209	253	0	0
17	411	Springvale	315	368	0.86	3.25	250	296	288	0	1
18	LW5	Mandalong	160	179	0.89	3.70	143	166	154	0	1
19	LW5	Dendrobium	245	255	0.96	3.75	195	229	-	-	-
20	LW1	Wye	216	206	1.05	3.44	165	193	-	-	-
21	LW1	Invincible	145	116	1.25	2.70	104	116	111	0	1
22	TE1	Abel	120	95	1.26	2.30	86	95	75	1	1
23	LWs	Ashton	216	154	1.40	2.55	134	154	130	1	1
24	LW40	WWD	179	113	1.58	3.80	111	113	108	1	1
25	LWE1	South Bulga	259	155	1.67	2.55	134	155	150	0	1
26	LW41	WWD	179	105	1.70	3.80	104	105	100	1	1
27	LW9	Crinum	280	155	1.81	3.50	142	155	150	0	1
28	LW39	WWD	179	97	1.84	3.90	92	97	92	0	1
29	TE-3D	Wye North	355	185	1.92	1.90	148	174	143	1	1
30	TE-355	Wye North (LW4)	355	180	1.97	1.90	144	170	-	-	-
31	Panel2	Abel	150	76	1.97	1.88	71	76	71	0	1
32	TE-North B	Cooranbong	150	75	2.00	2.80	70	75	70	1	1
33	LW1	Oaky Ck	205	95	2.16	3.20	93	95	90	1	1
34	LW9/9a	Homestead	200	80	2.50	3.30	75	80	75	1	1
Percentage of Measured < Predicted Value										48	91

(iv) Parameter Sensitivities

A review of the sensitivity of the Pi-Term Models has been completed in **Merrick, 2014** and demonstrates that the model is not overly sensitive to changes to the input parameters, W, H and T. The influence of the effective strata thickness t' has a greater impact on the height of fracturing for values < 20 m than the cases with $t' > 20$ m. This is not surprising as the spanning capabilities of the strata units will probably decrease rapidly below this thickness range as it corresponds with the point where the bending beam stress starts to exceed the UCS of the rock mass.

The model variable sensitivity charts are presented in **Figures A43e to A43h**.

(v) Comparison with other models

Three critical cases were identified in the analysis where the A-Zone extended to within 10 m of the surface (Invincible, South Bulga, and Homestead Mines) with a minimum t' value of 10 m assumed. Adopting a minimum beam thickness of 10 m will generally indicate the maximum likely height of continuous fracturing for all cases in the database (see **Figure A42g**).

For completeness, four case studies have been selected from the sub-critical, critical and supercritical panel geometries and plotted with varying panel widths in **Figures A43i to A43l** to demonstrate the sensitivity of the models to changes in mining geometry. Several sub-surface fracture height models (**Foster, 1995; SCT, 2008; ACARP, 2007** and **Tammetta, 2013**) that have been referred to by OEH and PACs during recent project approval applications are also plotted with the Pi-term model results. It is apparent that the models are based on a smaller number of key variables and some were developed from data in a particular coalfield only. The application of the models in other coalfields with significantly different geological conditions and mining geometries are considered to have resulted in a larger range of 'error' compared to the Pi-term models.

Finally, the width-based models also do not consider the effect of cover depth or mining height and assume the A-Zone will continue to increase above *supercritical* panel geometries. This usually means that surface to seam connectivity will always be predicted for critical and supercritical panel widths. It is noted that only 2 or 3 cases out of 14 (15% - 20%) or 1 in 5 supercritical longwalls have resulted in surface to seam connectivity; see **Figure 43m**.

This outcome suggests that other factors such as cover depth, mining height and geological conditions should also be considered than just the panel width alone when estimating heights of fracturing above longwall panels.

A11.5.11 Definition of Surface Cracking Zone

During the development of the Pi-term model it has also been necessary to better define the surface cracking zone depth. The depth of the surface cracking zone has been estimated from subsidence data, surface crack observations and published measurements as follows:

- The literature review findings presented in **Section A11.3** indicate that surface cracking depths above longwalls are likely to be < 15 m generally.
- The Mean and median strain/curvature ratios of 5.3 m and 7.4 m mentioned earlier in Section derived from subsidence data measurements for Newcastle Coalfield (see **Figures A43n** and **A43o**) indicates the *average surface cracking depth*. The ratio is considered to be a direct measurement of the depth to the neutral axis of bending where tensile strains cross over to compressive strain. This also suggests near surface strata beam thicknesses are twice the depth to the neutral axis of bending or 11 m to 15 m. It is apparent that these values are consistent with near surface beam thicknesses assumed in the Pi-Term Geology Model.
- Borehole measurement devices measured depths of cracking at the base of sandstone valleys in the Southern Coalfield of up to 12 m after mine subsidence effects (refer **Mills, 2007**).
- Measured crack depths of up to 20 m have been measured along the crests of steep slopes above LW41 (ref to **RCA, 2013**).

Based on the above information, it is assessed that the following conservative crack depths presented in **Table A6.9** may be assumed when assessing surface to seam connectivity potential above longwalls beneath varying topography:

Table A6.9 - Suggested Maximum Cracking Depths for Impact Assessment

Location and Topography	Surface Cracking Depth (m)
	Newcastle/Hunter Valley - Southern/Western Coalfield
Flat Terrain with Moderate Slopes up to 18°	7.5 - 12
Bases of Valleys	12 - 15
Low side of panel beneath steep slopes > 18° (not valley floor)	3.5 - 5
Crests or high side of panel beneath steep slopes > 18°	15 - 20

A11.5.12 Summary

The geometry and geology Pi-term models presented in **Section A11.5** for estimating the A-Zone and B-Zone fracture horizons are generally consistent with the prevailing view that the panel width, cover depth and mining height will have the greatest influence on fracture development heights above longwall panels. The Pi-term models for A and B-Zone Fracture

Heights are also generally consistent with **Whittaker and Reddish, 1990, Singh & Kendorski, 1991** and the analytical models presented earlier.

The spanning or non-spanning capability of strata units in the overburden cannot be ignored however, when assessing the potential fracturing heights above a longwall panel. Where local extensometer and piezometric data are available, the influence of spanning strata may be used to calibrate the Geology Pi-term model to a given site.

Predictions based on the up-dated Strain, Overburden Curvature Index and Fracture Height Angle Models are still also considered relevant and will provide similar, if not more conservative outcomes. These models may be used to provide a range of predictions at a greenfields site for risk assessment purposes. It should be understood however, that only the Geology Pi-term model will allow the influence of strata unit thickness or local site geology to be included directly in the predictions of sub-surface fracture height.

It should be understood that the vagaries of the rock mass do not usually allow the strata unit thickness term to be assessed directly from borehole data without back analysis of overburden performance measurements. The database presented in this appendix has been used to derive a minimum beam thickness of 10 m to estimate worst-case heights of fracturing for adverse rock mass conditions. A thickness of 15 m to 20 m corresponds to the minimum beam thicknesses assessed from surface strain and curvature measurements (and a cracking depth of 7.5 m to 10 m).

Subsequent measurements of continuous heights of fracturing may require a thinner strata unit thickness to be used to calibrate the model. At this stage, there are three cases in the database that have been reported to have fractured through to the surface, which required a beam thickness of 6 to 11 m to match the Pi-term model exactly and intersect the surface cracking zone (or D-Zone). One of the cases (South Bulga LWE1) however, may have included the B-Zone in the interpretation of the 'height of fracturing' at the time it was assessed.

It is assessed that the assumptions that the height of fracturing will be limited when either:

- critical panel widths exceed $1.4H$;
- spanning strata exists that can bridge the fractured zone or the presence of plastic, low strength strata that tends to shear along bedding partings when deformed through bending action, rather than crack vertically, may also limit continuous cracking heights.

All of these outcomes are intuitively correct and correlate well with observed behaviour across sub-critical to supercritical mining geometries. It is also noted that the strata unit thickness term enables all of the database and subsequent regression equations to be used with a reasonable level of confidence, such that the predicted worst-case values will not be unduly biased by the database itself. The geology Pi-term t'/W was back analysed for each of the 34 case studies to give an exact fit between the predicted and measured fracture heights. The set of measured t' values were correlated with the predicted t' with a high R^2 of 0.9. The

predicted v. measured heights of continuous fracturing were also correlated and returned an R^2 value of 0.8, which is also a good fit.

For estimates of HoF above partial pillar extraction panels, the HoF zones may be based on the effective mining height, T_e (if remnant pillars are likely to fail) or the maximum span between stable remnant pillars.

The use of the Pi-term models for multi-seam mining environments will also require consideration of the interburden thicknesses and cumulative effects of the A-Zones if they likely to intersect overlying longwall goafs. The multi-seam affect may be estimated for an overlying seam by converting the multi-seam subsidence increase to an effective mining height.

A12 Far-Field Displacements and Strain Predictions

A12.1 Background

The term far-field displacements (FFD) generally refer to the horizontal surface movements that occur outside the vertical subsidence limit or angle of draw to an extracted pillar panel or longwall block. It is currently understood that FFDs are a phenomenon caused by the reduction of horizontal stress when collapse of overburden rock (i.e. goafing) occurs above an extracted area. There also appears to be a strong correlation between the FFDs and the surface subsidence magnitude (which is also an indicator of horizontal stress relief). A conceptual model of the mechanics of FFDs is presented in **Figure A44a**.

Horizontal stress in rock is normally greater than the vertical stress at a given depth of cover; it has been 'locked' into the strata by tectonic movements and over-consolidation pressures (i.e. stress). Over-consolidation stresses occur in sedimentary rock after uplift and erosion over millennia has gradually removed the overlying material since the time of formation. Tectonic induced stress usually results in strong directional bias between the major and minor principal stress magnitudes, with variation due to stiffness of the lithological units as well (refer to **Nemcik et al, 2005, Pells, 2004, McQueen, 2004, Enever, 1999 and Walker, 2004**).

It is considered that both of the abovementioned horizontal stress development mechanisms are likely to be present in the near surface rocks in the western area of the Newcastle Coalfield.

FFD's have only recently become an issue in the Newcastle Coalfield because of adverse surface impact experiences in the Southern Coalfield (e.g. horizontal movements of around 25 mm have been measured over 1.5 km away from extracted longwall panels on a concrete dam wall. No cracking damage occurred to the dam wall because of these movements however).

The strains associated with FFDs are usually very low, however, there is one case in the Southern Coalfield where a bridge was subject to lateral shearing of approximately 50 mm along the river bed axis.

To-date, it is understood that there are no precedents in the Newcastle Coalfield where similar FFD effects (measured or inferred via damage) have occurred around longwalls or total extraction panels. Horizontal movements have been measured outside the angle of draw limits from mine workings however, albeit at smaller distances and magnitudes (eg. 20 mm of horizontal movement has been measured in undulating terrain at 250 m from one longwall block where the cover depth was 135 m).

The horizontal stress in the Newcastle Coal Measures has been measured at several locations along the F3 Freeway to the west of Wyong and Newcastle (**Lohe and Dean-Jones, 1995**). The magnitude of the measured horizontal stress indicates that it is relatively high, with magnitudes that are 1.5 to >5 times the vertical stress, in relatively flat or moderately undulated terrain.

The major principal horizontal stress is usually orientated N to NE in the Western Newcastle Coalfield, but it can be re-orientated parallel to the axis of a ridge due to natural weathering processes near the surface (which cause lateral unloading towards the gullies); refer to **Lohe and Dean Jones, 1995**.

A12.2 In-situ Stress Field

Reference to stress measurement data in **Lohe and Dean-Jones, 1995** indicates that the 'shallow' (ie < 100 m below the surface) regional stress field in the undulating terrain along the eastern and eastern sides of Lake Macquarie is likely to have its major principal horizontal stress > 5 x vertical stress (and assuming horizontal stress is zero at the surface). Deeper strata at depths > 150 m is likely to have its major principal horizontal stress <2 x vertical stress.

The stress data from the above reference was measured using over-coring / HI-Cell techniques and is presented in Table A4.

Table A6 - Horizontal Stress Field Measurements in Newcastle Coalfield Relevant to Tasman

Location	Depth (m)	In-situ Stress Measurements*			
		Major Sigma 1 (MPa)	Minor Sigma 2 (MPa)	Vertical Sigma 3 (MPa)	Sigma1+ / Sigma 3
Wakefield	24	10.4	0.42	0.6	17.3
Wallsend Borehole	100	13.3	9.7	2.5	5.3
West Wallsend No. 2	190	27.4	20.3	4.75	5.8
Kangy Angy	70	11.8	4.2	1.75	6.7
Moonee	90	11.7	8.3	2.25	5.2
West Wallsend	170	6.4	n/a	4.25	1.5
Ellalong	320	6.5	4.6	8.0	0.8

* - All measurements in medium strength sandstone.

+ - ratio assumes horizontal stress is zero at the surface (which is not always correct).

The shallow stress data is plotted in **Figure A44b** and indicates that the major principal horizontal stress could be as high as 6 MPa at the surface (unless weathered rock and soil is present) with the Major and Minor Principal Horizontal stresses equal to approximately 4 times the vertical stress for depths up to 250 m.

This high Sigma 1 reading, however, may be associated with a sandstone / conglomerate ridgeline and not typical for the areas away from ridgelines (although a residual 'surface' horizontal stress range from 1.5 to 6.5 MPa has also been assessed for the Sydney Metropolitan area in **McQueen, 1999** and **Pells, 2002**).

Another commonly used assumption in the NSW Coalfields is that the major principal horizontal stress is approximately 2 x the vertical stress and the minor principal horizontal stress is 1.4 ~ 1.5 x the vertical stress (or the Major Principal Horizontal Stress is 1.33~1.4 x the Minor Principal Horizontal Stress). It is also acknowledged that the horizontal stress in the

Newcastle and Sydney areas can be 4 to 5 times the vertical stress, based on shallow rock mass data at depths < 50 m; refer to **Lohe and Dean Jones, 1995**. The sources of this stress field imbalance has been explained in **Enever, 1999, Pells, 2002** and **Fell *et al*, 1992** as being due to:

- (i) the ‘over consolidation’ ratio; where the vertical pressure due to ancient surface at the time of consolidation has since been eroded away, leaving a ‘locked’ in horizontal stress component in today’s sedimentary rock mass. The OCR can be shown to decrease exponentially with depth and is equal in all directions at a given point.
- (ii) Tectonic strain; where crustal plate movements apply a strain to the rock mass and the resultant stress is dependent on the stiffness of the individual beds and direction of movement.
- (iii) Geological structure (faults/dykes); where discontinuities can change the magnitude and orientations of the regional stress field significantly.
- (iv) Topographic relief (ridges/valleys/gorges); where the magnitude and direction of the regional stress field can vary due to geometric affects.

The influence of underground mining can also result in changes (both increases and decreases) in horizontal and vertical stress field magnitudes as the rock mass adjusts to a new equilibrium state.

Based on the measured stress conditions, the horizontal stress magnitudes may be estimated based on the equations presented in **Nemcik et al, 2005**:

$$\sigma_H = K\sigma_v + E\varepsilon = \sigma_v [(v/1-v)OCR] + E\varepsilon$$

$$\sigma_h = f(\sigma_H) \text{ and } \sigma_v = 0.025H \text{ (MPa)}$$

where,

σ_H = Major Horizontal Principal Stress;

σ_h = Minor Horizontal Principal Stress;

σ_v = Vertical Stress;

v = Poisson’s Ratio (normally ranges between 0.15 and 0.4 in coal measure rocks);

$(v/1-v)$ = Horizontal to vertical stress ratio factor (K_o) due to Poisson’s Ratio effect on its own;

OCR = The over-consolidation ratio, which relates vertical pre-consolidation pressure (σ_{vo}) with current vertical pressure (σ_v) as follows, $OCR = \sigma_{vo}/\sigma_v = H_o/H$.

(Note: This is an additional term that has been introduced by DgS, and has been mentioned (but not derived) in Pells, 2002 and calculated in Fell et al, 1992).

E = Young's Modulus for rock-mass unit;

ε = Tectonic Stress Factor (TSF) or Tectonic Strain.

Due to the wide range of horizontal stress values noted in the literature, it is recommended that the horizontal stress magnitudes be measured in-situ at several lithological horizons before high extraction mining commences.

Based on the apparent complexity and large variation between the interpretations of published stress field data, it was considered necessary to conduct a sensitivity analysis on the stress field profiles during the calibration of Map-3D[®] using the flat terrain data (see **Section A12.3** for details).

Total horizontal displacement measurements outside the ends and corners of several longwall panels in the Newcastle Coalfield (Newstan and West Wallsend Collieries), have been plotted against distance from the panel goaf edge / cover depth at the panel; refer to **Figure A45**.

Curves of best fit have been fitted to identify data trends from various locations from the ends and corners of the panels (note: the movements outside the corners of a longwall are typically smaller than the panel ends). The data has been obtained using GPS / EDM traverse techniques with quoted accuracy limits of +/- 7 to 10 mm.

The data in **Figure A45** has also been normalised to maximum measured subsidence (S_{\max}) above a given panel and is presented in **Figure A46**. It is considered that presenting the data in this format allows all of the available data to be used appropriately to make subsequent FFD predictions.

The data presented in **Figures A47** was measured from the sides of several longwall panels using in-line, steel tape measurements. This method is considered more accurate than the EDM techniques, however, they do not capture all of the displacement. The measured values have subsequently been adjusted to absolute movements, based on the EDM measurements presented in **Figures A45** and **A46**.

A combined graph of normalised total displacement data from the ends and sides of the longwall panels is presented in **Figure A48** with worst-case design curves from ends, corners and sides of a longwall panel for flat terrain conditions.

The empirical models may be used for calibrating the numerical models input parameters when proposed mining layouts and topographical conditions are considered to be well outside the available database (see **DgS, 2007**).

A12.3 Numerical Far-Field Displacement Modelling

The numerical modelling program Map-3D[®] has been applied at several mines in the Newcastle Coalfield to-date for the purposes of estimating FFD movements. The model was chosen mainly due to its suitability for modelling large-scale rock masses.

The program is a 3-dimensional elastic, isotropic, boundary-element model, which essentially starts with an infinite solid space and calculates the effects of excavations, geological structure, varying material types, and free-surfaces on the regional stresses and strains. Further details about the software can be found at the Map-3D[®] web site.

The model is firstly calibrated to measured displacement data for a given mining geometry, regional horizontal stress field and surface topography. The Young's Modulus or stiffness of the overburden is then adjusted above an extracted panel (or panels) and assumed caving zone until a reasonable match is achieved.

Although the empirical models indicate that subsidence is a key parameter for predicting FFDs, numerical modelling of horizontal stress relief effects does not require the subsidence above the panels to be matched (by the model) because the extraction of coal and subsequent goafing behaviour can be calibrated to measured far-field displacements instead. Therefore, the modelling outcomes are not linked to the modelled subsidence directly.

Non-linearity can be introduced into the model to analyse the effects of fault planes and bedding using displacement-discontinuity elements with normal and shear stiffness and Mohr-Coulomb friction and cohesive strength properties.

Multiple mining stages and irregular topography can also be defined to enable mechanistic extrapolation of existing empirical databases with a reasonable degree of confidence.

An example of a predicted far-field displacement pattern around a high extraction pillar panel mine is presented in **Figure A49**.

A12.5 Empirical Strain Prediction Model

Strain measurements from the side of several longwall panels from West Wallsend and Newstan Collieries and were also normalised to maximum panel subsidence. The data are presented in **Figure A50**.

Several curves are shown with the data in the above figure, one is the best-fit or mean curve and two are upper limit confidence limit curves for the data (U95%CL and U99%CL). The confidence limit curves have been defined using weighted non-linear statistical techniques and the residual errors about the mean curve.

A13 References

- ACARP, 1998a. **Chain Pillar Design (Calibration of ALPS)**. ACARP Project No. C6036, Colwell, M. Colwell Geotechnical Services.
- ACARP, 1998b, **Project No. C5024, Establishing the Strength of Rectangular and Irregular Pillars**. J.M.Galvin, B.K. Hebblewhite, M.D.G. Salamon and B.B.Lin. School of Mining, UNSW.
- ACARP, 2003. **Review of Industry Subsidence Data in Relation to the Impact of Significant Variations in Overburden Lithology and Initial Assessment of Sub-Surface Fracturing on Groundwater**. ACARP Project No. C10023. S. Ditton and R. Frith, Strata Engineering Report No. 00-181-ACR/1.
- ACARP, 2006. **Techniques to Predict and Measure Subsidence & its Impacts on the Groundwater Regime above Shallow Longwalls**. ACARP Project No. C23920 Report by Seedsman Geotechnics Pty Ltd and Geoterra Pty Ltd (March).
- ACARP, 2007. **Hydrological Response to Longwall Mining**. CSIRO Exploration & Mining. H. Guo, D. Adhikary, D. Gaveva. Report No. C14033 (October).
- Bulli Seam PAC, 2010. **Bulli Seam Operations Review Report**. NSW Government Planning Assessment Commission (10 July).
- Colwell,1993. **Water Inflow Investigation for a Longwall Operation**. M. Colwell. Published in Queensland Coal Geology Groups Conference Proceedings, New Developments in Coal Geology, Brisbane.
- Diedrichs and Kaiser, 1999. **Stability of Large Excavations in Laminated Hard Rock Masses: the Voussoir Analogue Revisited**. M.S. Diedrichs and P.K. Kaiser. International Journal of Rock Mechanics and Mining Sciences 36.
- DgS, 2007. **Prediction of Far-Field Displacements Due to Pillar Extraction or Longwall Mining in Mountainous Terrain**. S. Ditton. Proceedings of the 7th Triennial MSTs Conference on Mine Subsidence, University of Wollongong (November 26-27)
- DMR, 1987. **Mining Subsidence in NSW: 2. Surface Subsidence Prediction in the Newcastle Coalfield**. L. Holla. Department of Minerals Resources (June).
- Enever, 1999. **Near Surface In-situ Stress and its Counterpart at Depth in the Sydney Metropolitan Area**. Enever, J.R. Published in Australian Geomechanics Society (AGS) Conference Proceedings of the 8th Annual Conference on Geomechanics, Hobart.
- Fell *et al*, 1992. **Geotechnical Engineering of Embankment Dams**. Fell, R., MacGregor, P. and Stapledon, D.A.A. Balkema.

Forster and Enever, 1992. **Hydrogeological Response of Overburden Strata to Underground Mining, Central Coast, NSW.** I.R. Forster (Pacific Power) and J. Enever (CSIRO).

Forster, 1995. **Impact of Underground Coal Mining on the Hydrogeological Regime, Central Coast, NSW.** I.R. Forster. Published in Australian Geomechanics Society (AGS) Conference Proceedings (February), Engineering Geology of Newcastle – Gosford Region, University of Newcastle.

Frith, 2006. **Geotechnical Assessment of Overburden Fracturing Related to the Bulli Seam Extraction along the Line of the Proposed Endeavour Drift.** Frith Consulting Pty Ltd. Internal Report to BHP Billiton (October).

Holla, 1991. **Some Aspects of Strata Movement relating to Mining Under Water Bodies in NSW, Australia.** L. Holla. Published proceedings of 4th Int. Water Congress, Ljubljana, Slovenia, Yugoslavia (September).

Holla and Barclay, 2000. **Mine Subsidence in the Southern Coalfield.** L.Holla and E.Barclay. Department of Minerals Resources (June).

Karmis, et al, 1987. **Surface Deformation Characteristics Above Undermined Areas: Experiences from the Eastern United States Coalfields.** M. Karmis, A. Jarosz, P. Schilizzi & Z. Agioutantis. Published in Civil Engineering Transactions Journal, Institution of Engineers, Australia.

Kendorski, F.S., 1993. **Effect of High Extraction Coal Mining on Surface and Ground Water.** Proceedings of the 12th Conference on Ground Control in Mining, Morgantown, WV.

Li and Cairns, 2000. **Strata control experiences in longwall mining over old mine workings.** Li, G. and Cairns, R. AJM 3rd Annual Longwall Mining Summit, Yeppoon.

Lohe and Dean-Jones, 1995. **Structural Geology of the Newcastle-Gosford Region.** E.M. Lohe and G.L. Dean-Jones. Published in Australian Geomechanics Society (AGS) Conference Proceedings (February), Engineering Geology of Newcastle - Gosford Region, University of Newcastle.

McQueen, 2004. **In-situ Rock Stress and Its Effect in Tunnels and Deep Excavations in Sydney.** McQueen. L.B. Article presented in Australian Geomechanics Journal Vol 39. No. 3 (September).

MSEC, 2011. **Review of Under Surface and Groundwater Resources at Shallow Depths of Cover for the Proposed LWs 41 to 50, West Wallsend Colliery.** MSEC Report No. 519 (Rev A) - August.

Nemcik et al, 2005. **Statistical Analysis of Underground Stress Measurements in Australian Coal Mines.** Nemcik, J., Gale, W. and Mills, K. Published in proceedings of the Bowen Basin Geology Symposium.

Pells, 2002. **Developments in the Design of Tunnels and Caverns in the Triassic Rocks of the Sydney Region**. International Journal of Rock Mechanics and Mining Sciences No. 39. Pells, P.J.N.

Pells, 2004. **Substance and Mass Properties for the Design of Engineering Structures in the Hawkesbury Sandstone**. Article presented in Australian Geomechanics Journal Vol 39. No. 3 (September).

Peng and Chiang, 1984. **Longwall Mining**. S.S. Peng & H.S. Chiang. Wiley.

RCA, 2013. **End of Panel Longwall 41, Surface Subsidence Mapping Report, West Wallsend Colliery**. Robert Carr and Associates Pty Ltd. *Report Pending*.

Reynolds, 1977. **Coal Mining Under Stored Water**. Report on an Inquiry into Coal Mining Under or in the Vicinity of Stored Waters of the Nepean, Avon, Cordeaux, Cataract and Woronora Reservoirs, NSW for the NSW Government.

SCT, 2001. **Geotechnical Assessment for the Dendrobium Project**. SCT Operations Pty Ltd Report No. DEN1950 (5th June).

SCT, 2008. **Assessment of Longwall Panel Widths and Potential Hydraulic Connection to Bowmans Creek – Ashton Mine**. SCT Operations Pty Ltd Report to Ashton Coal, September.

Seedsman, 2010. **Calibrated Parameters for the Prediction of Subsidence at Mandalong Mine**. R.W. Seedsman. Coal Operators' Conference, University of Wollongong (February).

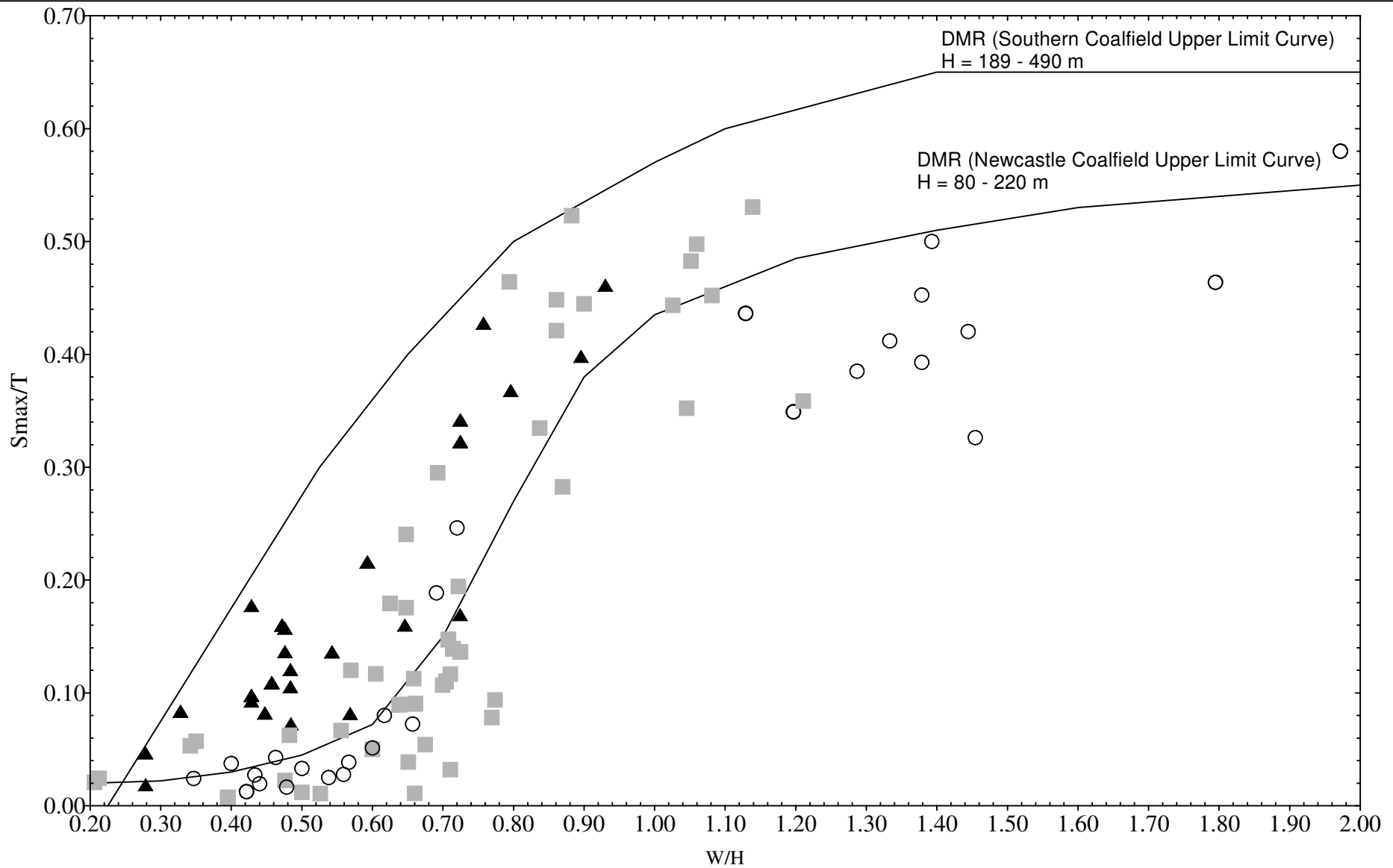
Singh and Kendorski, 1981. **Strata Disturbance Prediction for Mining Beneath Surface Water and Waste Empoundments**. M.M. Singh and F.S Kendorski. First Conference in Ground Control in Mining, West Virginia University, 76-89.

Tammetta, 2013. **Estimation of the Height of Complete Groundwater Drainage Above Mined Longwall Panels**. Paul Tammetta. Paper published in Groundwater Journal (Vol 51, No. 5, Sep-Oct 2013).

Walker, 2004. **Stress Relief on Hillsides and Hillside Excavations**. Walker, B.F. Article presented in Australian Geomechanics Journal Vol 39. No. 3 (September).

Wardell, 1975. **Mining Under Tidal Waters**. Wardell and Partners Report prepared for NSW Government.

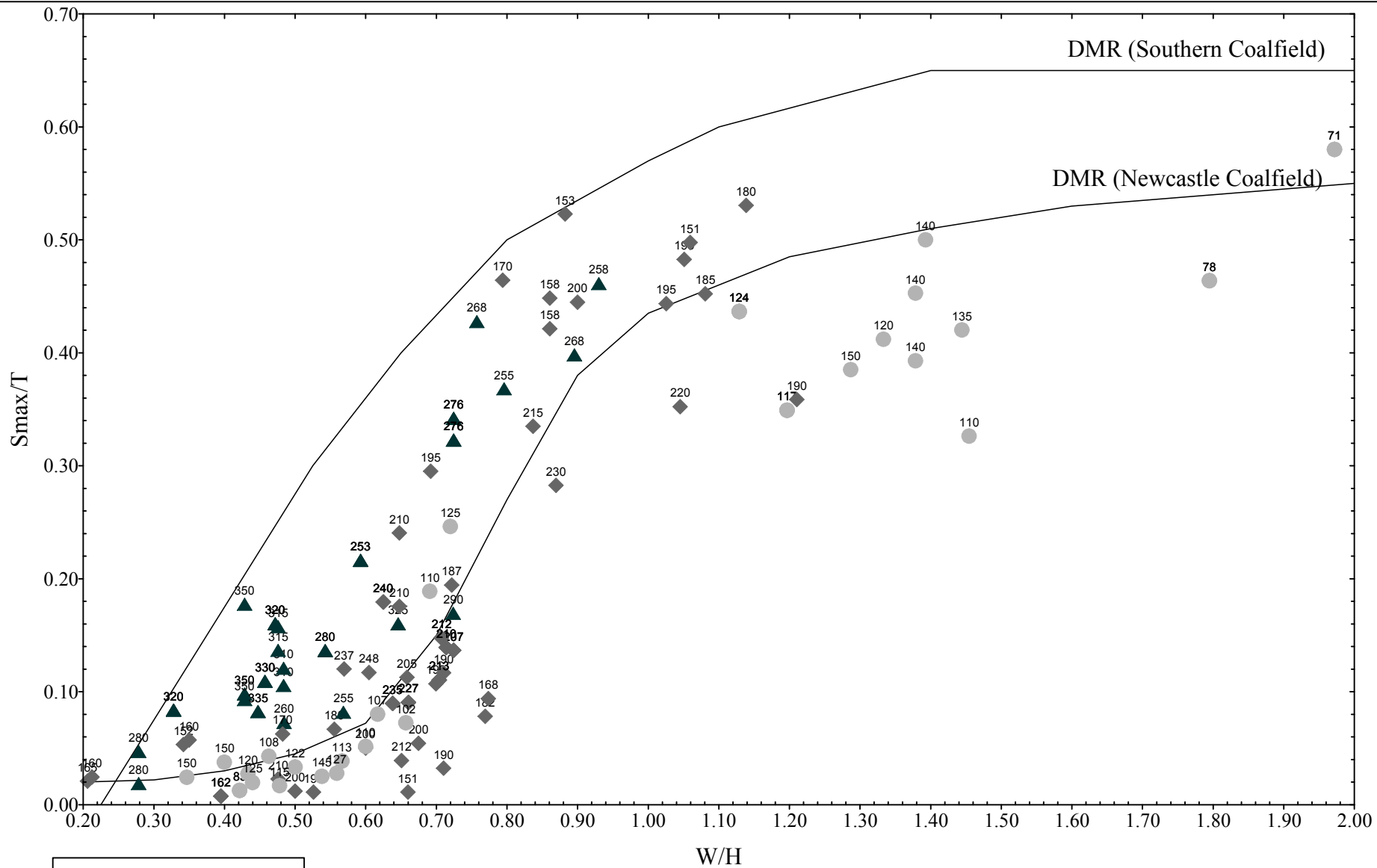
Whittaker & Reddish, 1989. **Subsidence, Occurrence, Prediction and Control**. B. N. Whittaker and D.J. Reddish. Department of Mining Engineering, University of Nottingham, UK.



LEGEND	
Cover Depth, H (m)	
○	H = 70m to H = 151m
■	H = 151m to H = 251m
▲	H = 251m to H = 350m



Engineer:	S.Ditton	Client:	Adapted from ACARP, 2003	
Drawn:	S.Ditton			
Date:	08.06.08	Title:	Project Database and DMR Subsidence Prediction Curves for Single Longwall Panels in Newcastle Coalfield	
Ditton Geotechnical Services Pty Ltd				
Scale:	NTS	Figure No.:	A1	



LEGEND	
●	Data Point
	Cover Depth, H (m)
●	H = 70m to H = 151m
◆	H = 151m to H = 251m
▲	H = 251m to H = 350m



Engineer:	S.Ditton	Client:	Adapted from ACARP, 2003	
Drawn:	S.Ditton			
Date:	08.06.08	Title:	Project Database for Single Longwall Panels in Newcastle Coalfield showing Cover Depth for Each Point	
Ditton Geotechnical Services Pty Ltd				
Scale:	NTS	Figure No:	A2.1	

Continuous or clamped elastic beam in overburden with horizontal stress.

Simply supported beam analogy for cracked beam analysis

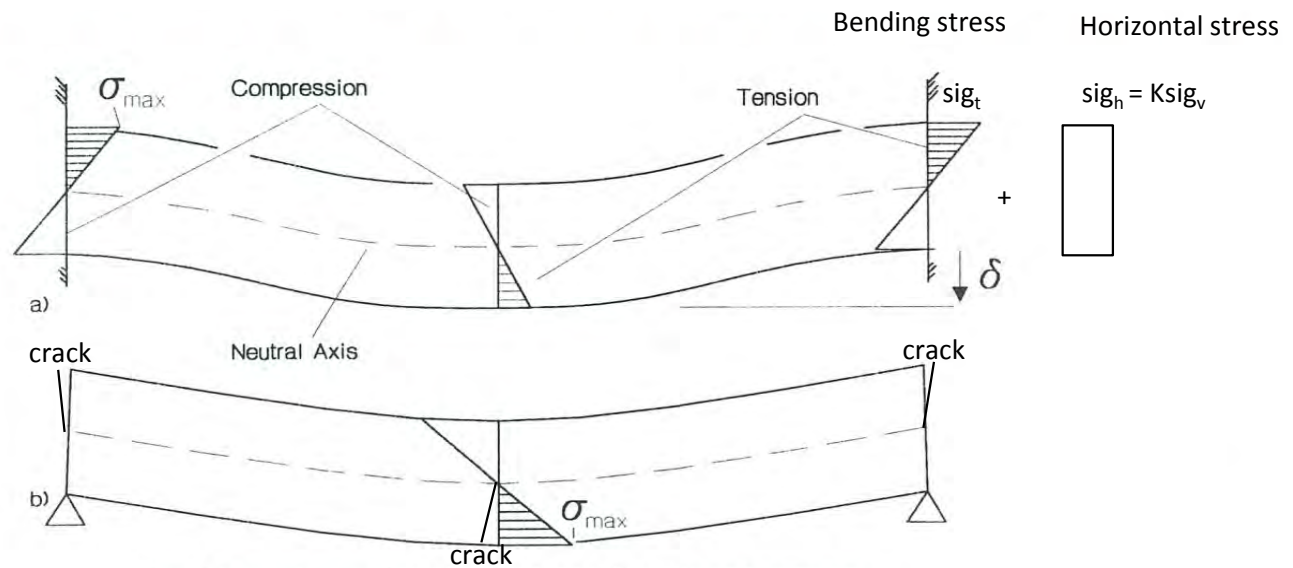


Fig. 4. Elastic beam with (a) fixed ends and (b) simple (pin) supports.

Note: Elastic beam cracks if $\sigma_t + \sigma_h > 0$, where tensile stress is positive.

Ref: Diedrichs & Kaiser, 1999

	Engineer:	S.Ditton	Client:	Adapted from ACARP, 2003	
	Drawn:	S.Ditton	Title:	Internal Compressive Stress Arch Geometry	
	Date:	03.06.13	Scale:	NTS	Figure No:
	Ditton Geotechnical Services Pty Ltd				A2.2

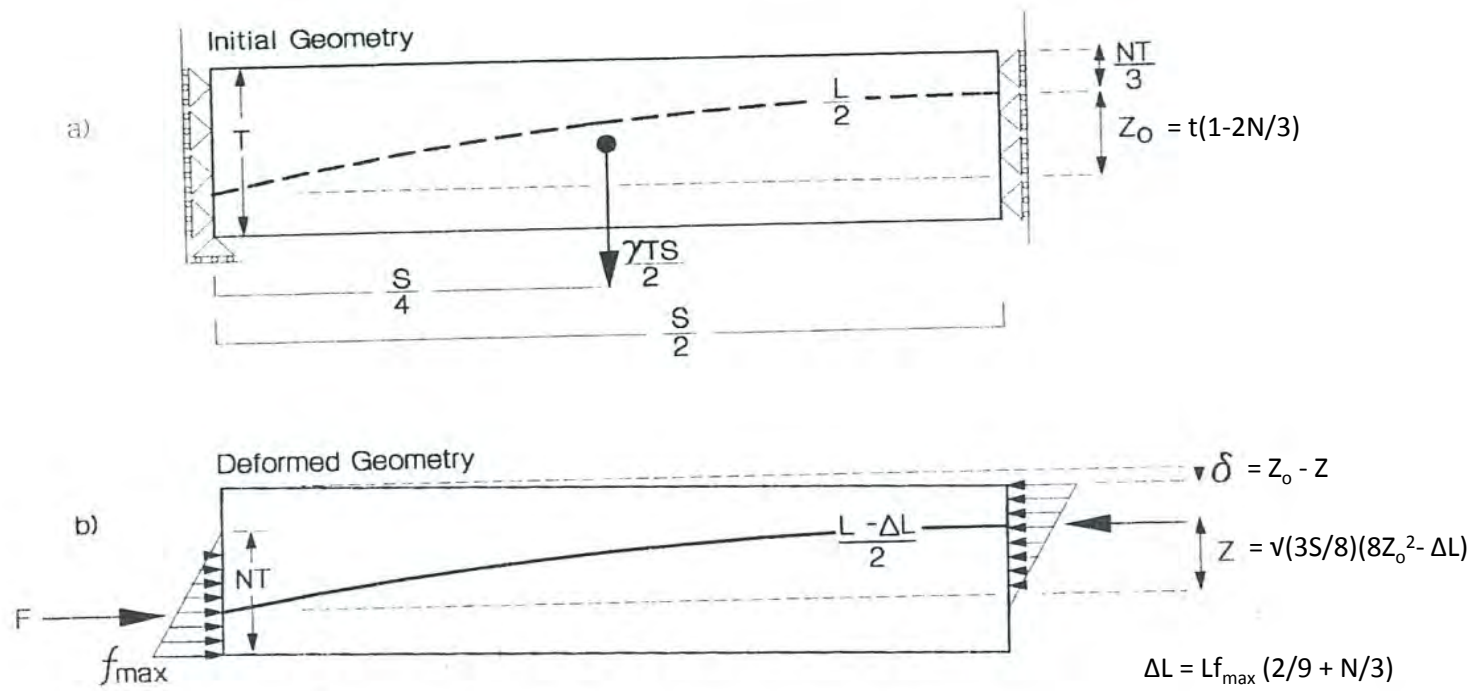
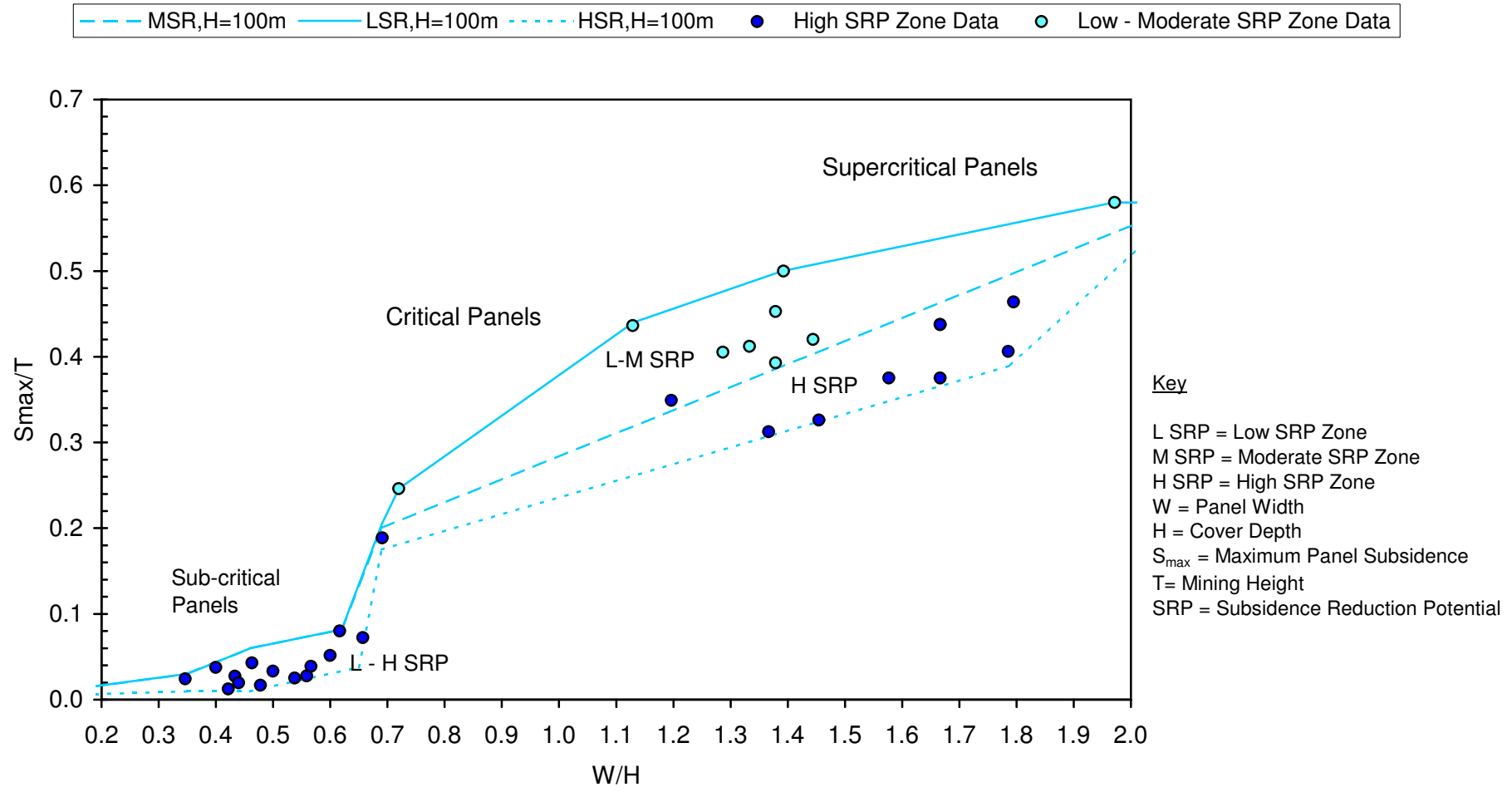


Fig. 5. Voussoir beam (half-span shown) and nomenclature.

Ref: Diedrichs & Kaiser, 1999

	Engineer:	S.Ditton	Client:	Adapted from ACARP, 2003	
	Drawn:	S.Ditton			
	Date:	03.06.13	Title:	Internal Compressive Stress Arch Development in Simply Supported Beam (i.e. Voussoir Beam Analogy)	
	Ditton Geotechnical Services Pty Ltd			Scale:	NTS

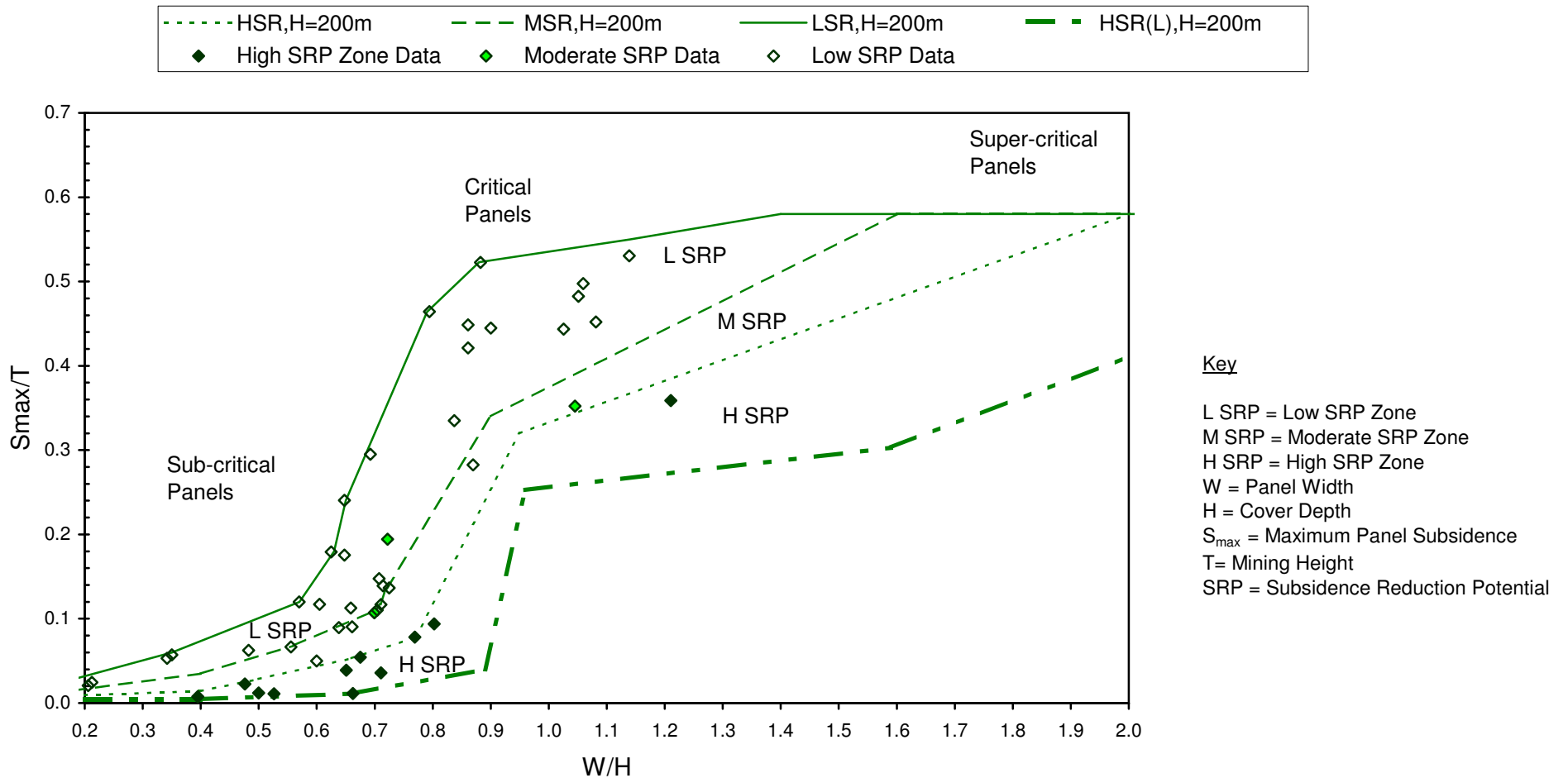


Key

L SRP = Low SRP Zone
M SRP = Moderate SRP Zone
H SRP = High SRP Zone
W = Panel Width
H = Cover Depth
 S_{max} = Maximum Panel Subsidence
T = Mining Height
SRP = Subsidence Reduction Potential

Note: No SRP distinguishment for panels with $W/H < 0.65$

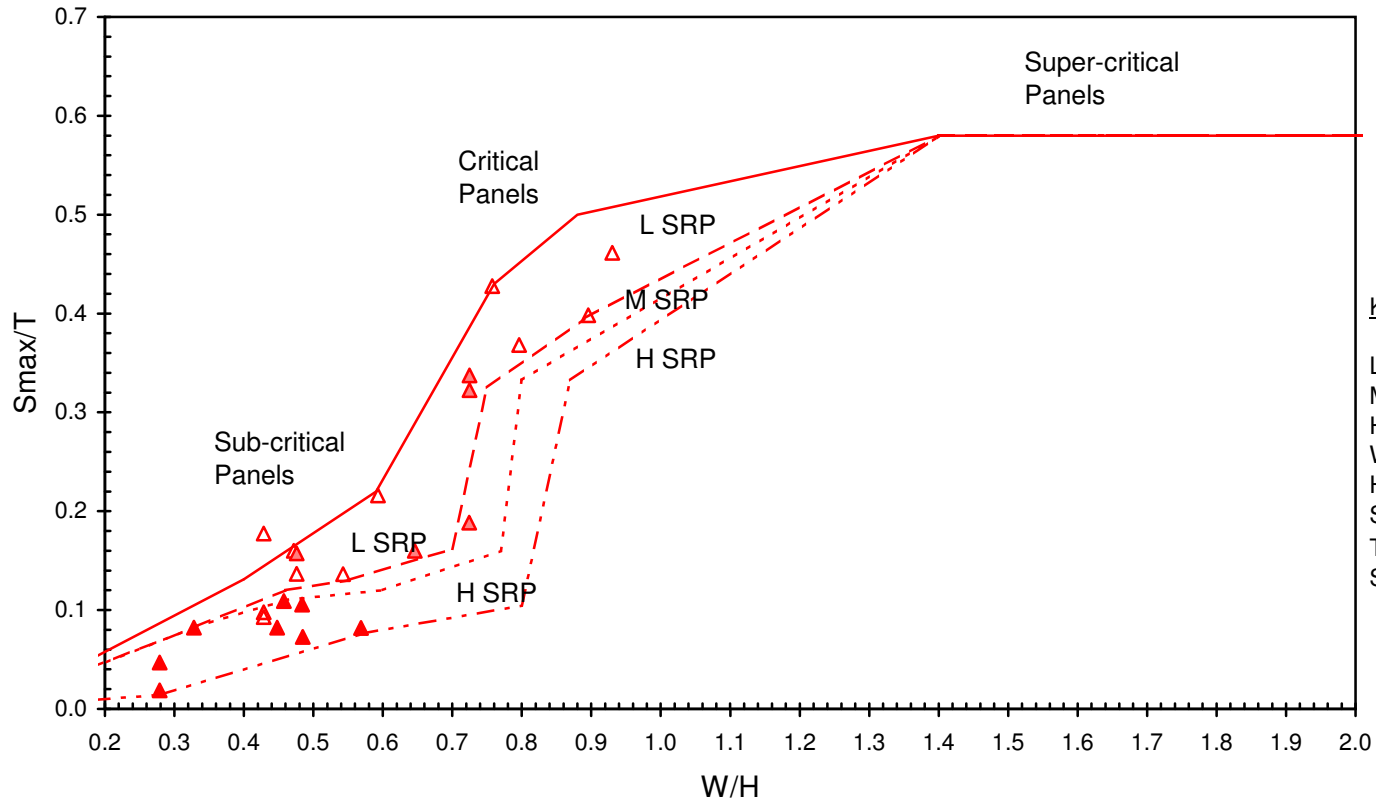
	Engineer:	S.Ditton	Client:	Adapted from ACARP, 2003	
	Drawn:	S.Ditton			
	Date:	08.08.08	Title:	Empirical Model for Predicting Subsidence Above Panels with Cover Depths Between 50 and 150 m and Low to High SRP Zones	
	Ditton Geotechnical Services Pty Ltd			Scale:	NTS



Key

L SRP = Low SRP Zone
M SRP = Moderate SRP Zone
H SRP = High SRP Zone
W = Panel Width
H = Cover Depth
 S_{max} = Maximum Panel Subsidence
T = Mining Height
SRP = Subsidence Reduction Potential

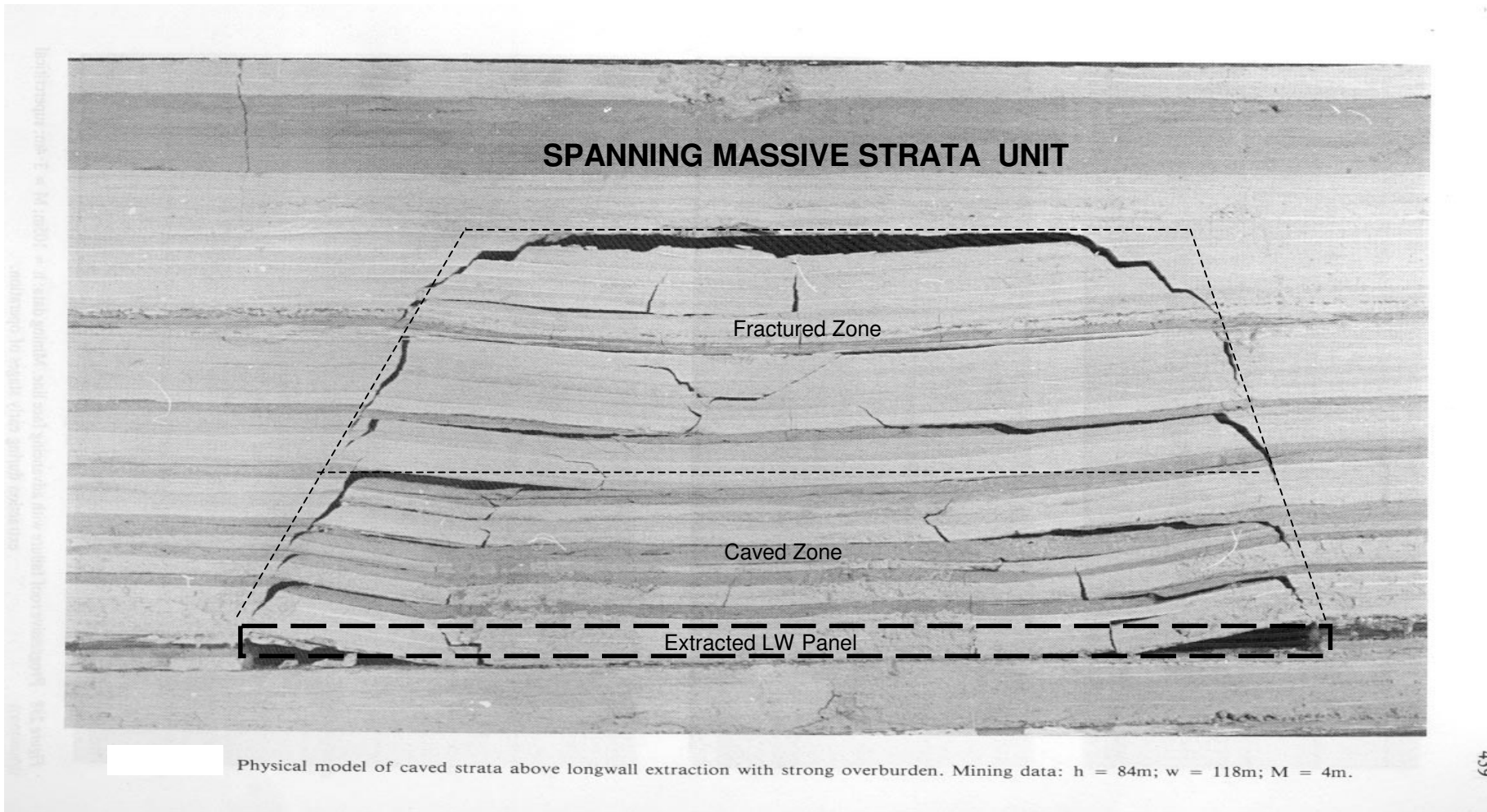
	Engineer:	S.Ditton	Client:	Adapted from ACARP, 2003	
	Drawn:	S.Ditton	Title:	Empirical Model for Predicting Subsidence Above Panels with Cover Depths	
	Date:	08.08.08	Between 250 and 350 m and Low to High SRP Zones		
	Ditton Geotechnical Services Pty Ltd		Scale:	NTS	Figure No:



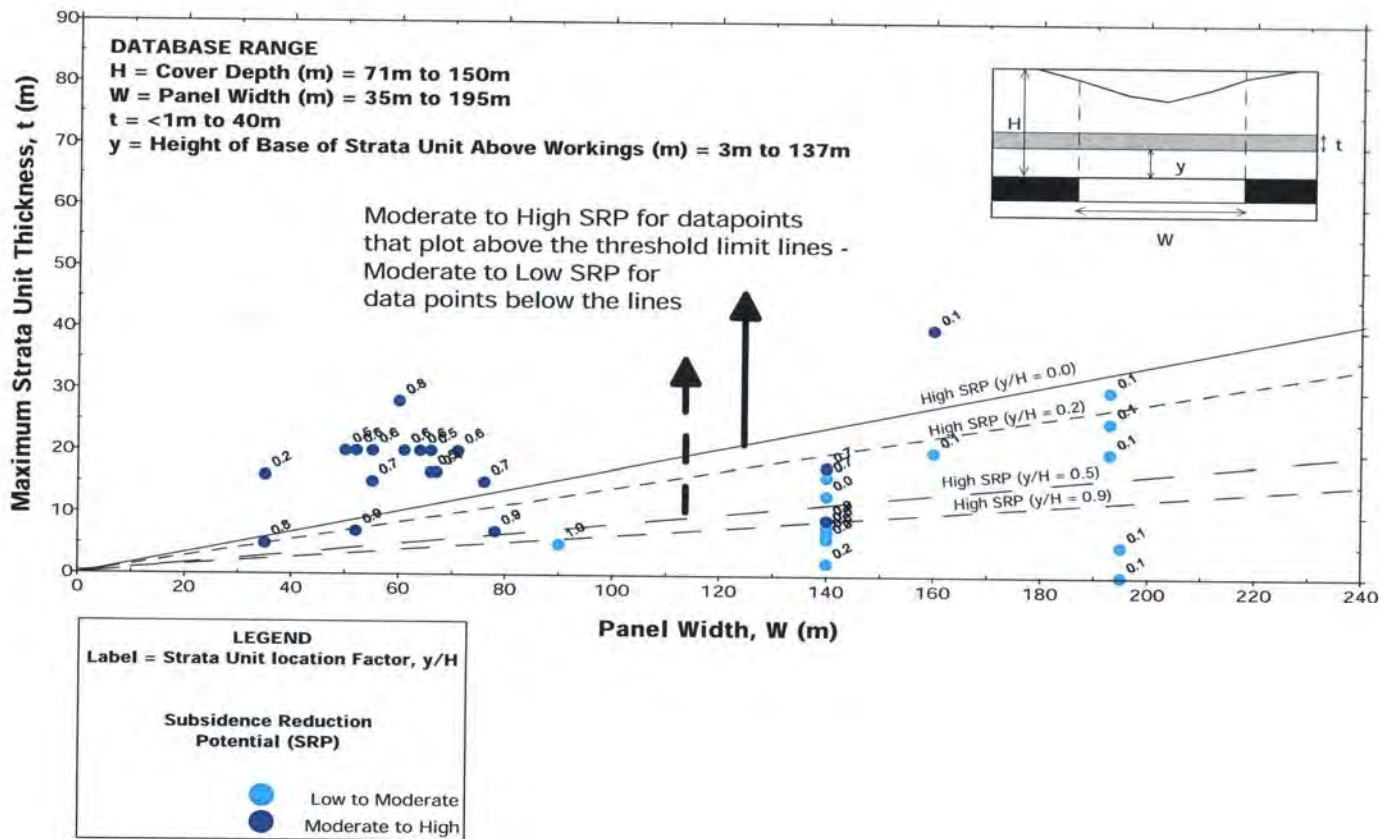
Key

L SRP = Low SRP Zone
M SRP = Moderate SRP Zone
H SRP = High SRP Zone
W = Panel Width
H = Cover Depth
 S_{max} = Maximum Panel Subsidence
T = Mining Height
SRP = Subsidence Reduction Potential

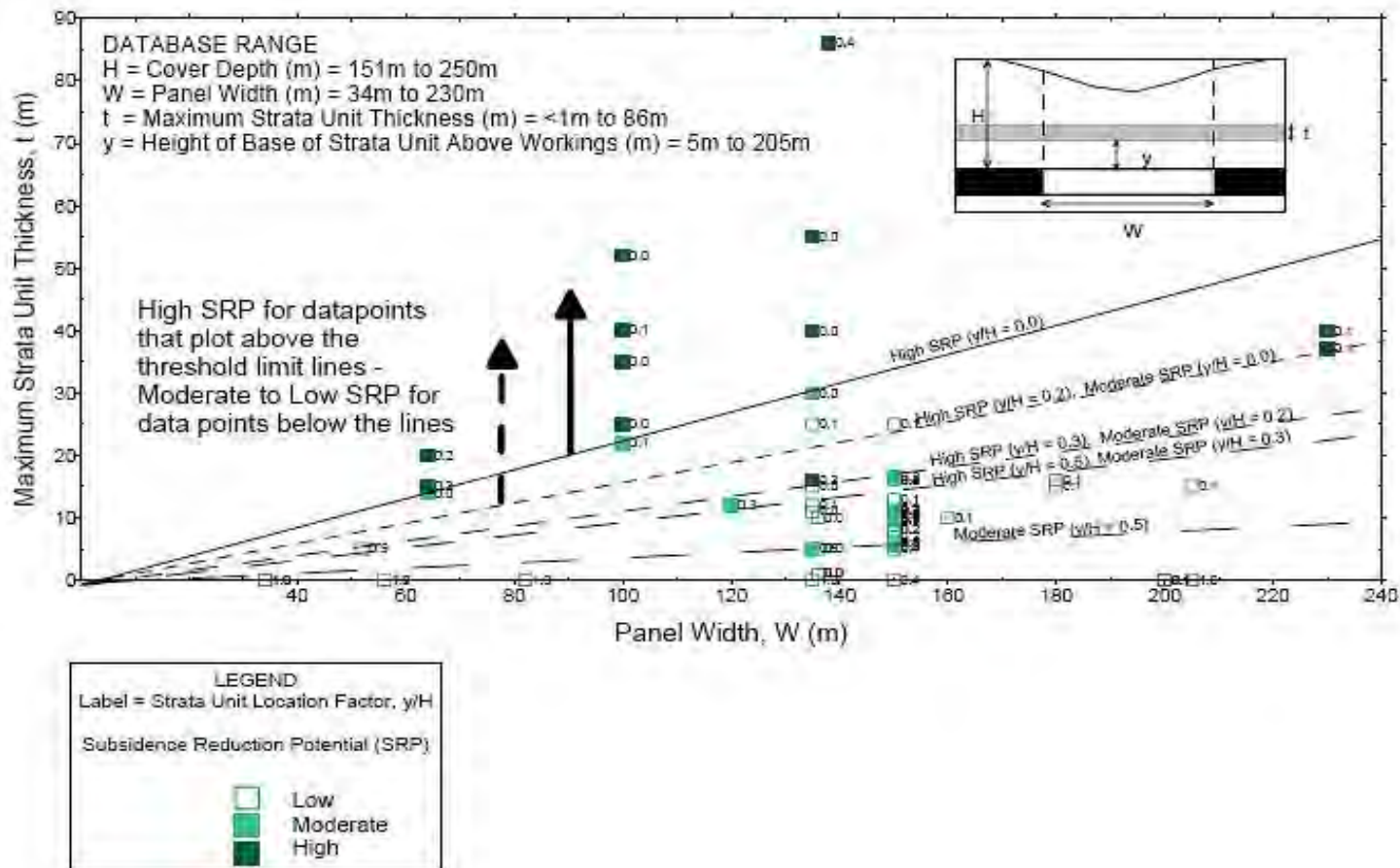
	Engineer:	S.Ditton	Client:	Adapted from ACARP, 2003	
	Drawn:	S.Ditton		Title:	Empirical Model for Predicting Subsidence Above Panels with Cover Depths
	Date:	08.08.08	Between 250 and 350 m and Low to High SRP Zones		
	Ditton Geotechnical Services Pty Ltd		Scale:		NTS



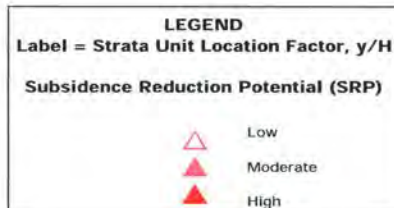
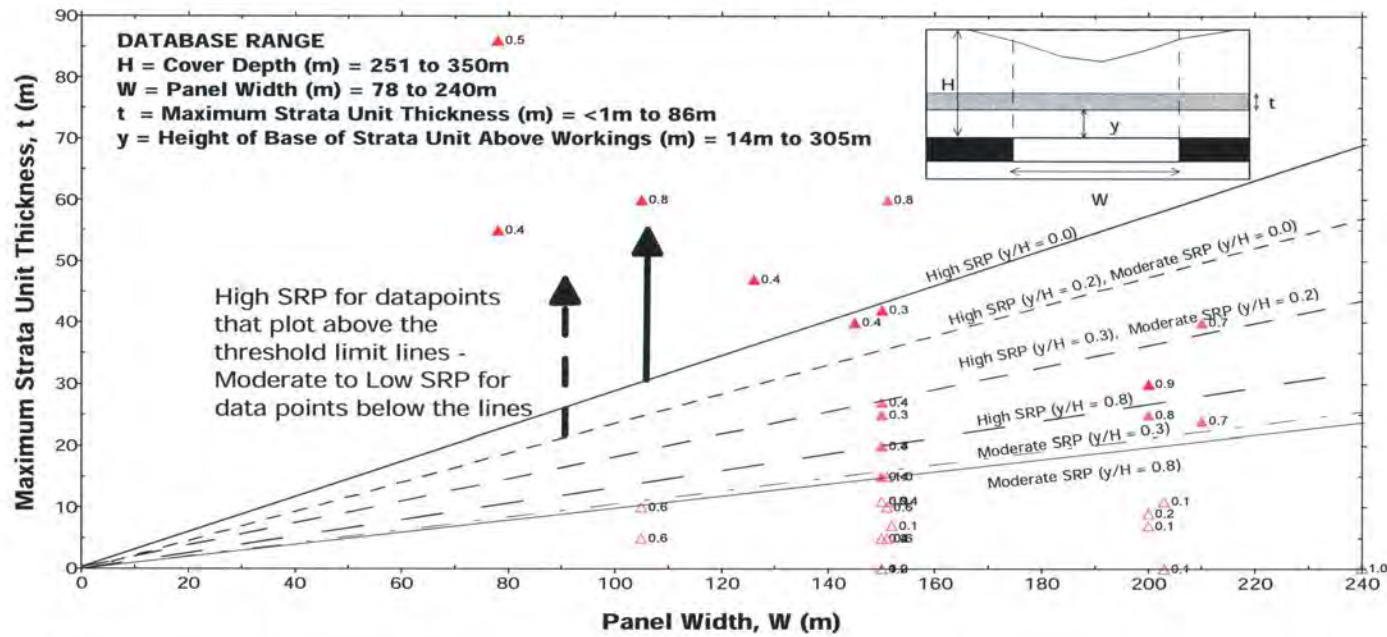
	Engineer:	S.Ditton	Client:	Adapted from ACARP, 2003	
	Drawn:	S.Ditton			
	Date:	08.08.08	Title:	Physical Overburden Model Showing the Subsidence Reducing Effect of a Massive Strata Unit At the Surface	
	Ditton Geotechnical Services Pty Ltd				
Scale:	NTS		Figure No:	A6	



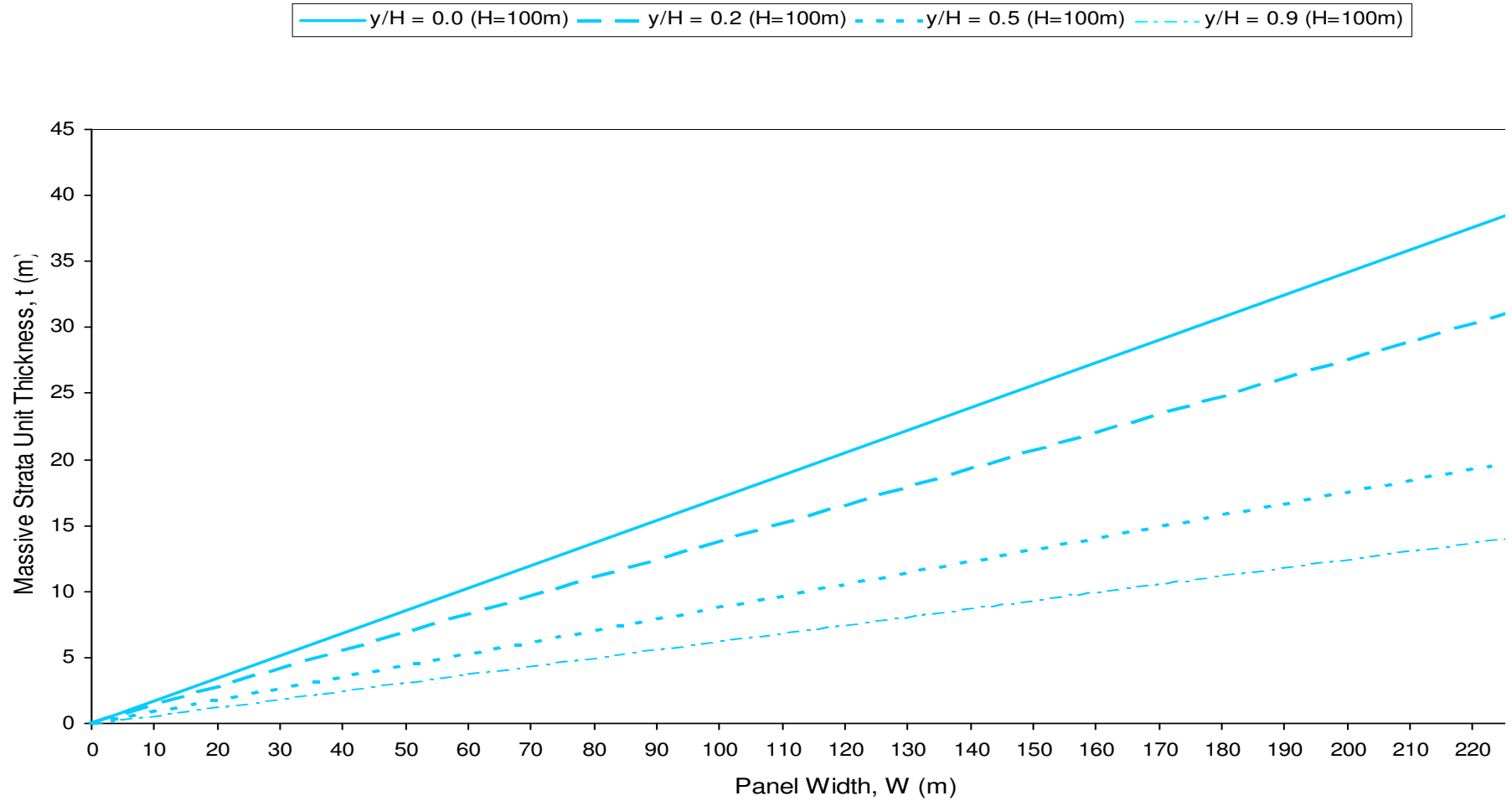
	Engineer:	S.Ditton	Client:	Extract from ACARP, 2003
	Drawn:	S.Ditton	Title:	Project Database of Maximum Strata Unit Thickness and SRP Threshold Limit Lines for H=50 m to 150 m
	Date:	08.08.08	Scale:	NTS
	Ditton Geotechnical Services Pty Ltd		Figure No:	A7.1



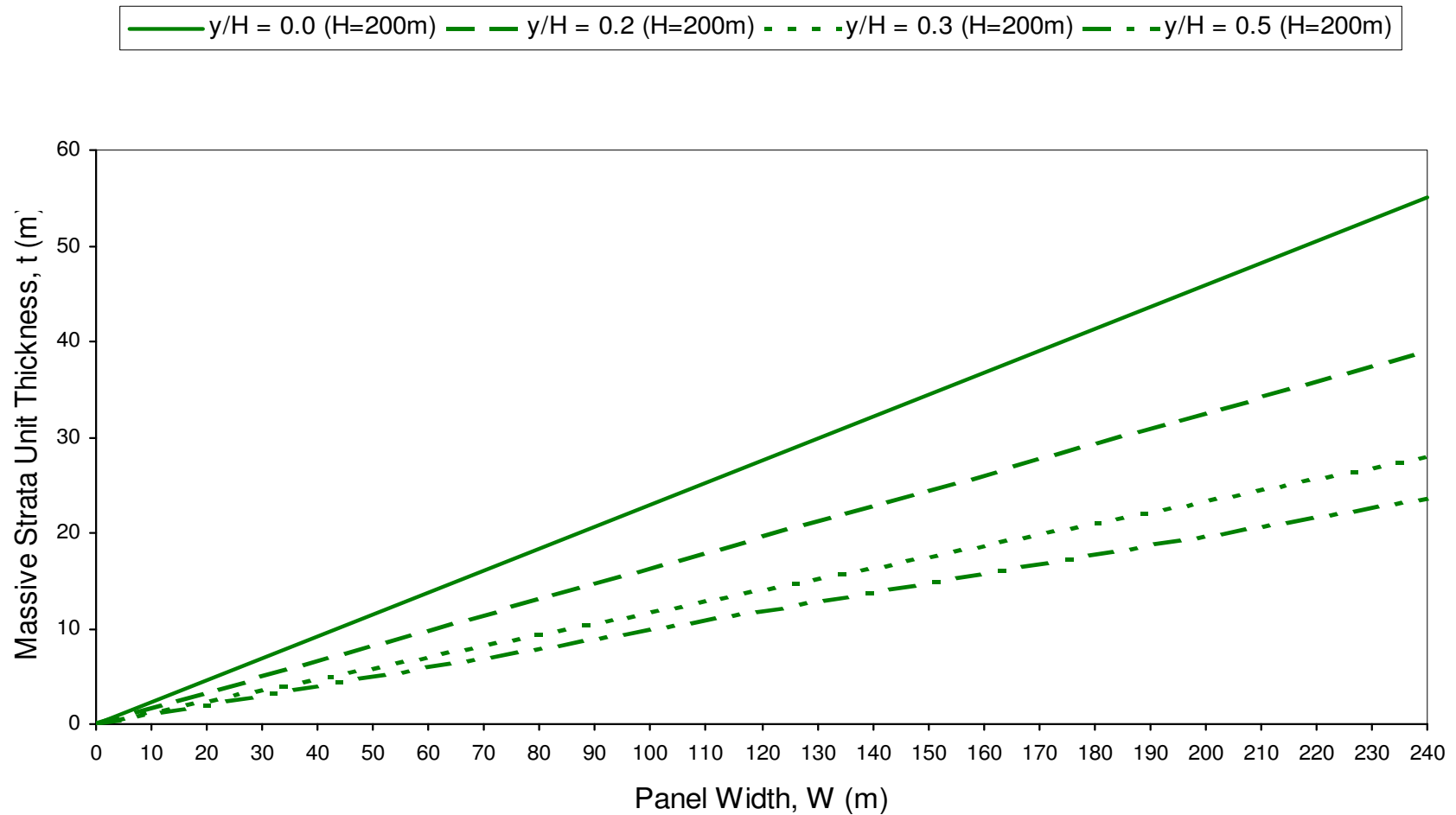
	Engineer:	S.Ditton	Client:	Extract from ACARP, 2003	
	Drawn:	S.Ditton			
	Date:	08.08.08	Title:	Project Database of Maximum Strata Unit Thickness and SRP Threshold Limit Lines for H=150 m to 250 m	
	Ditton Geotechnical Services Pty Ltd			Scale:	NTS



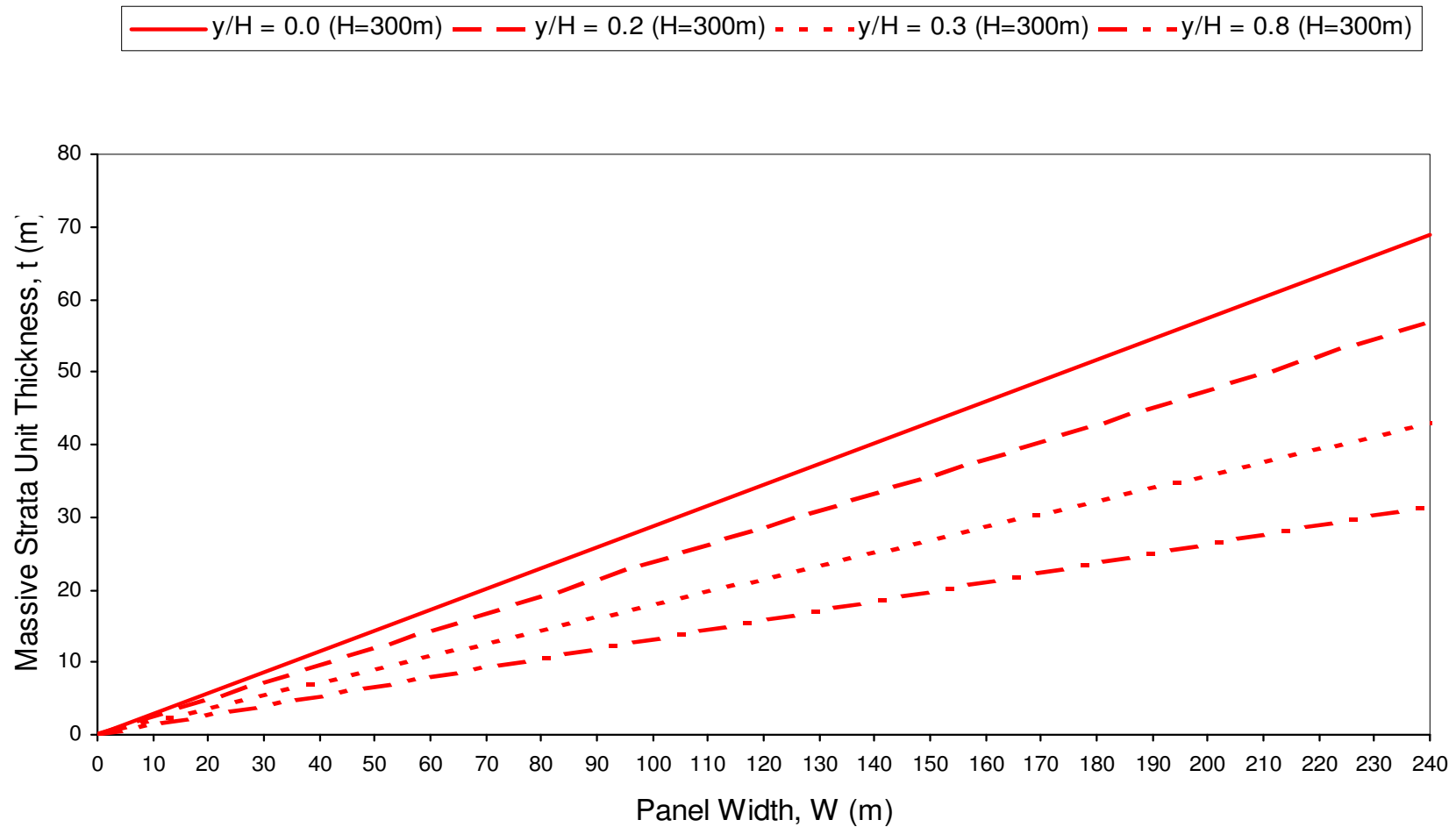
	Engineer:	S.Ditton	Client:	Extract from ACARP, 2003	
	Drawn:	S.Ditton			
	Date:	08.08.08	Title:	Project Database of Maximum Strata Unit Thickness and SRP Threshold Limit Lines for H=250 m to 350 m	
	Ditton Geotechnical Services Pty Ltd			Scale:	NTS



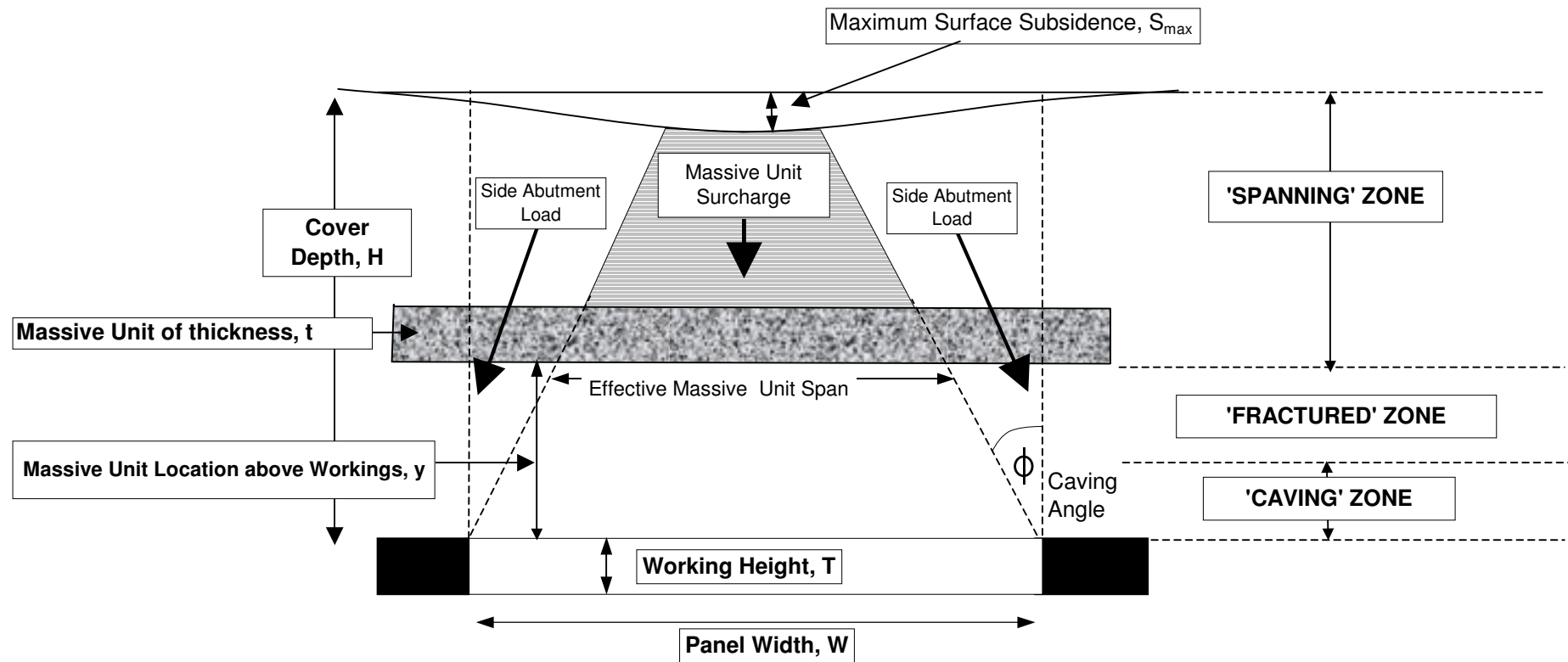
	Engineer:	S.Ditton	Client:	Adapted from ACARP, 2003	
	Drawn:	S.Ditton			
	Date:	08.08.08	Title:	Empirical Model for Predicting Subsidence Reduction Potential Above Panels with Cover Depths Between 50 and 150 m	
	Ditton Geotechnical Services Pty Ltd			Scale:	NTS



	Engineer:	S.Ditton	Client:	Adapted from ACARP, 2003		
	Drawn:	S.Ditton				
	Date:	08.08.08	Title:	Empirical Model for Predicting Subsidence Reduction Potential Above Panels with Cover Depths Between 150 and 250 m		
	Ditton Geotechnical Services Pty Ltd			Scale:	NTS	Figure No:



	Engineer:	S.Ditton	Client:	Adapted from ACARP, 2003	
	Drawn:	S.Ditton			
	Date:	08.08.08	Title:	Empirical Model for Predicting Subsidence Reduction Potential Above Panels with Cover Depths Between 250 and 350 m	
	Ditton Geotechnical Services Pty Ltd			Scale:	NTS



	Engineer:	S.Ditton	Client:	Adapted from ACARP, 2003	
	Drawn:	S.Ditton	Title:	Overburden with Massive Strata Unit Behaviour Concept Model and Key Parameter	
	Date:	08.08.08	Definitions:		
	Ditton Geotechnical Services Pty Ltd		Scale:	NTS	Figure No:

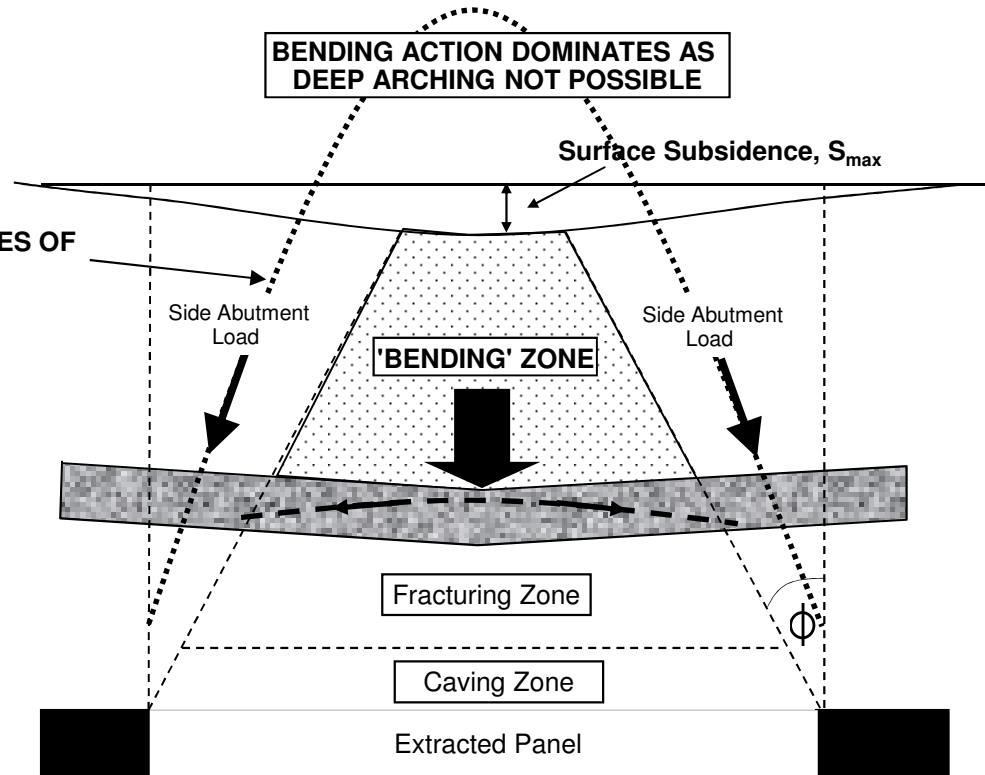
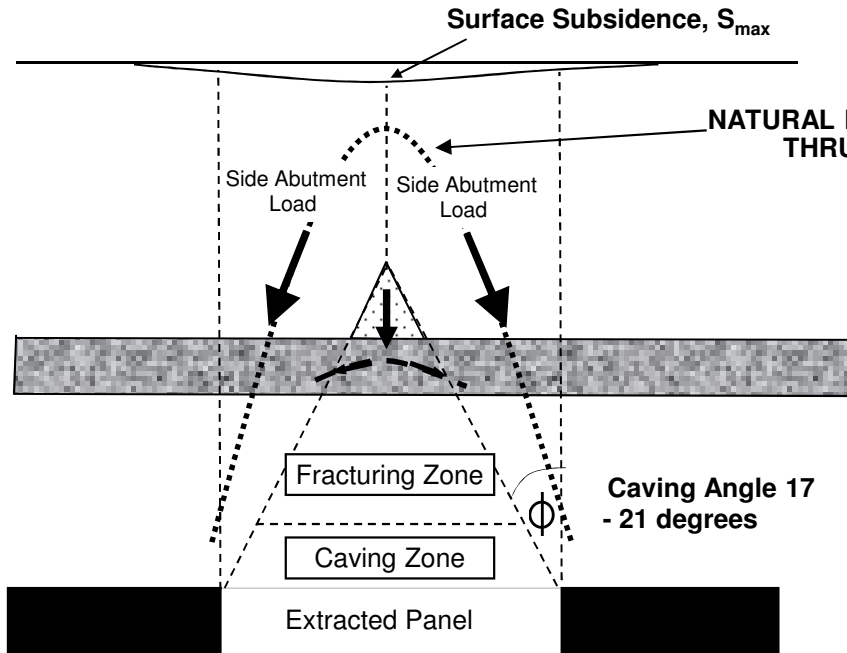
DEEP 'BEAM' BEHAVIOUR
($W/H < 0.7$)

Geometrical

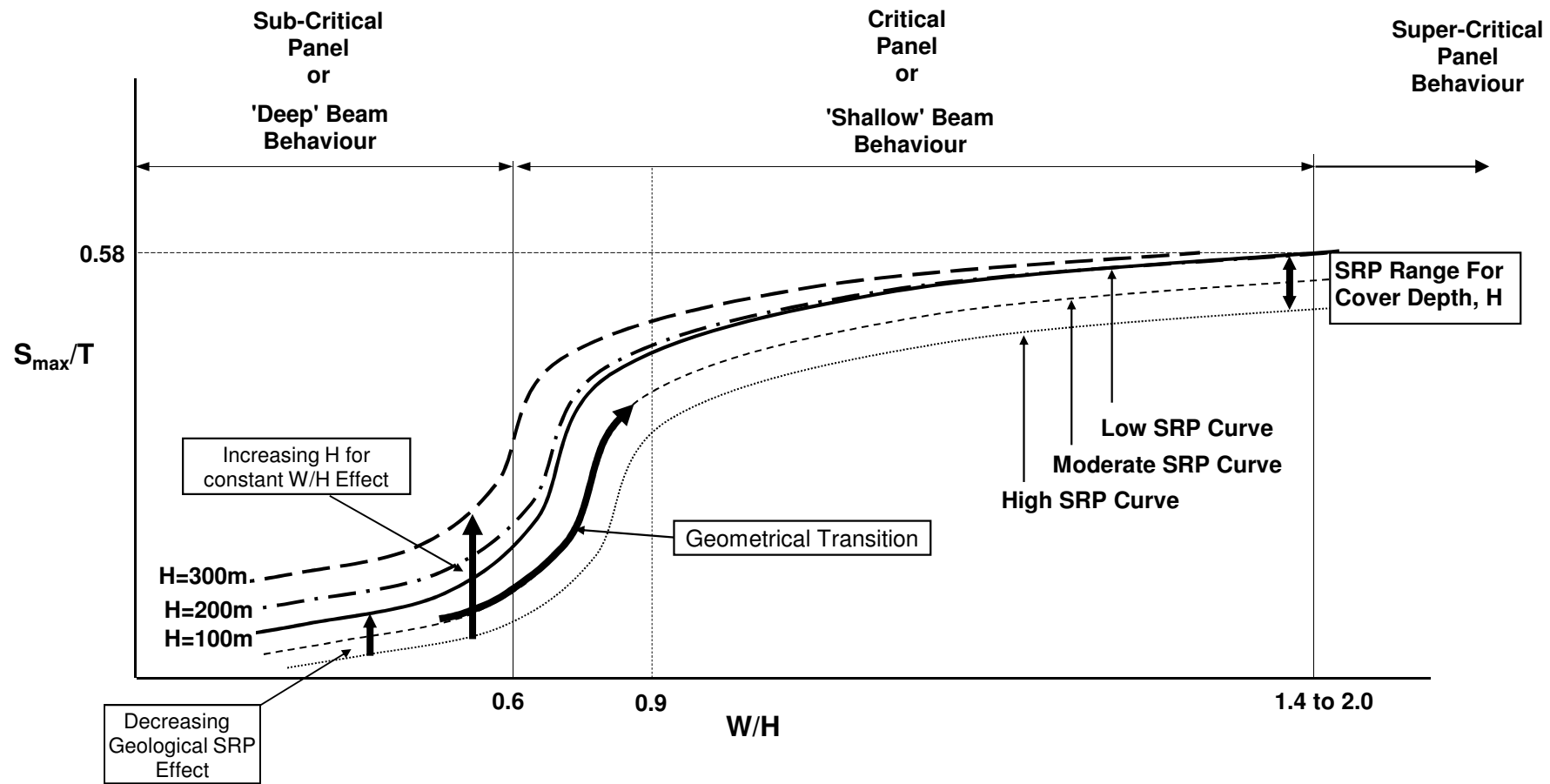
SHALLOW 'BEAM' BEHAVIOUR
($W/H > 0.7$)

AXIAL ACTION OR
DEEP 'ARCHING' DOMINATES
SMALL BENDING ZONE

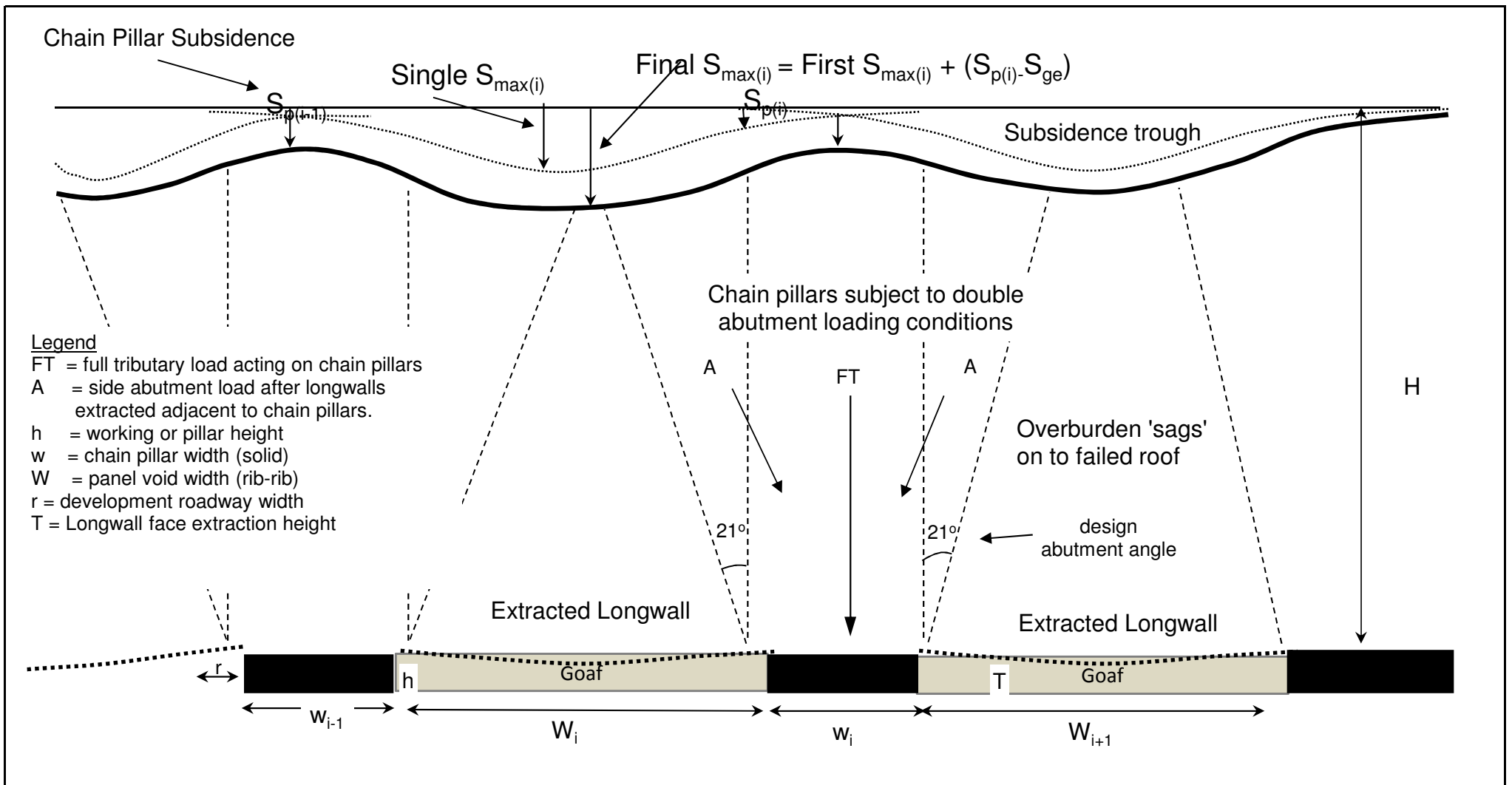
BENDING ACTION DOMINATES AS
DEEP ARCHING NOT POSSIBLE



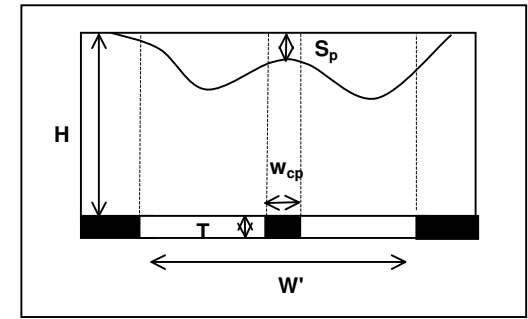
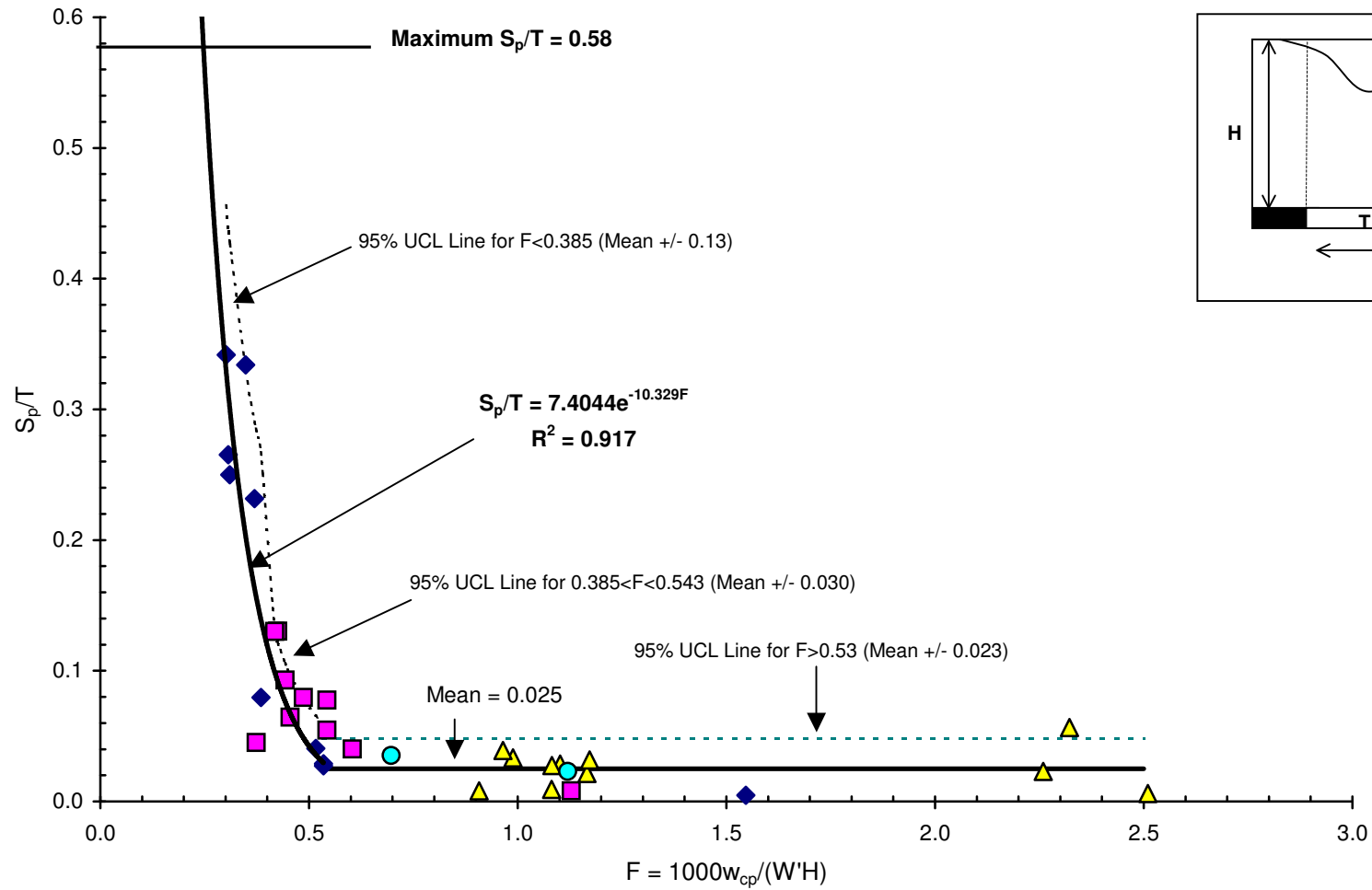
	Engineer:	S.Ditton	Client:	Adapted from ACARP, 2003	
	Drawn:	S.Ditton	Title:	Overburden with Massive Strata Units Behaviour Concept Models of Beam Action Types for Subcritical and Supercritical Longwall Panels	
	Date:	08.08.08	Scale:	NTS	Figure No: A12
	Ditton Geotechnical Services Pty Ltd				



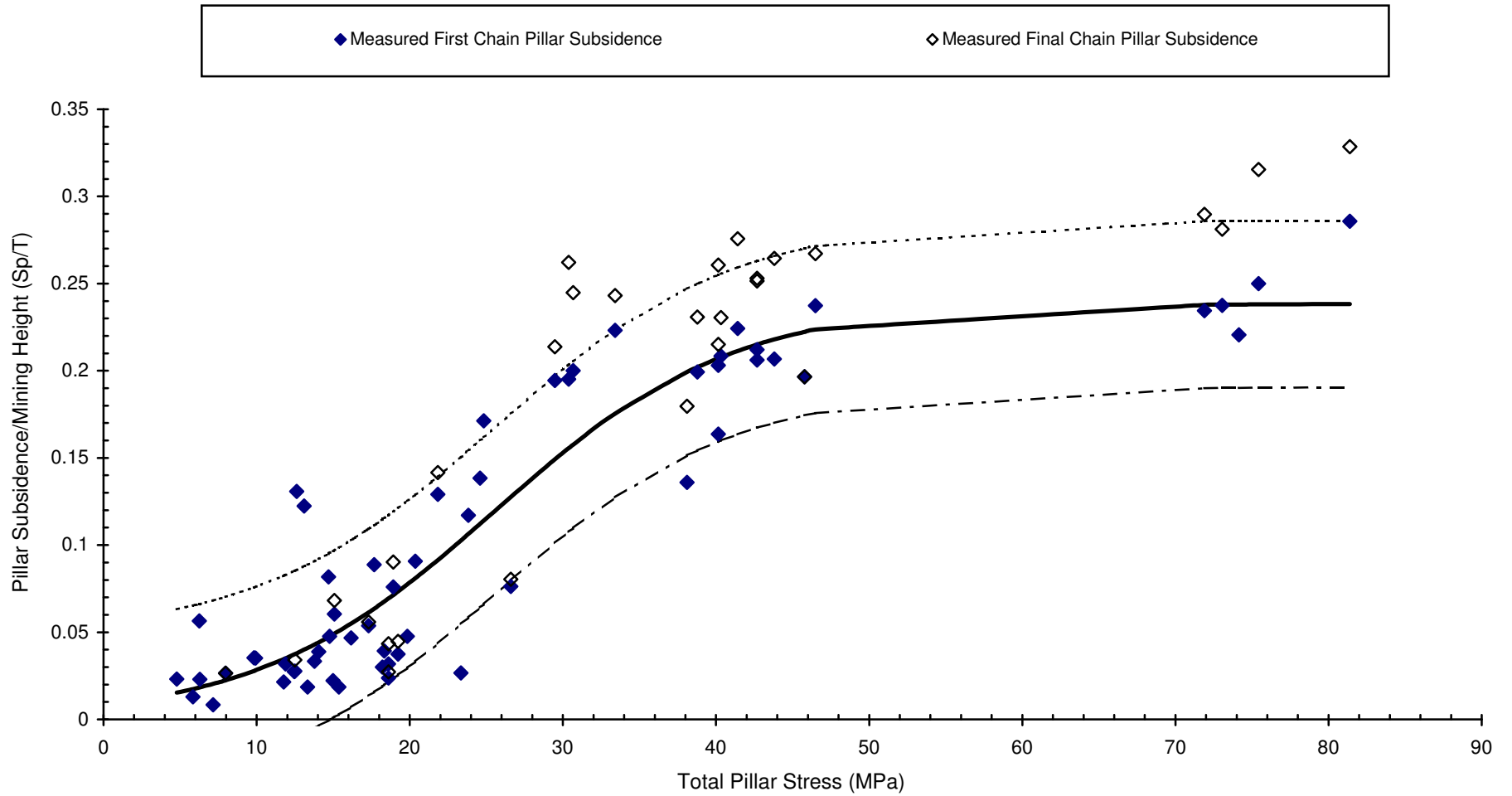
	Engineer:	S.Ditton	Client:	Adapted from ACARP, 2003	
	Drawn:	S.Ditton			
	Date:	08.08.08	Title:	Geomechanical and Geological Effects of Overburden Behaviour on Maximum Subsidence for Single Panels	
	Ditton Geotechnical Services Pty Ltd		Scale:	NTS	Figure No:



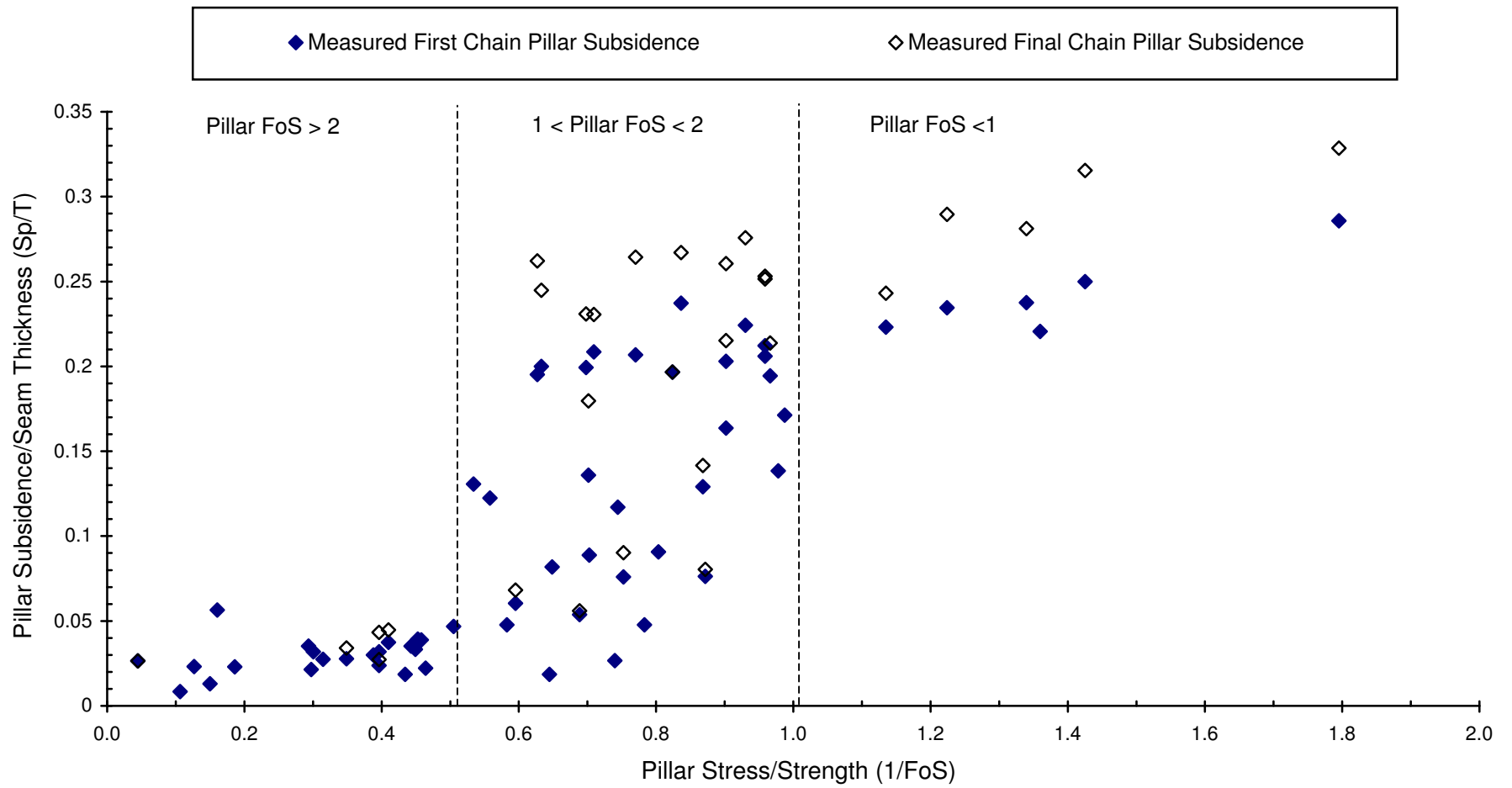
	Engineer:	S.Ditton	Client:	Adapted from ACARP, 2003	
	Drawn:	S.Ditton	Title:	Multiple Longwall Panel Subsidence Mechanism Concepts	
	Date:	19.07.12	Scale:	NTS	Figure No: A14
	Ditton Geotechnical Services Pty Ltd				



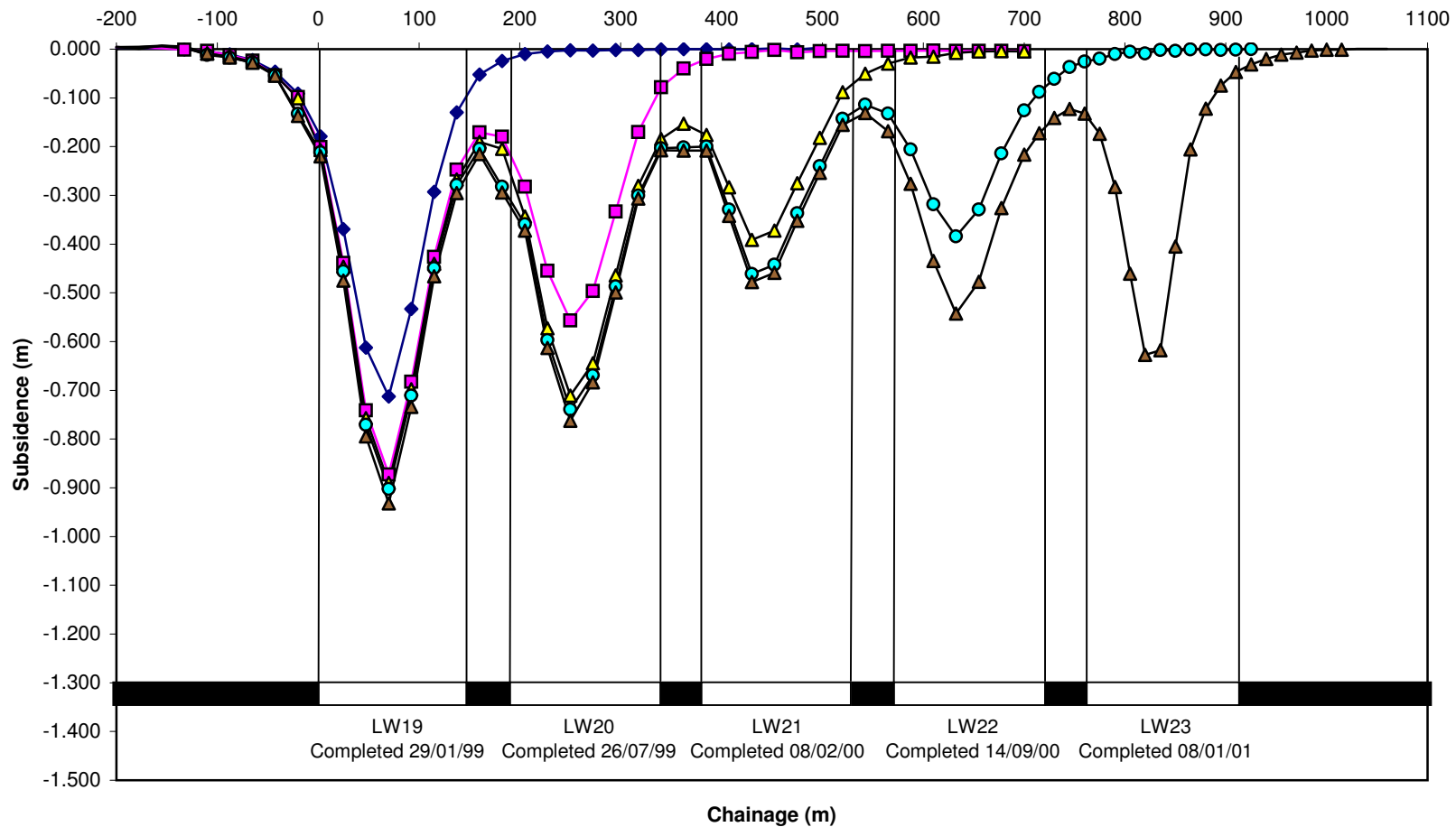
	Engineer:	S.Ditton	Client:	Extract from ACARP, 2003
	Drawn:	S.Ditton	Title:	2003 Empirical Model for Predicting Subsidence above Chain Pillars Subject to Double Abutment Loading
	Date:	08.08.08	Scale:	NTS
	Ditton Geotechnical Services Pty Ltd		Figure No:	A15



	Engineer:	S.Ditton	Client:	Adapted from ACARP, 2003	
	Drawn:	S.Ditton	Title:	2008 Empirical Model (DgS) for Predicting Subsidence above Chain Pillars Subject to Double Abutment Loading	
	Date:	08.08.08	Scale:	NTS	Figure No:
	Ditton Geotechnical Services Pty Ltd				A16



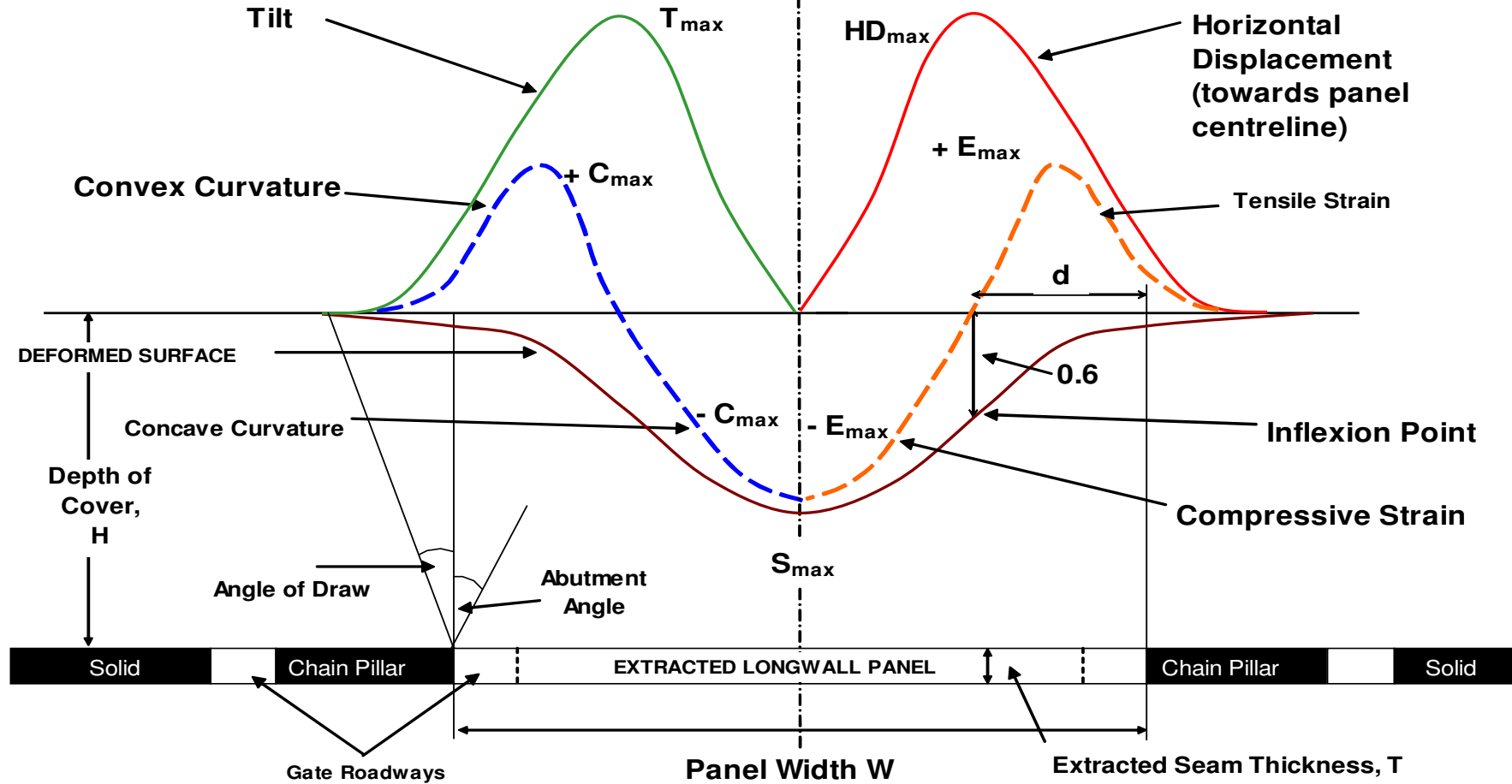
	Engineer:	S.Ditton	Client:	Adapted from ACARP, 2003	
	Drawn:	S.Ditton			
	Date:	08.08.08	Title:	Empirical DgS, 2008 Model Data of 1/FoS v. Subsidence above Chain Pillars Subject to Double Abutment Loading	
	Ditton Geotechnical Services Pty Ltd			Scale:	NTS



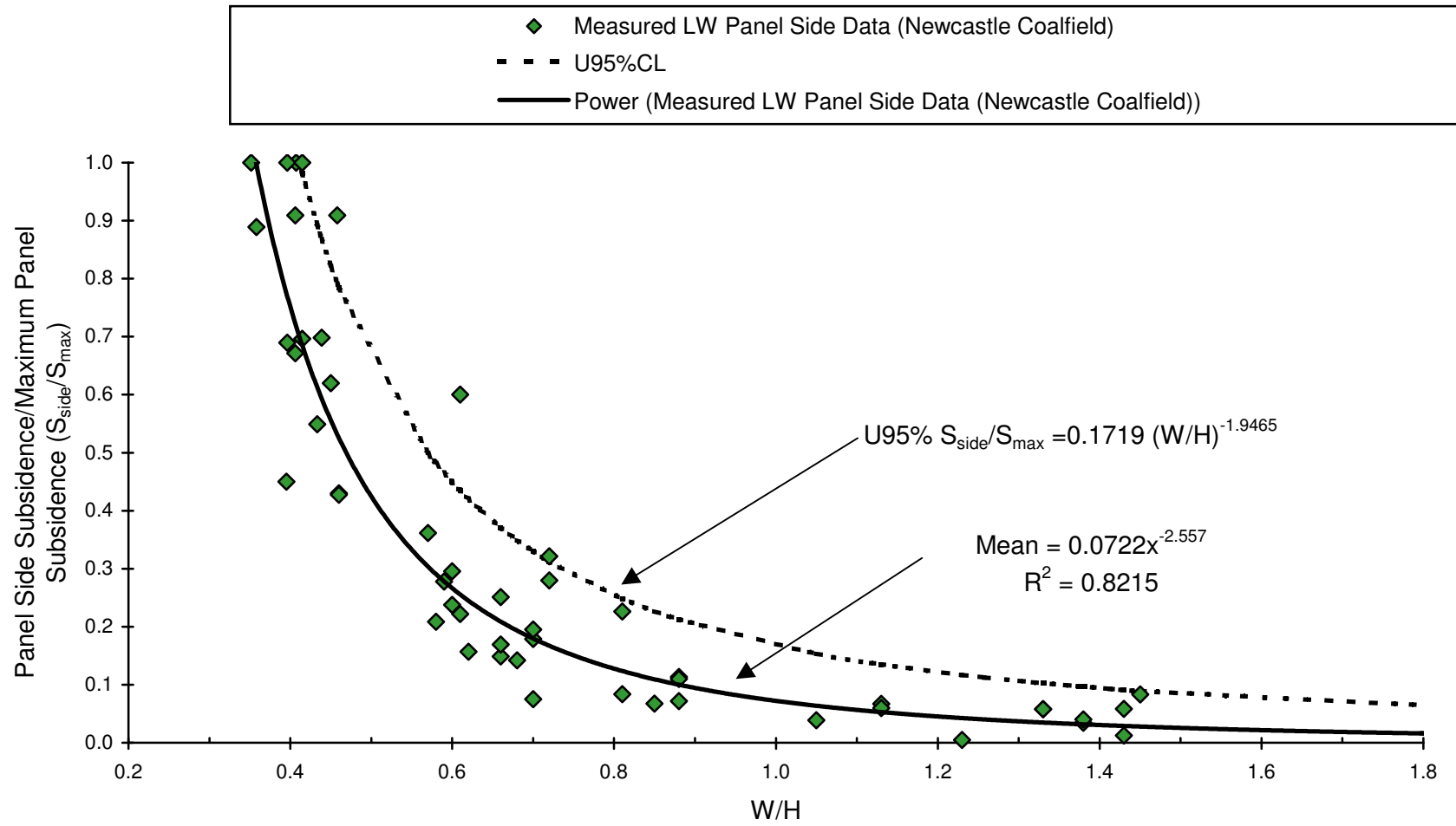
	Engineer:	S.Ditton	Client:	Adapted from ACARP, 2003	
	Drawn:	S.Ditton	Title:	Measured Multiple Longwall Panel Subsidence in Newcastle Coalfield	
	Date:	08.08.08	Scale:	NTS	Figure No:
	Ditton Geotechnical Services Pty Ltd				A18

VERTICAL DISPLACEMENT PARAMETER PROFILES

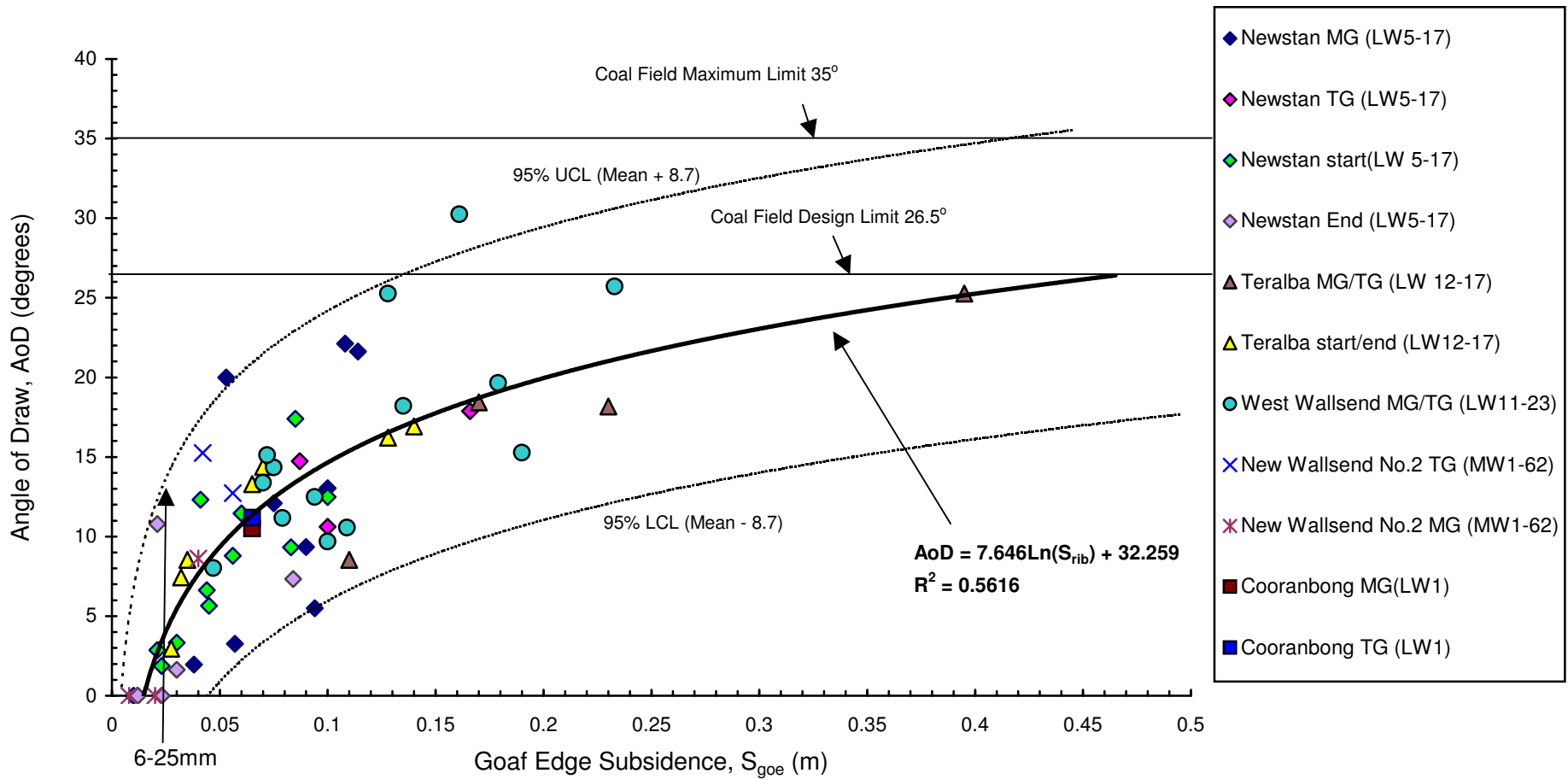
HORIZONTAL DISPLACEMENT PARAMETER PROFILES



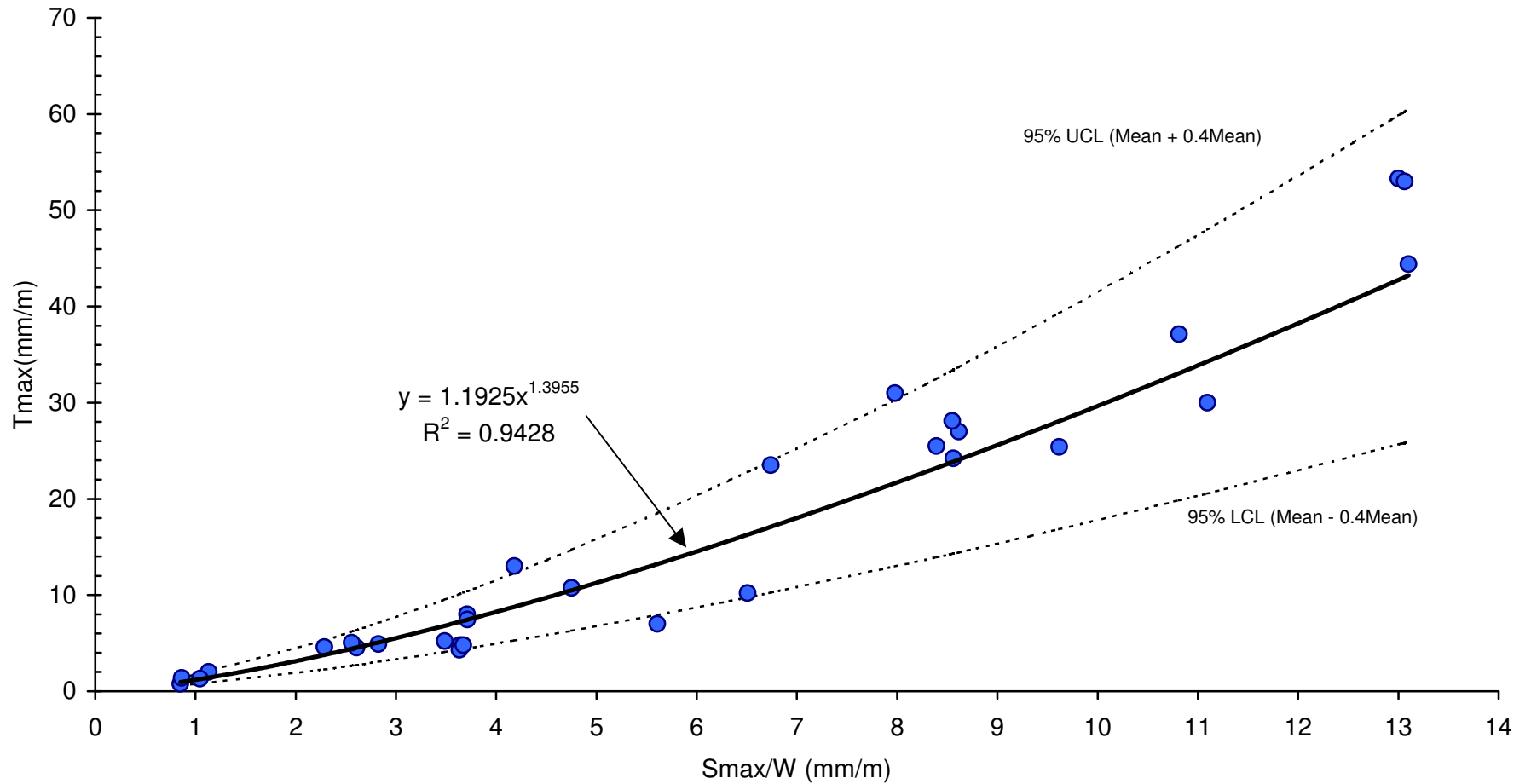
	Engineer:	S.Ditton	Client:	Extract from ACARP, 2003
	Drawn:	S.Ditton	Title:	Mine Subsidence Trough Deformation Parameters (adapted from Holla, 1987)
	Date:	08.08.08	Scale:	NTS
	Ditton Geotechnical Services Pty Ltd		Figure No:	A19



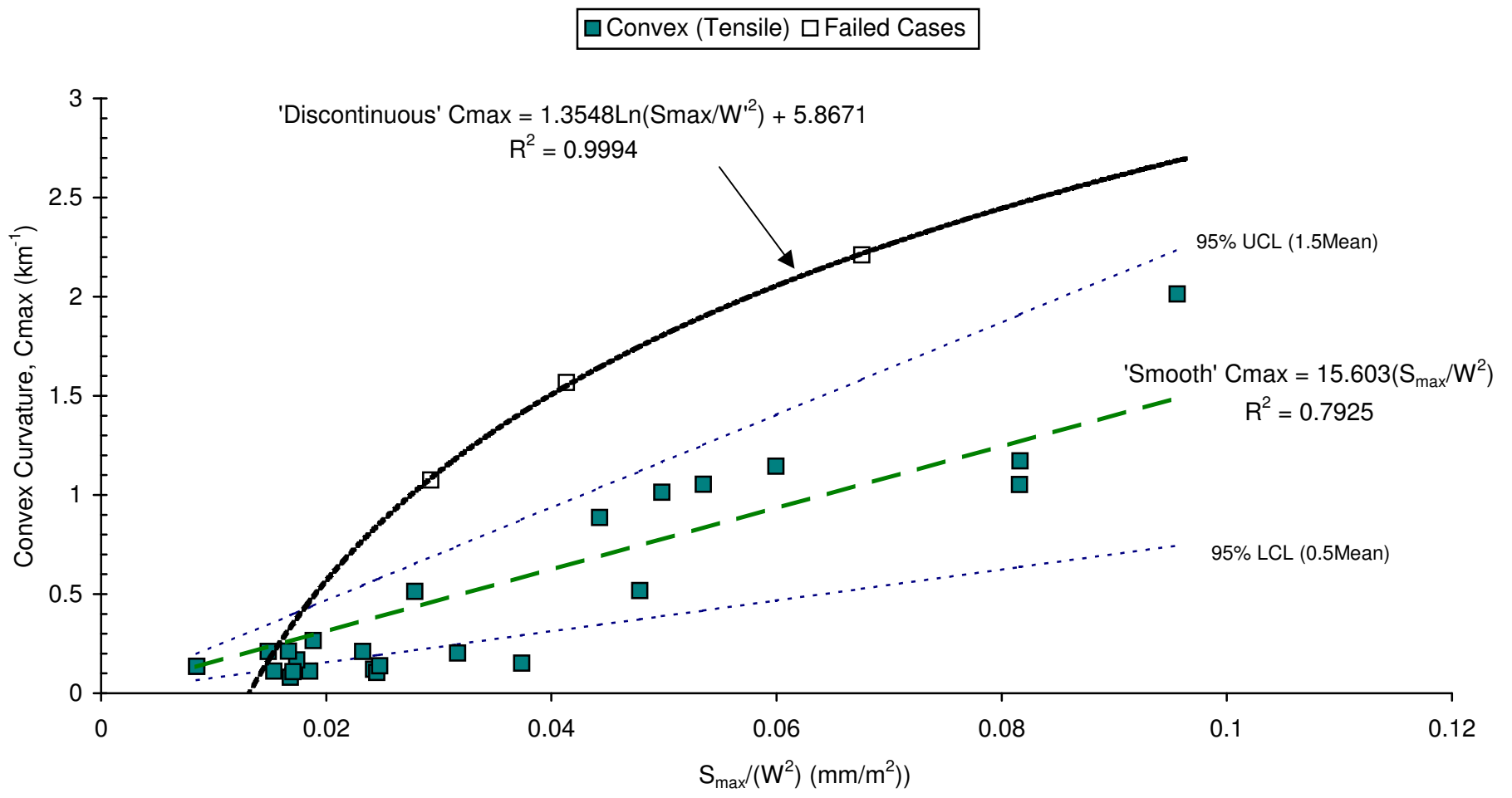
	Engineer:	S.Ditton	Client:	Adapted from ACARP, 2003	
	Drawn:	S.Ditton			
	Date:	08.08.08	Title:	Empirical Model for Goaf Edge Subsidence Prediction Above Longwall Panels	
	Ditton Geotechnical Services Pty Ltd				
Scale:			NTS	Figure No:	A20



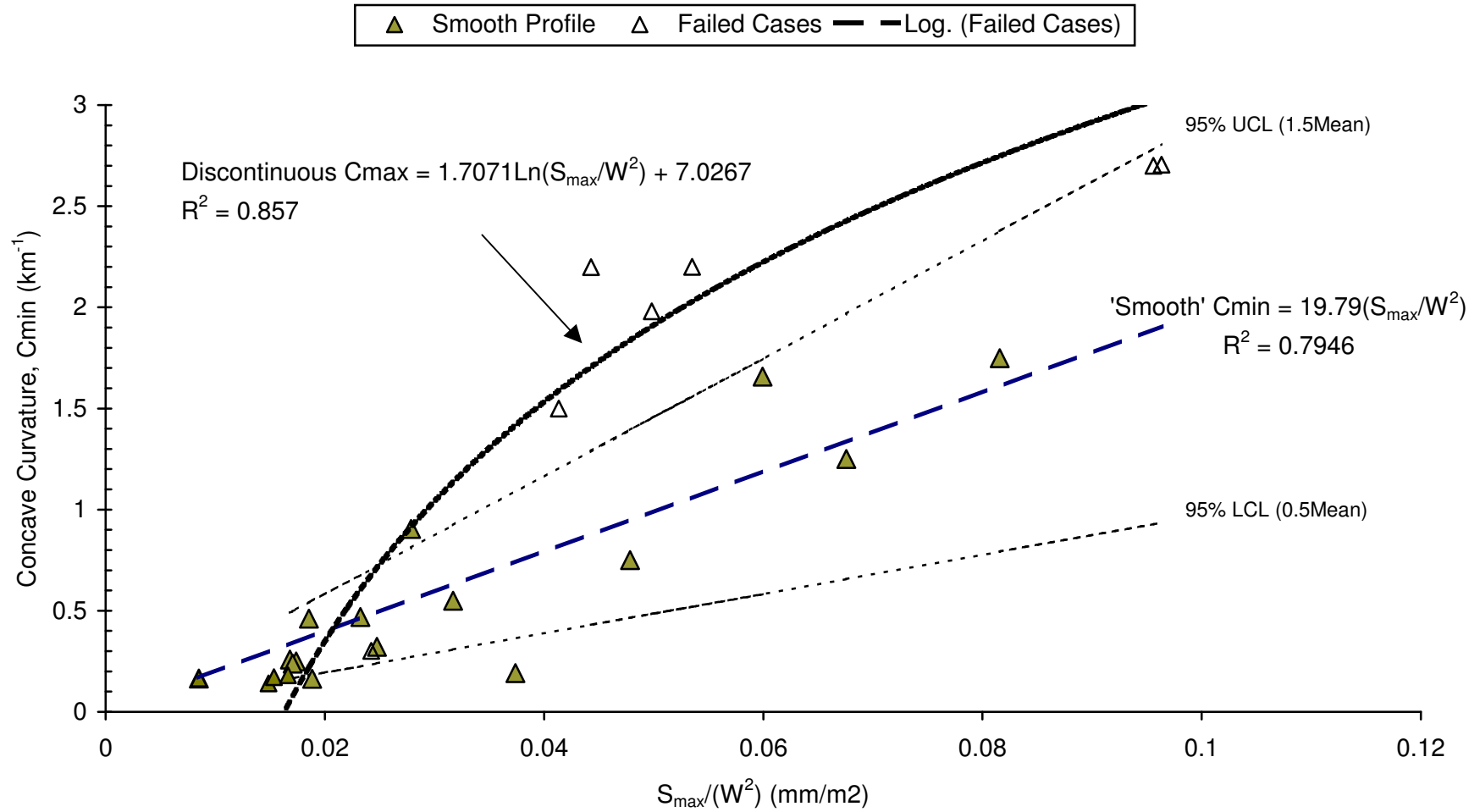
	Engineer:	S.Ditton	Client:	Extracted from ACARP, 2003	
	Drawn:	S.Ditton			
	Date:	08.08.08	Title:	Empirical Prediction Model for Longwall Panel Angle of Draw	
	Ditton Geotechnical Services Pty Ltd				
Scale:	NTS		Figure No:	A21	



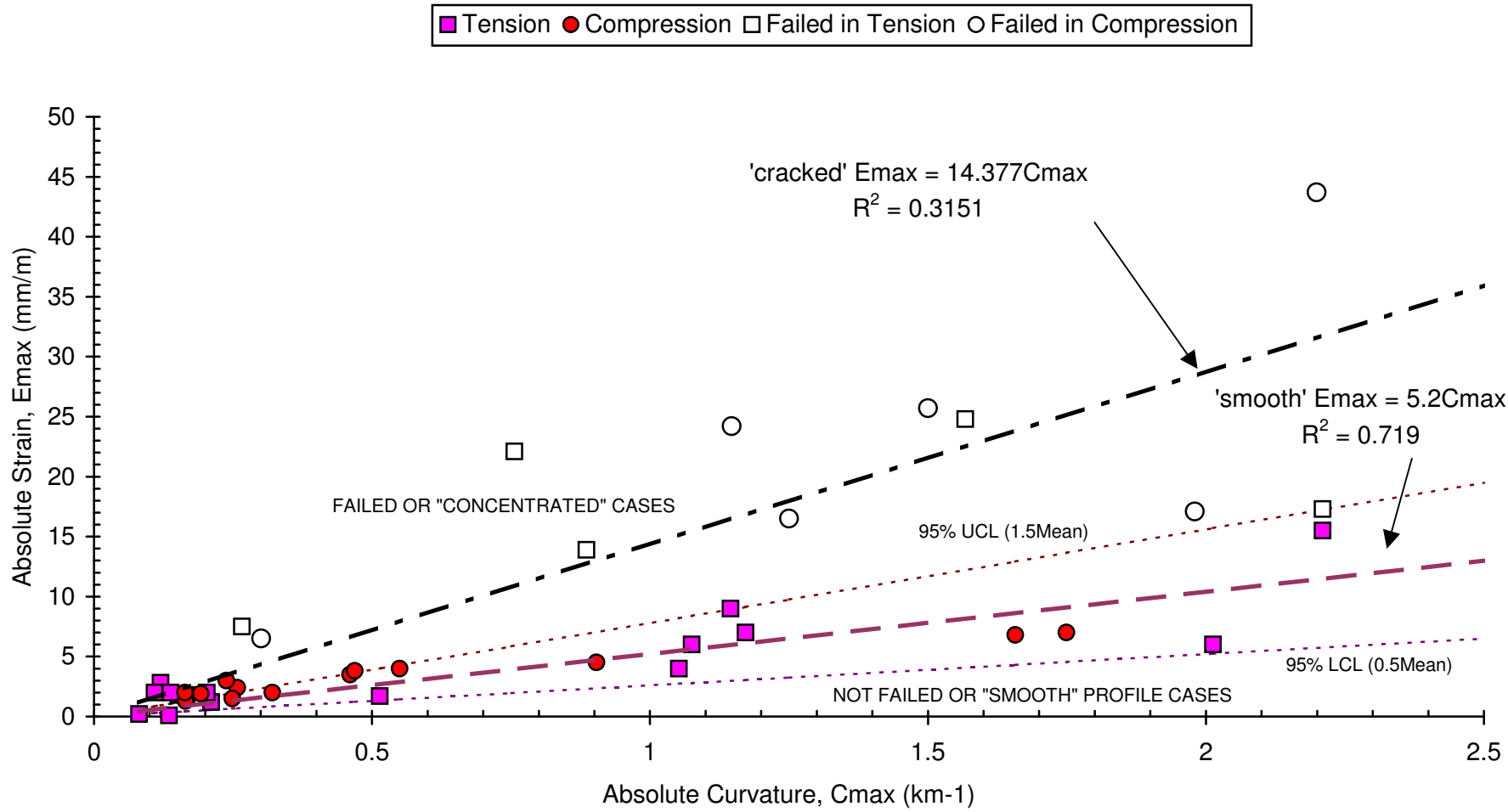
	Engineer:	S.Ditton	Client:	Extract from ACARP, 2003	
	Drawn:	S.Ditton			
	Date:	08.08.08	Title:	Empirical Model for Maximum Panel Tilt Prediction Above Longwall Panels	
	Ditton Geotechnical Services Pty Ltd				
Scale:	NTS		Figure No:	A22	



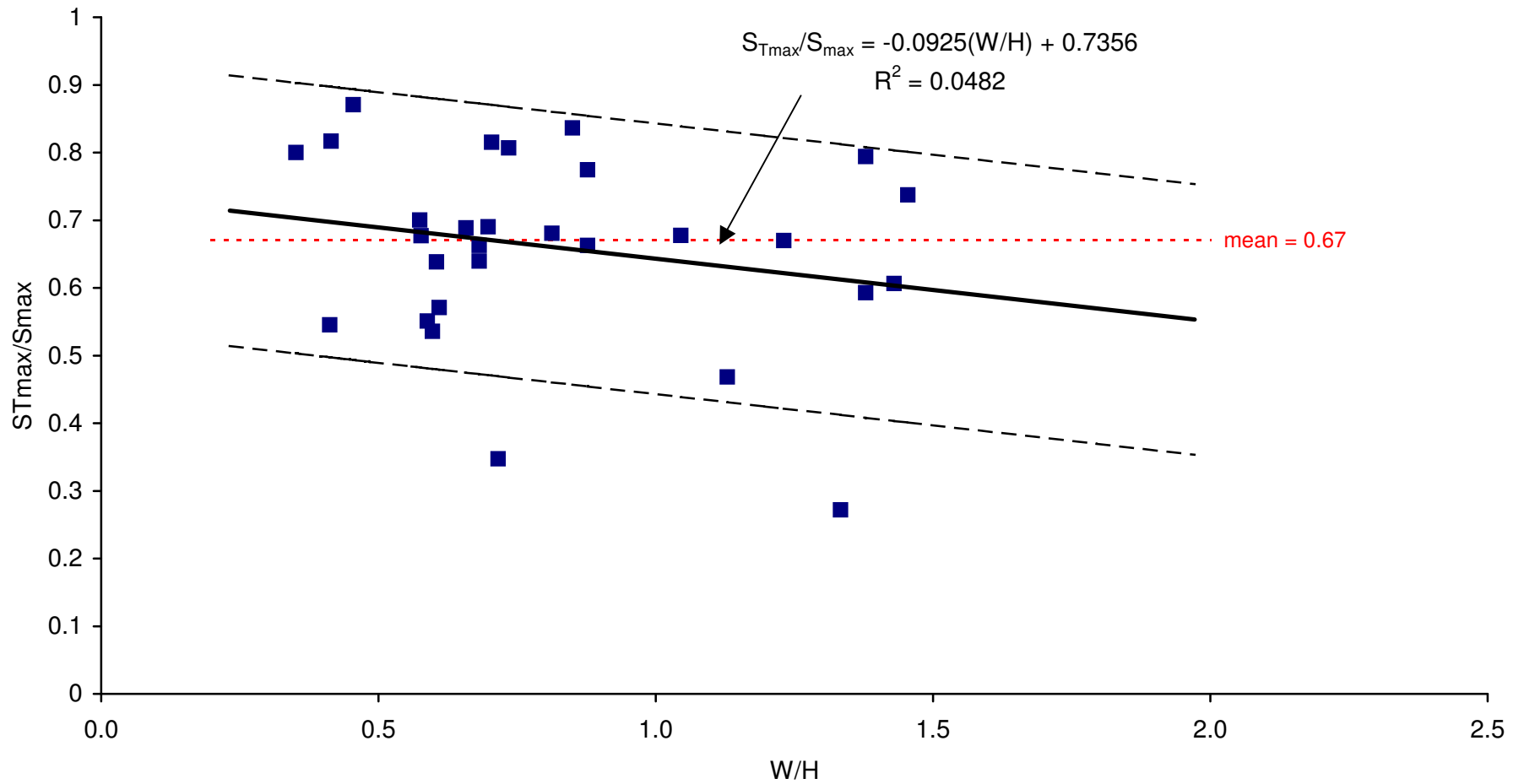
	Engineer:	S.Ditton	Client:	Extract from ACARP, 2003	
	Drawn:	S.Ditton	Title:	Empirical Model for Maximum Panel Convex Curvature Prediction Above Longwall Panels for Smooth and Discontinuous Profiles	
	Date:	08.08.08	Scale:	NTS	Figure No: A23
	Ditton Geotechnical Services Pty Ltd				



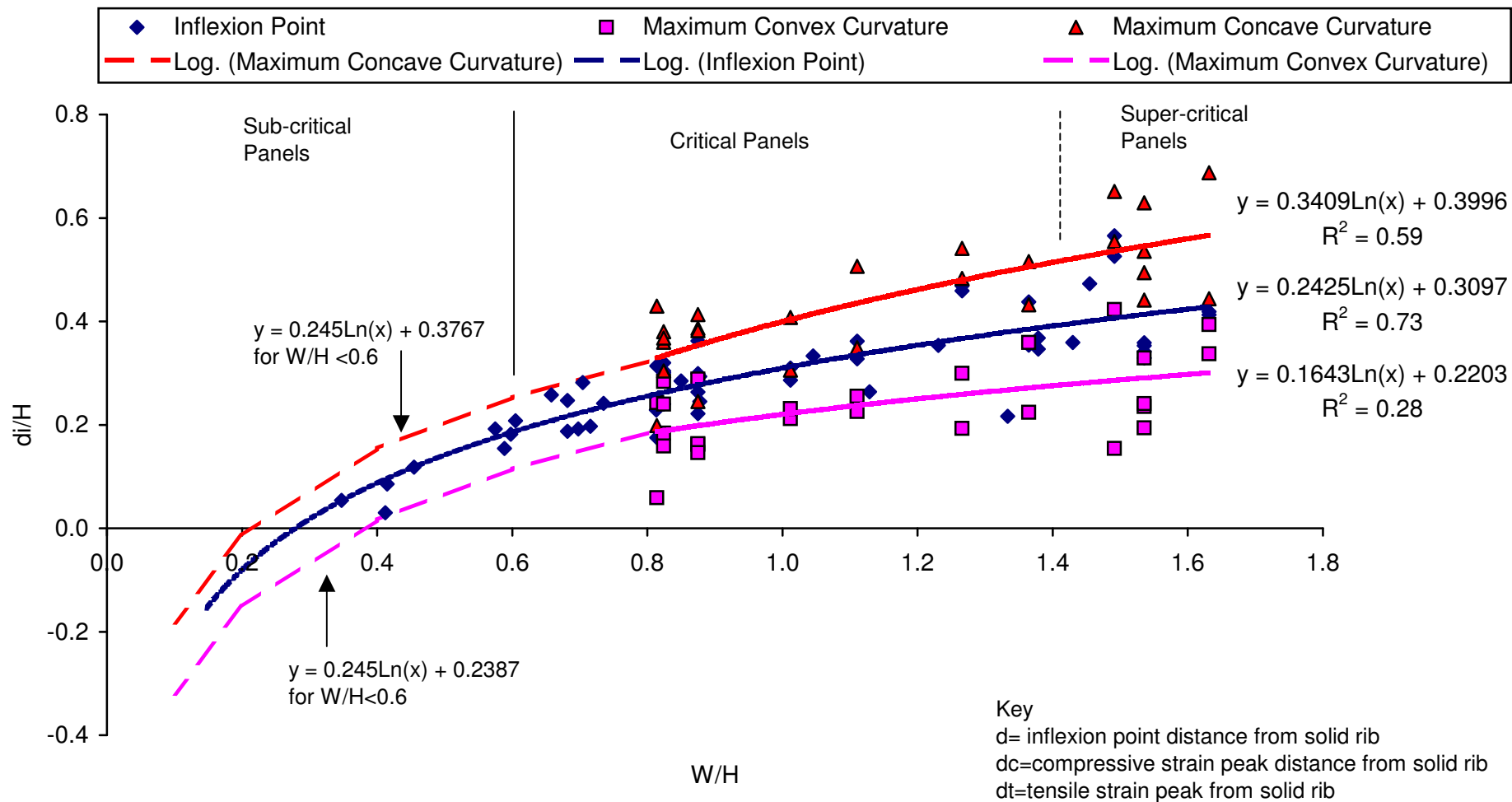
	Engineer:	S.Ditton	Client:	Extract from ACARP, 2003	
	Drawn:	S.Ditton	Title:	Empirical Model for Maximum Panel Concave Curvature Prediction Above Longwall Panels for Smooth and Discontinuous Profiles	
	Date:	08.08.08	Scale:	NTS	Figure No:
	Ditton Geotechnical Services Pty Ltd				A24



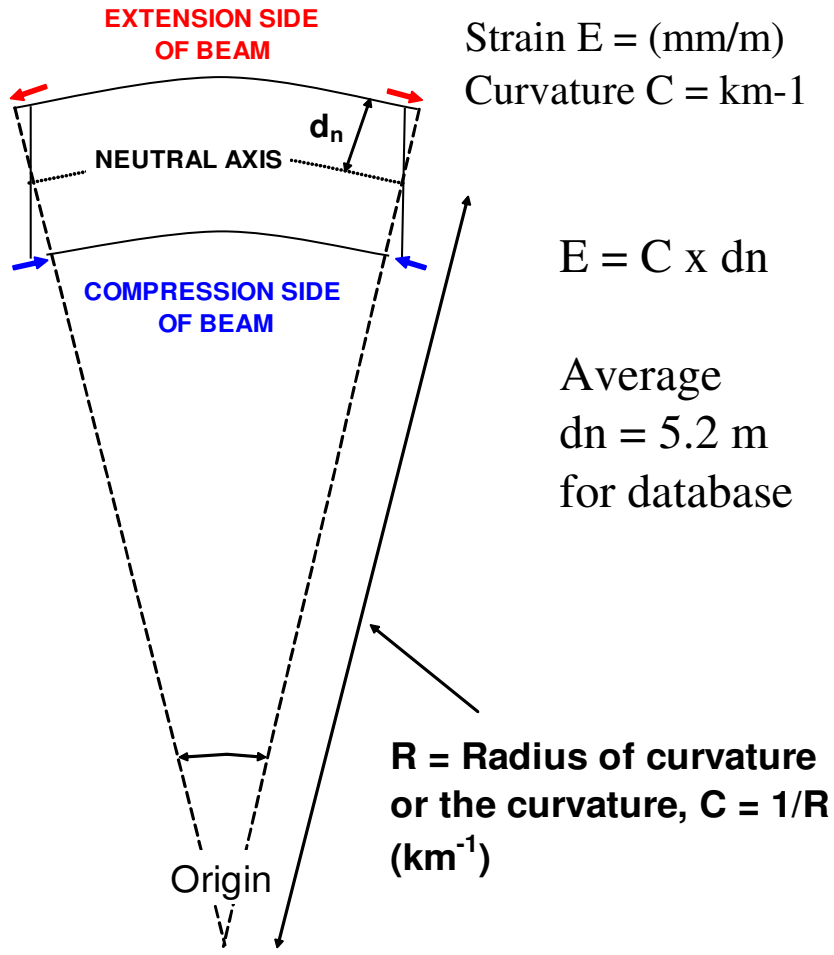
	Engineer:	S.Ditton	Client:	Extract from ACARP, 2003		
	Drawn:	S.Ditton		Title:	Empirical Model for Maximum Panel Strain Prediction Above Longwall Panels for Smooth and Cracked Profiles	
	Date:	08.08.08	Scale:		NTS	
	Ditton Geotechnical Services Pty Ltd				Figure No:	A25



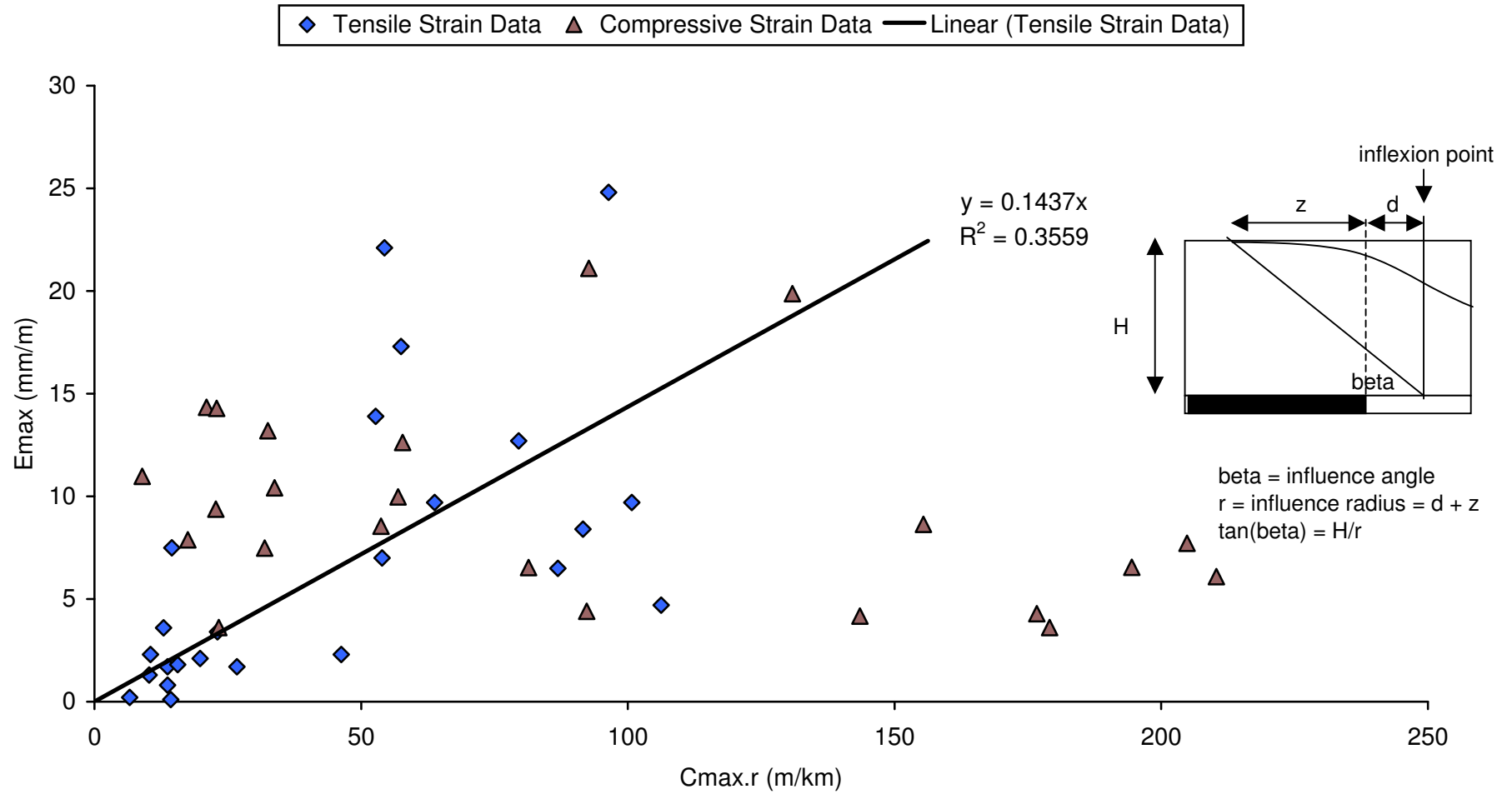
	Engineer:	S.Ditton	Client:	Extract from ACARP, 2003	
	Drawn:	S.Ditton			
	Date:	08.08.08	Title:	Empirical Model for Subsidence at Maximum Tilt Above Longwall Panels	
	Ditton Geotechnical Services Pty Ltd				
Scale:	NTS		Figure No:	A26	



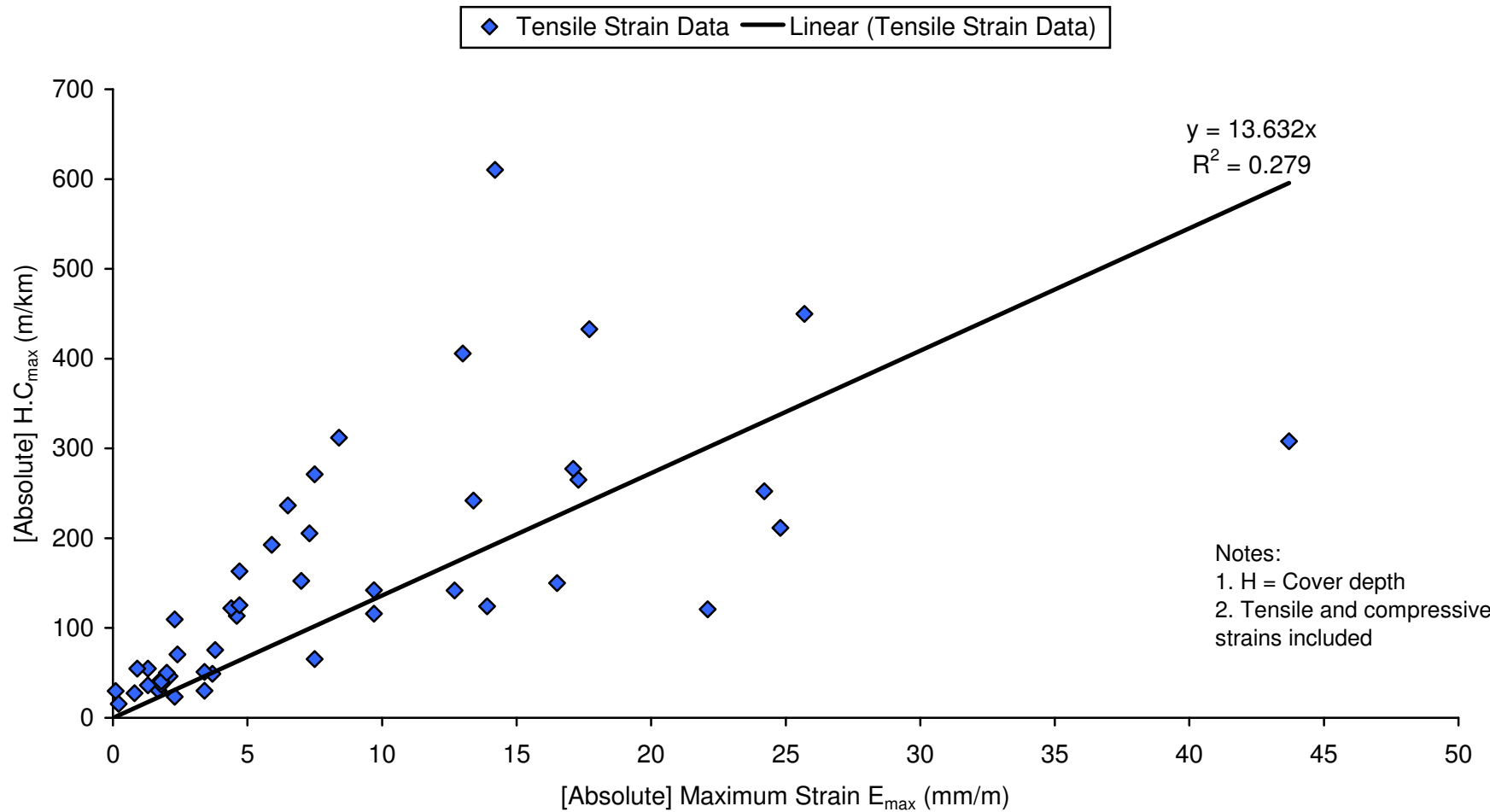
	Engineer:	S.Ditton	Client:	Adapted from ACARP, 2003	
	Drawn:	S.Ditton	Title:	Empirical Model for Predicting the Location of Inflexion Point, Maximum Tensile and Compressive Strain Peaks due to Longwall Panel Subsidence in the Newcastle Coalfield	
	Date:	08.08.08	Scale:	NTS	Figure No:
	Ditton Geotechnical Services Pty Ltd				A27



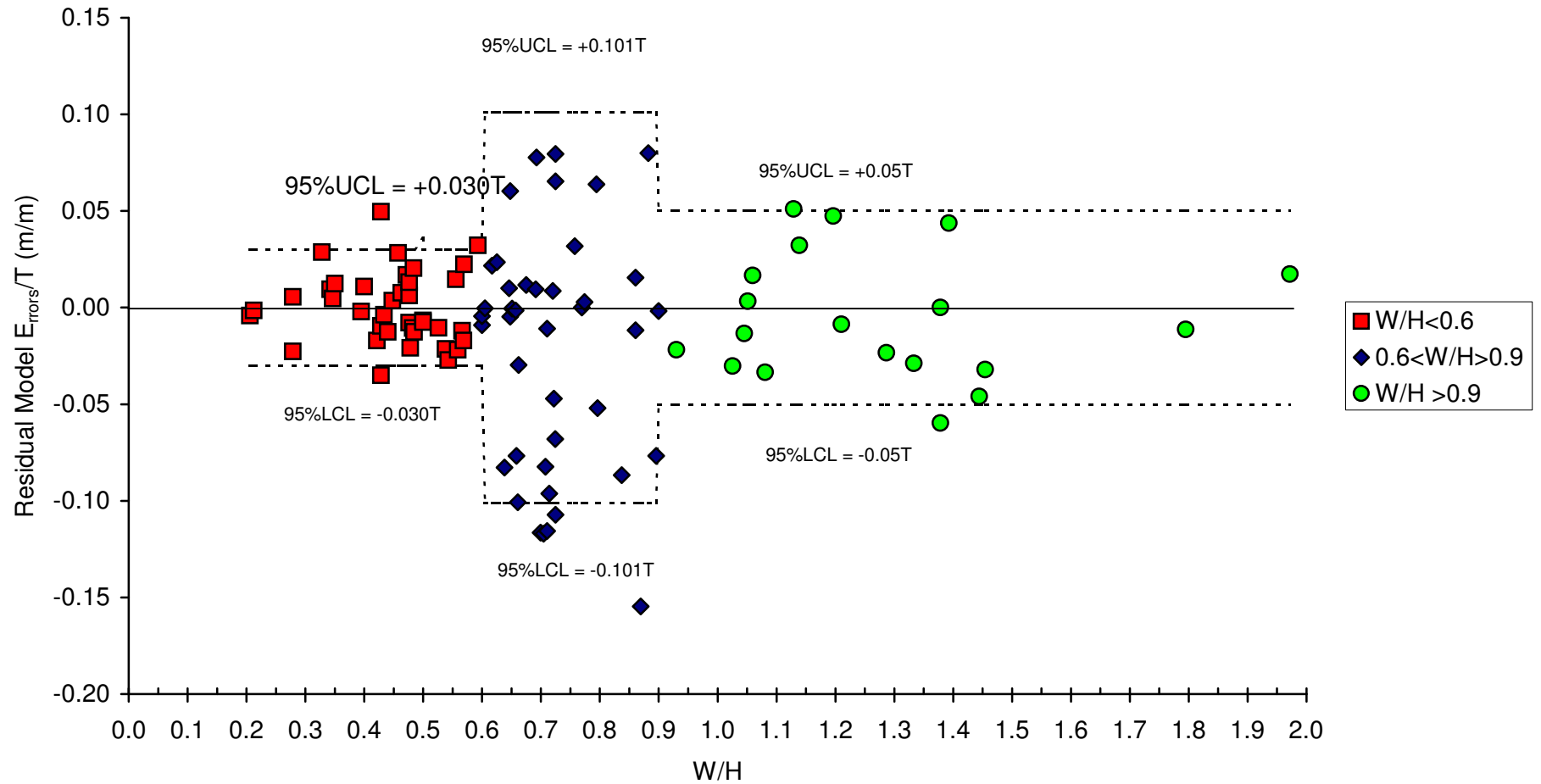
	Engineer:	S.Ditton	Client:	Extract from ACARP, 2003	
	Drawn:	S.Ditton			
	Date:	08.08.08	Title:	Bending Beam Theory for Strain Prediction from Curvature Measurements	
	Ditton Geotechnical Services Pty Ltd		Scale:		Figure No:



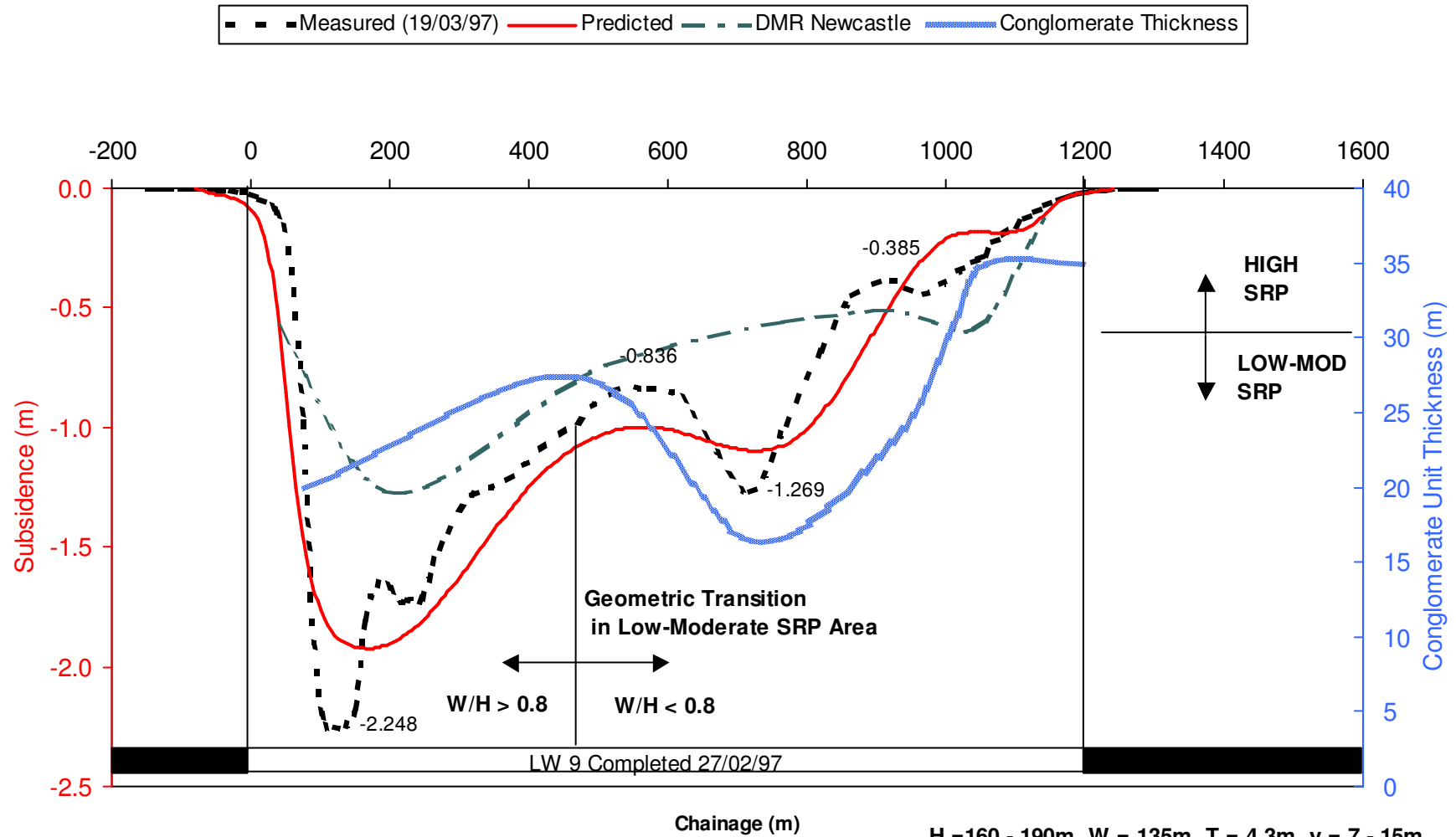
	Engineer:	S.Ditton	Client:	Karmis, 1987 Adapted for ACARP, 2003	
	Drawn:	S.Ditton	Title:	Empirical Model Recommended by Karmis et al, 1987 for Predicting Strain from Curvature	
	Date:	08.08.08	Above Longwall Panels in Newcastle Coalfield		
	Ditton Geotechnical Services Pty Ltd		Scale:	NTS	Figure No:



	Engineer:	S.Ditton	Client:	Holla and Barclay, 2000 Adapted for ACARP, 2003	
	Drawn:	S.Ditton			
	Date:	08.08.08	Title:	Empirical Model Recommended by Holla and Barclay, 2000 for Predicting Curvature from Maximum Strain Above Longwall Panels in the Newcastle Coalfield	
	Ditton Geotechnical Services Pty Ltd			Scale:	NTS



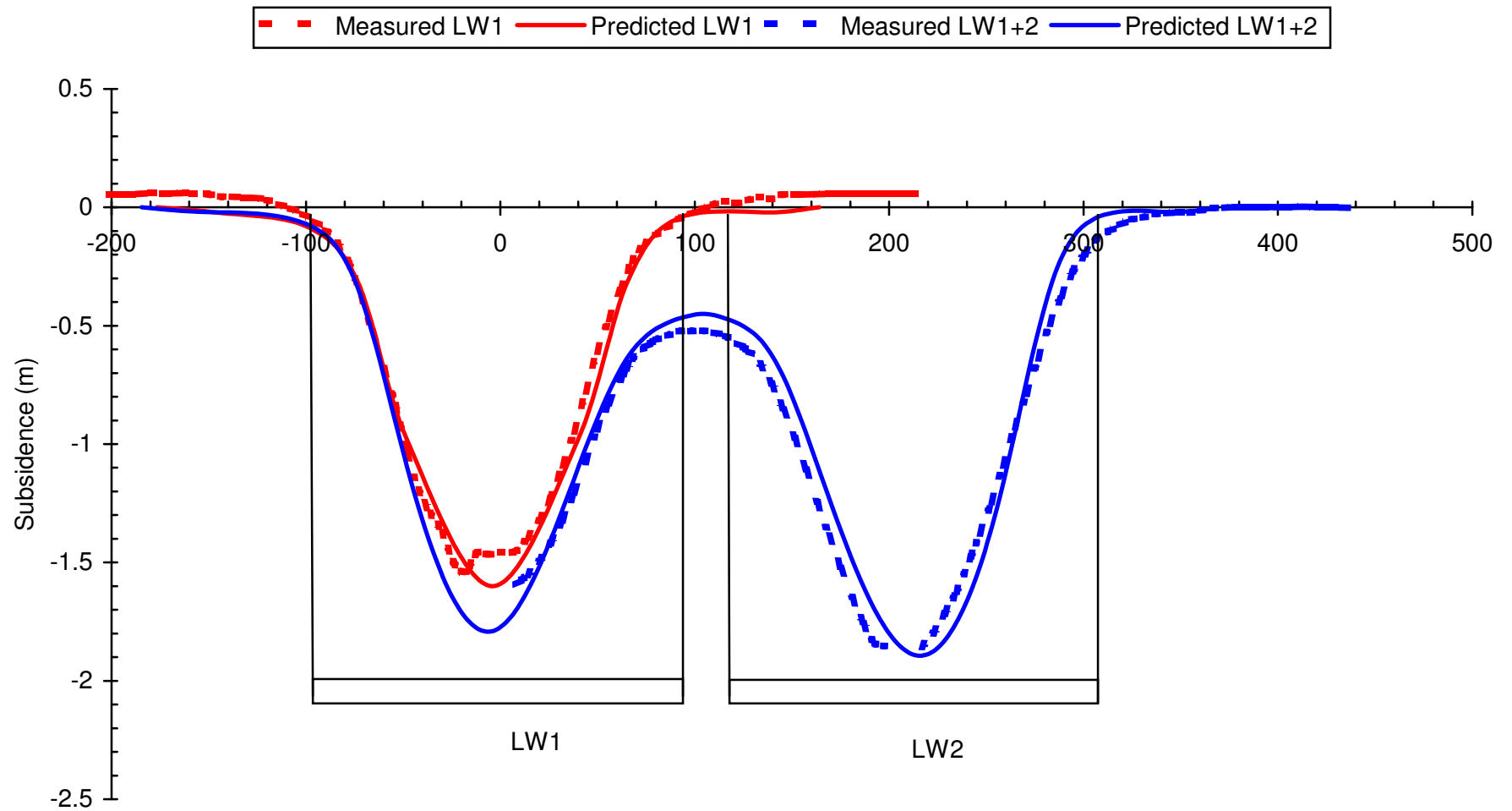
	Engineer:	S.Ditton	Client:	Extract from ACARP, 2003	
	Drawn:	S.Ditton	Title:	Residual Errors of Database for Single Panel Prediction Model above Longwalls in the Newcastle Coalfield	
	Date:	08.08.08	Scale:	NTS	Figure No:
	Ditton Geotechnical Services Pty Ltd				A30



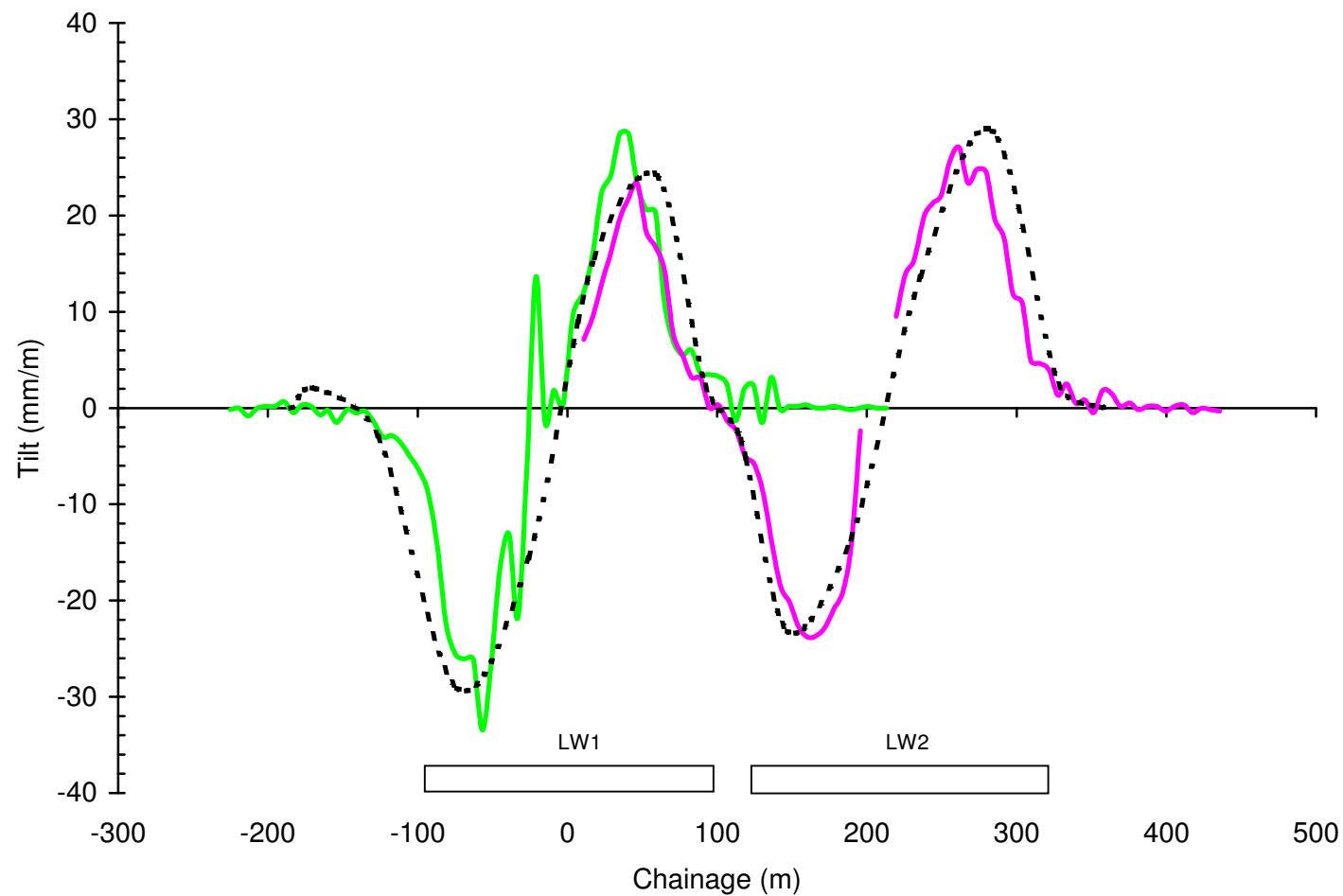
Chainage (m)

H = 160 - 190m, W = 135m, T = 4.3m, y = 7 - 15m

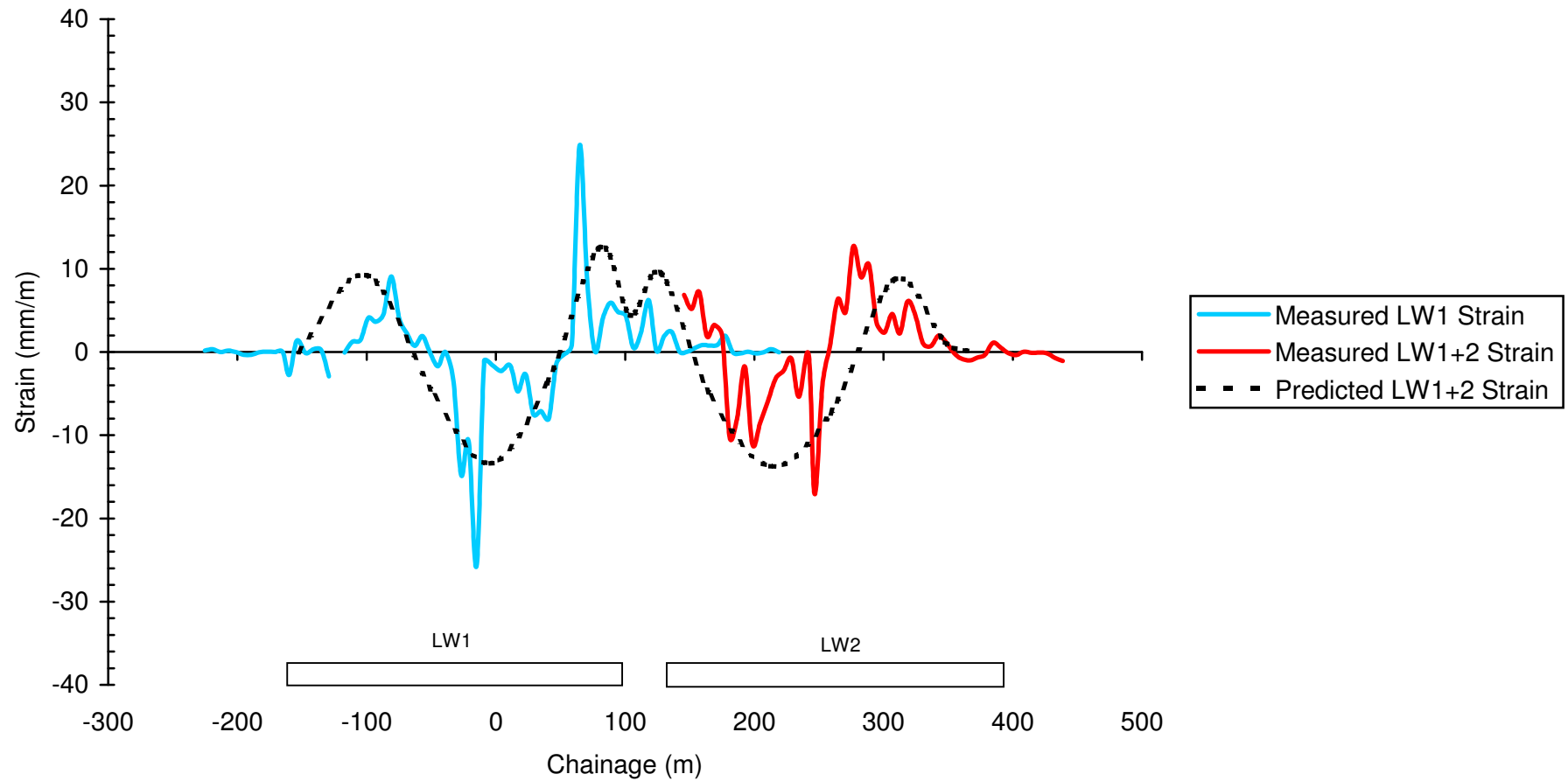
	Engineer:	S.Ditton	Client:	Extract from ACARP, 2003	
	Drawn:	S.Ditton	Title:	Predicted v. Measured Centreline Subsidence Profiles for a Newcastle Coalfield Longwall with Massive Conglomerate Strata and Sub-Critical to Supercritical Transition	
	Date:	08.08.08	Scale:	NTS	Figure No:
	Ditton Geotechnical Services Pty Ltd				A31



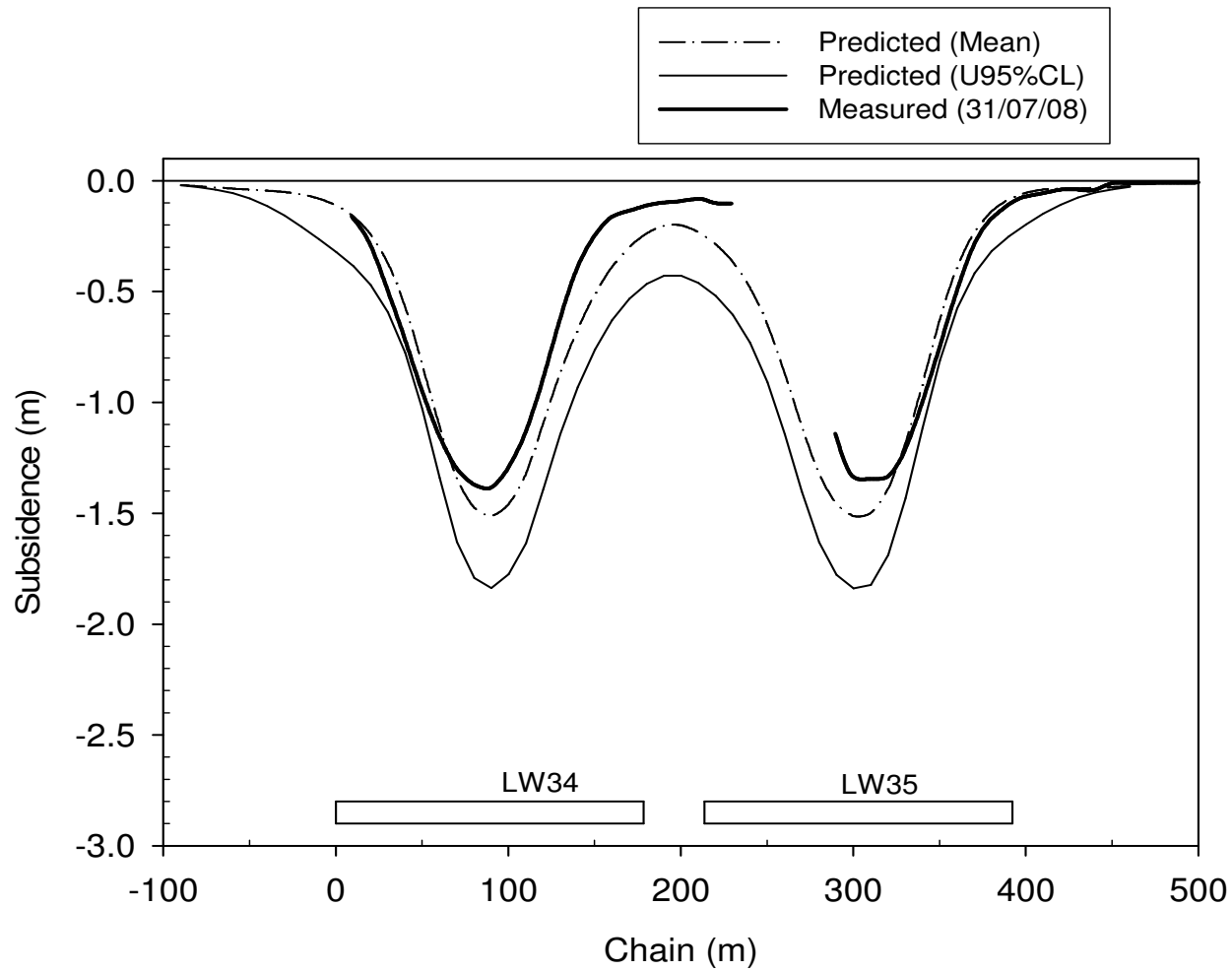
	Engineer:	S.Ditton	Client:	Extract from ACARP, 2003	
	Drawn:	S.Ditton			
	Date:	08.08.08	Title:	Predicted v. Measured Crossline Subsidence Profiles for a Newcastle Coalfield Longwall Mine	
	Ditton Geotechnical Services Pty Ltd			Scale:	NTS



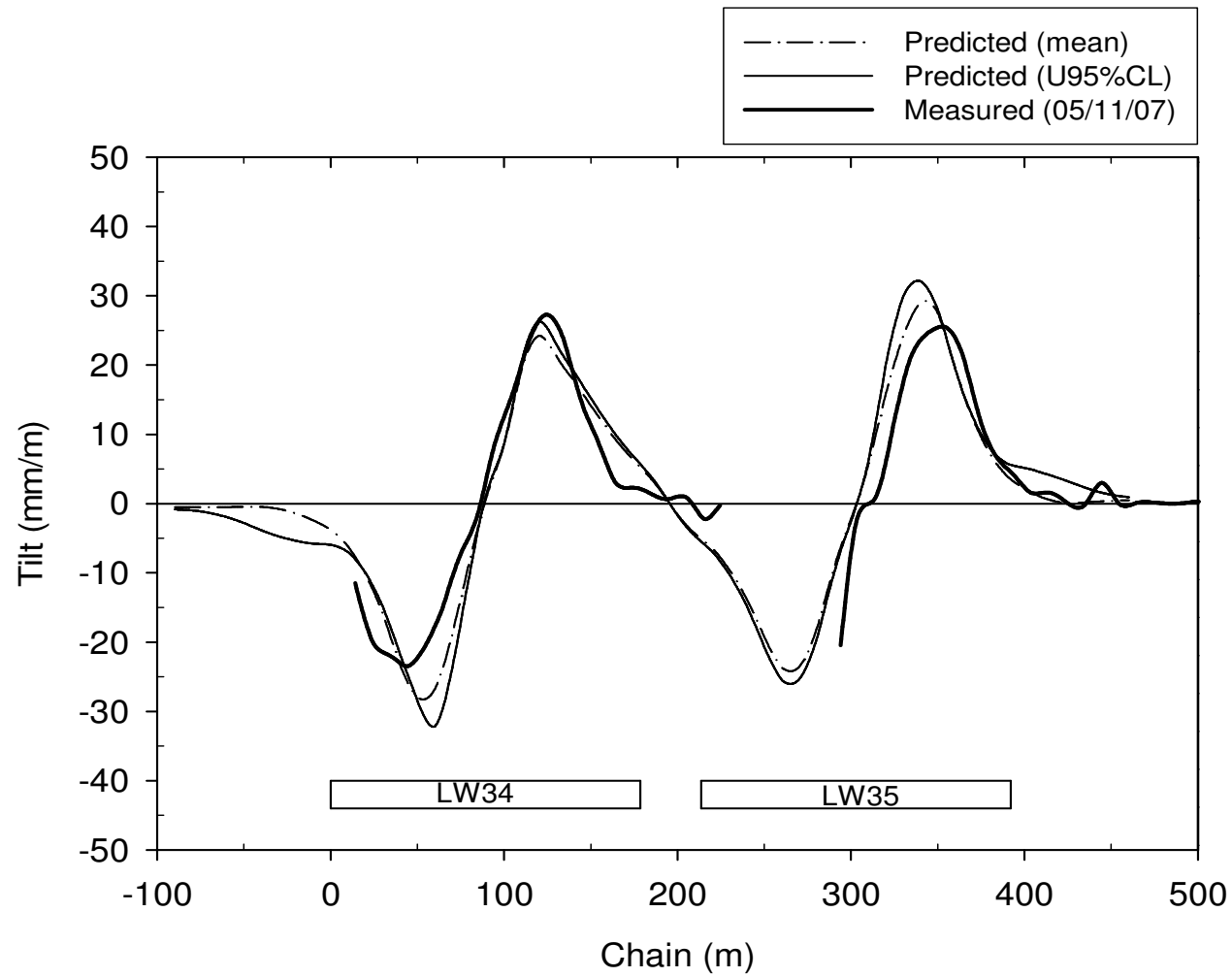
	Engineer:	S.Ditton	Client:	Extract from ACARP, 2003		
	Drawn:	S.Ditton		Title:	Predicted v. Measured Crossline Tilt Profiles for a Newcastle Coalfield Longwall Mine	
	Date:	08.08.08	Scale:		NTS	Figure No:
	Ditton Geotechnical Services Pty Ltd					



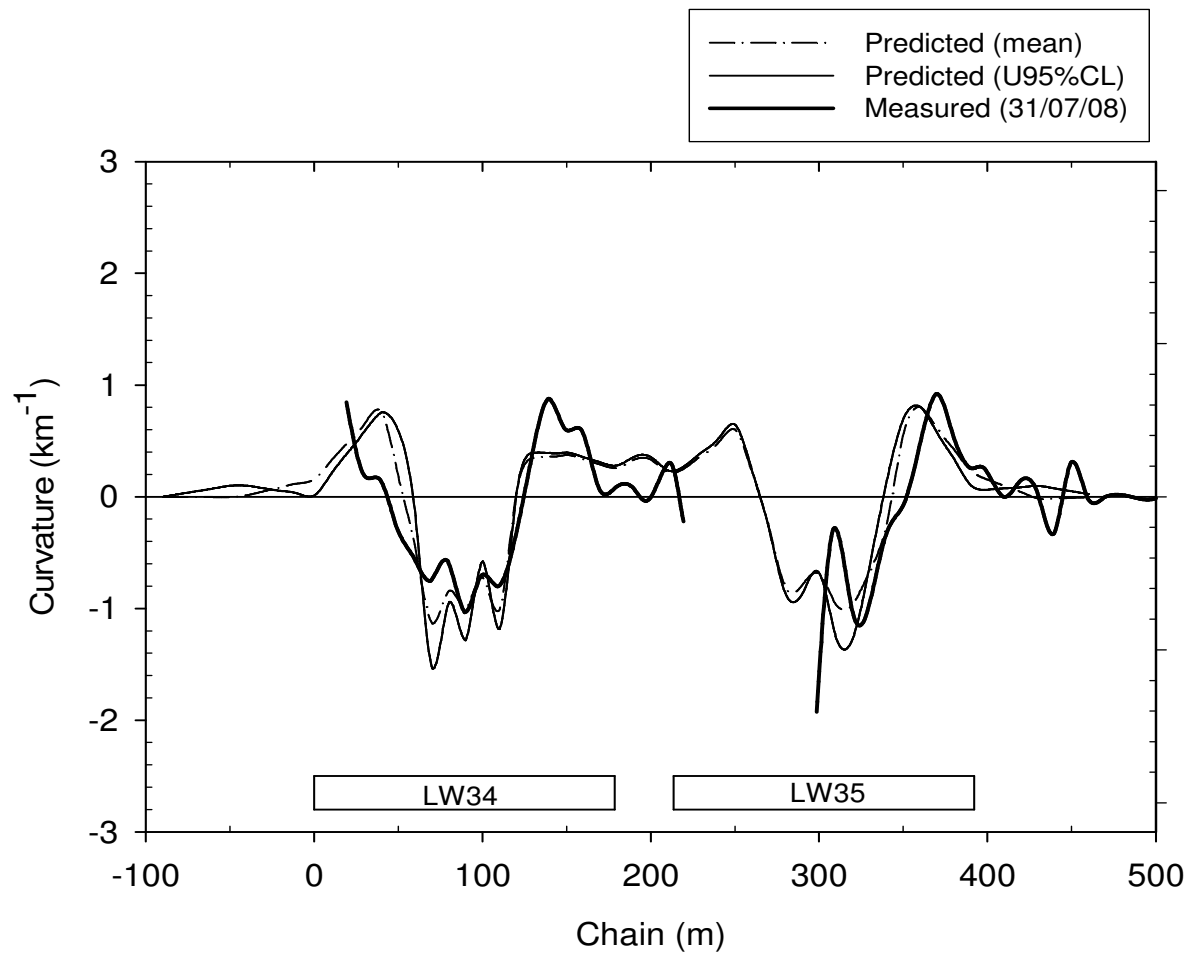
	Engineer:	S.Ditton	Client:	Extract from ACARP, 2003		
	Drawn:	S.Ditton		Title:	Predicted v. Measured Crossline Strain Profiles for a Newcastle Coalfield Longwall Mine	
	Date:	08.08.08	Scale:		NTS	Figure No:
	Ditton Geotechnical Services Pty Ltd					



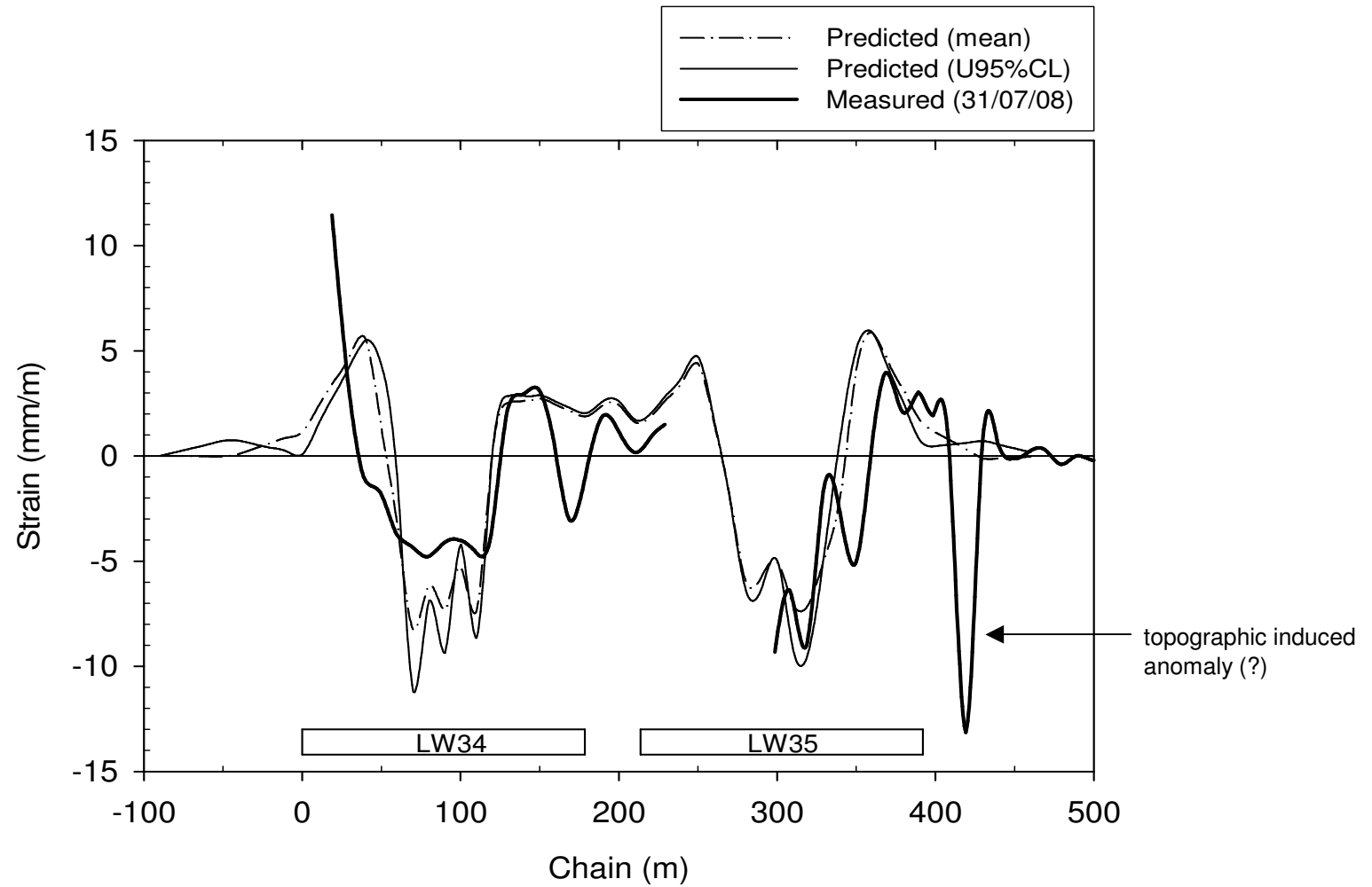
	Engineer:	S.Ditton	Client:	DgS, 2008 Modified ACARP, 2003 Model Outcomes	
	Drawn:	S.Ditton			
	Date:	07.09.08	Title:	Predicted v. Measured Crossline Subsidence Profiles for a Newcastle Coalfield Longwall Longwall Panel	
	Ditton Geotechnical Services Pty Ltd			Scale:	NTS



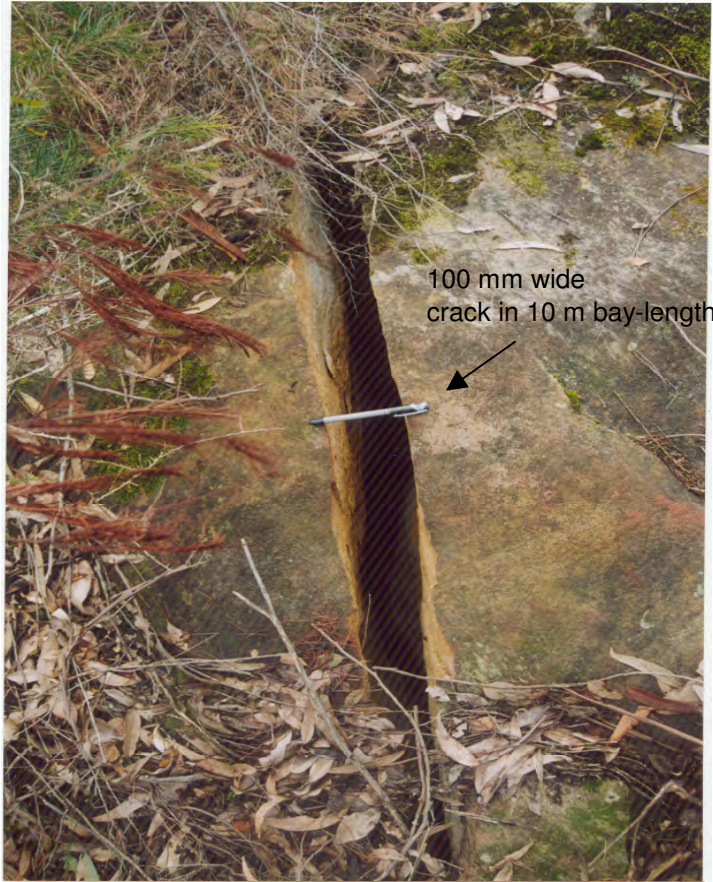
	Engineer:	S.Ditton	Client:	DgS, 2008 Modified ACARP, 2003 Model Outcomes		
	Drawn:	S.Ditton		Title:	Predicted v. Measured Crossline Tilt Profiles for a Newcastle Coalfield Longwall Mine	
	Date:	07.09.08	Scale:		NTS	Figure No: A36
	Ditton Geotechnical Services Pty Ltd					



	Engineer:	S.Ditton	Client:	DgS, 2008 Modified ACARP, 2003 Model Outcomes			
	Drawn:	S.Ditton		Title:	Predicted v. Measured Crossline Curvature Profiles for a Newcastle Coalfield Longwall Mine		
	Date:	07.09.08	Scale:		NTS	Figure No:	A37
	Ditton Geotechnical Services Pty Ltd						



	Engineer:	S.Ditton	Client:	DgS, 2008 Modified ACARP, 2003 Model Outcomes	
	Drawn:	S.Ditton	Title:	Predicted v. Measured Crossline Strain Profiles for a Newcastle Coalfield Longwall Mine	
	Date:	08.09.08	Scale:	NTS	Figure No:
	Ditton Geotechnical Services Pty Ltd				A38



Strain Concentration Factor Calculation for 10 m Baylength[^]

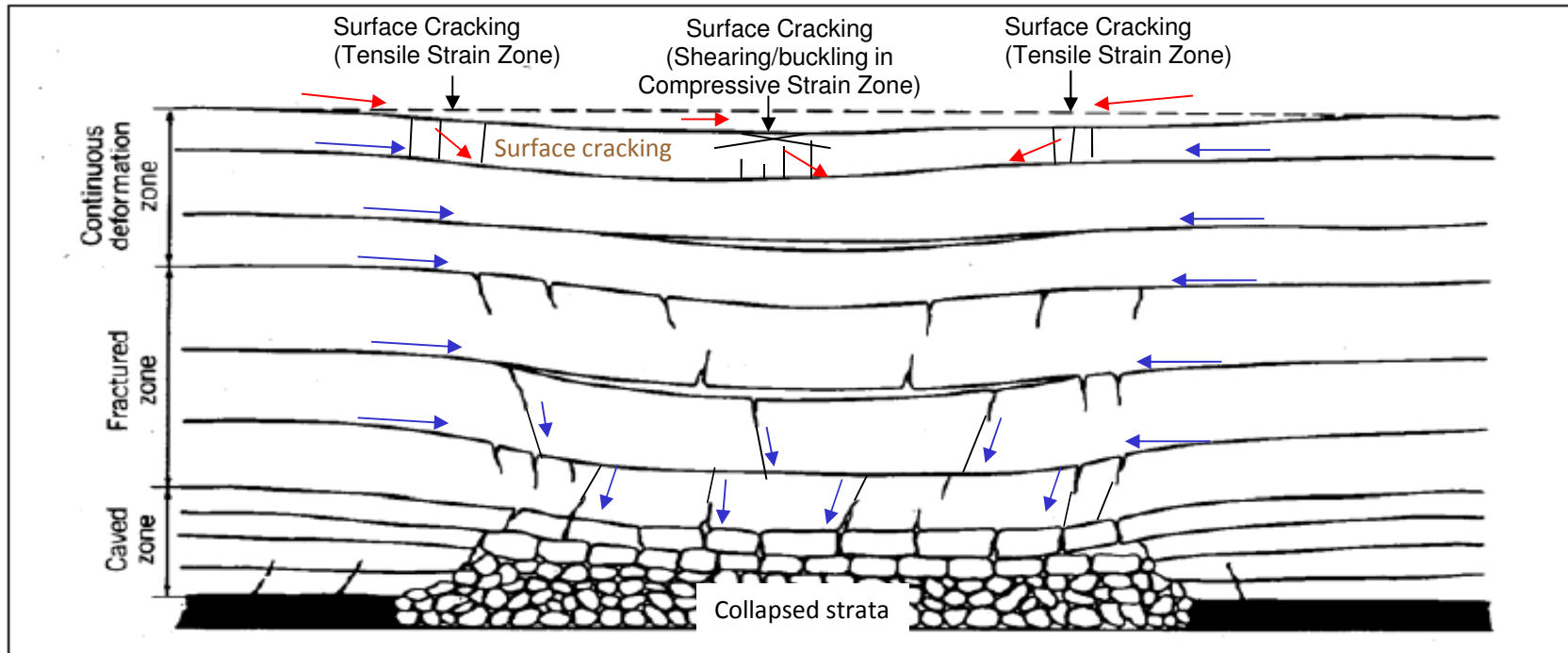
- Measured crack width = 100 mm.
- Measured crack depth >5 m
- Location = 27 m from solid rib.
S_{max} = 1.4 m.
- Cover depth, H = 180 m.
- LW panel width, W= 175 m.
(W/H = 0.97)
- Measured curvature,
C = 1.15 km⁻¹
(radius of 867 m)
- Measured strain over 10 m,
E = 5.8 mm/m*
- Concentrated strain = crack width/bay-length = 100/10 = 10 mm/m.

Therefore, concentrated strain = 10/5.8 = 1.7 x uniform strain.

*- peak strains measured 10 m to south of crack at same distance from rib.

[^] - It is likely that strain concentration includes strain from adjacent 'bays'.

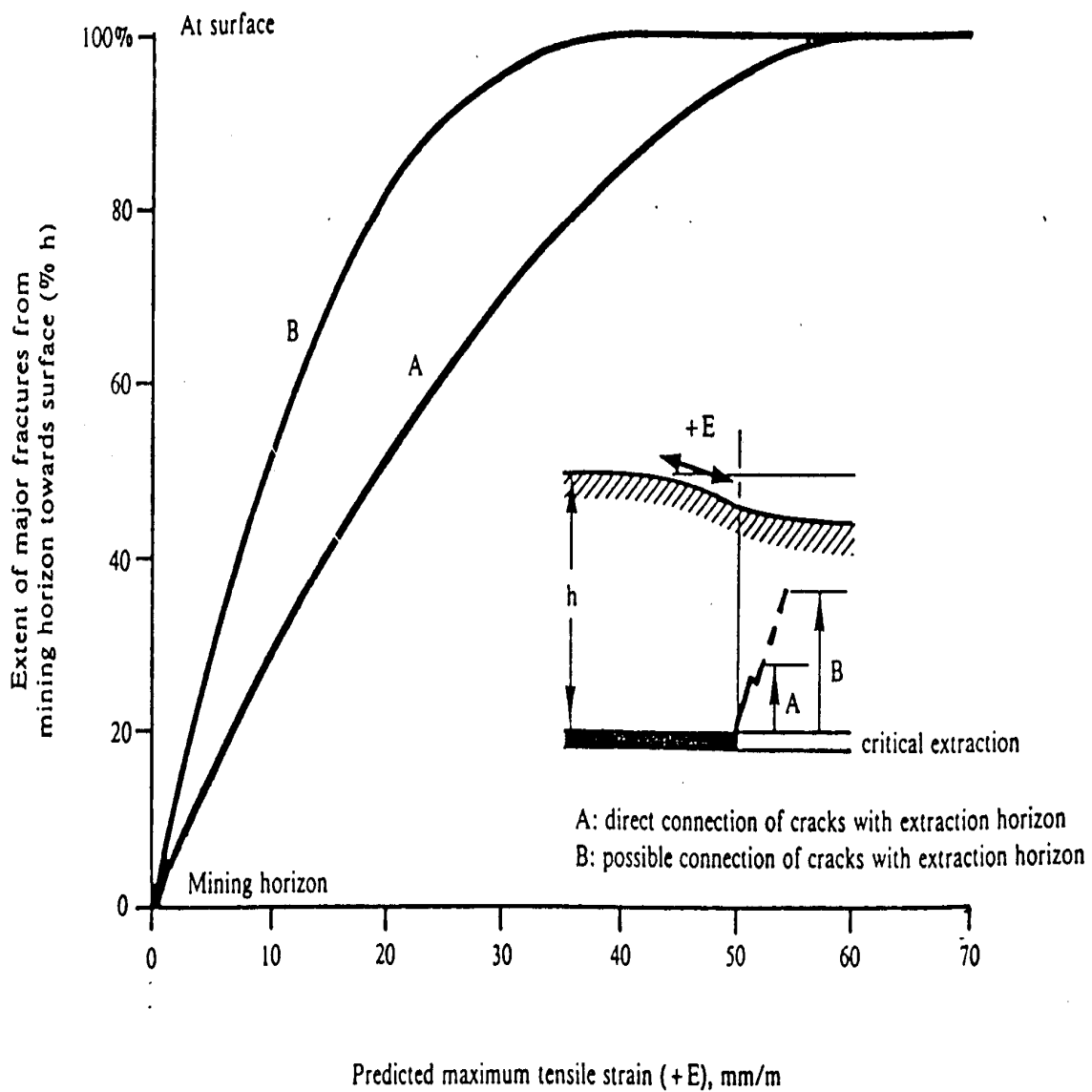
	Engineer:	S.Ditton	Client:	Adapted from ACARP, 2003		
	Drawn:	S.Ditton				
	Date:	08.08.08	Title:	Example of Strain Concentration Effect Above Longwall with Shallow Surface Rock		
	Ditton Geotechnical Services Pty Ltd					
Scale:	NTS		Figure No:	A39		



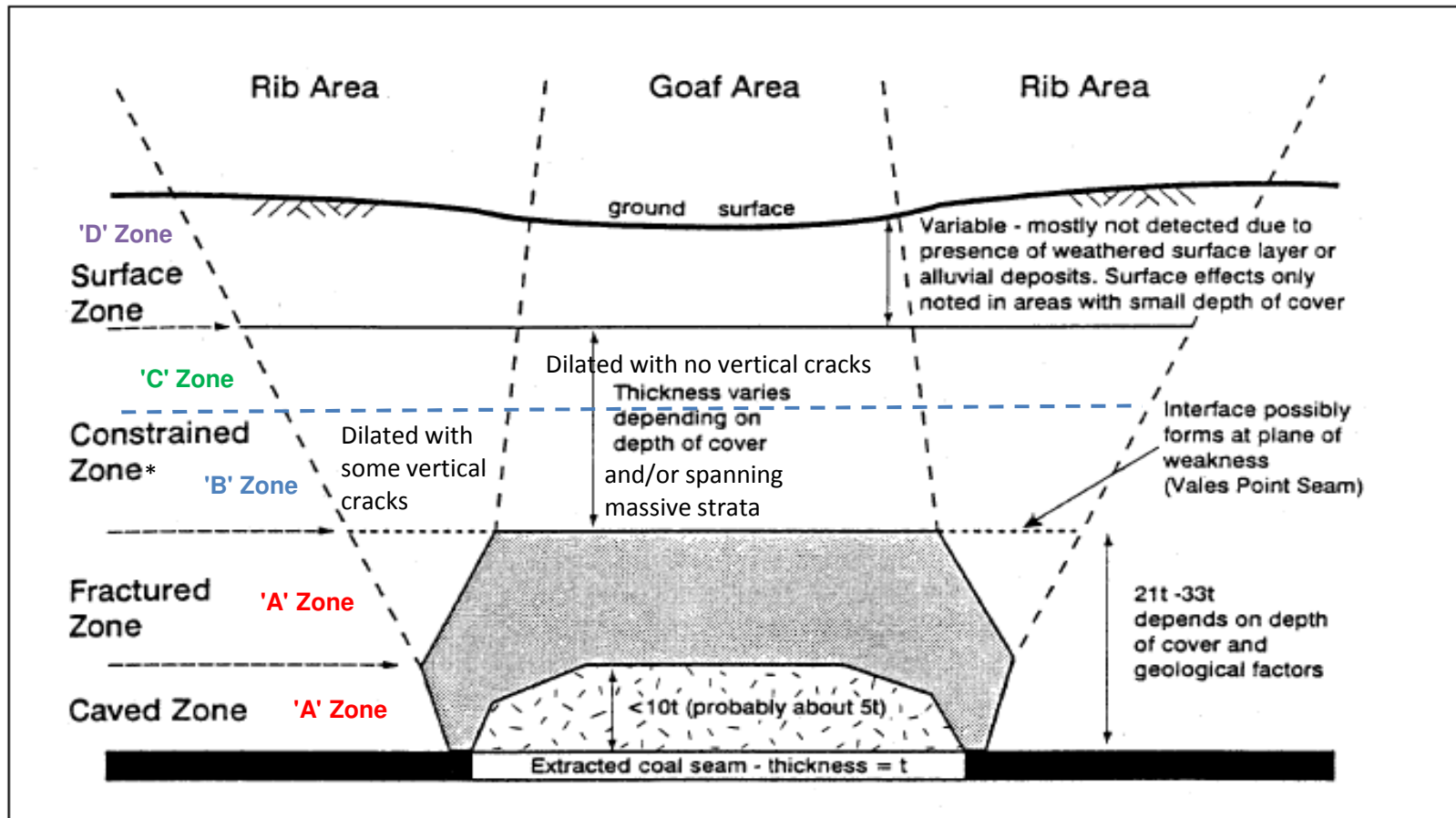
Zones in the Overburden According to Peng and Chiang (1984)

Key
 → Surface water flow path → Sub-surface water flow path

	Engineer: S.Ditton	Client: Appendix A	Title: Schematic Model of Overburden Fracture Zones Above Longwall Panels	
	Drawn: S.Ditton			
	Date: 23.11.12	Scale: NTS	Figure No: A40a	
	Ditton Geotechnical Services Pty Ltd			



Engineer:	S.Ditton	Client:	Extract from ACARP, 2003
Drawn:	S.Ditton		
Date:	30.04.07	Title:	Empirically Based Sub-Surface Fracturing Model Presented in Whittaker & Reddish, 1989
Ditton Geotechnical Services Pty Ltd		Scale:	NTS
		Figure No:	A40b



Zones in the Overburden according to Forster (1995)

* - Constrained Zone generally means B-Zone, but may include C-Zone, depending on W/H ratio and geology

	Engineer:	S.Ditton	Client:	Appendix A
	Drawn:	S.Ditton	Title:	Schematic Model of Overburden Fracture Zones in Forster, 1995 Model (based on Piezometric Data Above High Extraction Panels in the Newcastle Coalfield)
	Date:	23.11.12	Scale:	NTS
	Ditton Geotechnical Services Pty Ltd		Figure No:	A40c

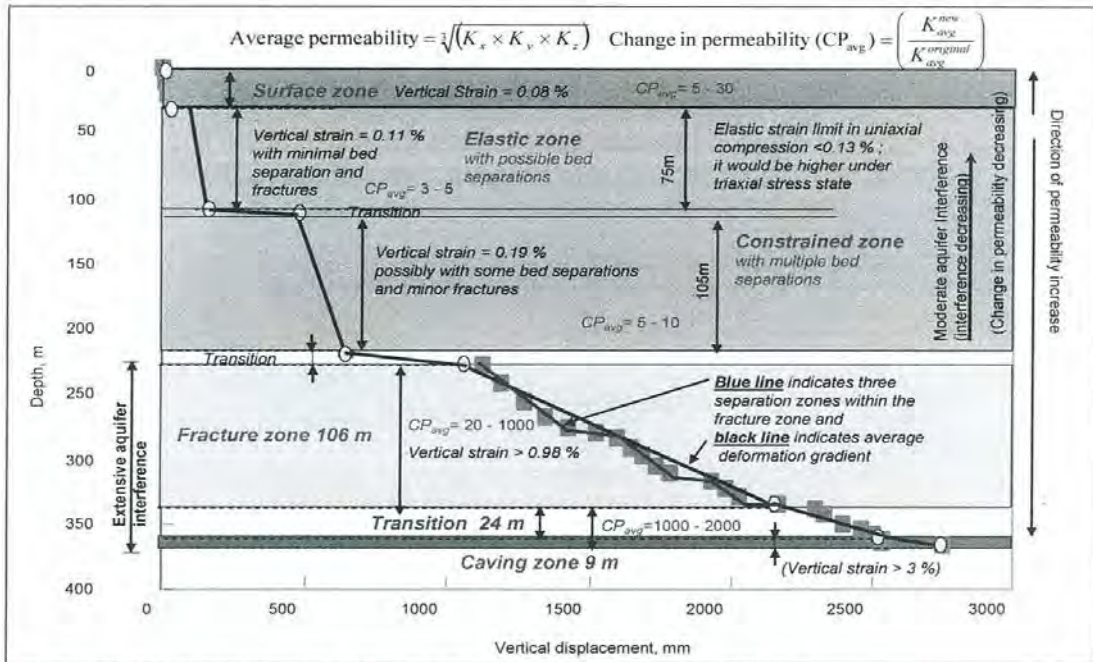


Figure H. Hydrogeological response model for Springvale Colliery

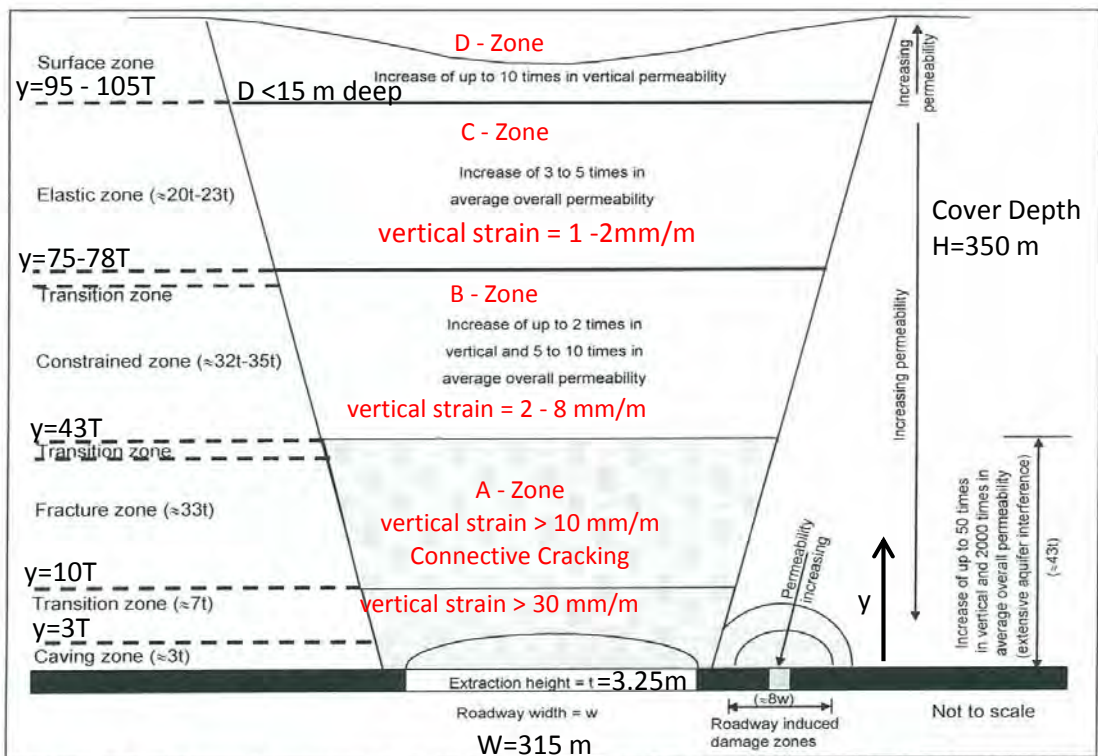


Figure I. A schematic representation of the hydrogeological response model of Springvale Colliery

	Engineer:	S.Ditton	Client:	Appendix A
	Drawn:	S.Ditton		
	Date:	23.11.12	Title:	Schematic Model of Overburden Fracture Zones in ACARP, 2007
	Ditton Geotechnical Services Pty Ltd		Scale:	Figure No: A40d

Figure 6 is a conceptual model that illustrates the type of damage that can be expected within the overburden due to subsidence above a full-extraction panel. Five broad zones can be identified [Singh and Kendorski 1981; Peng and Chiang 1984; Kendorski 1993, 2006]:

1. The *complete caving zone*, in which the roof rock is completely disrupted as it falls into the gob, normally extends two to four times the extracted seam height (h).
2. The *partial caving zone*, in which the beds are completely fractured but never lose contact with one another, extends up to $6-10 h$.
3. The *fracture zone*, within which the subsidence strains are great enough to cause new fracturing in the rock and create direct hydraulic connections to the lower seam. The top of this zone can be as high as $24 h$ above the lower seam.
4. The *dilated zone*, where the permeability is enhanced but little new fracturing is created, extends up to $60 h$.
5. The *confined zone*, where subsidence normally causes no change in strata properties other than occasional bed slippage. This zone extends from the top of the dilated zone to about 50 ft below the surface.

6. D - Zone (<15 m)

5. C - Zone

4. B - Zone

3. A - Zone

1, 2. A - Zone

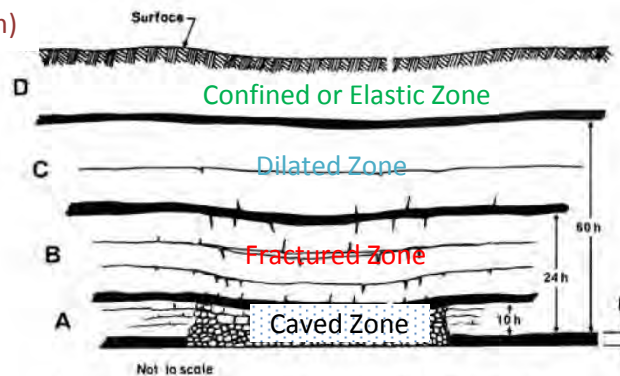


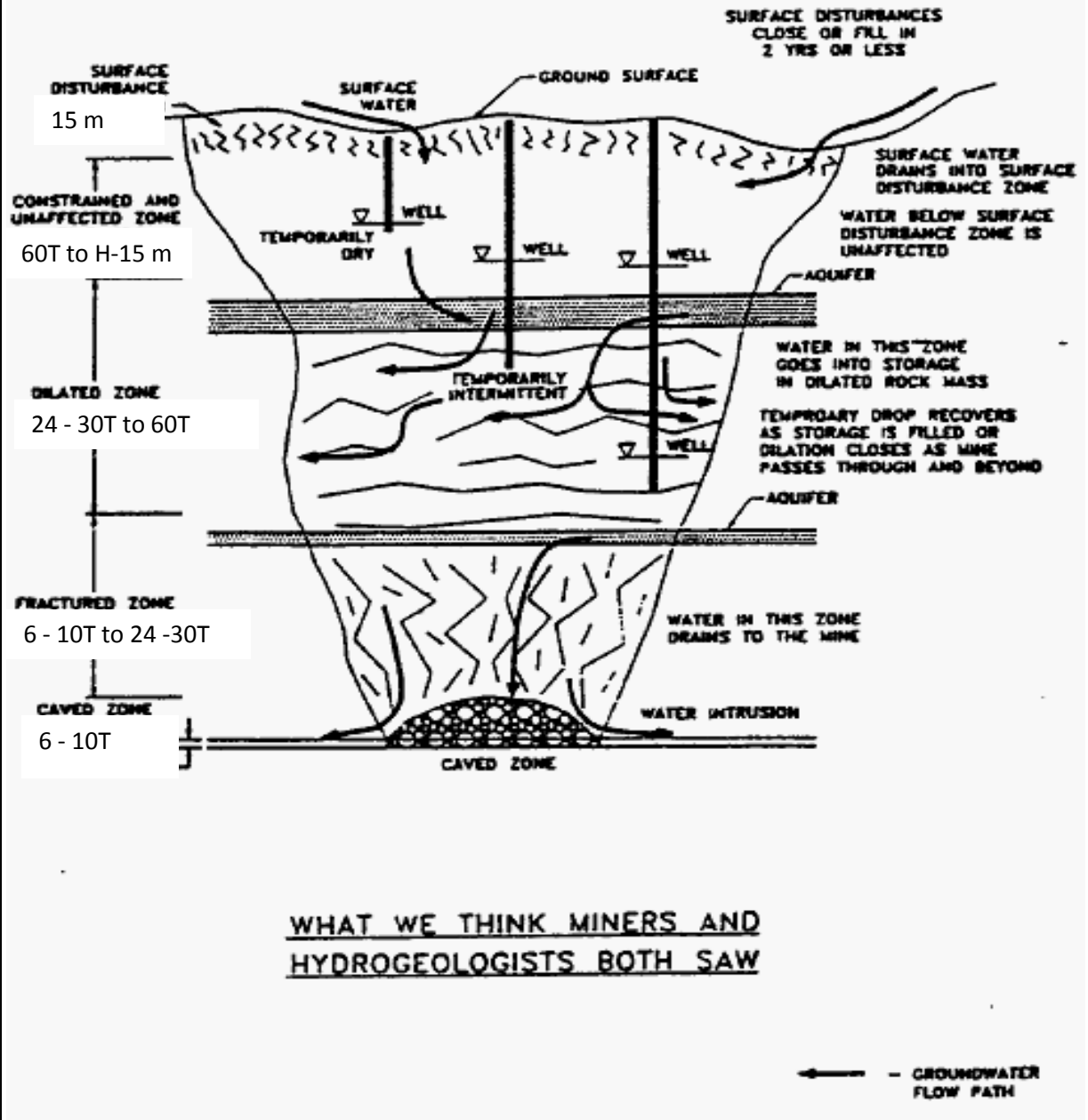
Figure 6.—Overburden response to full-extraction mining: (A) caving zones, (B) fracture zone, (C) dilated zone, and (D) confined zone.

The dimensions of these zones vary from panel to panel because of differences in geology and panel geometry. The implication of this model for multiple-seam mining is that when the interburden thickness exceeds approximately 6–10 times the lower seam thickness, the upper seam should be largely intact, although the roof may be fractured or otherwise damaged.

Note: Equivalent **ACARP, 2007** model zones A to D also shown down the left side.

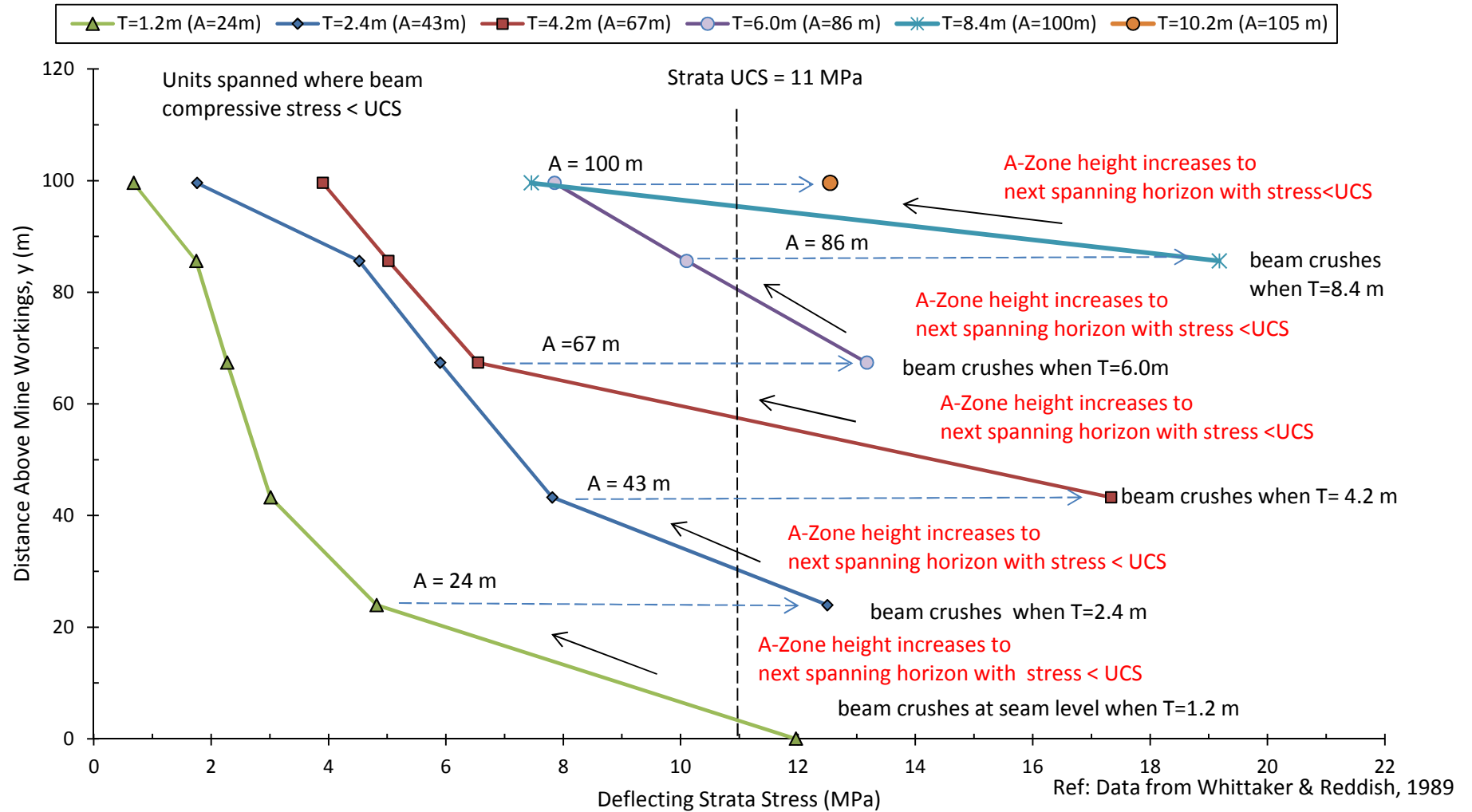
	Engineer:	S.Ditton	Client:	Appendix A	
	Drawn:	S.Ditton			
	Date:	03.06.13	Title:	Model of Overburden Fracture Zones above US Longwall Mines According to Mark, 2007	
	Ditton Geotechnical Services Pty Ltd		Scale:		Figure No:

Zone and Thickness Ranges
(based on Mining Height, T)

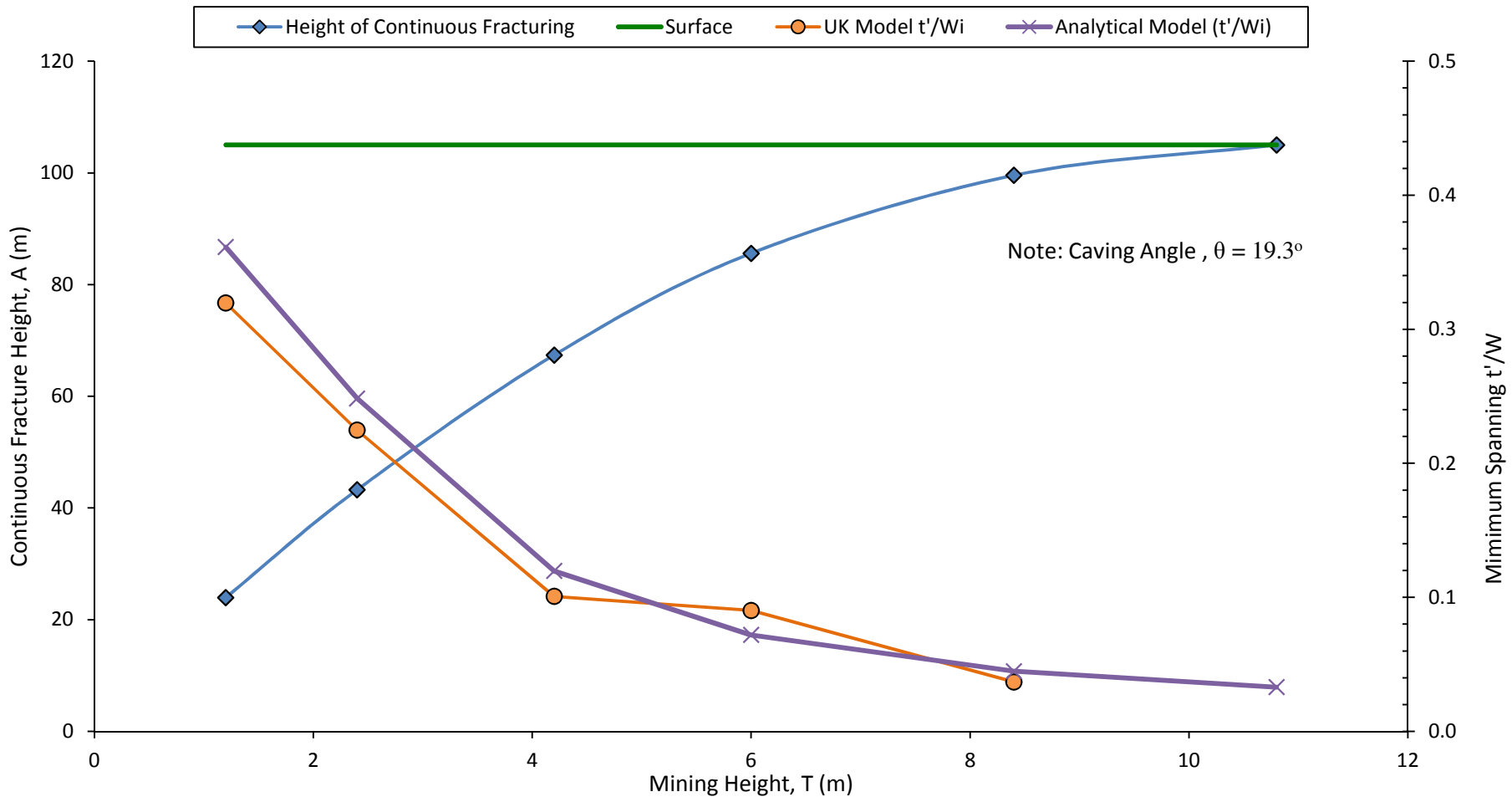


WHAT WE THINK MINERS AND
HYDROGEOLOGISTS BOTH SAW

	Engineer: S.Ditton	Client: Appendix A
	Drawn: S.Ditton	
	Date: 03.06.13	Title: Model of Overburden Fracture Zones above UK Longwall Mines According to Kendorski, 1993
	Ditton Geotechnical Services Pty Ltd	Scale: Figure No: A40f

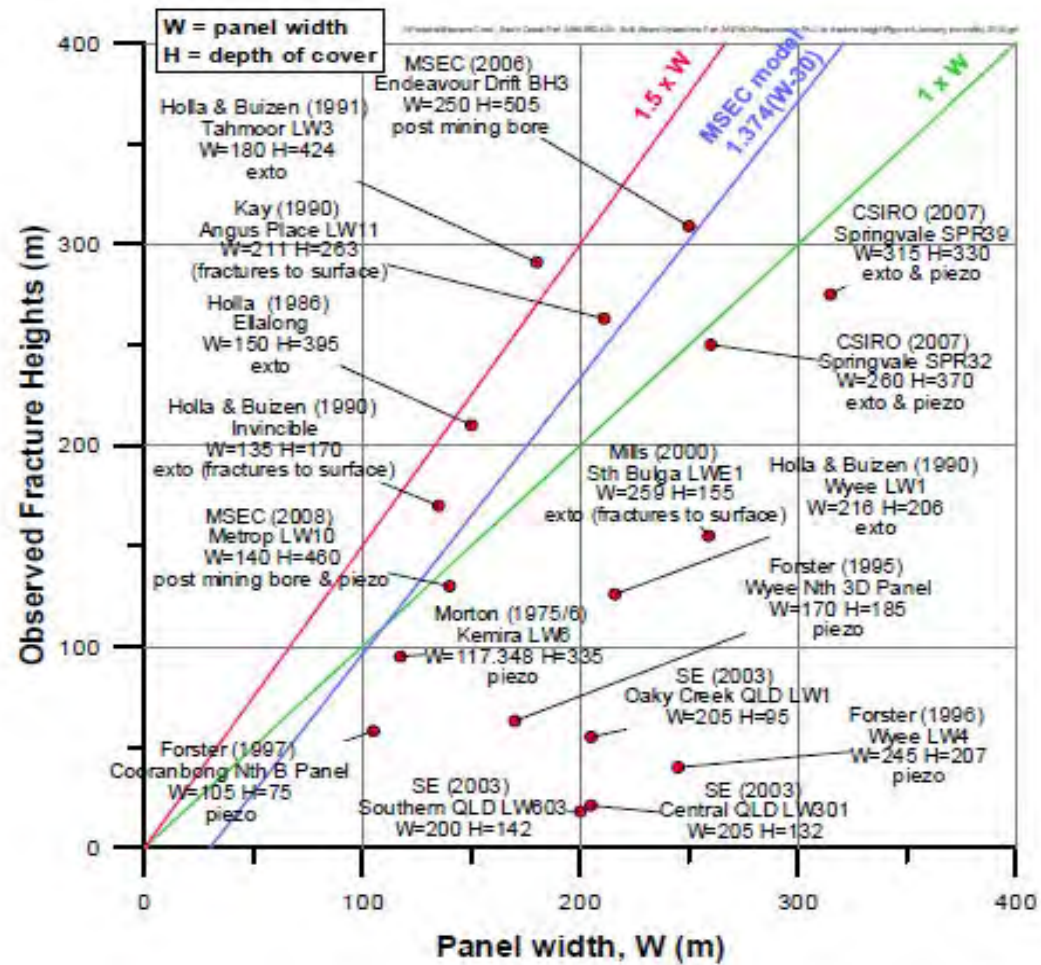


	Engineer:	S.Ditton	Client:	Review of Height of Fracturing Data	
	Drawn:	S.Ditton	Title:	Interpreted Beam Stress in Spanning Units of Physical Model of Laminated Overburden above a Longwall	
	Date:	07.06.13	Scale:	NTS	Figure No:
	Ditton Geotechnical Services Pty Ltd				A40g



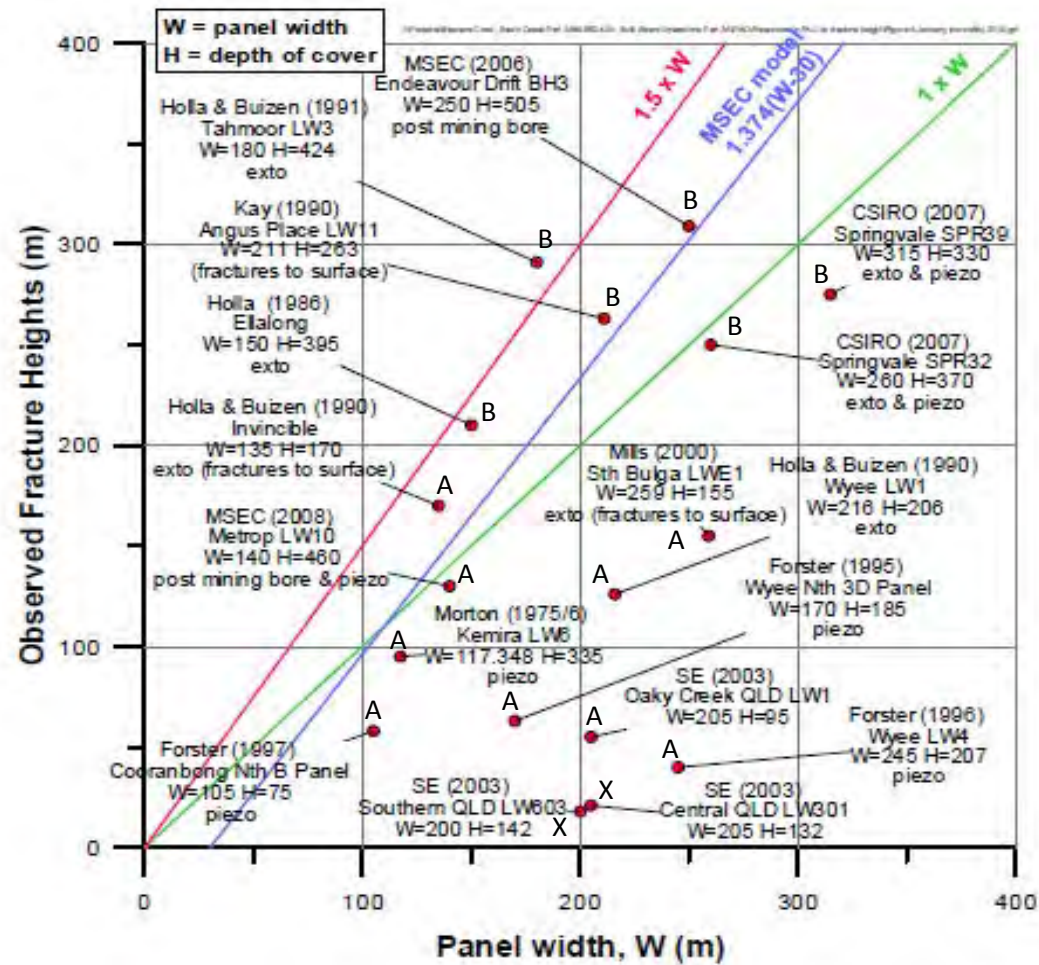
Ref: Data from Whittaker & Reddish, 1989

	Engineer:	S.Ditton	Client:	Review of Height of Fracturing Data		
	Drawn:	S.Ditton		Title:	Analytical v. Physical HoF Model Minimum Beam Thickness Required to Span the Continuous Fracture Zone	
	Date:	07.06.13	Scale:		NTS	Figure No: A40h
	Ditton Geotechnical Services Pty Ltd					



Ref: MSEC, 2011

	Engineer:	S.Ditton	Client:	Review of Height of Fracturing Data		
	Drawn:	S.Ditton		Title:	Observed Fracture Height Models presented by SCT and MSEC	
	Date:	07.06.13	Scale:		NTS	
	Ditton Geotechnical Services Pty Ltd				Figure No:	A40i



Key

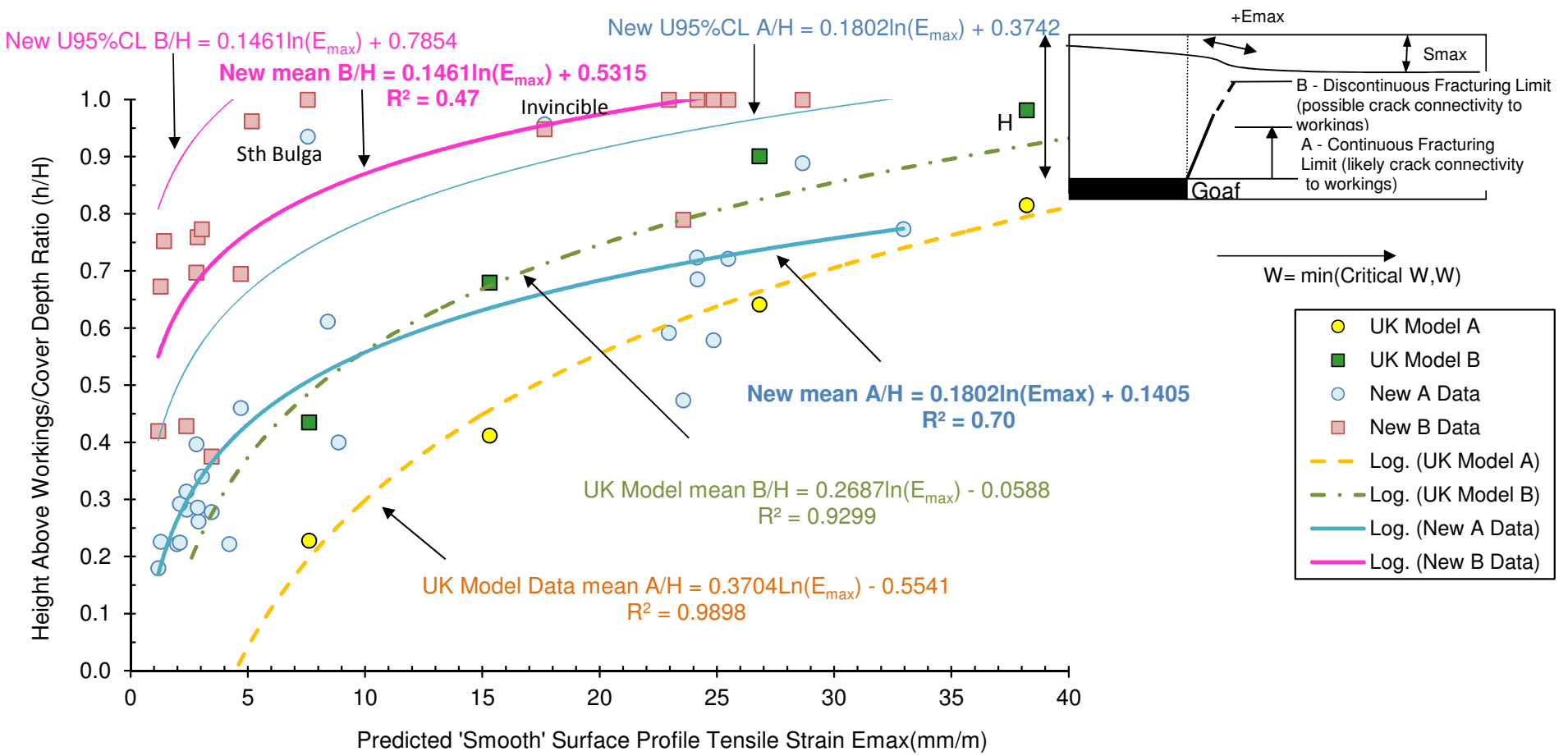
A: A-Zone Horizon

B: B-Zone Horizon

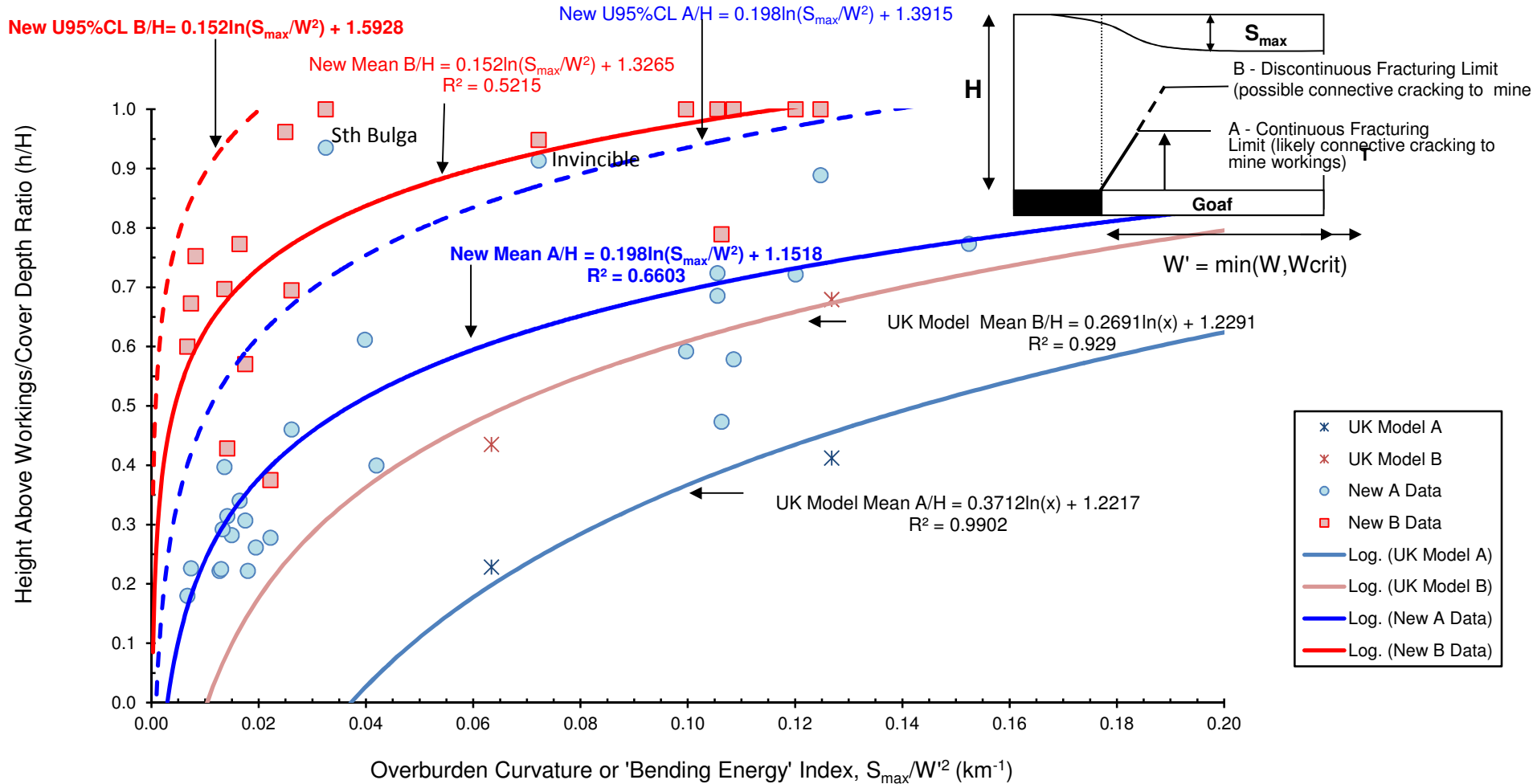
X: In-conclusive data

Ref: MSEC, 2011

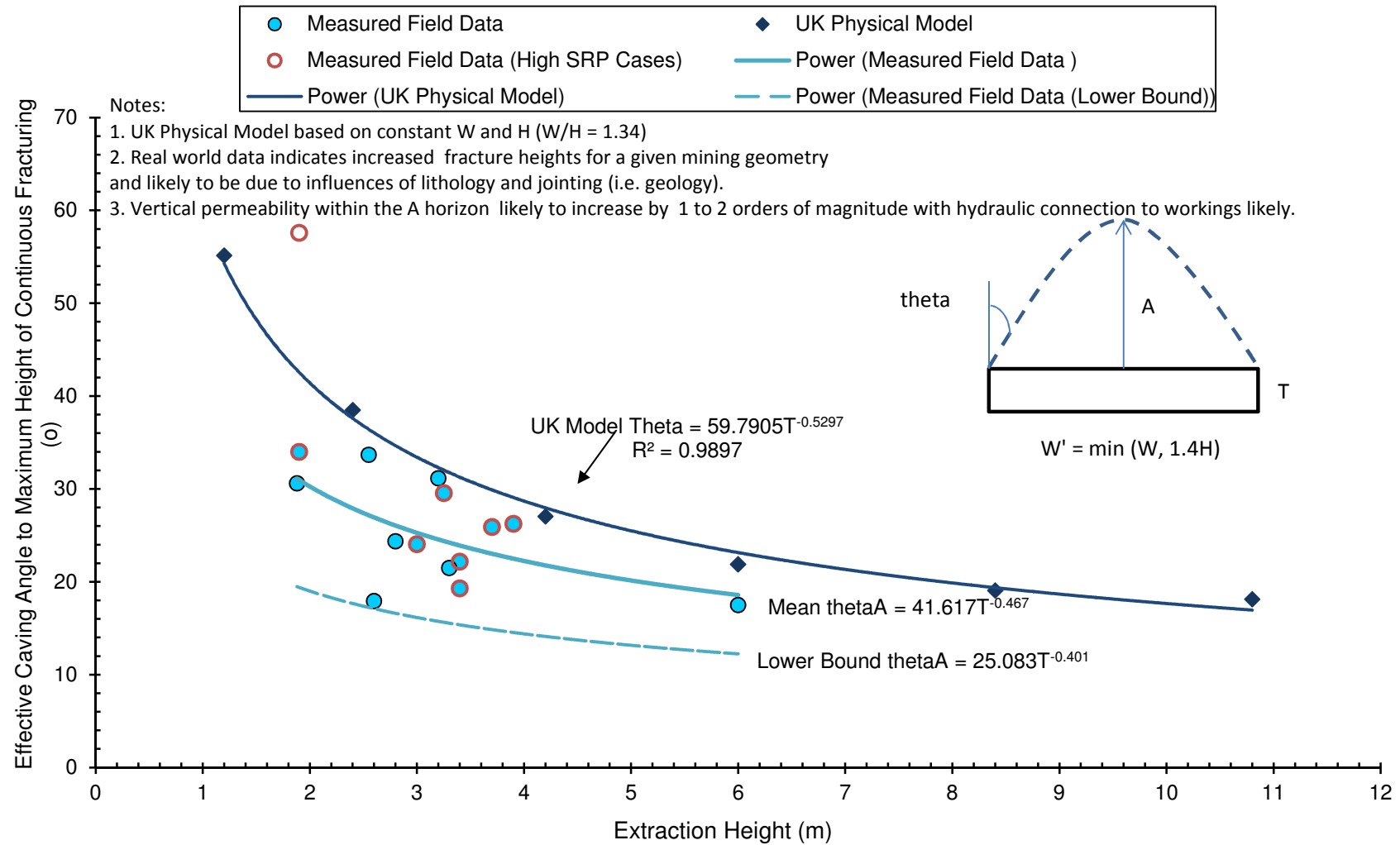
	Engineer: S.Ditton	Client: Review of Height of Fracturing Data
	Drawn: S.Ditton	
	Date: 07.06.13	Title: Review of Observed Fracture Height Models presented by SCT and MSEC v. Whittaker & Reddish Sub-Surface Fracture Model Zoning
	Ditton Geotechnical Services Pty Ltd	
Scale: NTS		Figure No: A40j



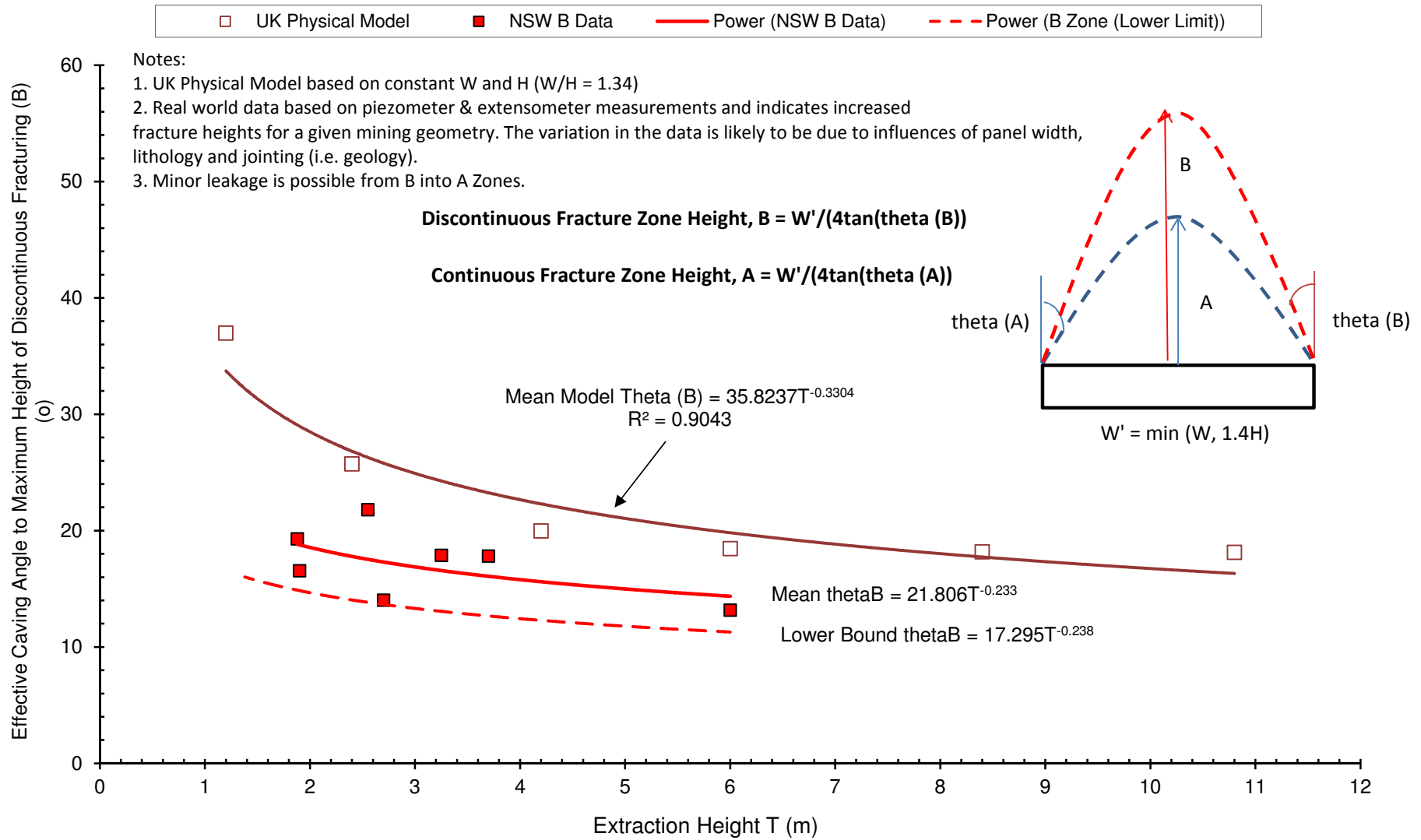
Engineer:	S.Ditton	Client:	Updated Whittaker and Reddish Model presented in ACARP, 2003	
Drawn:	S.Ditton			
Date:	18.11.12	Title:	Continuous and Discontinuous Sub-Surface Fracture Height Model above Longwalls using Surface Tensile Strains as the Key Indicator	
Ditton Geotechnical Services Pty Ltd		Scale:	NTS	Figure No: A41a



	Engineer: S.Ditton	Client: Updated from ACARP, 2003
	Drawn: S.Ditton	
	Date: 03.12.12	Title: Continuous and Discontinuous Sub-Surface Fracture Heights above Longwalls (based on ACARP, 2003)
	Ditton Geotechnical Services Pty Ltd	Scale: NTS
		Figure No: A41b



	Engineer:	S.Ditton	Client:	Modified from ACARP, 2003 (DgS,2012)	
	Drawn:	S.Ditton			
	Date:	15.11.12	Title:	Alternative ACARP, 2003 A-Zone Sub-Surface Fracture Height Model based on Panel Width and Mining Height as Key Parameters	
	Ditton Geotechnical Services Pty Ltd			Scale:	NTS

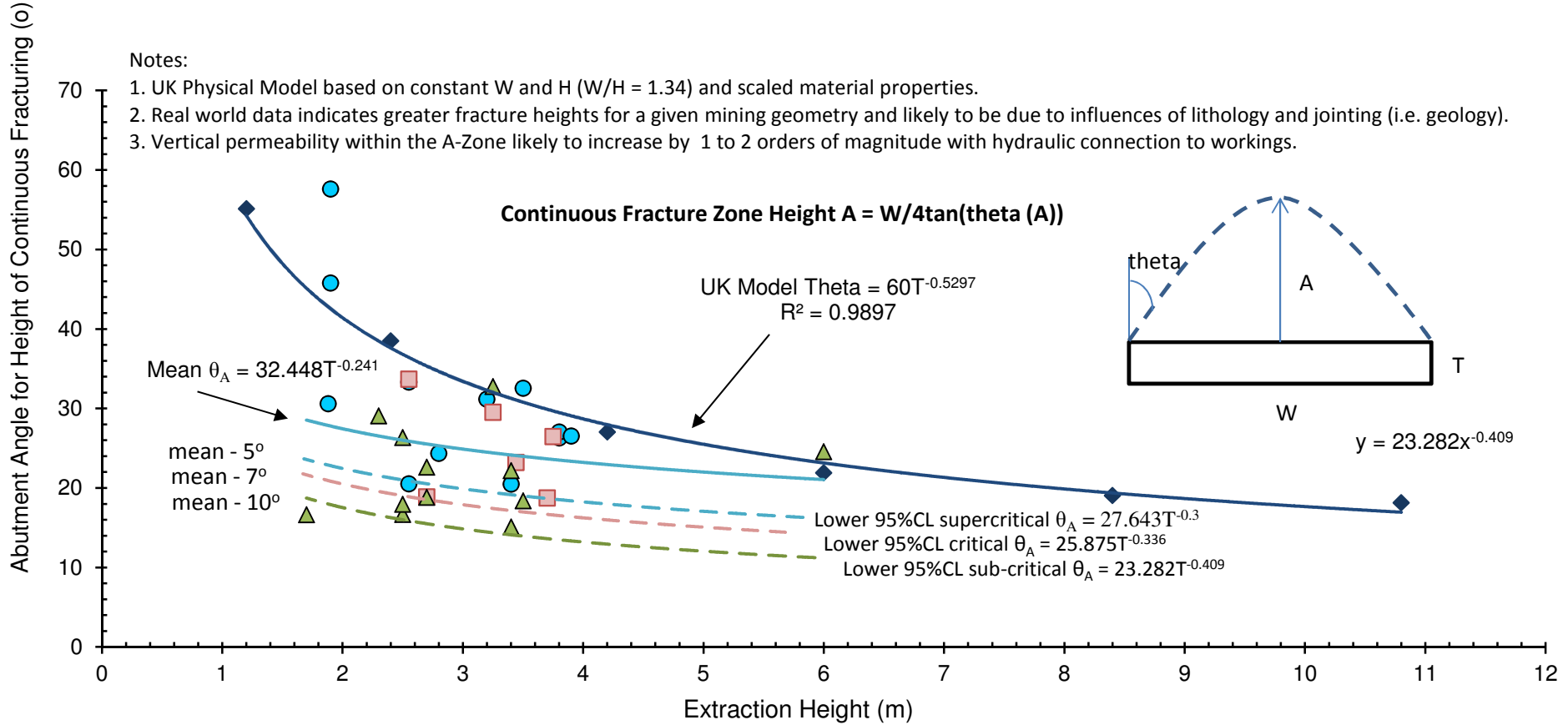


	Engineer:	S.Ditton	Client:	Modified from ACARP, 2003 (DgS,2012)	
	Drawn:	S.Ditton			
	Date:	15.11.12	Title:	Alternative ACARP, 2003 B-Zone Sub-Surface Fracture Height Model based on Panel Width and Mining Height as Key Parameters	
	Ditton Geotechnical Services Pty Ltd			Scale:	NTS

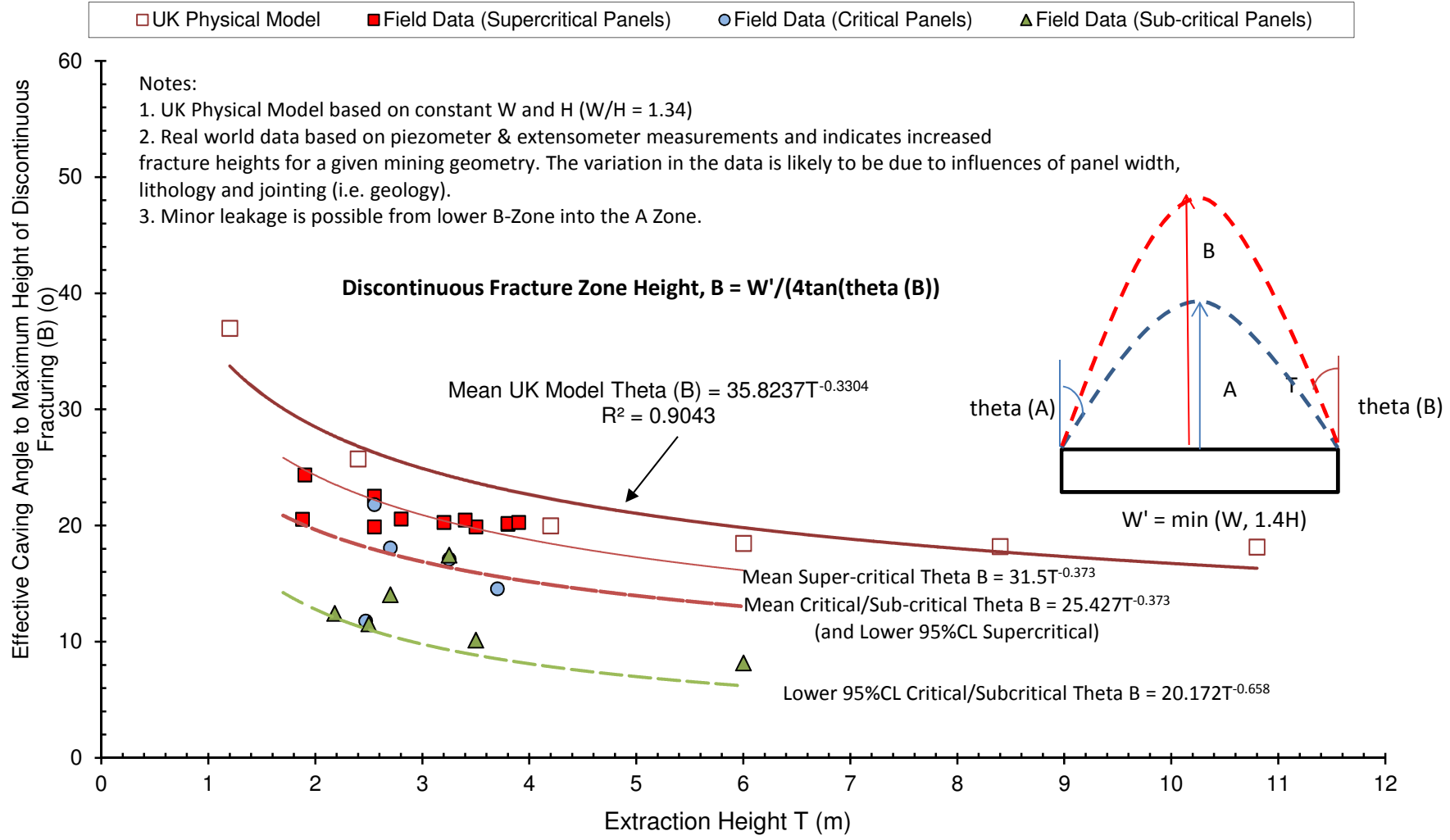


Notes:

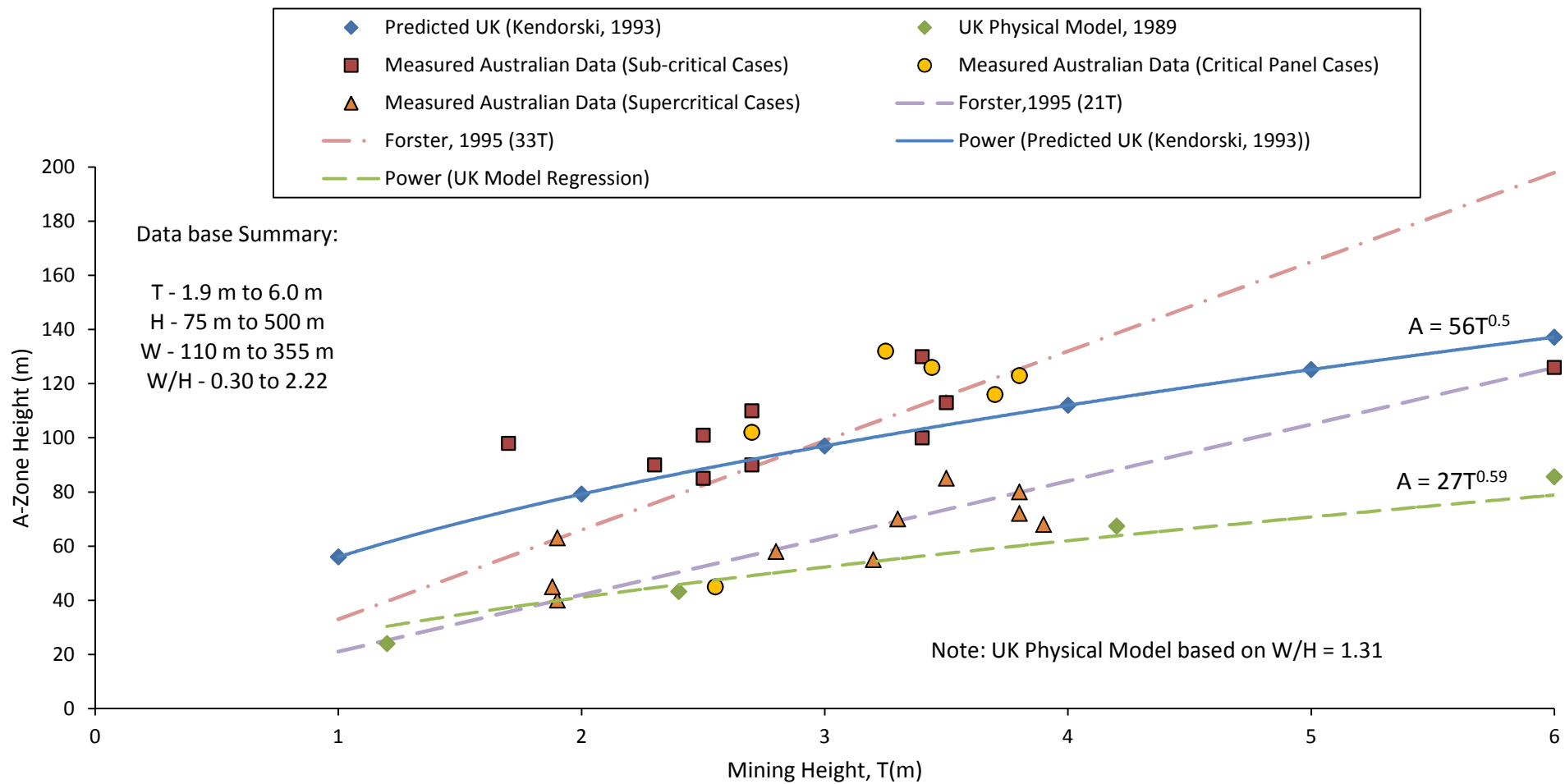
1. UK Physical Model based on constant W and H (W/H = 1.34) and scaled material properties.
2. Real world data indicates greater fracture heights for a given mining geometry and likely to be due to influences of lithology and jointing (i.e. geology).
3. Vertical permeability within the A-Zone likely to increase by 1 to 2 orders of magnitude with hydraulic connection to workings.



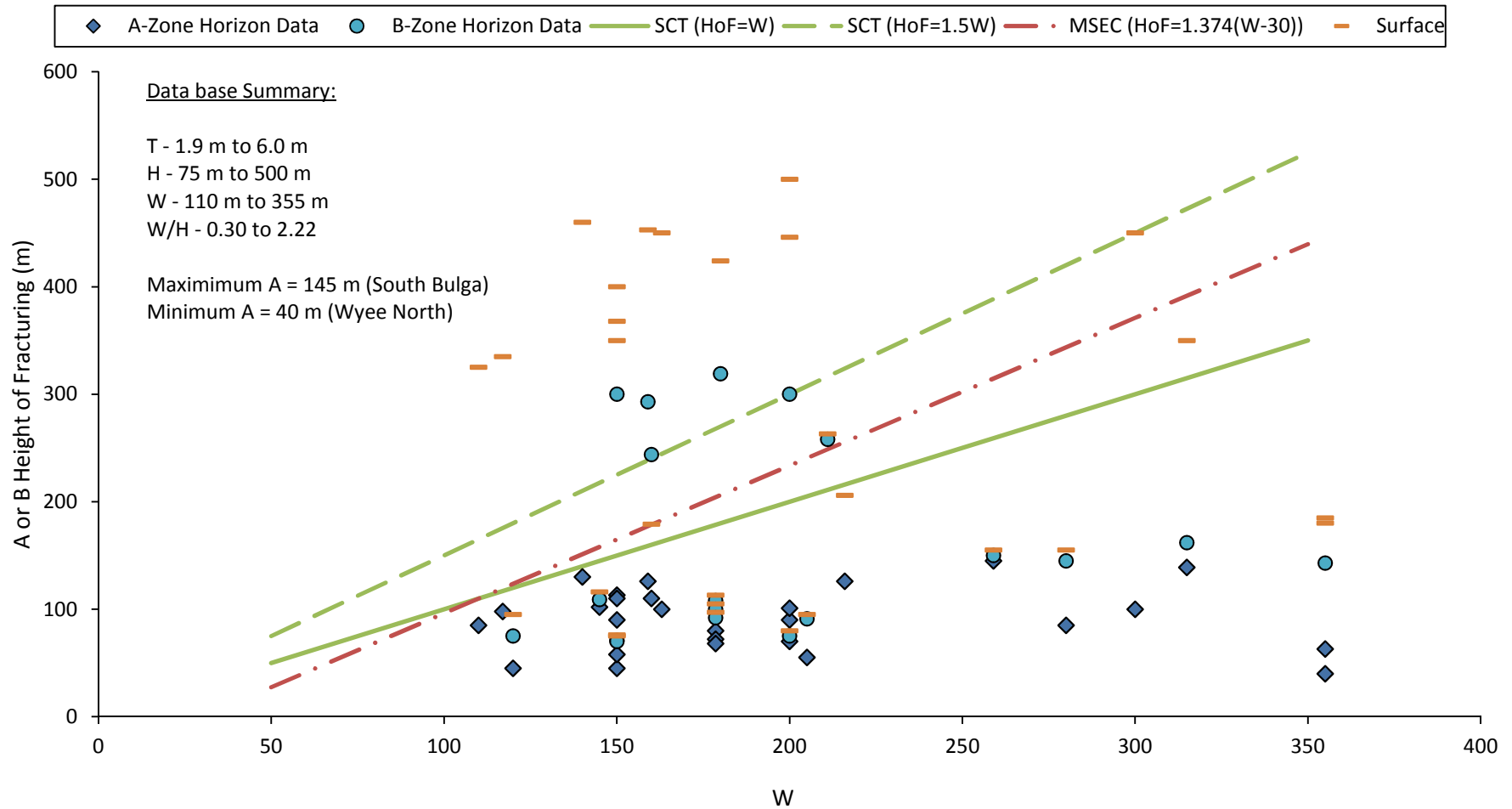
	Engineer:	S.Ditton	Client:	Modified from ACARP, 2003	
	Drawn:	S.Ditton	Title:	Predicted Height of Continuous Fracturing Based on HoF Angle and Mining Height	
	Date:	10.06.13	Scale:	NTS	Figure No: A41e
	Ditton Geotechnical Services Pty Ltd				



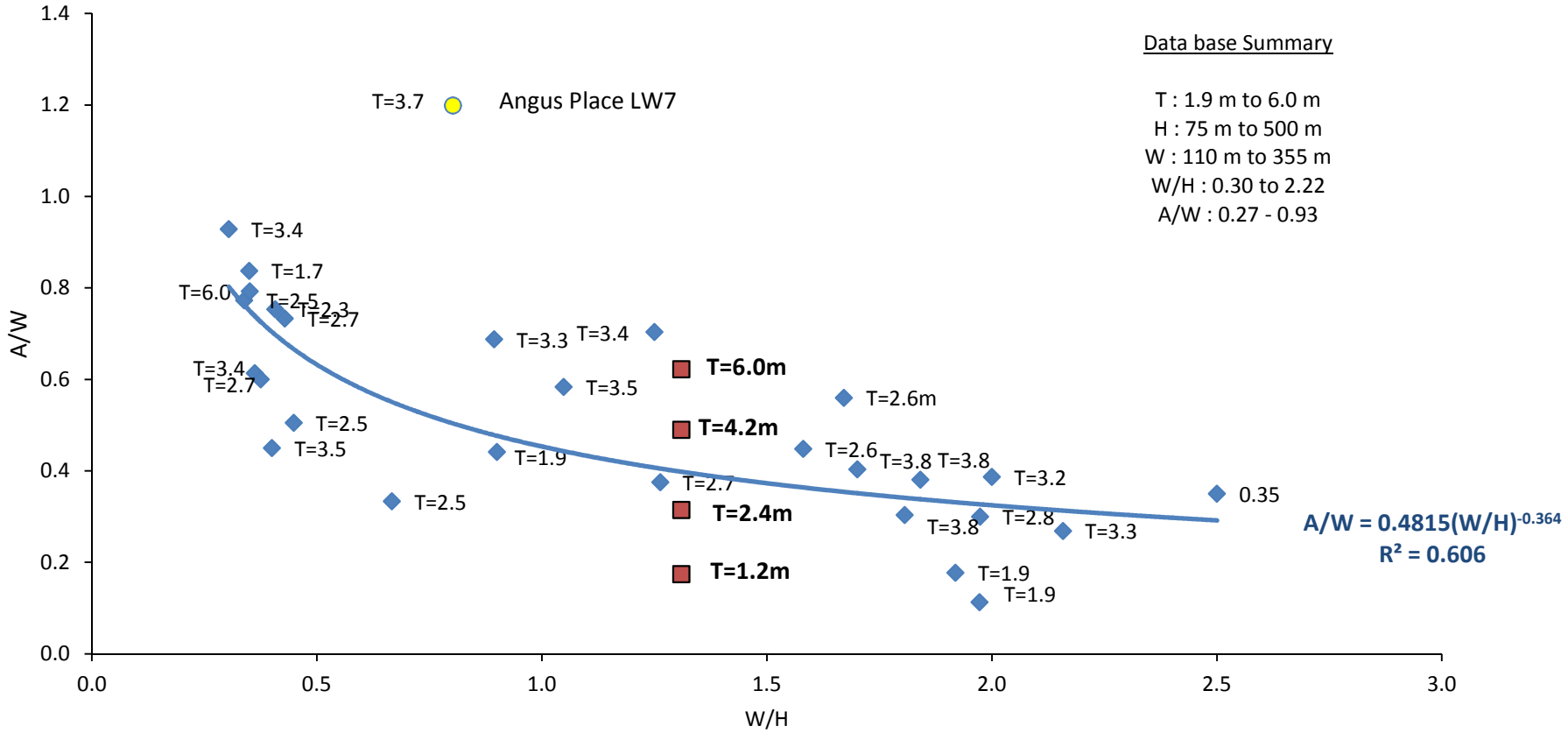
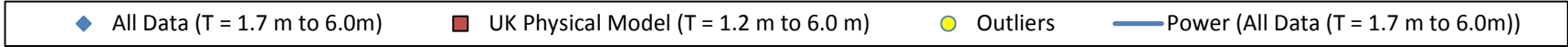
	Engineer:	S.Ditton	Client:	Modified from ACARP, 2003	
	Drawn:	S.Ditton			
	Date:	10.06.13	Title:	Predicted Height of Discontinuous Fracturing Based on Measured Heights of Discontinuous Fracture Angles and Mining Height	
	Ditton Geotechnical Services Pty Ltd		Scale:	NTS	Figure No:



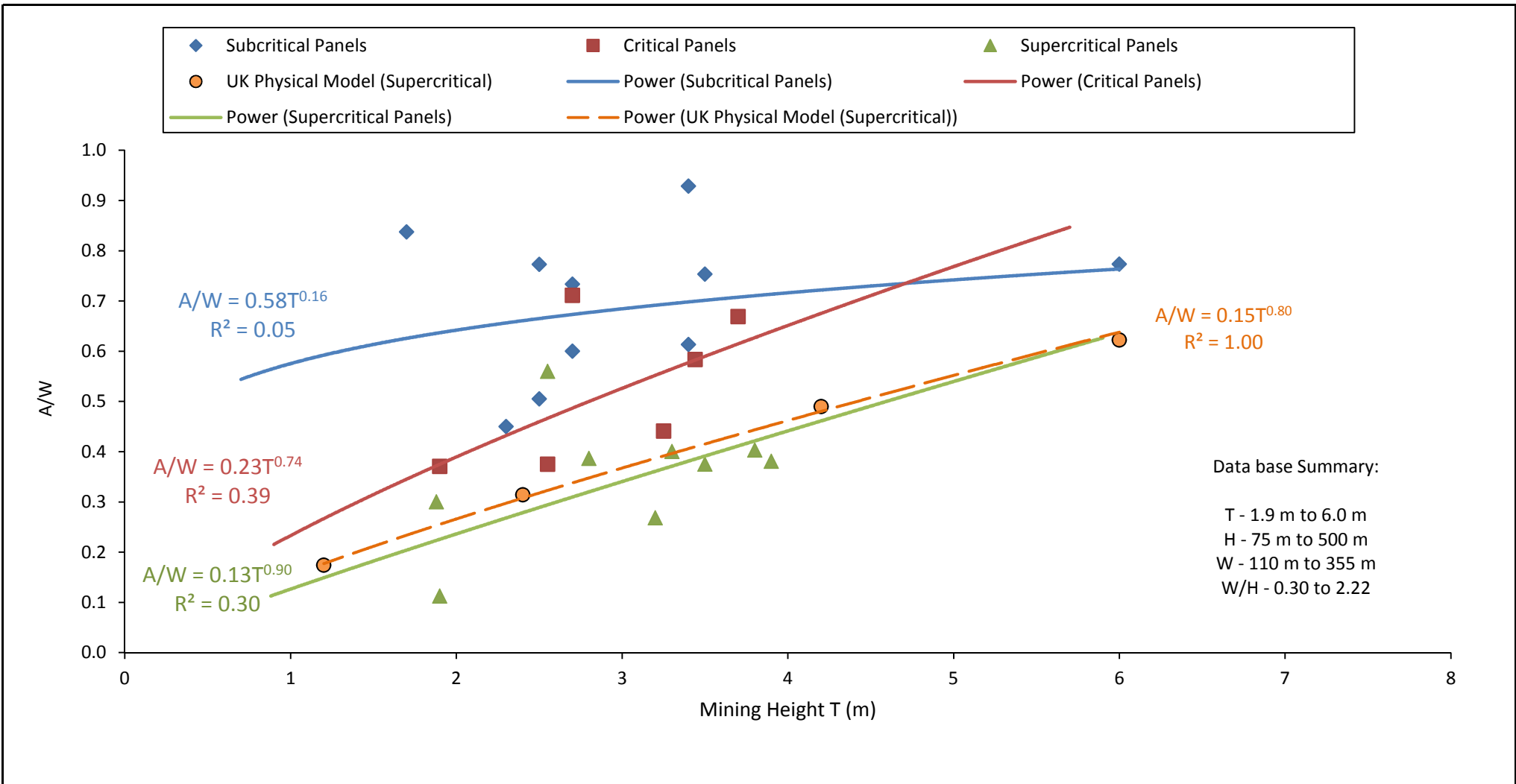
	Engineer:	S.Ditton	Client:	Review of Height of Fracturing Data	
	Drawn:	S.Ditton			
	Date:	07.06.13	Title:	Continuous UK Fracture Height Models based on Mining Height Only v. Measured Australian Database	
	Ditton Geotechnical Services Pty Ltd			Scale:	NTS



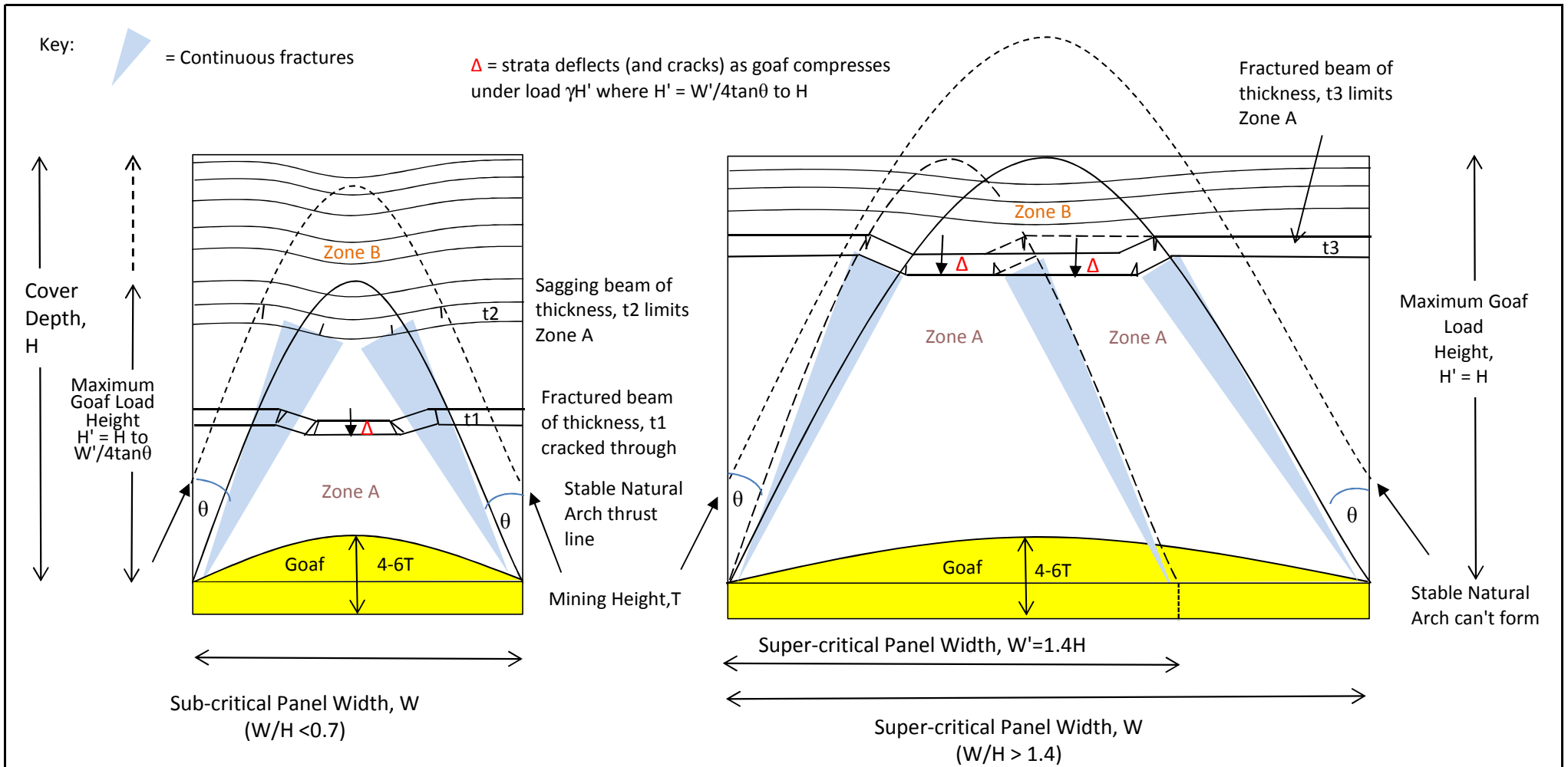
	Engineer:	S.Ditton	Client:	Review of Height of Fracturing Data	
	Drawn:	S.Ditton	Title:	Continuous Australian Fracture Height Model based on Panel Width Only	
	Date:	07.06.13		Database	
	Ditton Geotechnical Services Pty Ltd		Scale:	NTS	Figure No:



	Engineer:	S.Ditton	Client:	Review of Height of Fracturing Data		
	Drawn:	S.Ditton		Title:	Continuous Australian Fracture Height Model based on A normalised to Panel Width with Influence of Mining Height Included	
	Date:	07.06.13	Scale:		NTS	Figure No:
	Ditton Geotechnical Services Pty Ltd					

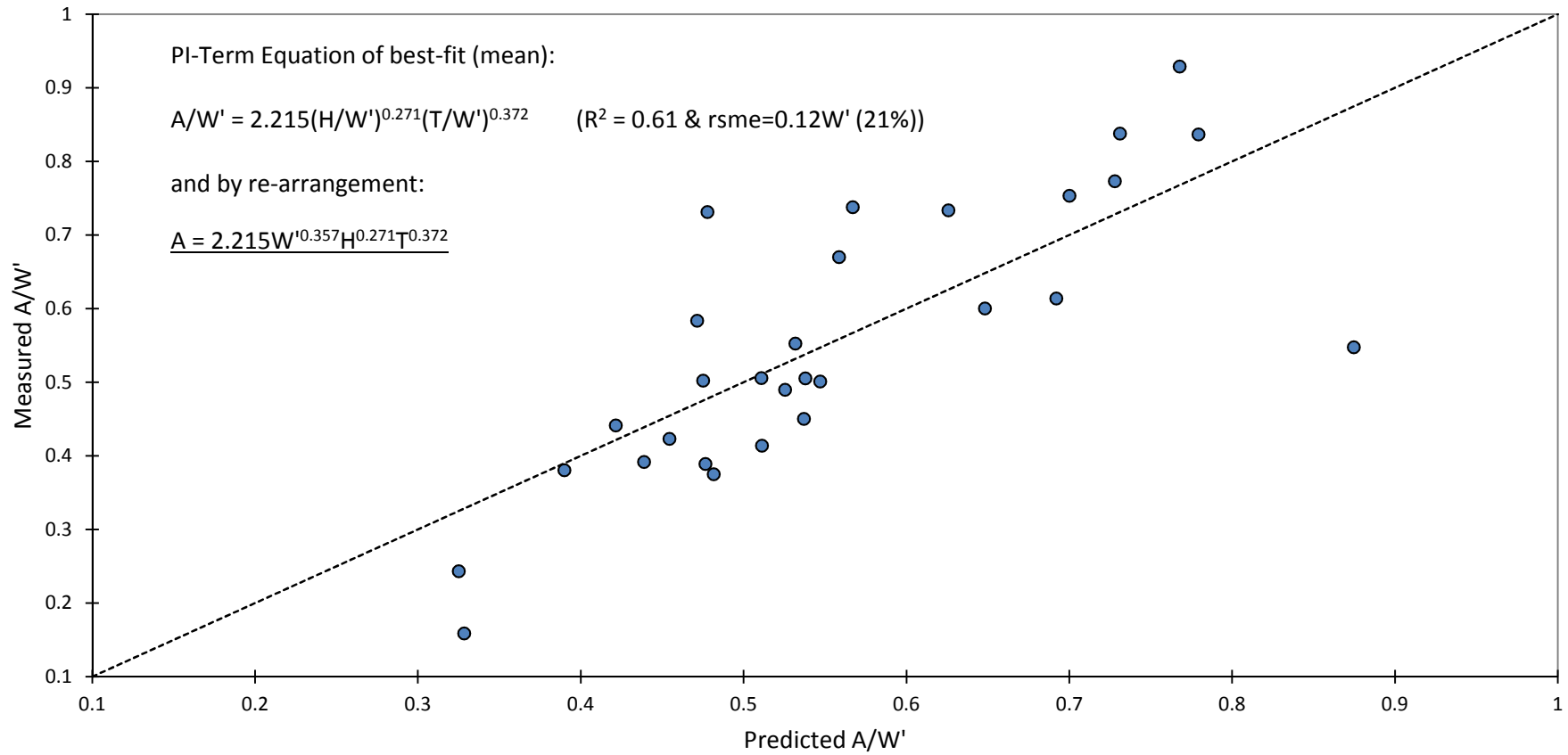


	Engineer:	S.Ditton	Client:	Review of Height of Fracturing Data		
	Drawn:	S.Ditton		Title:	Continuous Australian Fracture Height Model based on A normalised to Panel Width v. Mining Height	
	Date:	07.06.13	Scale:		NTS	
	Ditton Geotechnical Services Pty Ltd				Figure No:	A41j

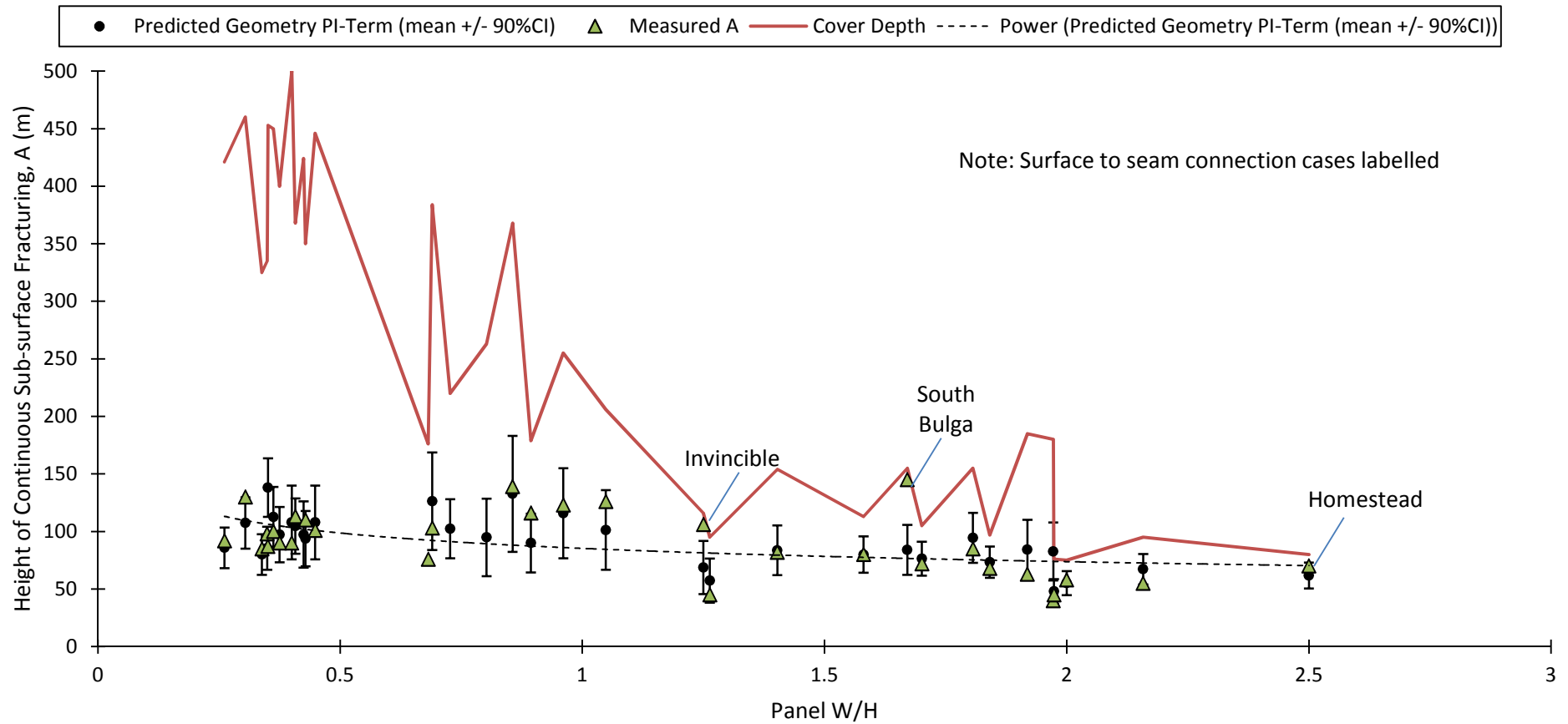


	Engineer:	S.Ditton	Client:	Review of Height of Fracturing Data
	Drawn:	S.Ditton	Title:	Conceptual Model for Development of Height of Continuous Fracturing Zone for a range of Longwall Panel Geometries
	Date:	26.08.13	Scale:	NTS
	Ditton Geotechnical Services Pty Ltd		Figure No:	A42a

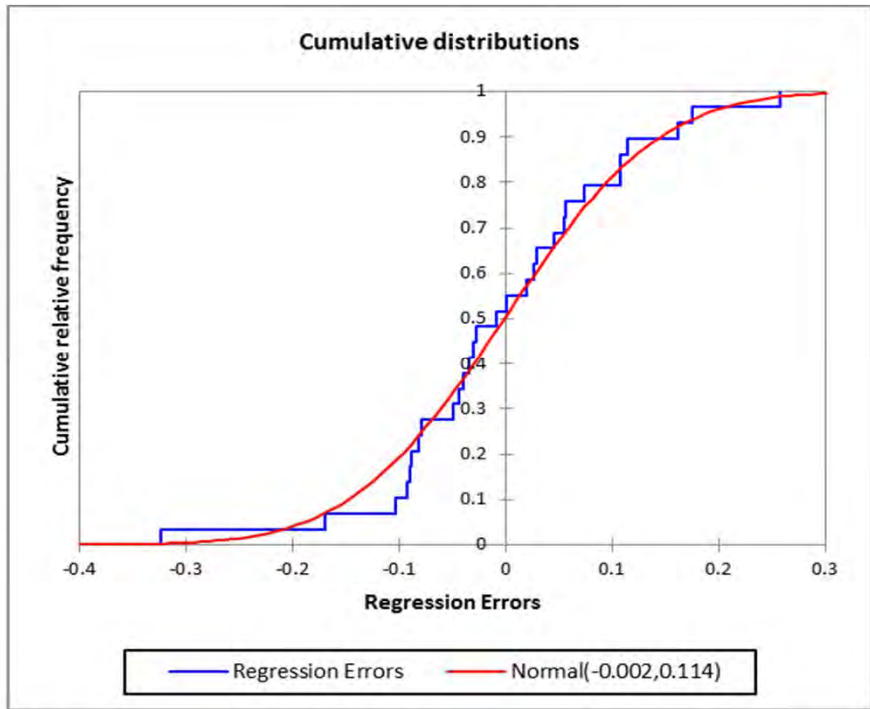
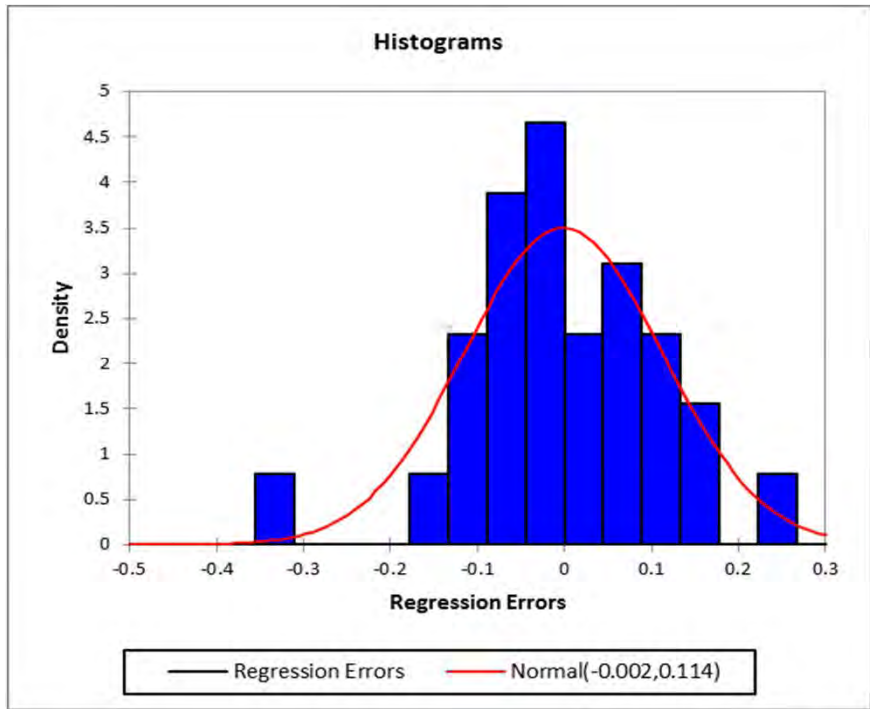
Mine Geometry Only PI-Term Model



	Engineer:	S.Ditton	Client:	Review of Height of Fracturing Data	
	Drawn:	S.Ditton			
	Date:	01.05.14	Title:	Results of Non-Linear Regression Analysis: Predicted v. Measured Value Analysis for Height of A-Zone Fracturing for the Geometry PI-Term Model	
	Ditton Geotechnical Services Pty Ltd		Scale:	NTS	Figure No:



	Engineer:	S.Ditton	Client:	Review of Height of Fracturing Data	
	Drawn:	S.Ditton	Title:	Results of Non-Linear Regression Error analysis for Geometry PI-Terms Only Height of A-Zone Prediction Model (Geology Pi-Term Not Included)	
	Date:	01.05.14	Scale:	NTS	Figure No:
	Ditton Geotechnical Services Pty Ltd				A42c



Kolmogorov-Smirnov test:

D	0.117
p-value	0.798
alpha	0.05

Test interpretation:

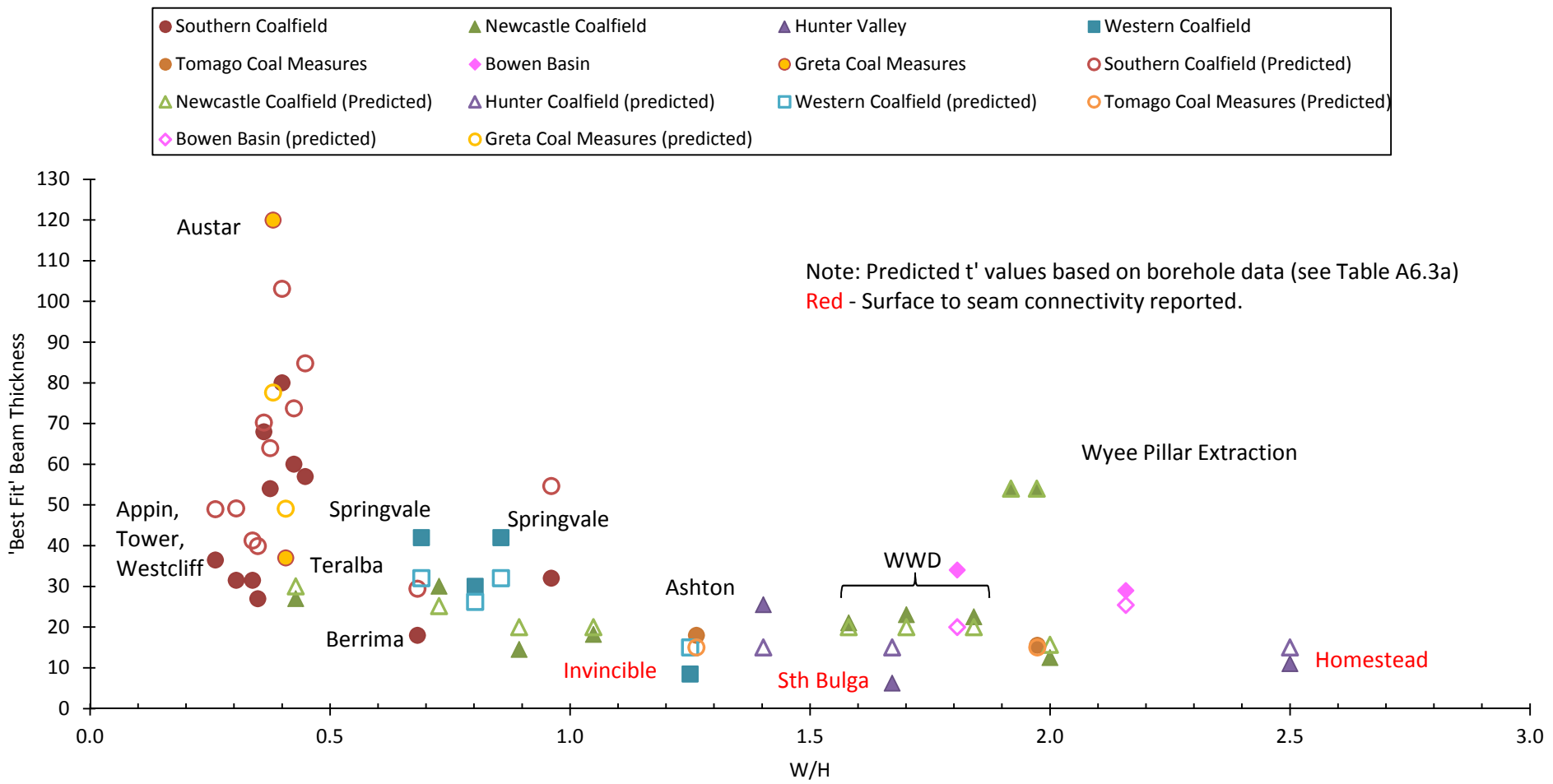
H0: The sample follows a Normal distribution

Ha: The sample does not follow a Normal distribution

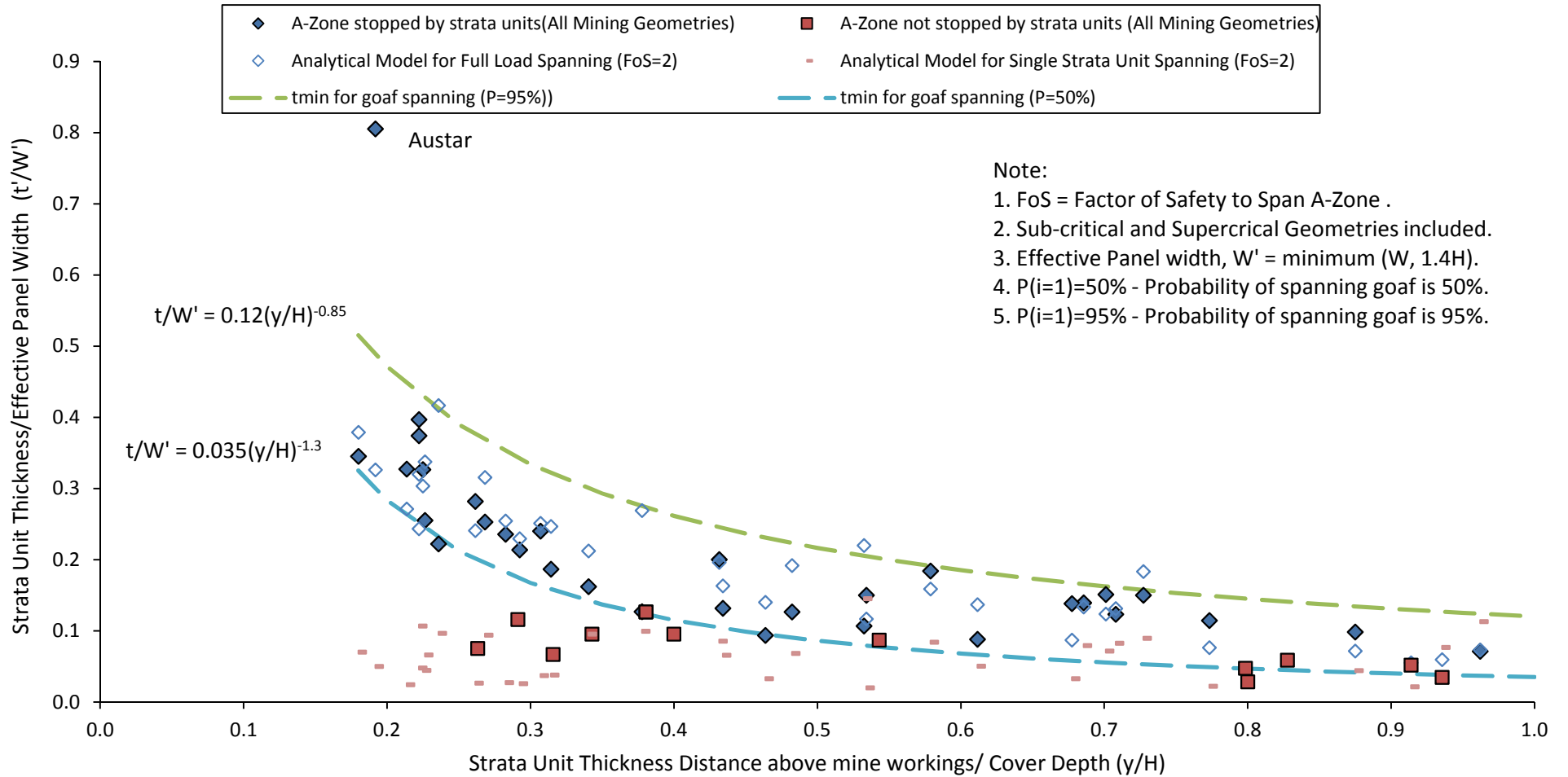
As the computed p-value is greater than the significance level $\alpha=0.05$, one cannot reject the null hypothesis H0.

The risk to reject the null hypothesis H0 while it is true is 79.75%.

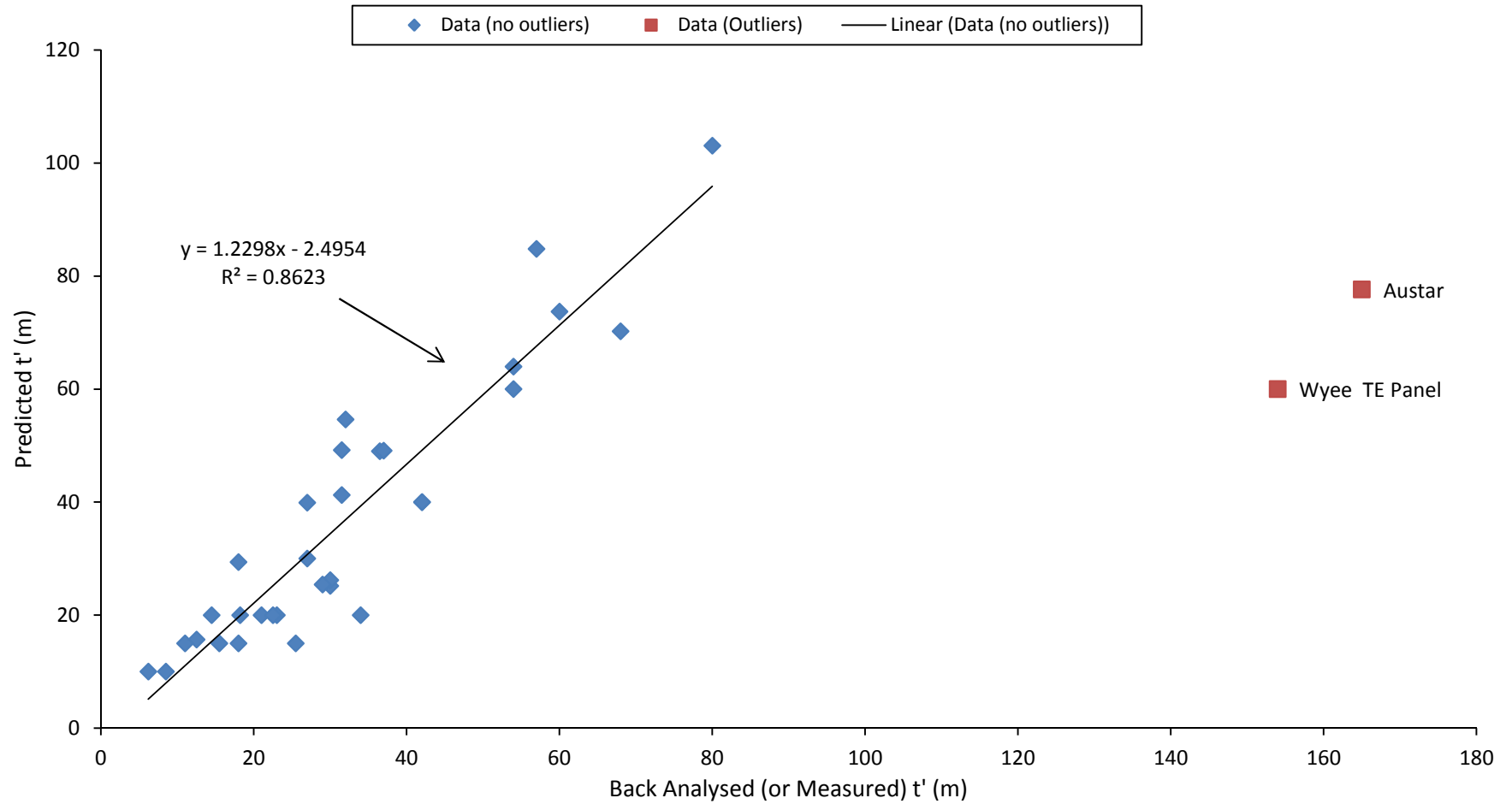
	Engineer:	S.Ditton	Client:	Review of Height of Fracturing Data	
	Drawn:	S.Ditton			
	Date:	01.05.14	Title:	Results of Non-Linear Regression Error analysis for Geometry Pi-Term Height of A-Zone	
	Ditton Geotechnical Services Pty Ltd			Prediction Model: Regression Error Normal Distribution Test	
Scale:			NTS	Figure No:	A42d



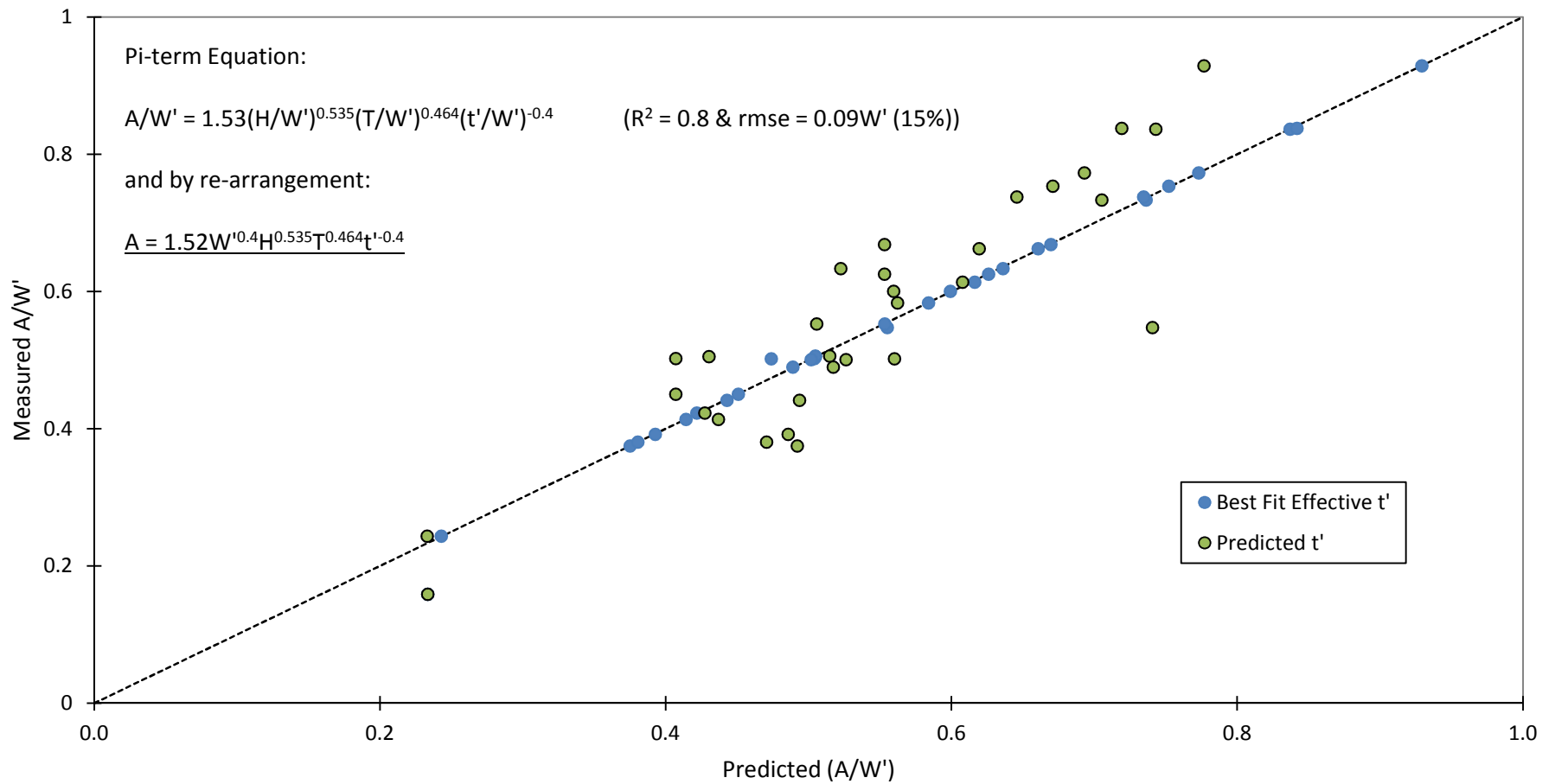
	Engineer:	S.Ditton	Client:	Review of Height of Fracturing Data	
	Drawn:	S.Ditton			
	Date:	01.05.14	Title:	Results of Back-analysis of Effective Strata Units required to Match the Observed A-Zone Heights above Longwall Panel Goafs using the Geology Pi-Term Model	
	Ditton Geotechnical Services Pty Ltd			Scale:	NTS



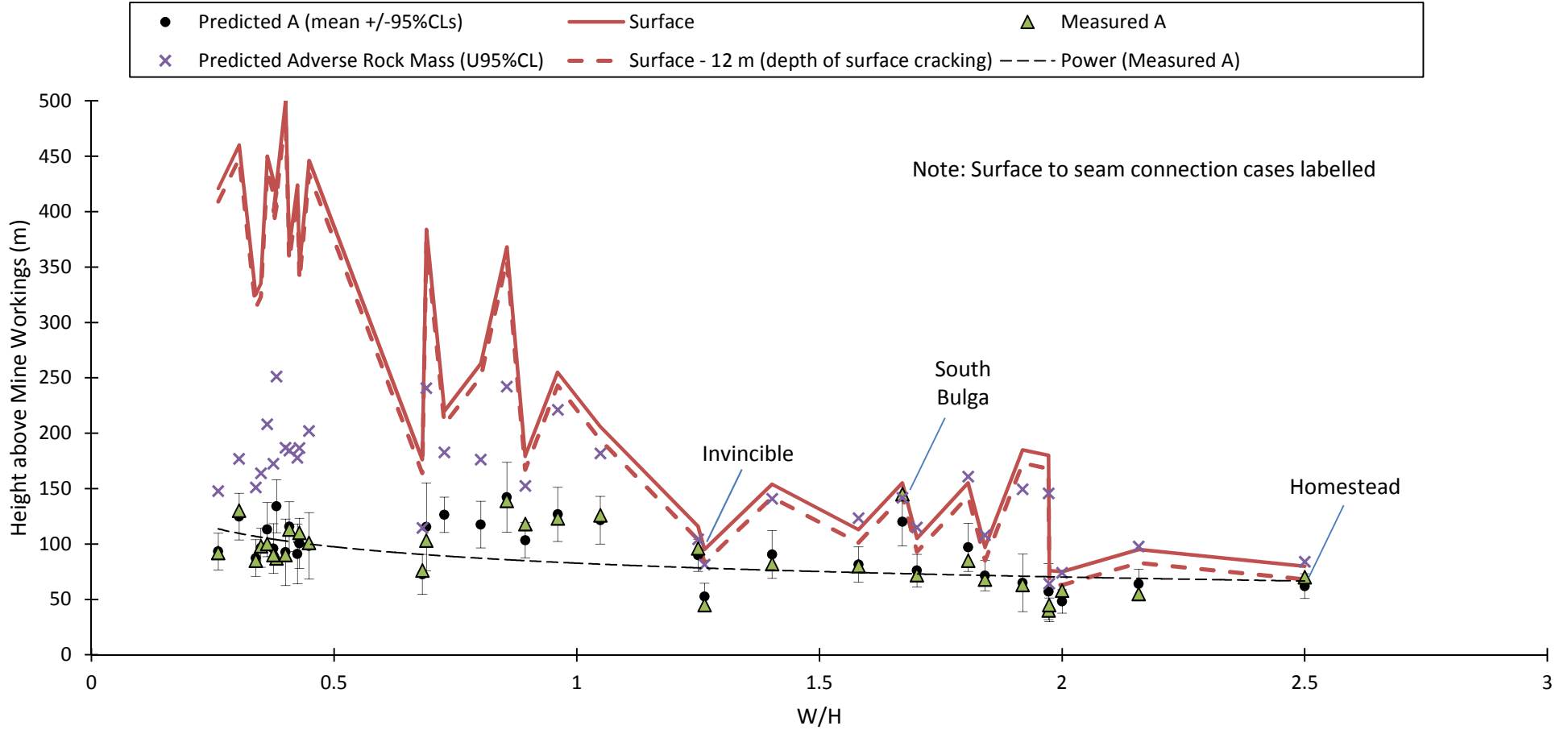
	Engineer:	S.Ditton	Client:	Review of Height of Fracturing Data	
	Drawn:	S.Ditton	Title:	Minimum Effective beam Thickness Required to Span the A-Zone, based on Back Analysis	
	Date:	01.05.14	Results for the Geology Pi-Term Model (see Figure A42e)		
	Ditton Geotechnical Services Pty Ltd		Scale:	NTS	Figure No:



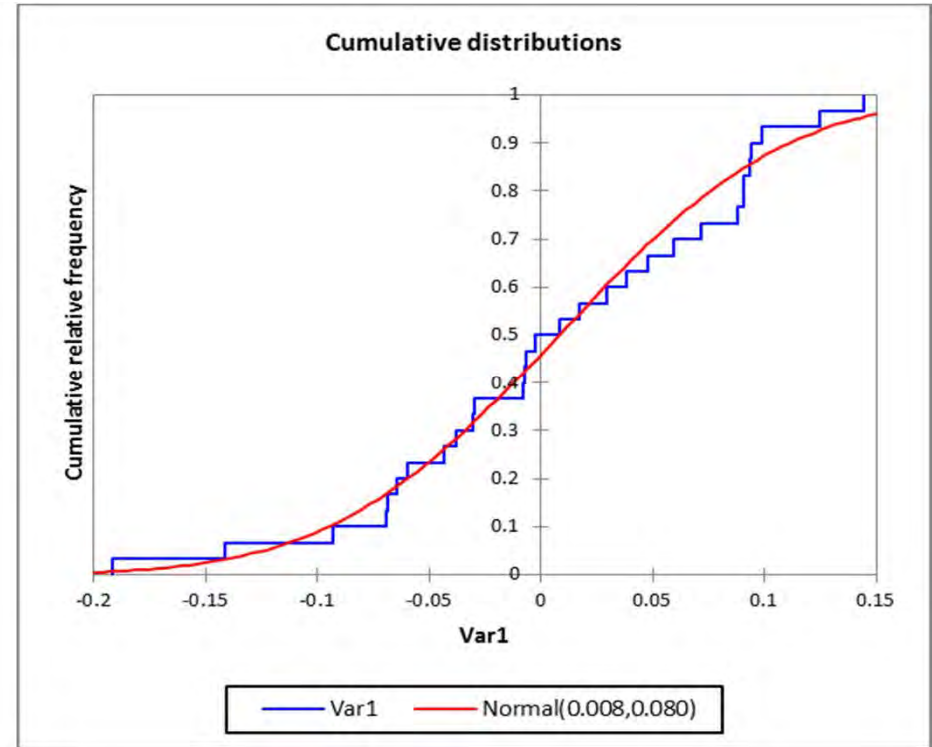
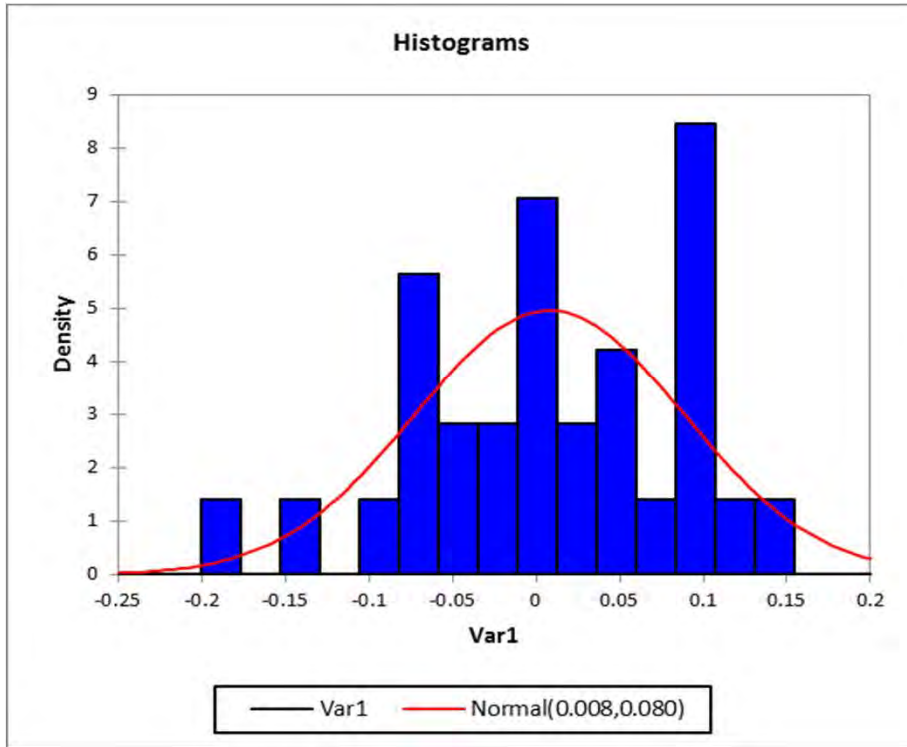
	Engineer:	S.Ditton	Client:	Review of Height of Fracturing Data		
	Drawn:	S.Ditton		Title:	Comparison of Back-Analysed (or measured (t') v. Predicted t' for the Geological PI-Term	
	Date:	01.05.14	Scale:		NTS	Figure No: A42g
	Ditton Geotechnical Services Pty Ltd					



	Engineer:	S.Ditton	Client:	Review of Height of Fracturing Data	
	Drawn:	S.Ditton	Title:	Results of Non-Linear Regression Analysis: Predicted v. Measured Value Analysis for Height of A-Zone Fracturing for Geology Pi-Term Model	
	Date:	01.05.14	Scale:	NTS	Figure No:
	Ditton Geotechnical Services Pty Ltd				A42h



	Engineer:	S.Ditton	Client:	Review of Height of Fracturing Data	
	Drawn:	S.Ditton			
	Date:	01.05.14	Title:	Results of Non-Linear Regression Error analysis for Height of A-Zone Prediction Model with Geology Included	
	Ditton Geotechnical Services Pty Ltd				
Scale:	NTS		Figure No:	A42i	



Kolmogorov-Smirnov test:

D	0.107
p-value	0.866
alpha	0.05

Test interpretation:

H0: The sample follows a Normal distribution

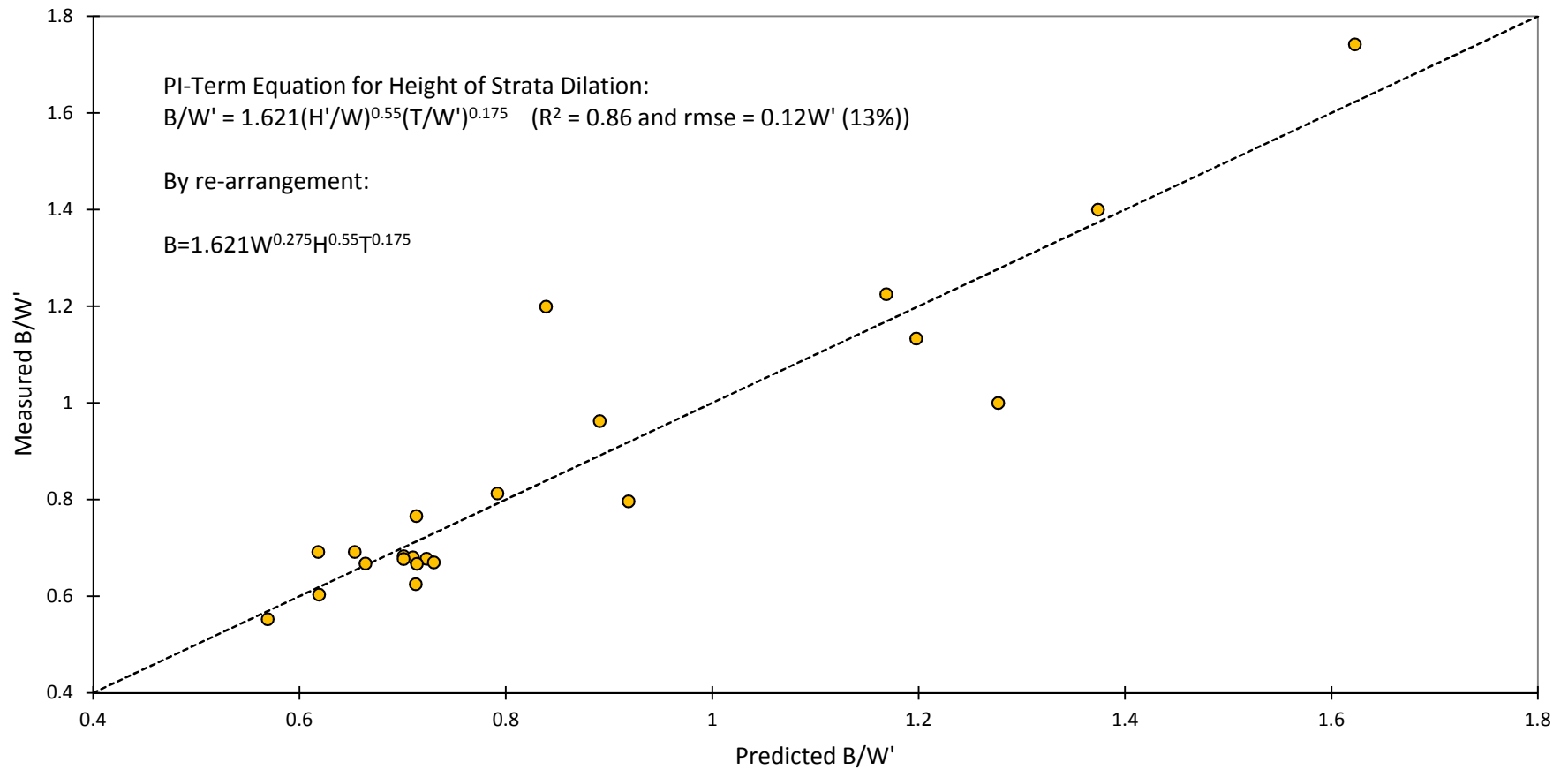
Ha: The sample does not follow a Normal distribution

As the computed p-value is greater than the significance level $\alpha=0.05$, one cannot reject the null hypothesis H0.

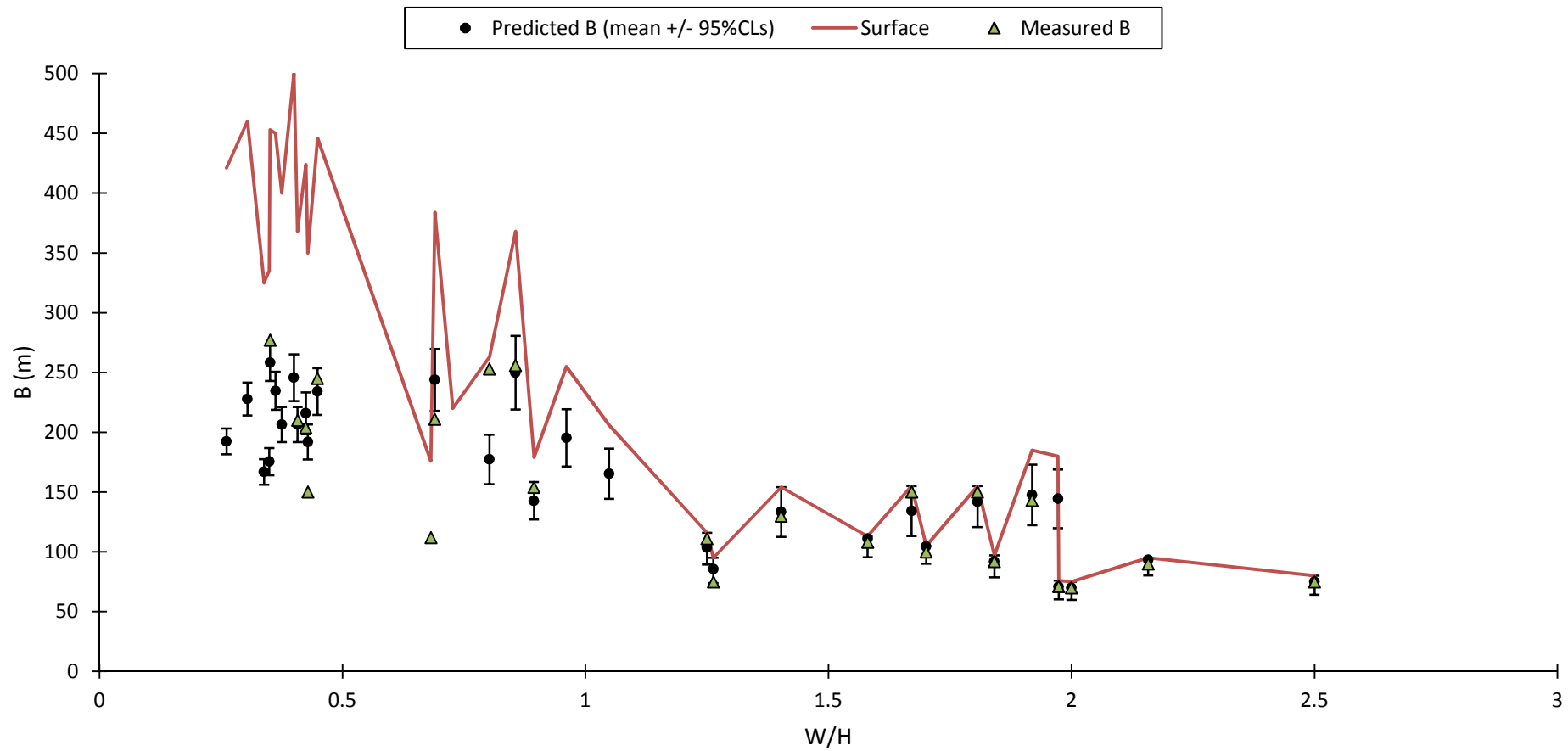
The risk to reject the null hypothesis H0 while it is true is 86.6%.

	Engineer:	S.Ditton	Client:	Review of Height of Fracturing Data	
	Drawn:	S.Ditton			
	Date:	01.05.14	Title:	Results of Non-Linear Regression Error analysis for Geology Pi-Term Height of A-Zone	
	Ditton Geotechnical Services Pty Ltd			Prediction Model: Regression Error Normal Distribution Test	
		Scale:	NTS	Figure No:	A42j

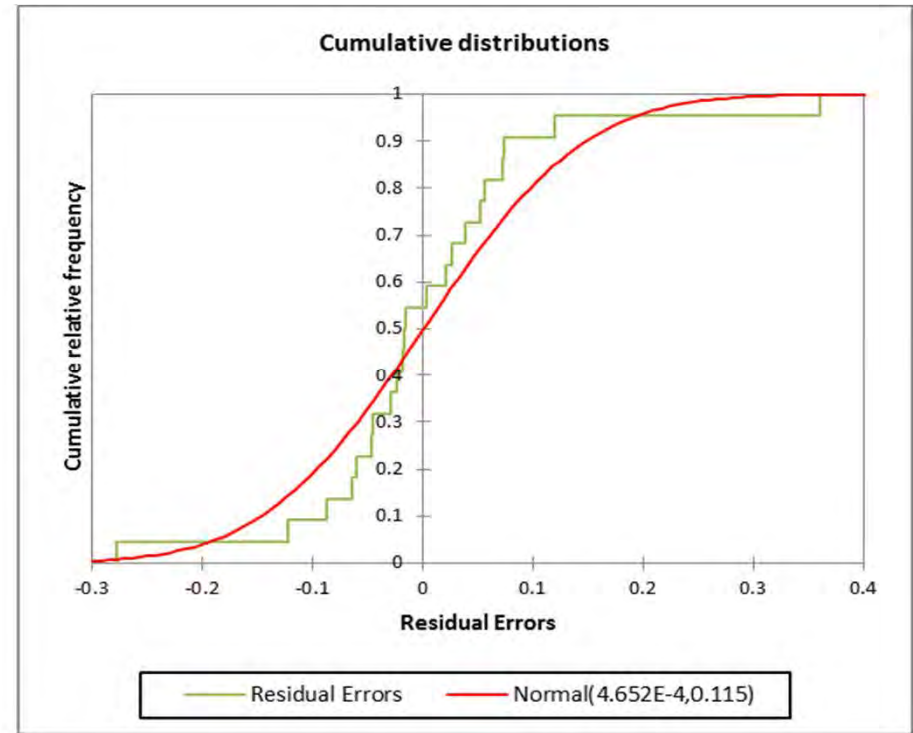
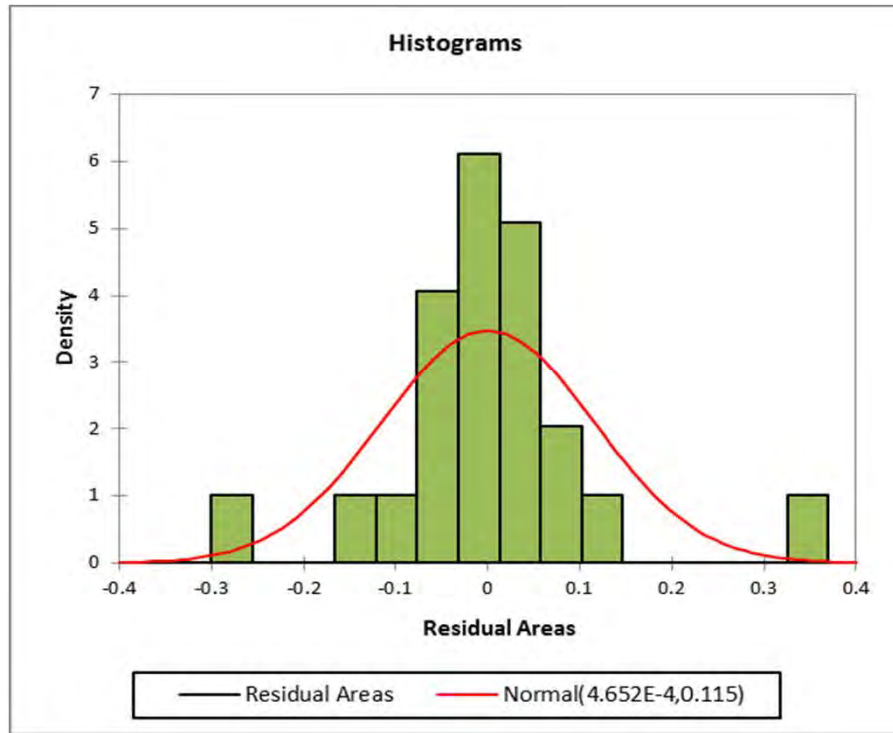
Geometry Model



	Engineer:	S.Ditton	Client:	Review of Height of Fracturing Data	
	Drawn:	S.Ditton			
	Date:	01.02.14	Title:	Results of Non-Linear Regression Error analysis for Height of B-Zone Predictions for Geometry Only Pi-Term Model	
	Ditton Geotechnical Services Pty Ltd			Scale:	NTS



	Engineer:	S.Ditton	Client:	Review of Height of Fracturing Data	
	Drawn:	S.Ditton	Title:	Results of Non-Linear Regression Error analysis for Height of B-Zone Predictions for Geometry Only Pi-Term Model	
	Date:	01.02.14	Scale:	NTS	Figure No:
	Ditton Geotechnical Services Pty Ltd				A42I



Kolmogorov-Smirnov test:

D	0.173
p-value	0.487
alpha	0.05

Test interpretation:

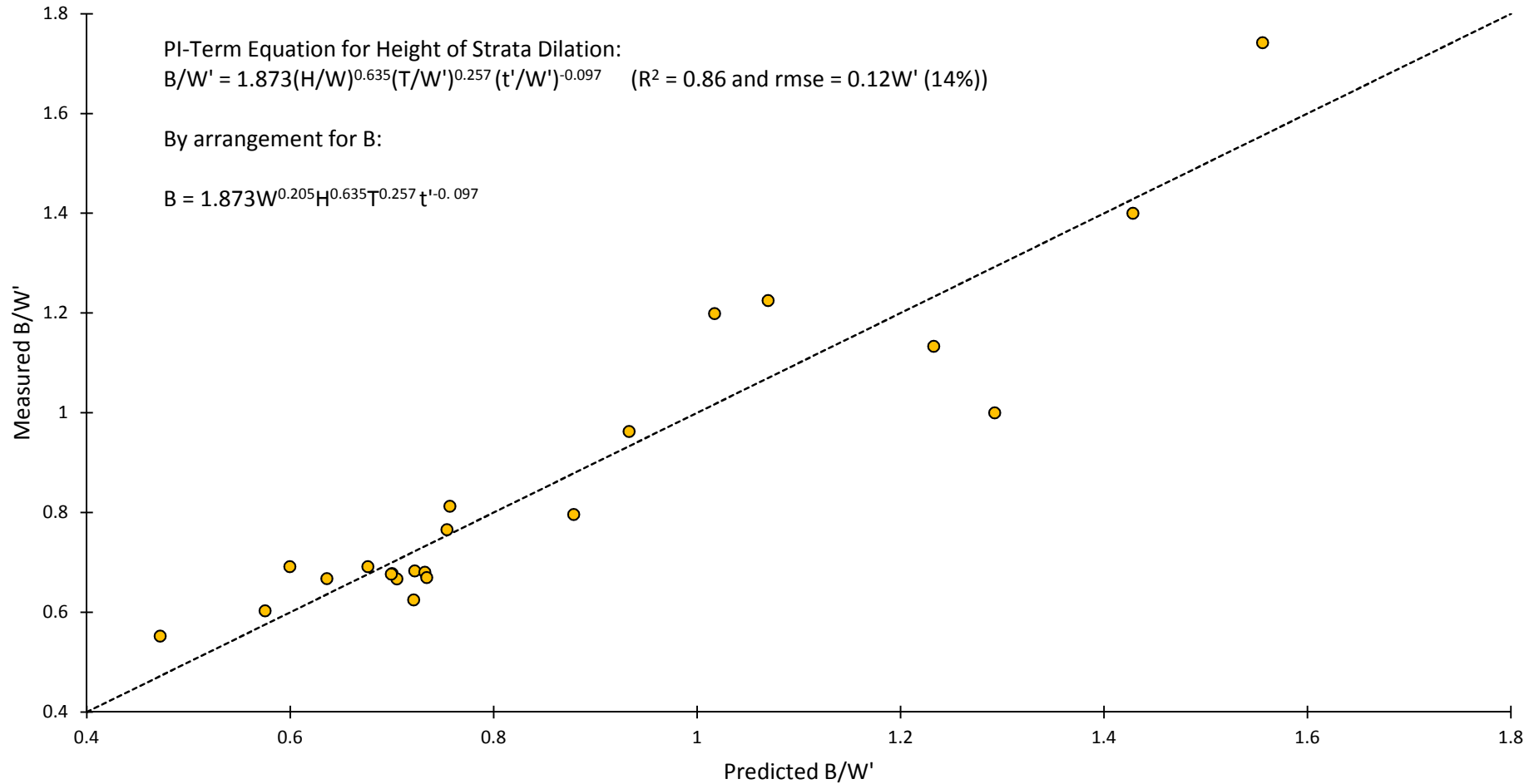
H0: The sample follows a Normal distribution

Ha: The sample does not follow a Normal distribution

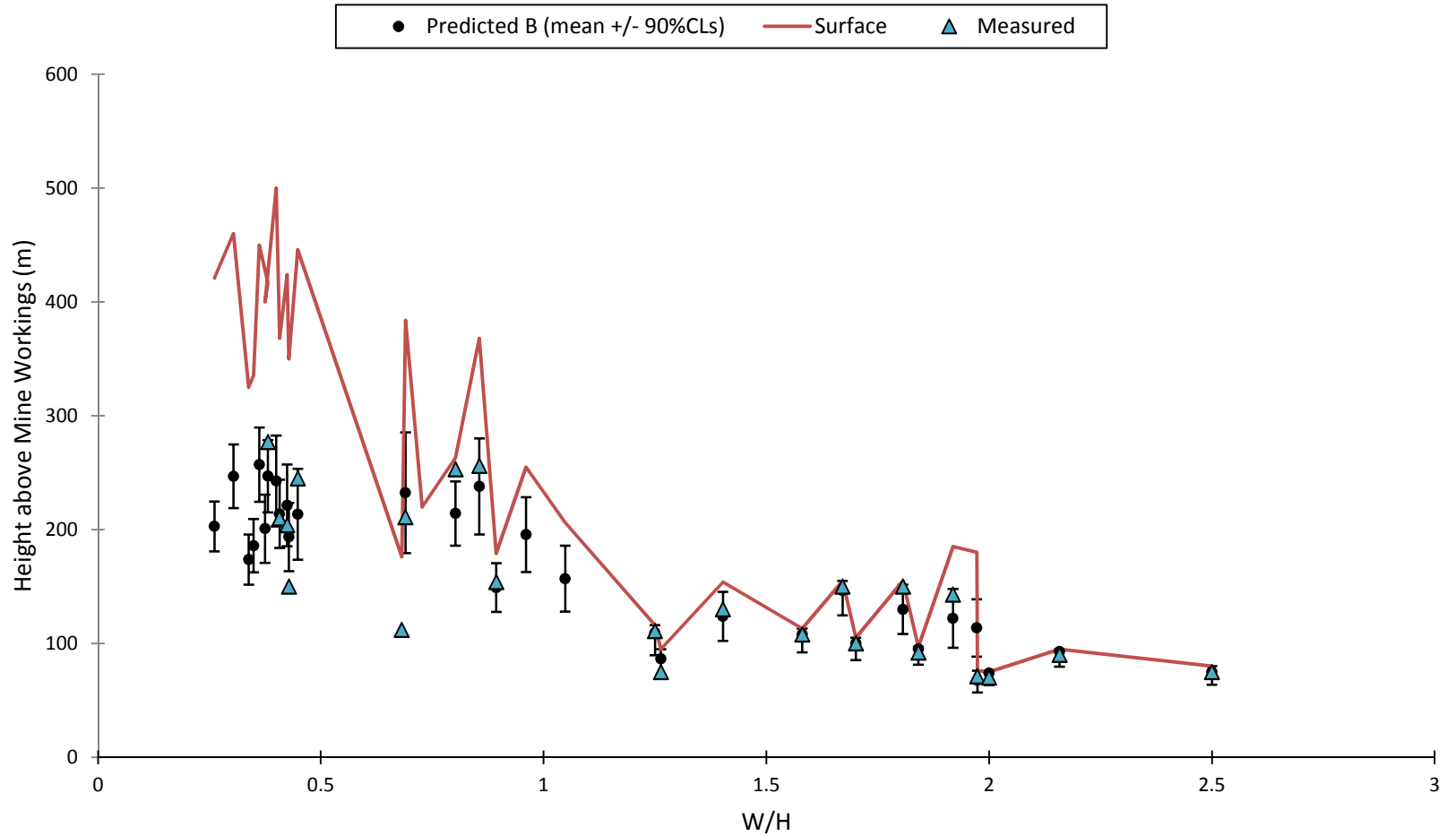
As the computed p-value is greater than the significance level $\alpha=0.05$, one cannot reject the null hypothesis H0.

The risk to reject the null hypothesis H0 while it is true is 48.70%.

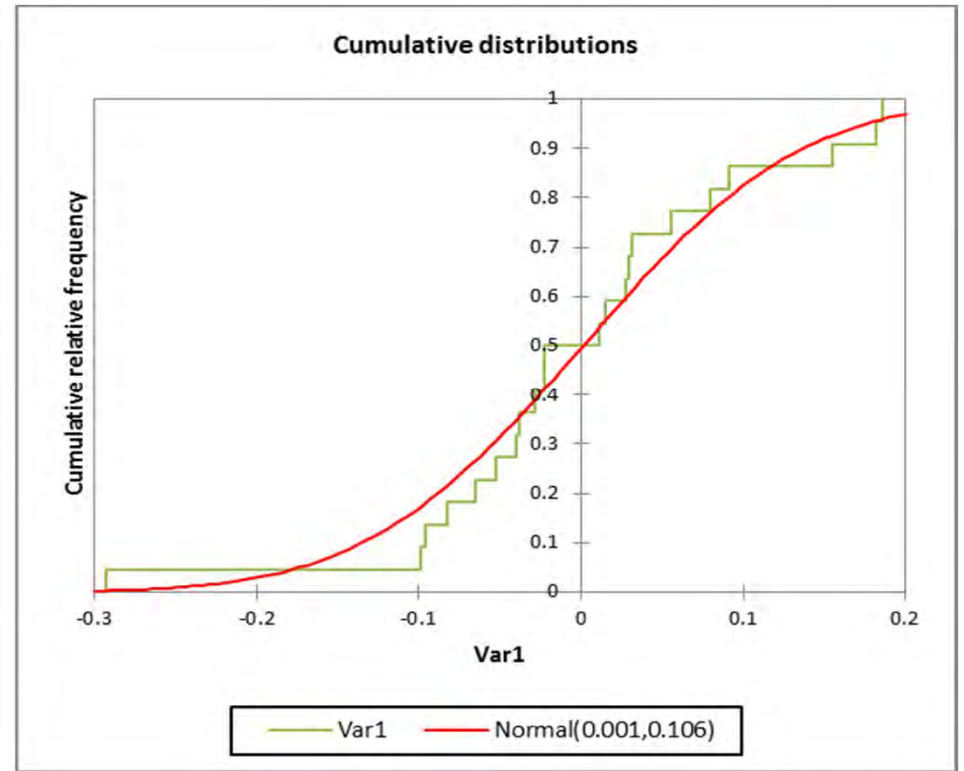
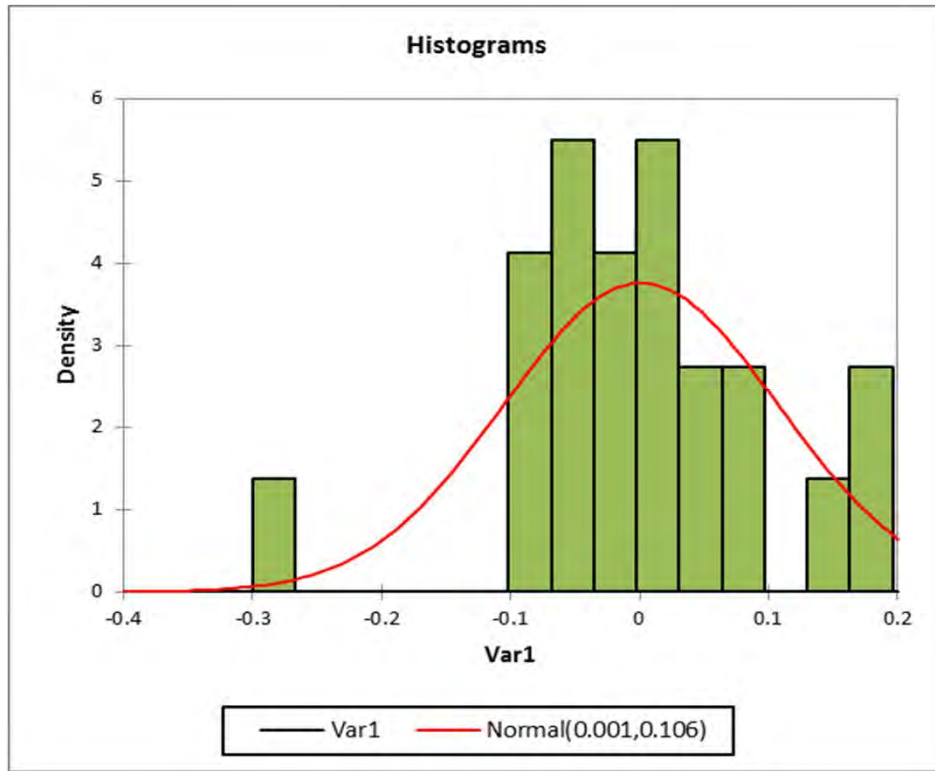
	Engineer:	S.Ditton	Client:	Review of Height of Fracturing Data	
	Drawn:	S.Ditton			
	Date:	01.02.14	Title:	Results of Non-Linear Regression Error analysis for Height of B-Zone Predictions for Geometry Only Pi-Term Model	
	Ditton Geotechnical Services Pty Ltd			Scale:	NTS



	Engineer:	S.Ditton	Client:	Review of Height of Fracturing Data		
	Drawn:	S.Ditton		Title:	Results of Non-Linear Regression Error analysis for Height of B-Zone Predictions for Geology Pi-Term Model	
	Date:	01.02.14	Scale:		NTS	
	Ditton Geotechnical Services Pty Ltd				Figure No:	A42n



	Engineer:	S.Ditton	Client:	Review of Height of Fracturing Data	
	Drawn:	S.Ditton			
	Date:	01.02.14	Title:	Results of Non-Linear Regression Error analysis for Height of B-Zone Predictions for Geology Pi-Term Model	
	Ditton Geotechnical Services Pty Ltd		Scale:	NTS	Figure No:



Kolmogorov-Smirnov test:

D	0.126
p-value	0.849
alpha	0.05

Test interpretation:

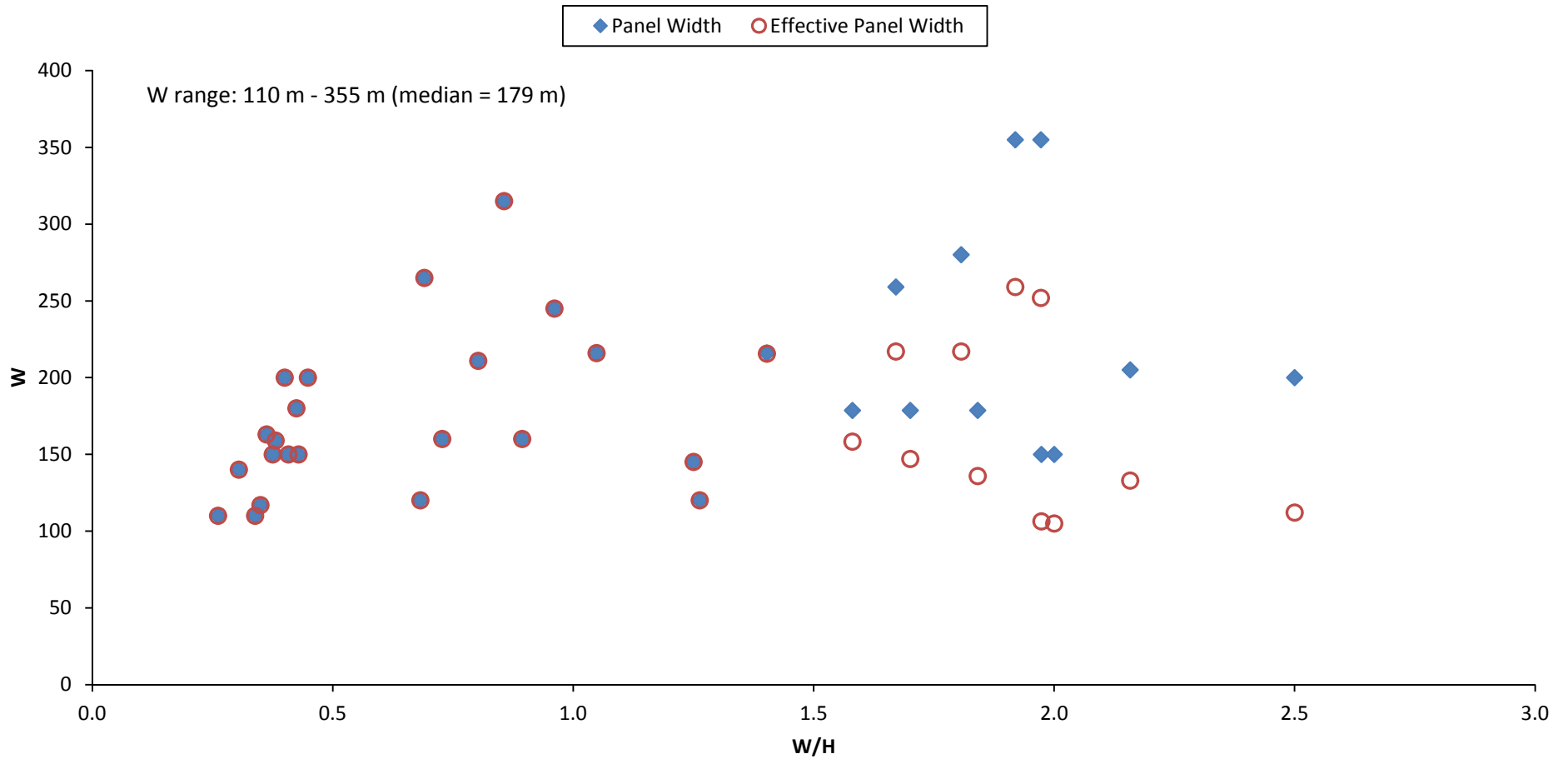
H0: The sample follows a Normal distribution

Ha: The sample does not follow a Normal distribution

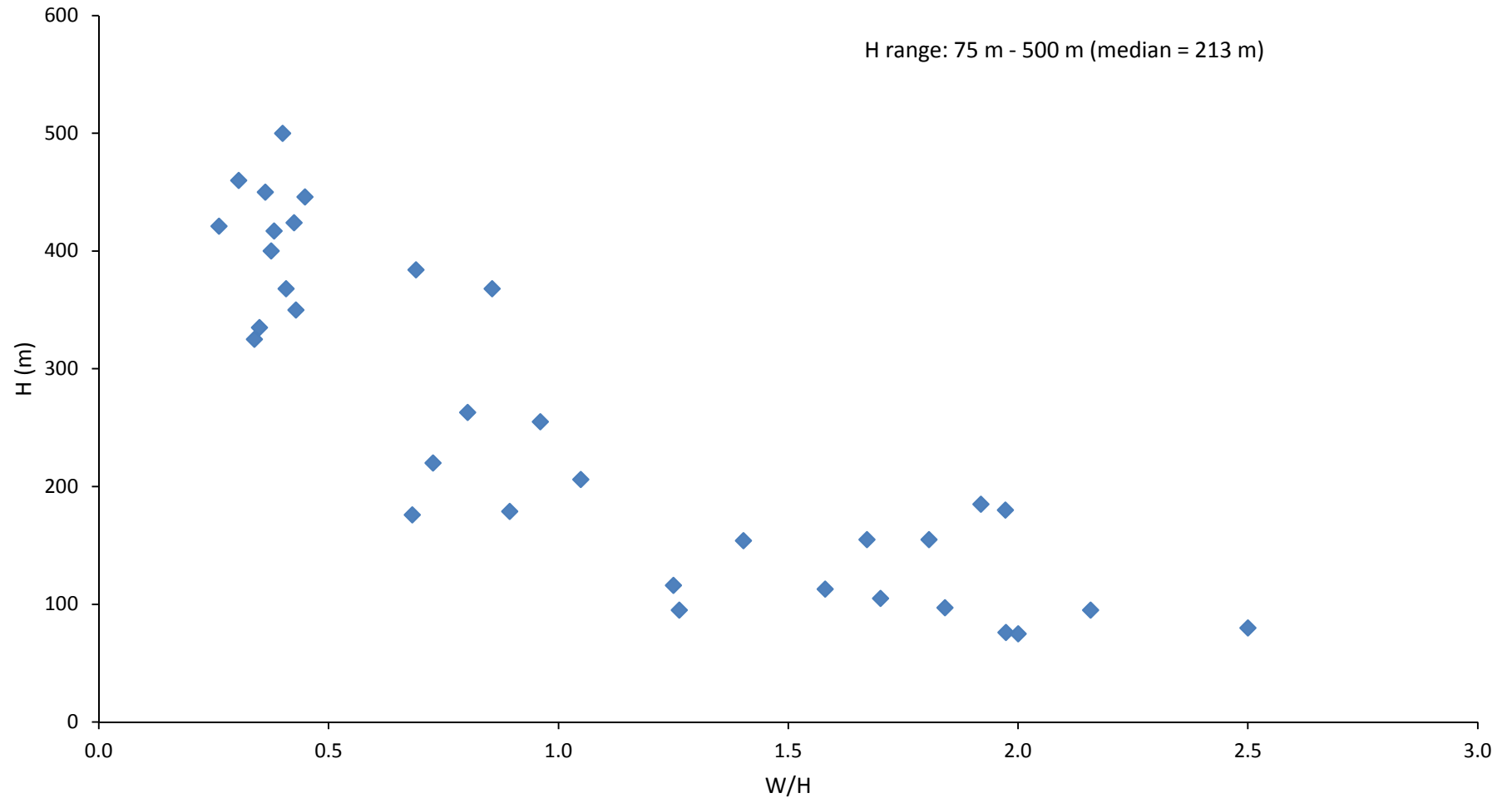
As the computed p-value is greater than the significance level $\alpha=0.05$, one cannot reject the null hypothesis H0.

The risk to reject the null hypothesis H0 while it is true is 84.89%.

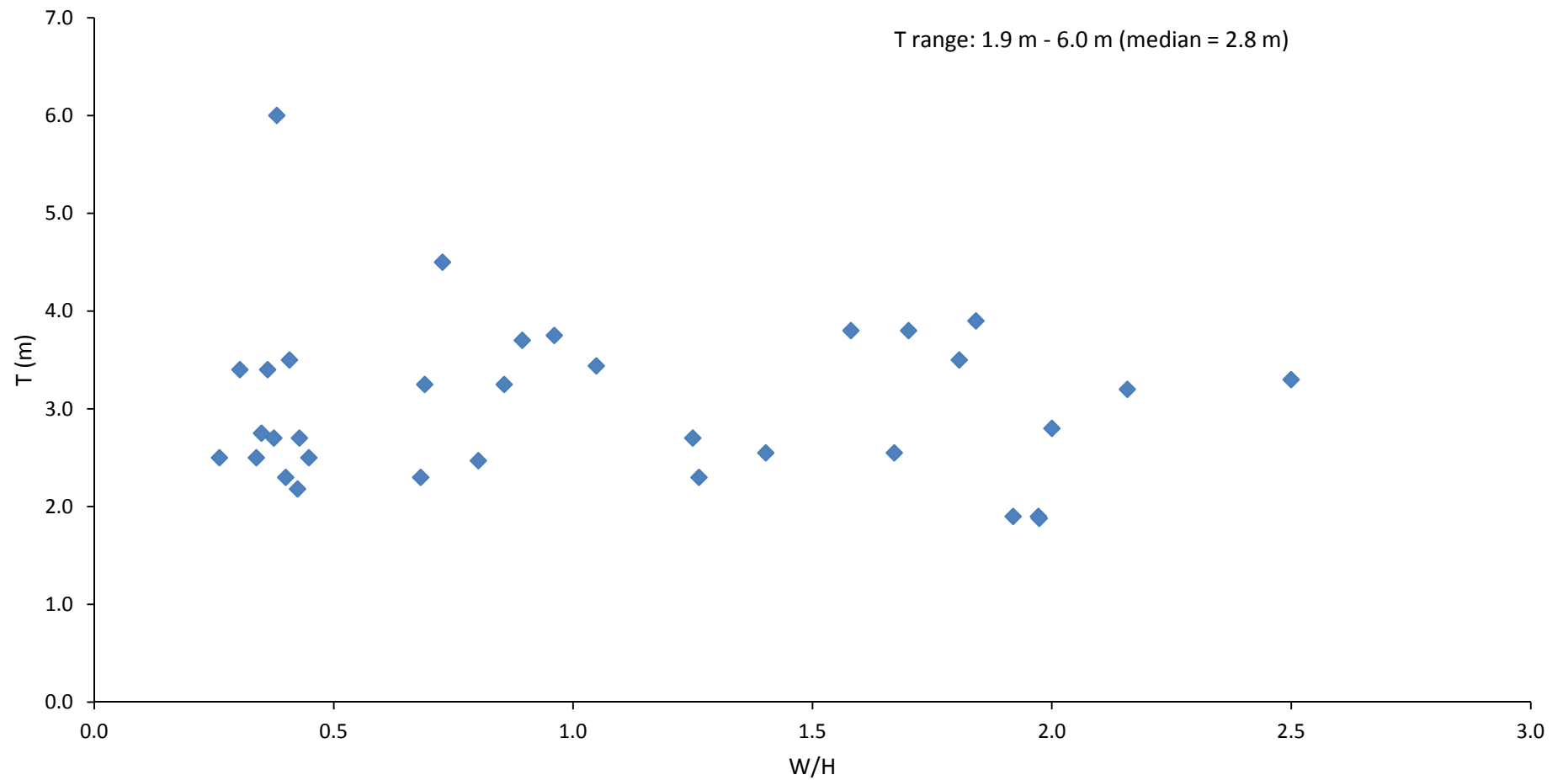
	Engineer:	S.Ditton	Client:	Review of Height of Fracturing Data	
	Drawn:	S.Ditton			
	Date:	01.02.14	Title:	Results of Non-Linear Regression Error analysis for Height of B-Zone Predictions for Geology Pi-Term Model	
	Ditton Geotechnical Services Pty Ltd			Scale:	NTS



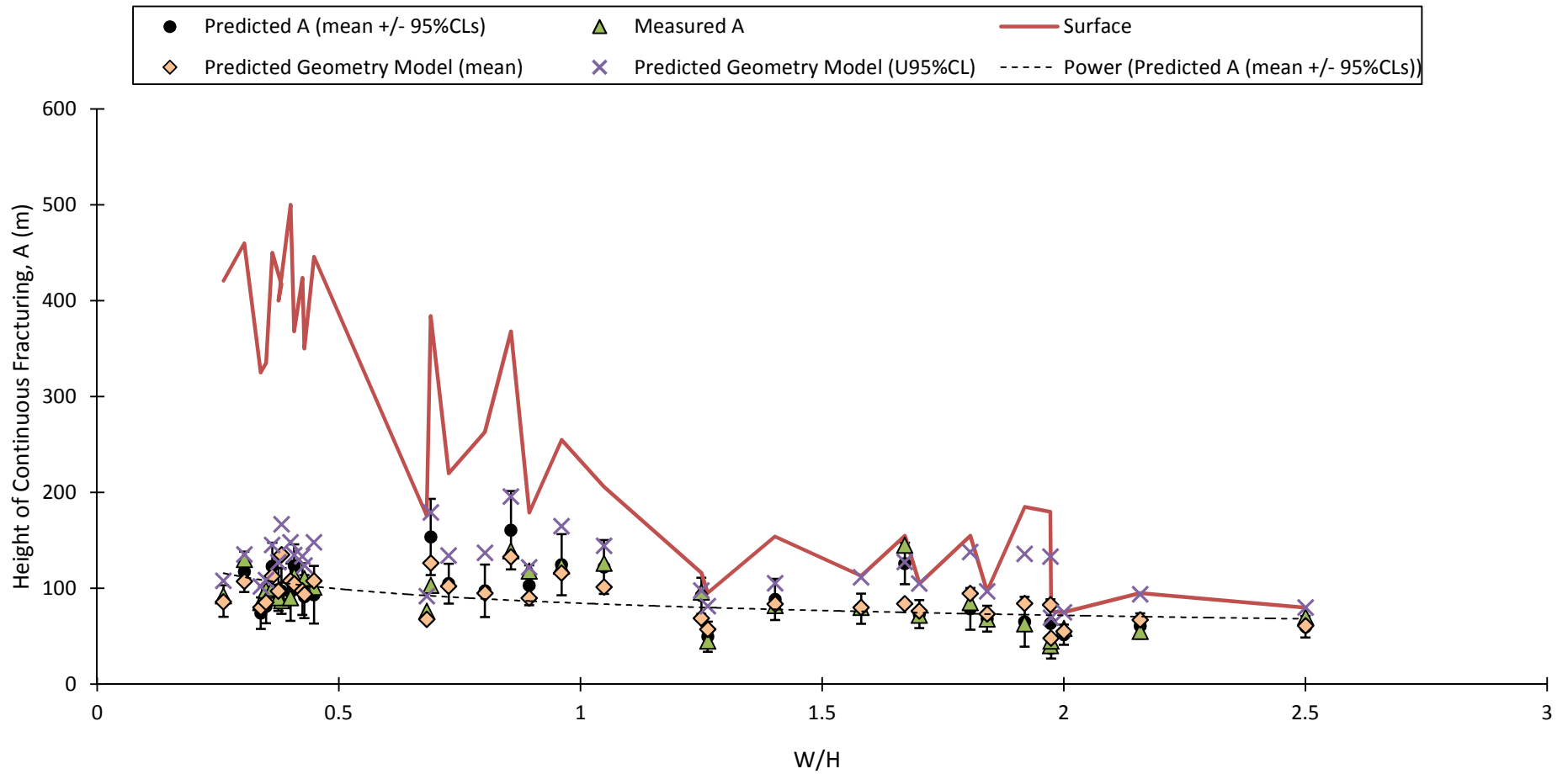
	Engineer:	S.Ditton	Client:	Modified from ACARP, 2003	
	Drawn:	S.Ditton			
	Date:	03.12.12	Title:	Panel Width v. W/H Database for Sub-surface Fracturing Model	
	Ditton Geotechnical Services Pty Ltd				
Scale:	NTS		Figure No:	A43a	



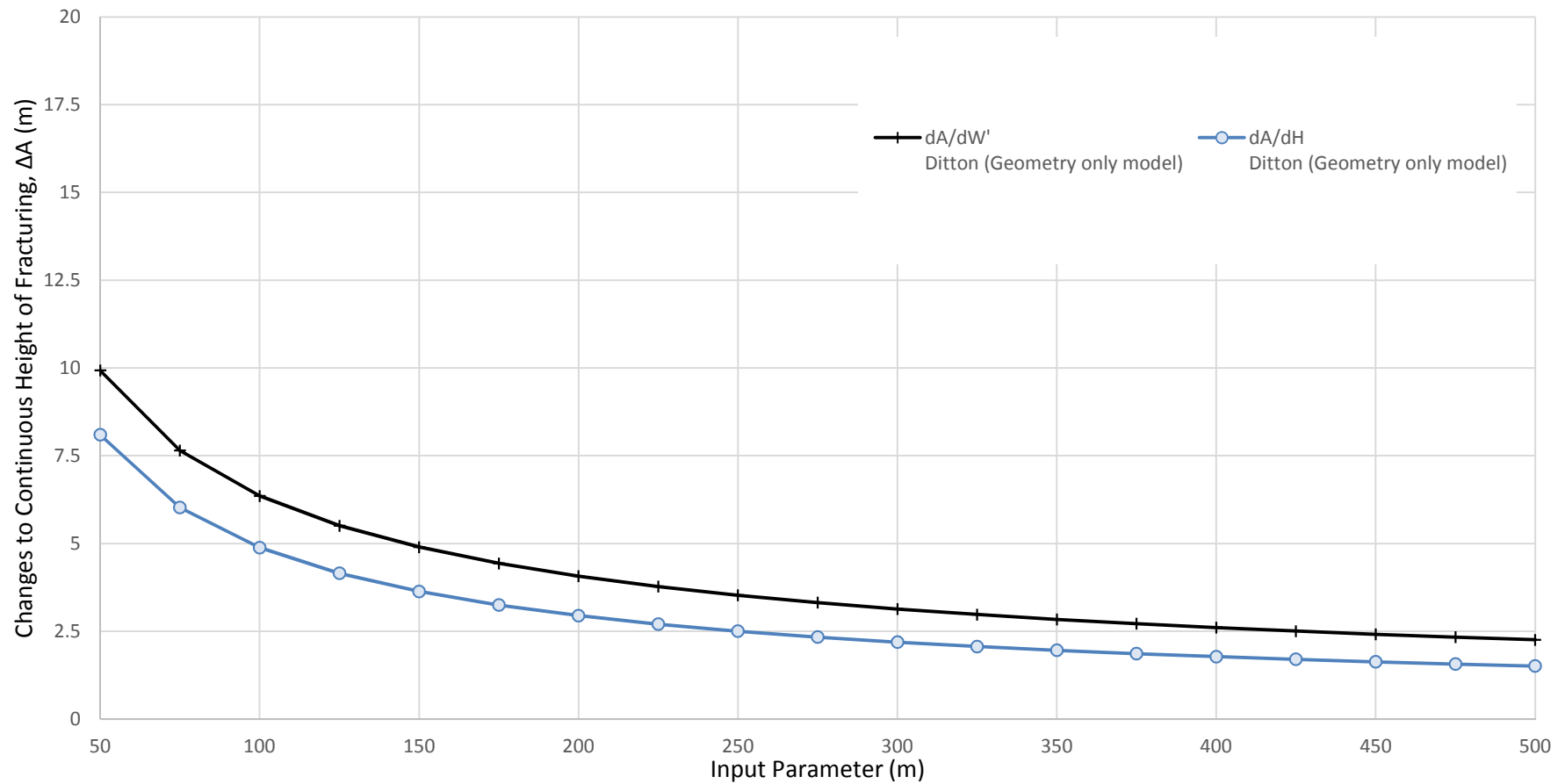
	Engineer:	S.Ditton	Client:	Modified from ACARP, 2003	
	Drawn:	S.Ditton			
	Date:	03.12.12	Title:	Cover Depth v. W/H Database for Sub-surface Fracturing Model	
	Ditton Geotechnical Services Pty Ltd				
Scale:	NTS		Figure No:	A43b	



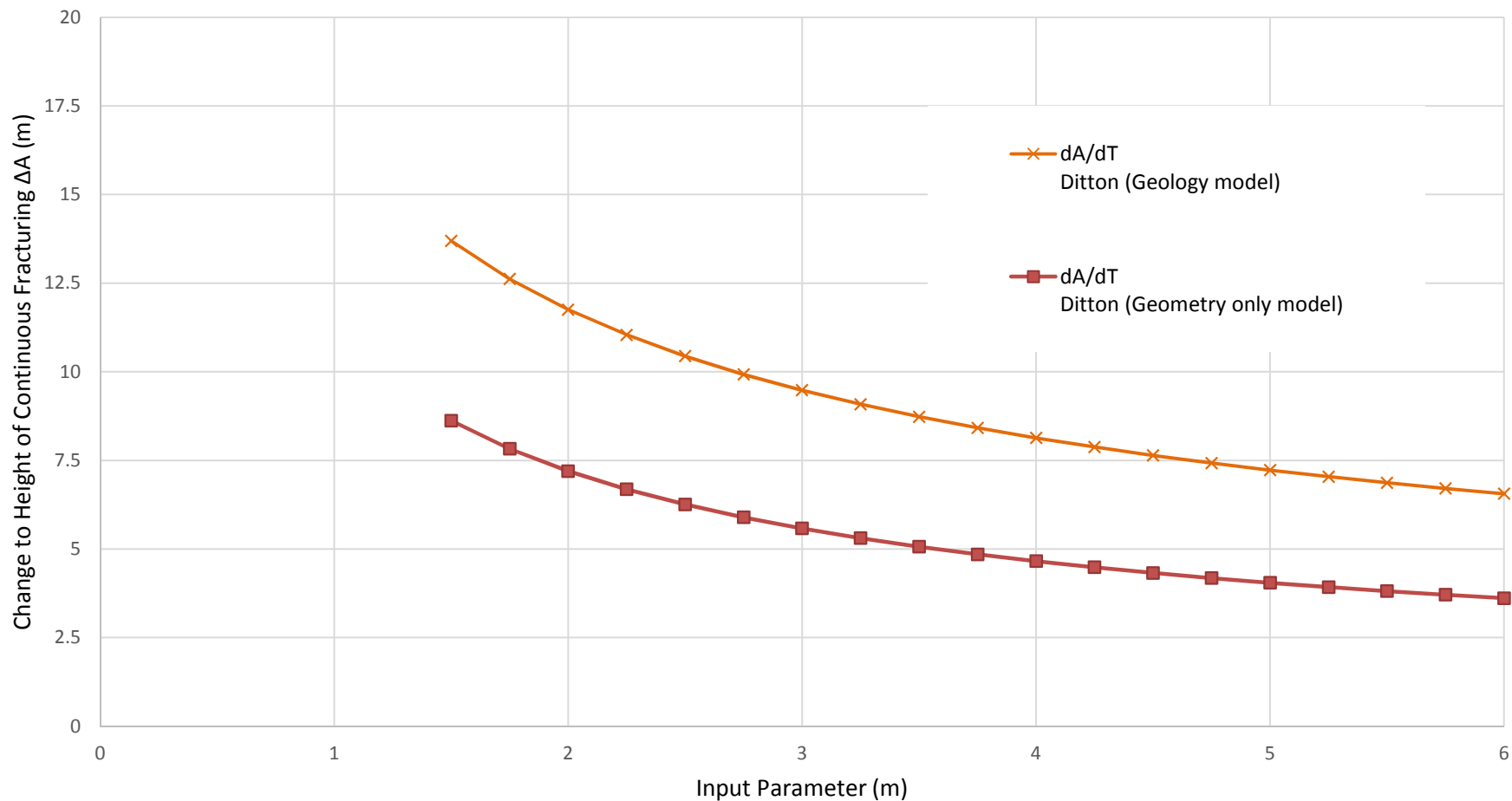
	Engineer:	S.Ditton	Client:	Modified from ACARP, 2003	
	Drawn:	S.Ditton			
	Date:	03.12.12	Title:	Mining Height v. W/H Database for Sub-surface Fracturing Model	
	Ditton Geotechnical Services Pty Ltd				
Scale:	NTS		Figure No:	A43c	



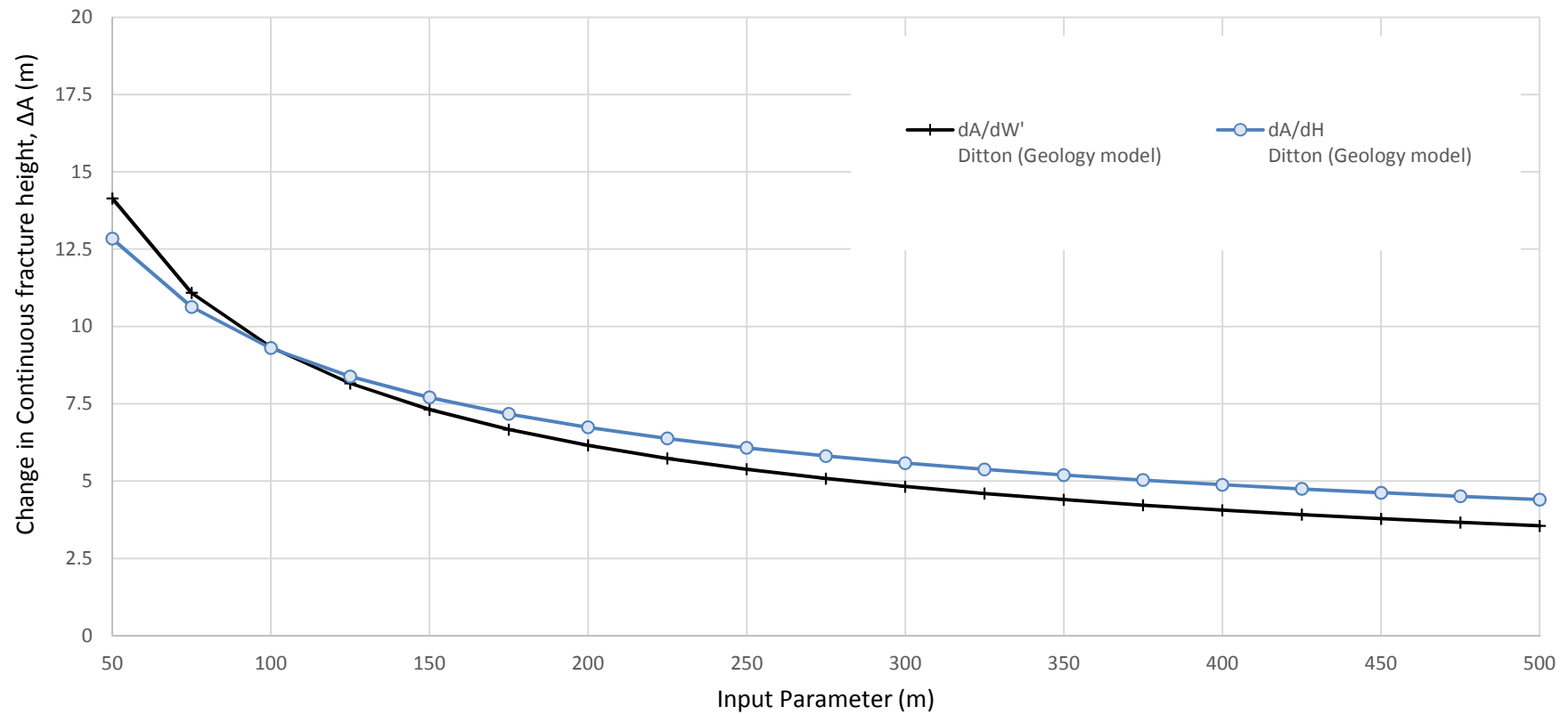
	Engineer:	S.Ditton	Client:	Review of Height of Fracturing Data		
	Drawn:	S.Ditton		Title:	Heights of Continuous Fracturing Predictions for the Geometry and Geology Pi-Term Models	
	Date:	01.05.14	Scale:		NTS	Figure No:
	Ditton Geotechnical Services Pty Ltd					



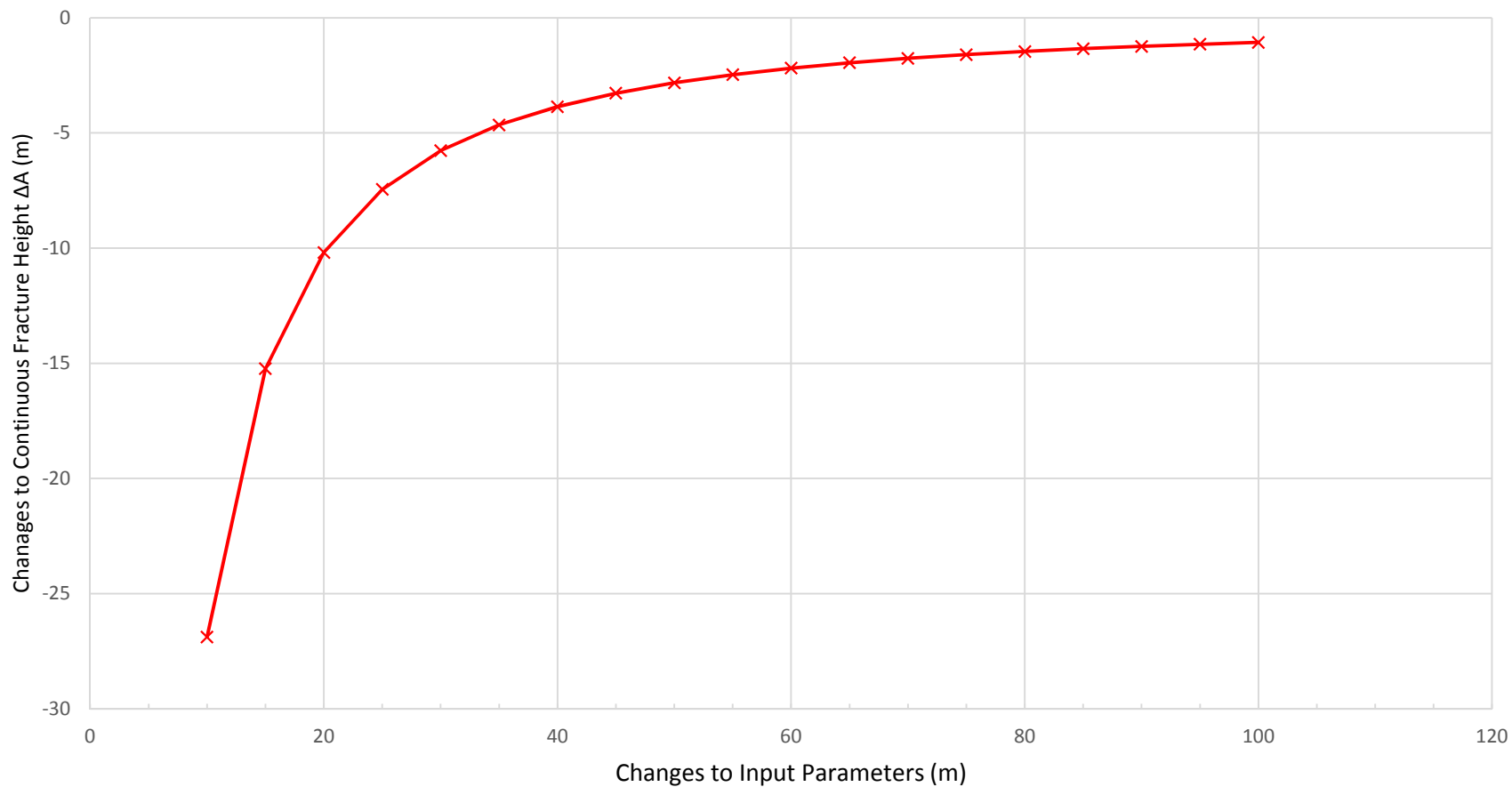
	Engineer:	S.Ditton	Client:	Modified from ACARP, 2003	
	Drawn:	S.Ditton			
	Date:	25.05.14	Title:	Sensitivity Analysis of Geometry Only Pi-Term Model Input Parameters on Predicted Height of Continuous Fracturing: W' and H (as per Merrick, 2014)	
	Ditton Geotechnical Services Pty Ltd				
Scale:	NTS		Figure No:	A43e	



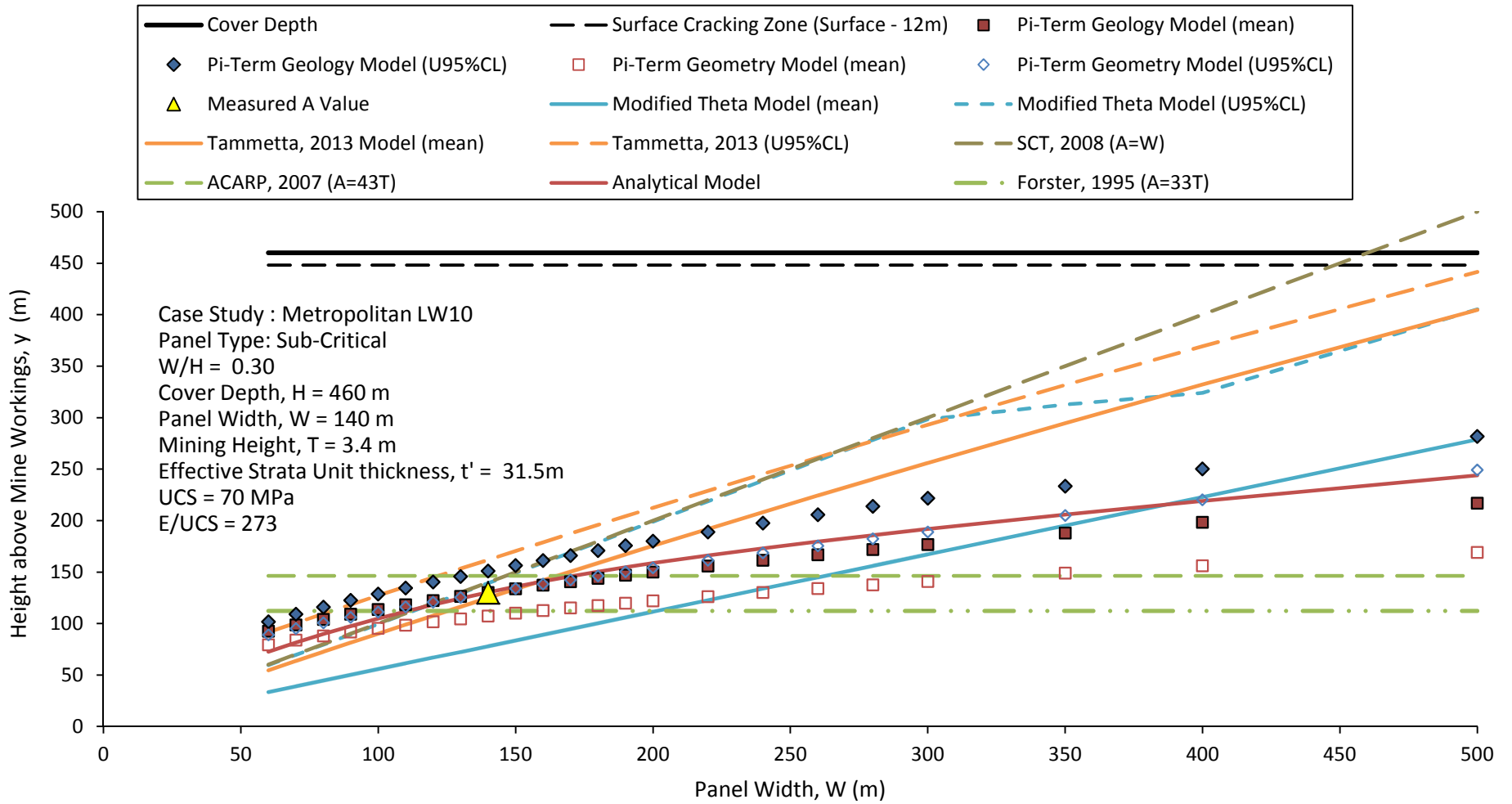
	Engineer:	S.Ditton	Client:	Modified from ACARP, 2003	
	Drawn:	S.Ditton			
	Date:	25.05.14	Title:	Sensitivity Analysis of Geology & Geometry Pi-Term Model Input Parameters on Predicted Height of Continuous Fracturing: T (as per Merrick, 2014)	
	Ditton Geotechnical Services Pty Ltd				
Scale:	NTS		Figure No:	A43f	



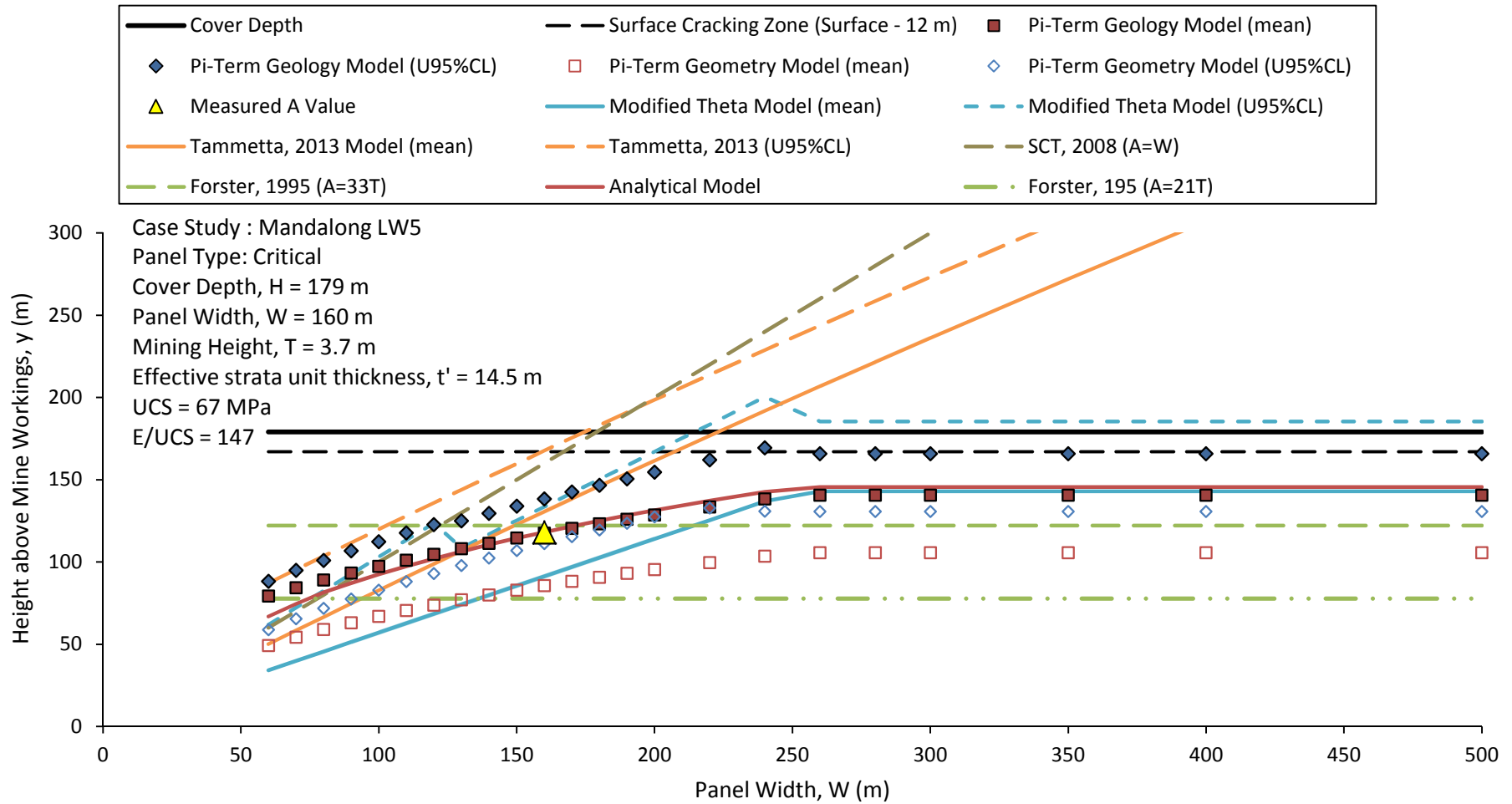
	Engineer:	S.Ditton	Client:	Modified from ACARP, 2003	
	Drawn:	S.Ditton			
	Date:	25.05.14	Title:	Sensitivity Analysis of Geology Pi-Term Model Input Parameters on Predicted Height of Continuous Fracturing: W' and H (as per Merrick, 2014)	
	Ditton Geotechnical Services Pty Ltd				
Scale:	NTS		Figure No:	A43g	



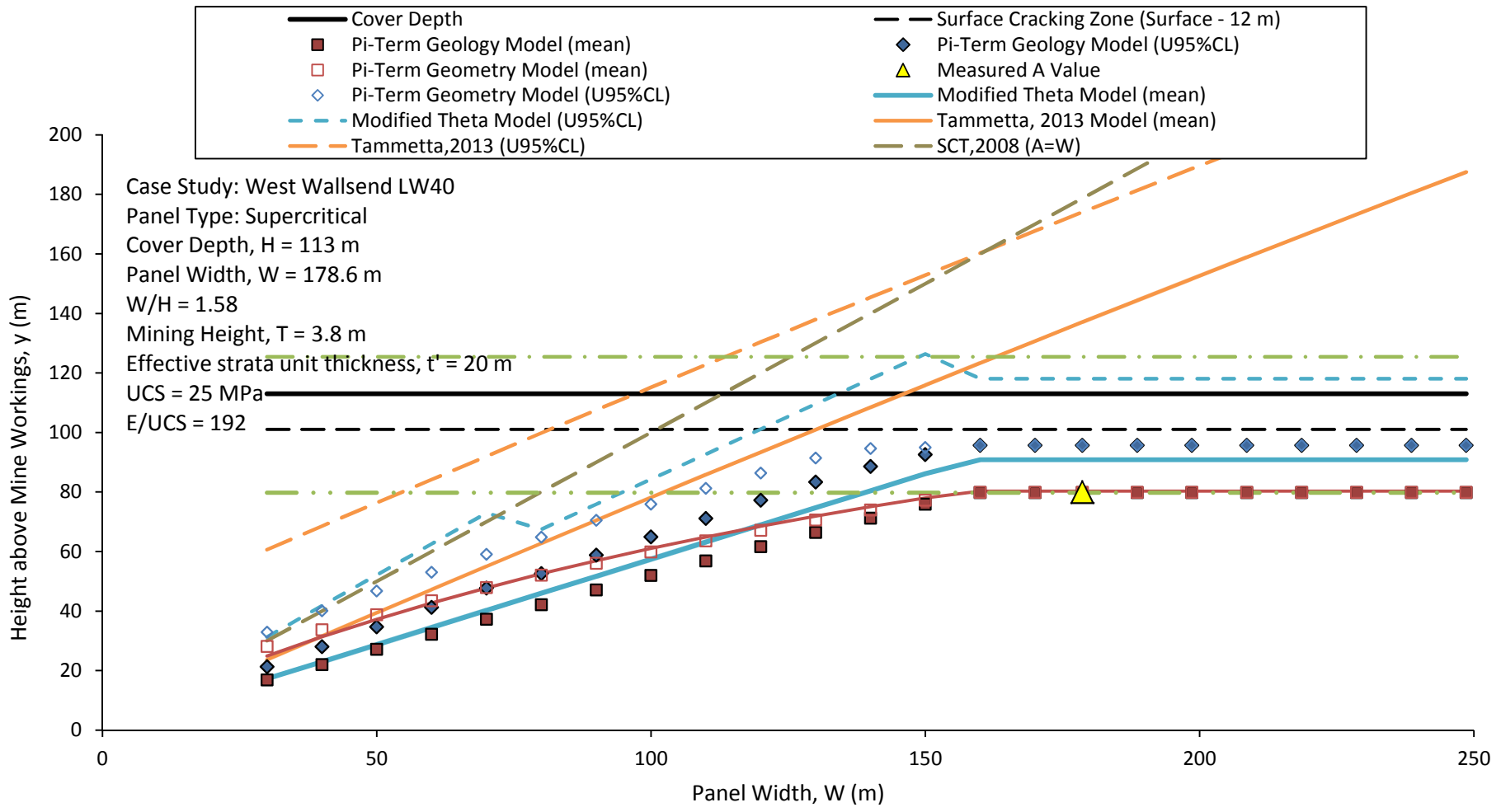
	Engineer:	S.Ditton	Client:	Modified from ACARP, 2003	
	Drawn:	S.Ditton			
	Date:	25.05.14	Title:	Sensitivity Analysis of Geology Pi-Term Model Input Parameters on Predicted Height of Continuous Fracturing: t' (as per Merrick, 2014)	
	Ditton Geotechnical Services Pty Ltd				
Scale:	NTS		Figure No:	A43h	



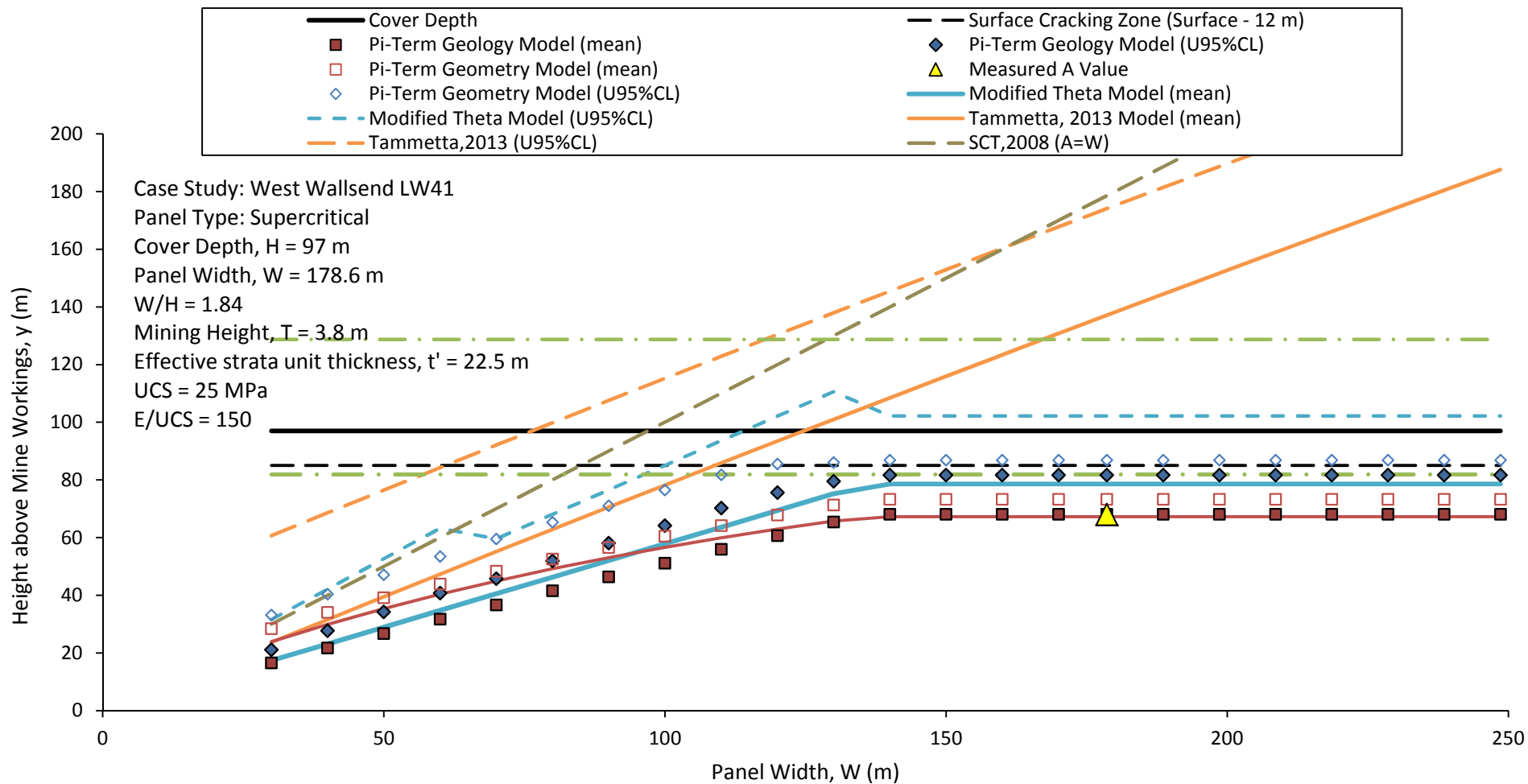
	Engineer:	S.Ditton	Client:	Modified from ACARP, 2003	
	Drawn:	S.Ditton			
	Date:	16.03.14	Title:	Predicted A-Zone Fracture Heights for Varying Panel Widths using Pi-Term Geometry and Geology Models and Current State of the Art Models	
	Ditton Geotechnical Services Pty Ltd			Scale:	NTS



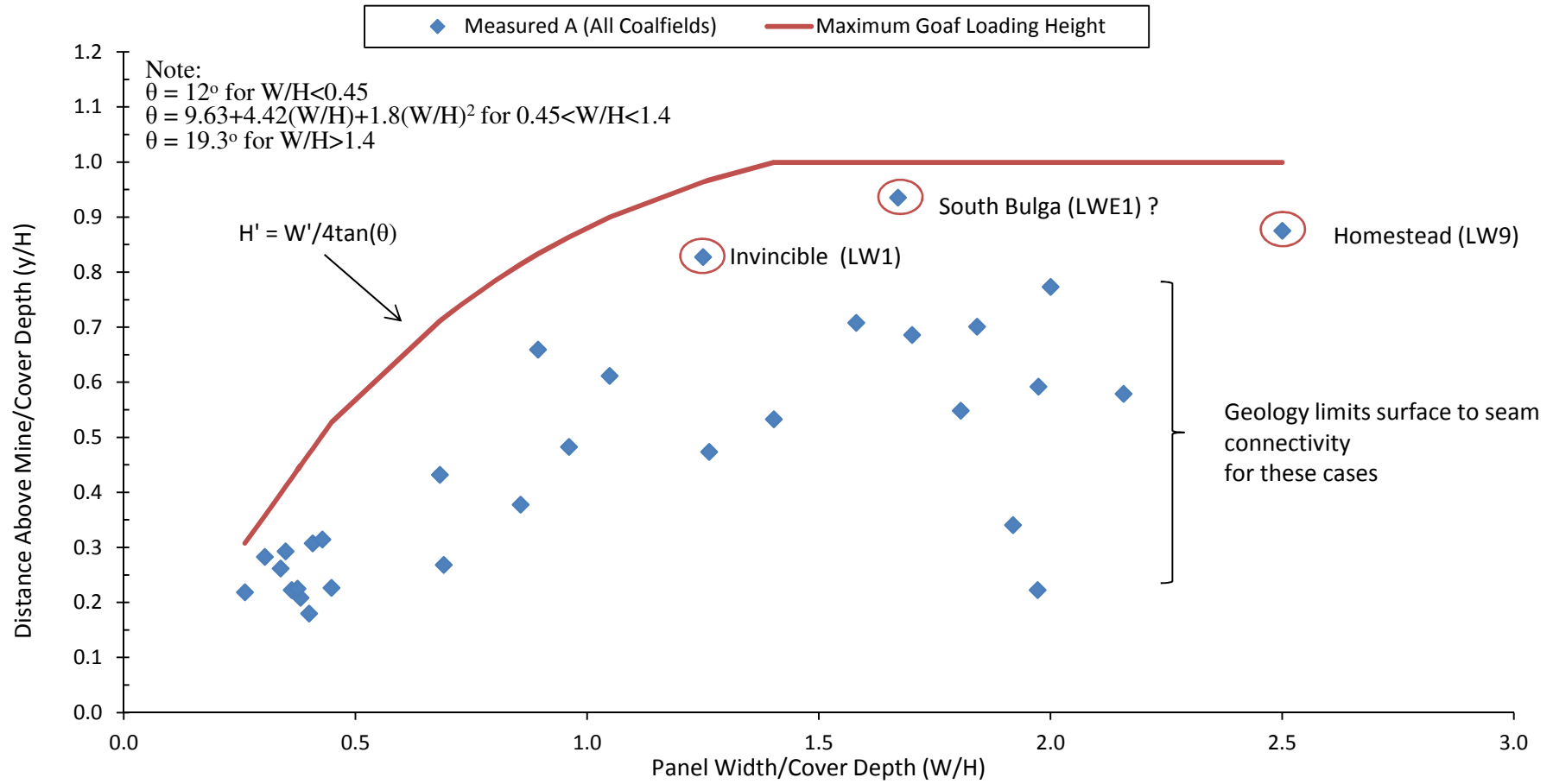
	Engineer:	S.Ditton	Client:	Modified from ACARP, 2003	
	Drawn:	S.Ditton			
	Date:	16.03.14	Title:	Predicted A-Zone Fracture Heights for Varying Panel Widths using Pi-Term Geometry and Geology Models and Current State of the Art Models	
	Ditton Geotechnical Services Pty Ltd				
Scale:	NTS		Figure No:	A43j	



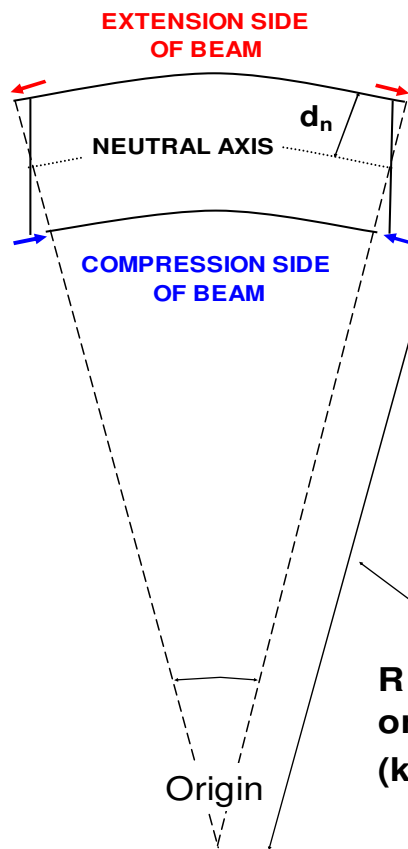
	Engineer:	S.Ditton	Client:	Modified from ACARP, 2003	
	Drawn:	S.Ditton			
	Date:	16.03.14	Title:	Predicted A-Zone Fracture Heights for Varying Panel Widths using Pi-Term Geometry and Geology Models and Current State of the Art Models	
	Ditton Geotechnical Services Pty Ltd				
Scale:	NTS		Figure No:	A43k	



	Engineer:	S.Ditton	Client:	Modified from ACARP, 2003	
	Drawn:	S.Ditton			
	Date:	16.03.14	Title:	Predicted A-Zone Fracture Heights for Varying Panel Widths using Pi-Term Geometry and Geology Models and Current State of the Art Models	
	Ditton Geotechnical Services Pty Ltd			Scale:	NTS



	Engineer:	S.Ditton	Client:	Review of Height of Fracturing Data	
	Drawn:	S.Ditton			
	Date:	01.05.14	Title:	Measured Heights of Continuous Fracturing in NSW and QLD Coalfields with Reported Surface to Seam Connectivity Cases and Theoretical Goaf Loading Height	
	Ditton Geotechnical Services Pty Ltd			Scale:	NTS



Strain $E = (\text{mm/m})$
 Curvature $C = \text{km}^{-1}$

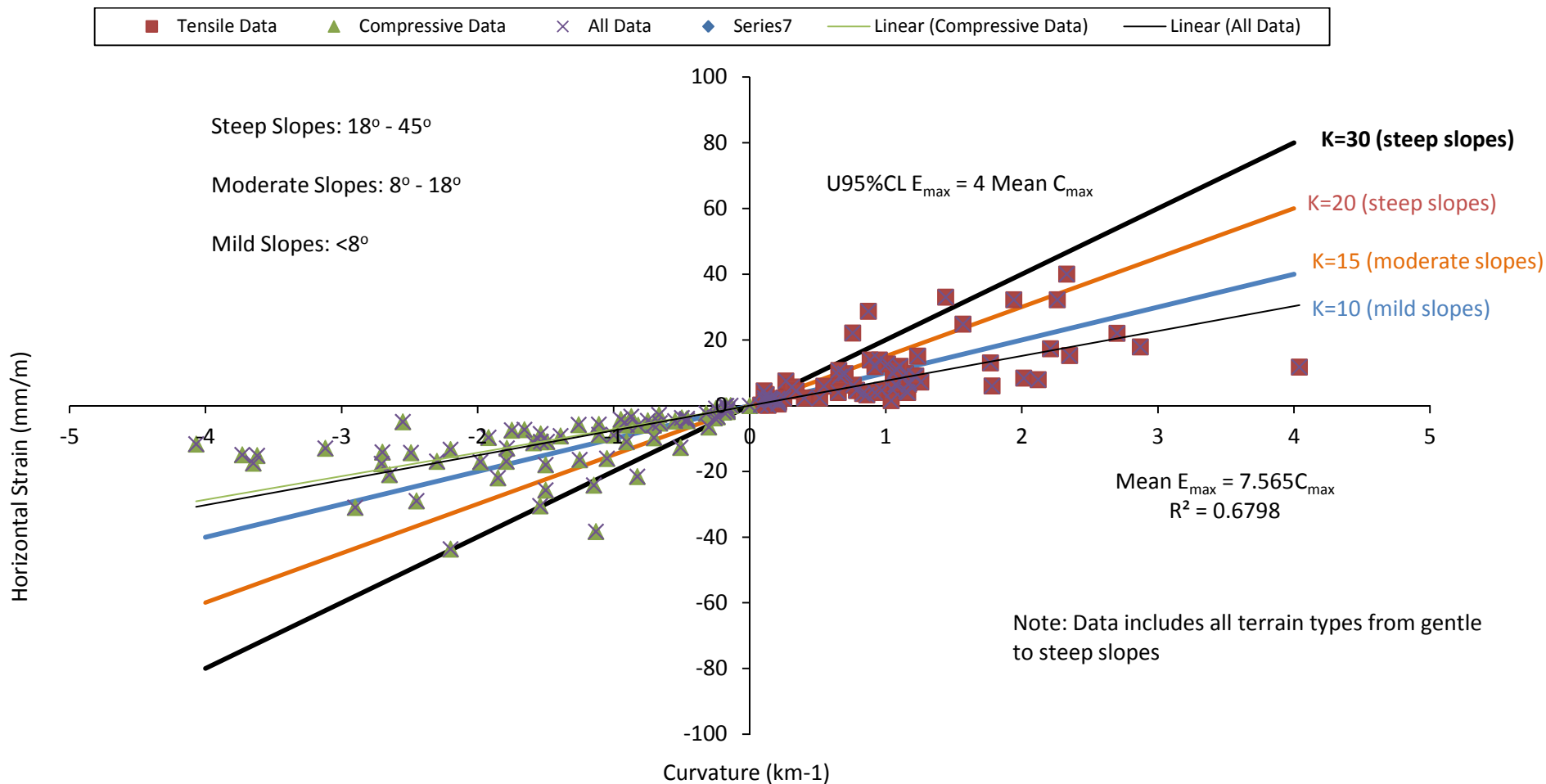
$$E = C \times d_n$$

= Depth of Cracking

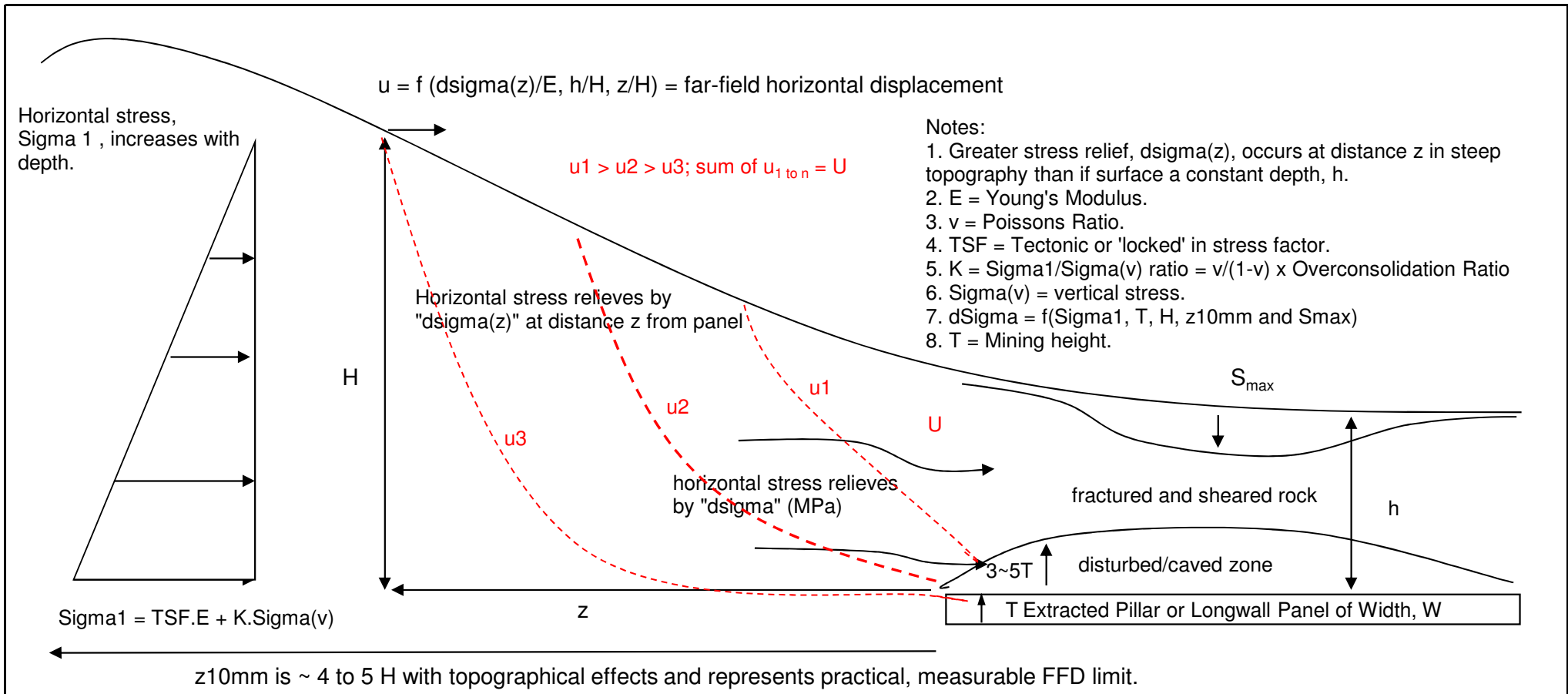
**R = Radius of curvature
 or the curvature, $C = 1/R$
 (km^{-1})**



Engineer:	S.Ditton	Client:	Extract from ACARP, 2003	
Drawn:	S.Ditton			
Date:	08.08.08	Title:	Bending Beam Theory for Strain Prediction from Curvature Measurements	
Ditton Geotechnical Services Pty Ltd		Scale:	NTS	Figure No: A43n



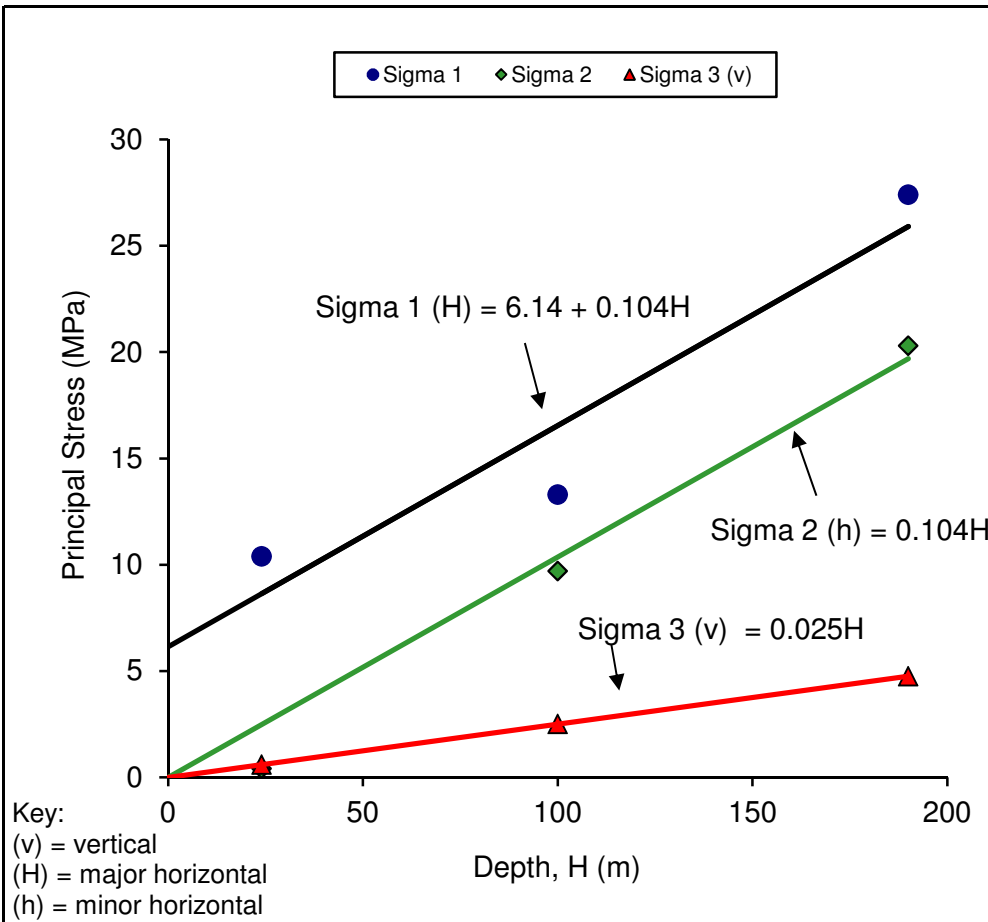
	Engineer:	S.Ditton	Client:	Extract from ACARP, 2003	
	Drawn:	S.Ditton			
	Date:	08.08.08	Title:	Empirical Model for Maximum Panel Strain Prediction Above Longwall Panels for Smooth and Cracked Profiles in the Newcastle Coalfield	
	Ditton Geotechnical Services Pty Ltd			Scale:	NTS



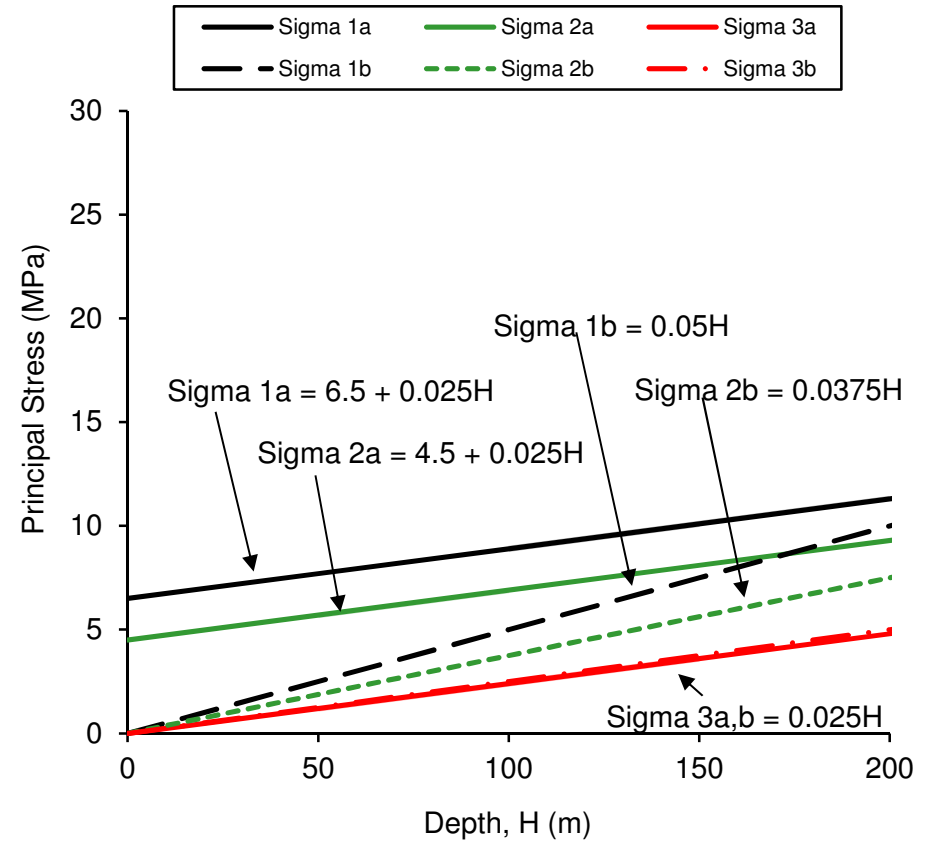
- Notes:
1. Greater stress relief, $d\Sigma(z)$, occurs at distance z in steep topography than if surface a constant depth, h .
 2. E = Young's Modulus.
 3. ν = Poissons Ratio.
 4. TSF = Tectonic or 'locked' in stress factor.
 5. $K = \Sigma_1/\Sigma(v)$ ratio = $\nu/(1-\nu) \times \text{Overconsolidation Ratio}$
 6. $\Sigma(v)$ = vertical stress.
 7. $d\Sigma = f(\Sigma_1, T, H, z_{10mm} \text{ and } S_{\max})$
 8. T = Mining height.

Simple Analytical Model for Predicting Total FFD : $U = 0.5(\Sigma_1 \times 12.3/2)z_{10mm}/[E(H+h)/2] + \text{'tail' of } 10mm + S_{\max} \text{ component (refer to text)}$

	Engineer:	S.Ditton	Client:	DgS, 2007		
	Drawn:	S.Ditton	Title:	Conceptual Model of Far-Field Displacement Outside Angle of Draw Limits from Pillar Extraction or Longwall Panels		
	Date:	22.05.07	Scale:	NTS	Figure No:	A44a
	Ditton Geotechnical Services Pty Ltd					

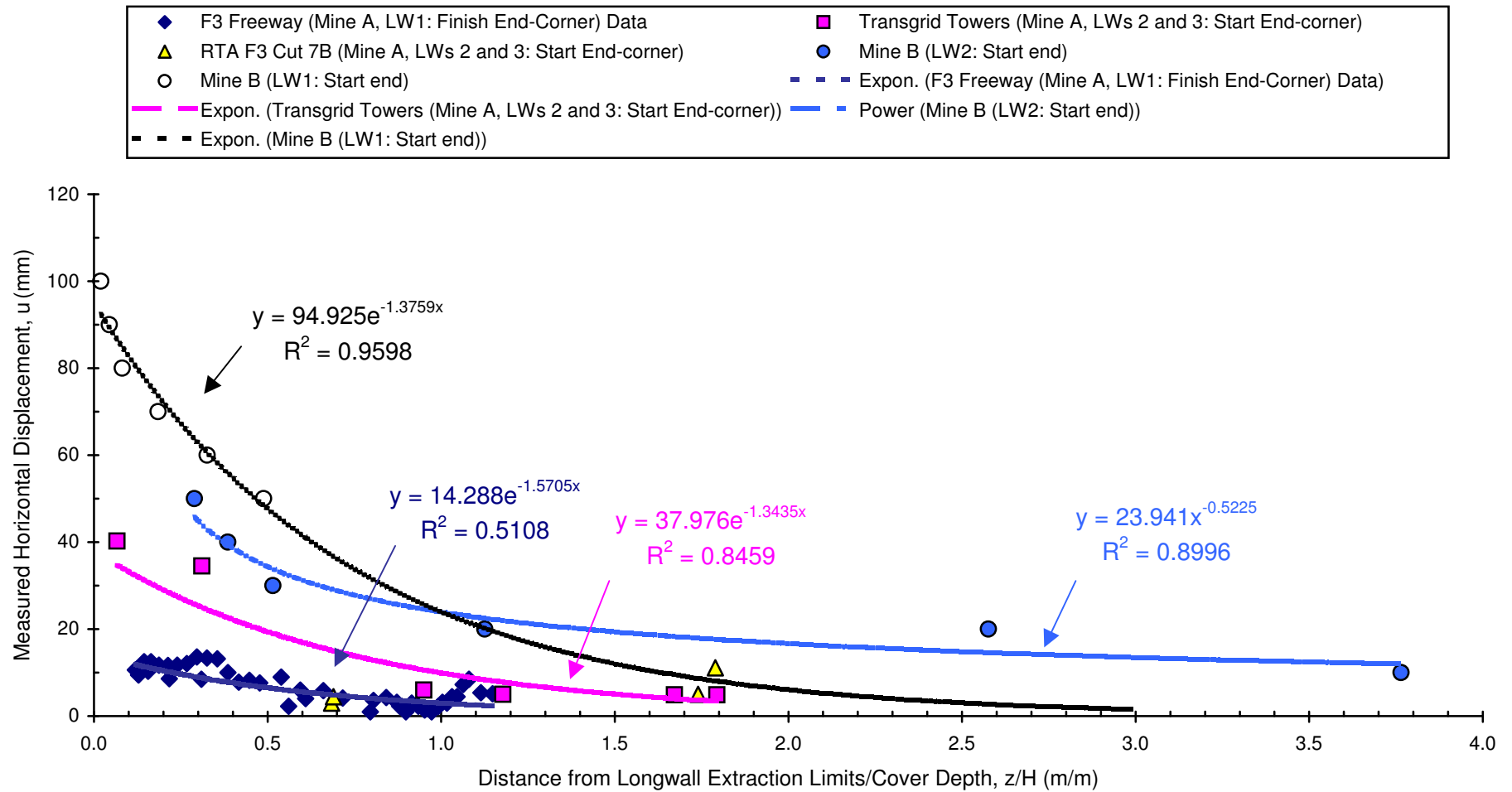


Measured Stress Field for F3 Freeway, West of Newcastle (Lohe & Dean Jones, 1995)

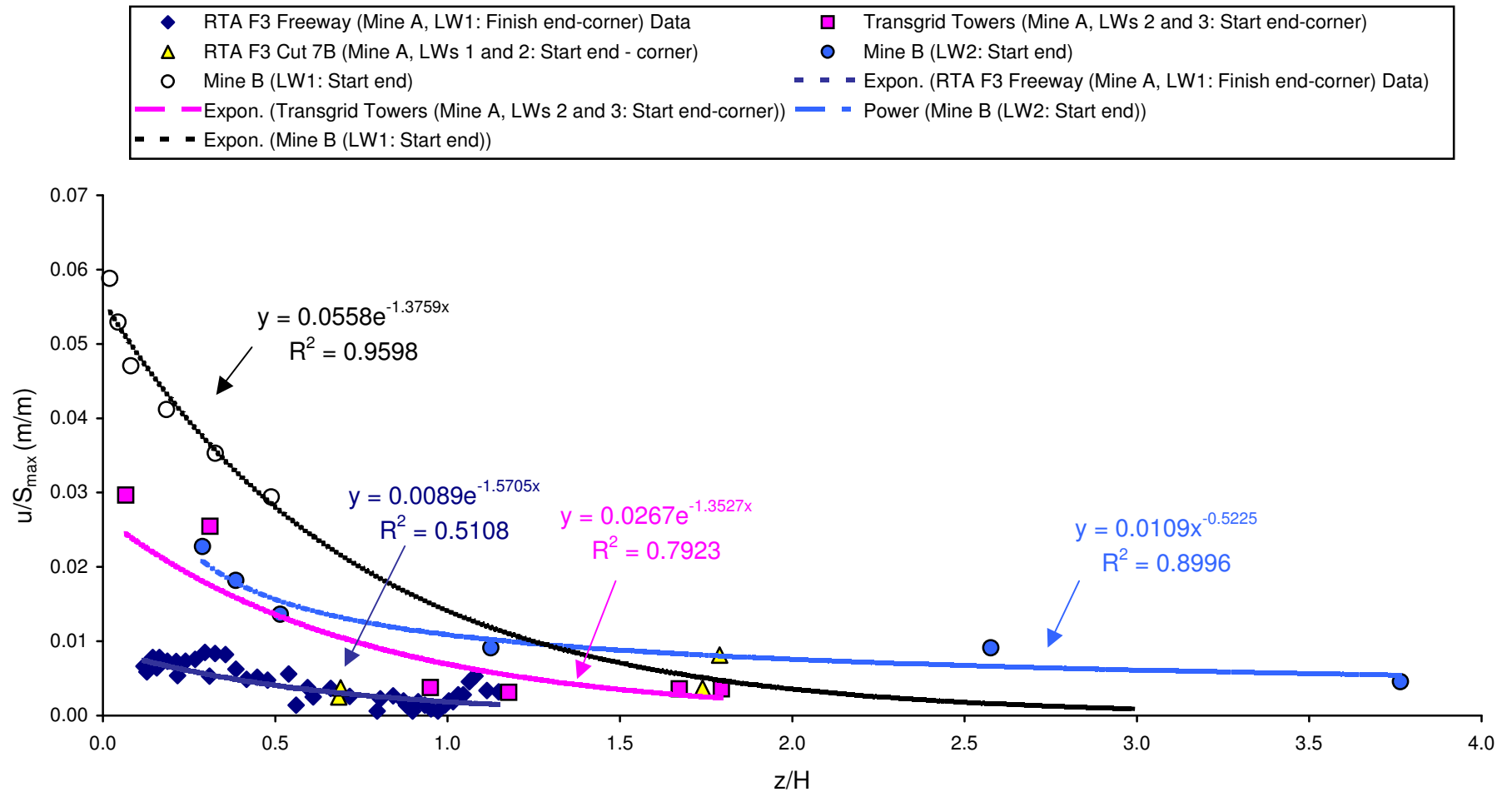


Typical Stress Field Models for Sydney Basin Overburden
 a) McQueen, 2004; b) Lohe & Dean Jones, 1995; c) Pells, 2002
 not shown for clarity (refer to text).

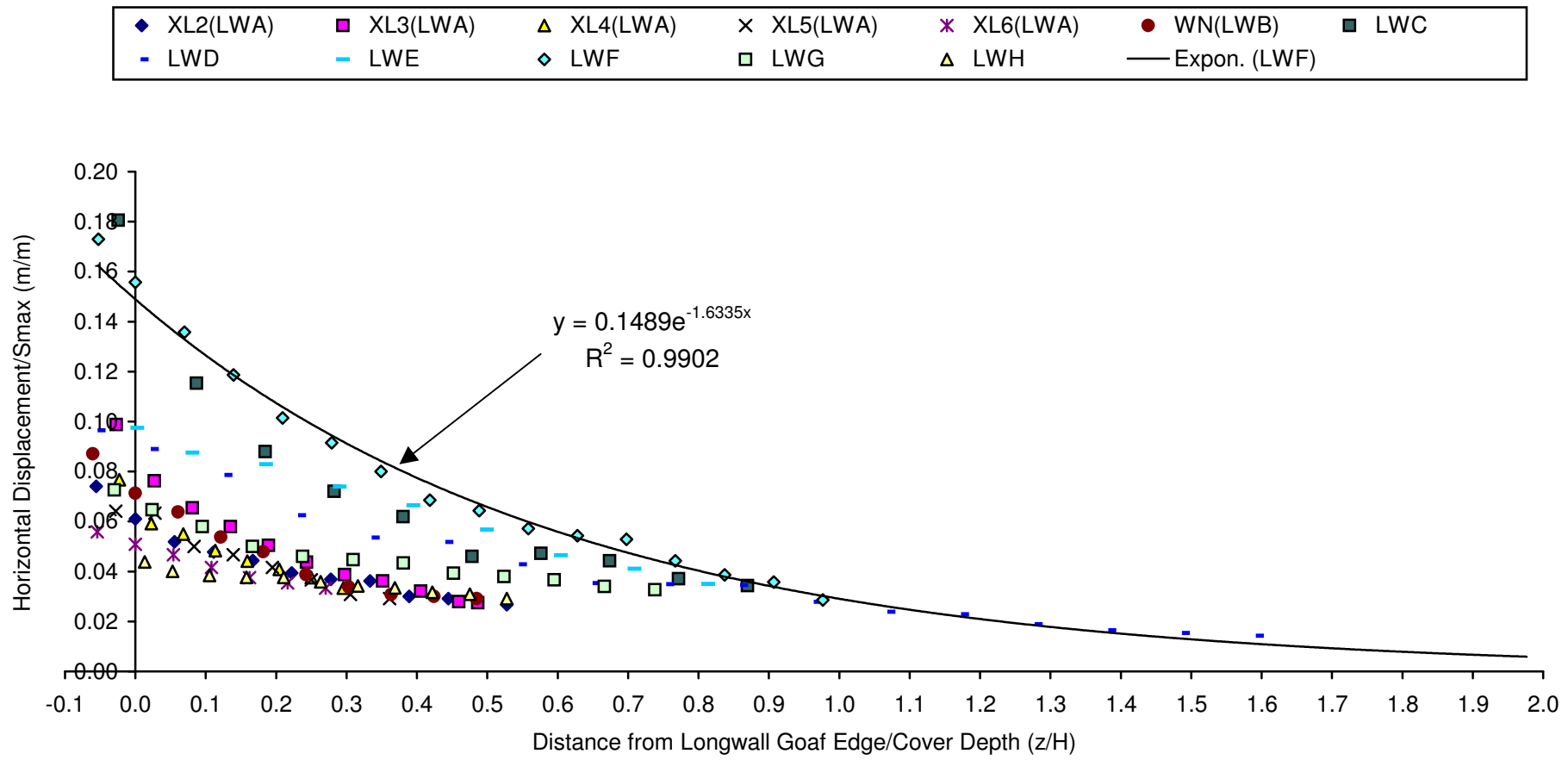
	Engineer:	S.Ditton	Client:	DgS, 2007	
	Drawn:	S.Ditton			
	Date:	12.07.07	Title:	Published Principal Stress Field Models for Sydney Basin and Western Area of Newcastle Coalfield	
	Ditton Geotechnical Services Pty Ltd			Scale:	NTS



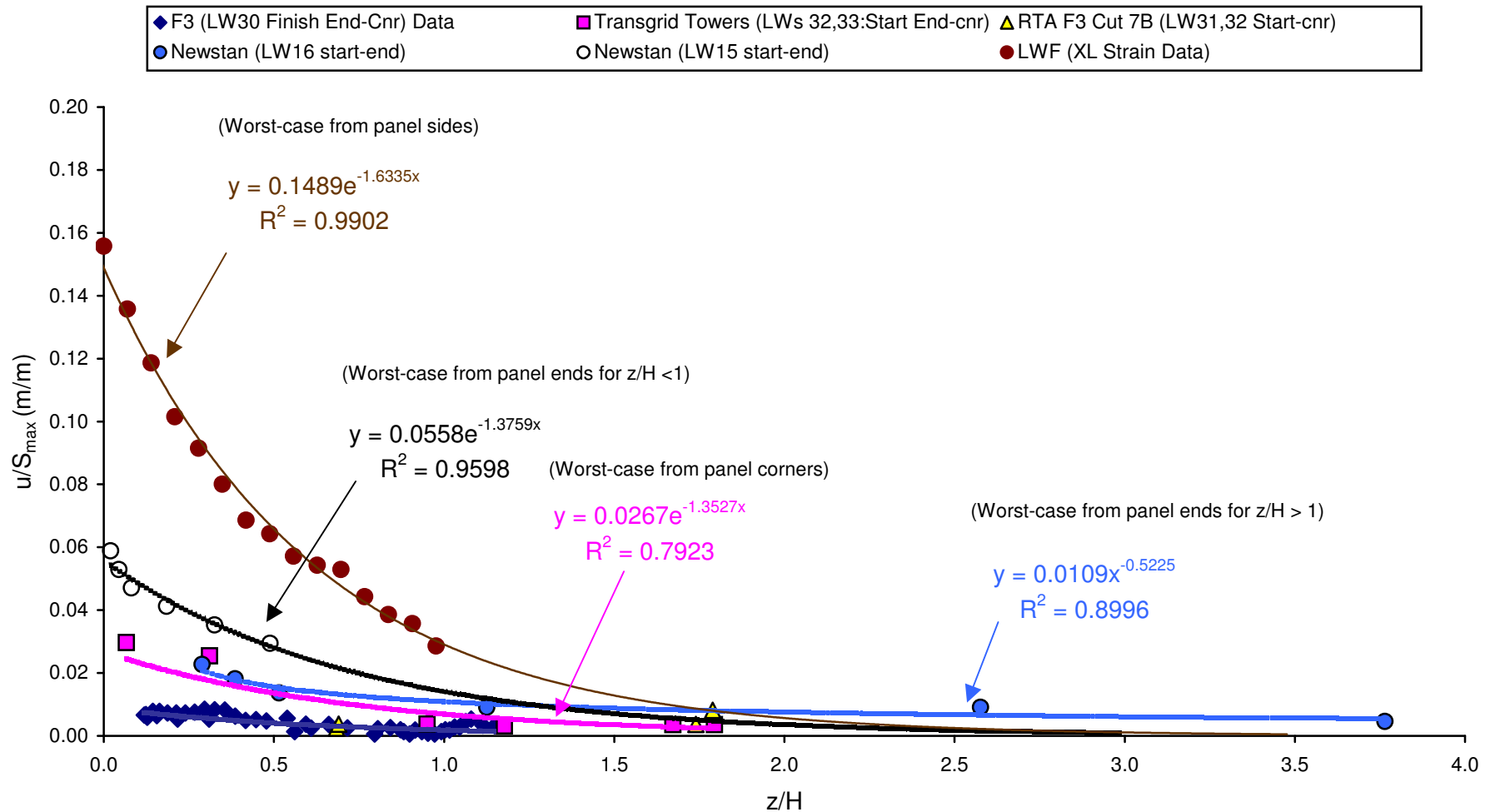
	Engineer:	S.Ditton	Client:	DgS, 2007	
	Drawn:	S.Ditton			
	Date:	22.05.07	Title:	Empirical far-field displacement prediction model using total station electronic distance measurements from longwall panel ends	
	Ditton Geotechnical Services Pty Ltd			Scale:	NTS



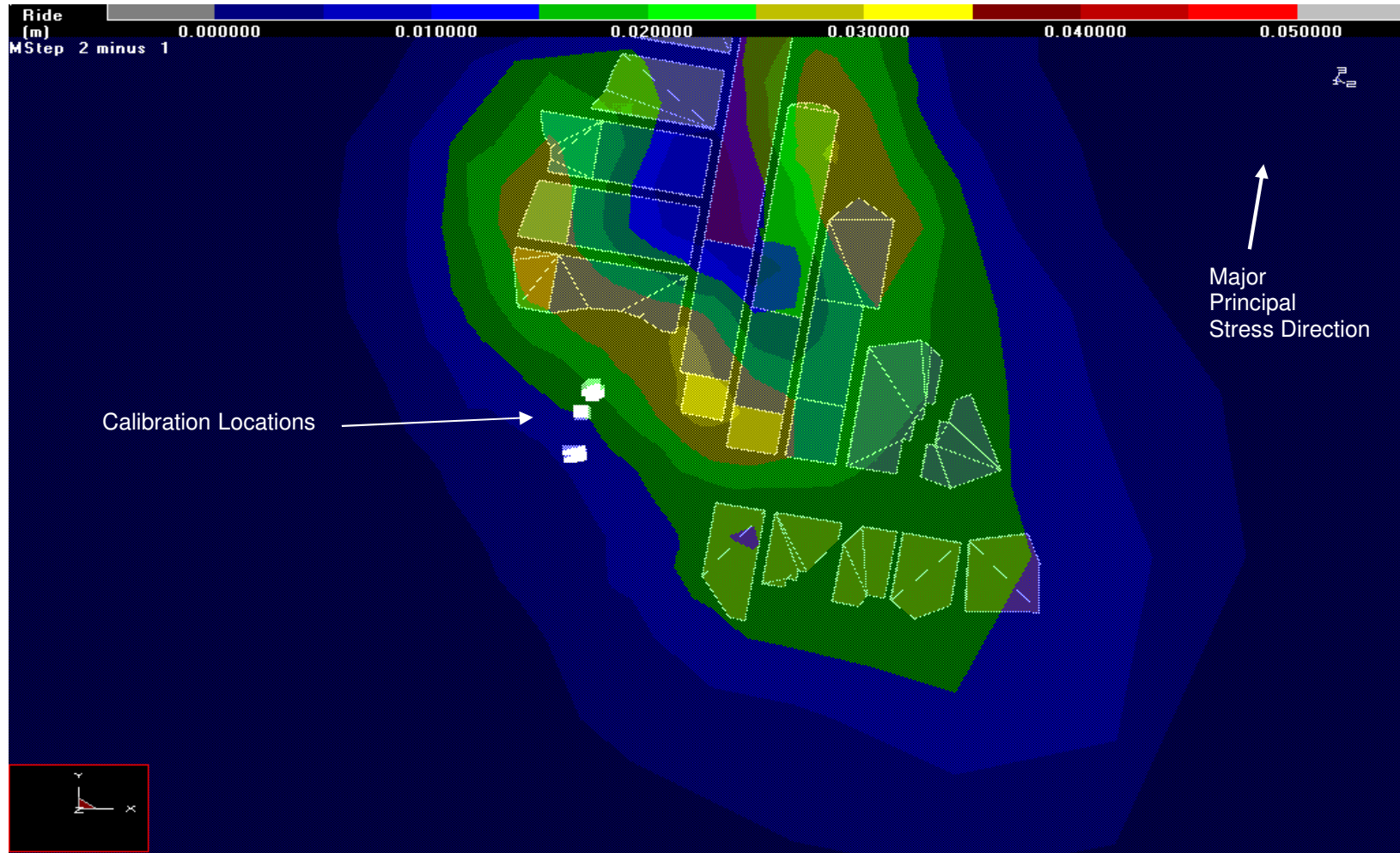
	Engineer:	S.Ditton	Client:	DgS, 2007	
	Drawn:	S.Ditton	Title:	Empirical far-field displacement prediction model using total station electronic distance measurements from longwall panel ends and normalised to maximum panel subsidence	
	Date:	22.05.07	Scale:	NTS	Figure No:
	Ditton Geotechnical Services Pty Ltd				A46



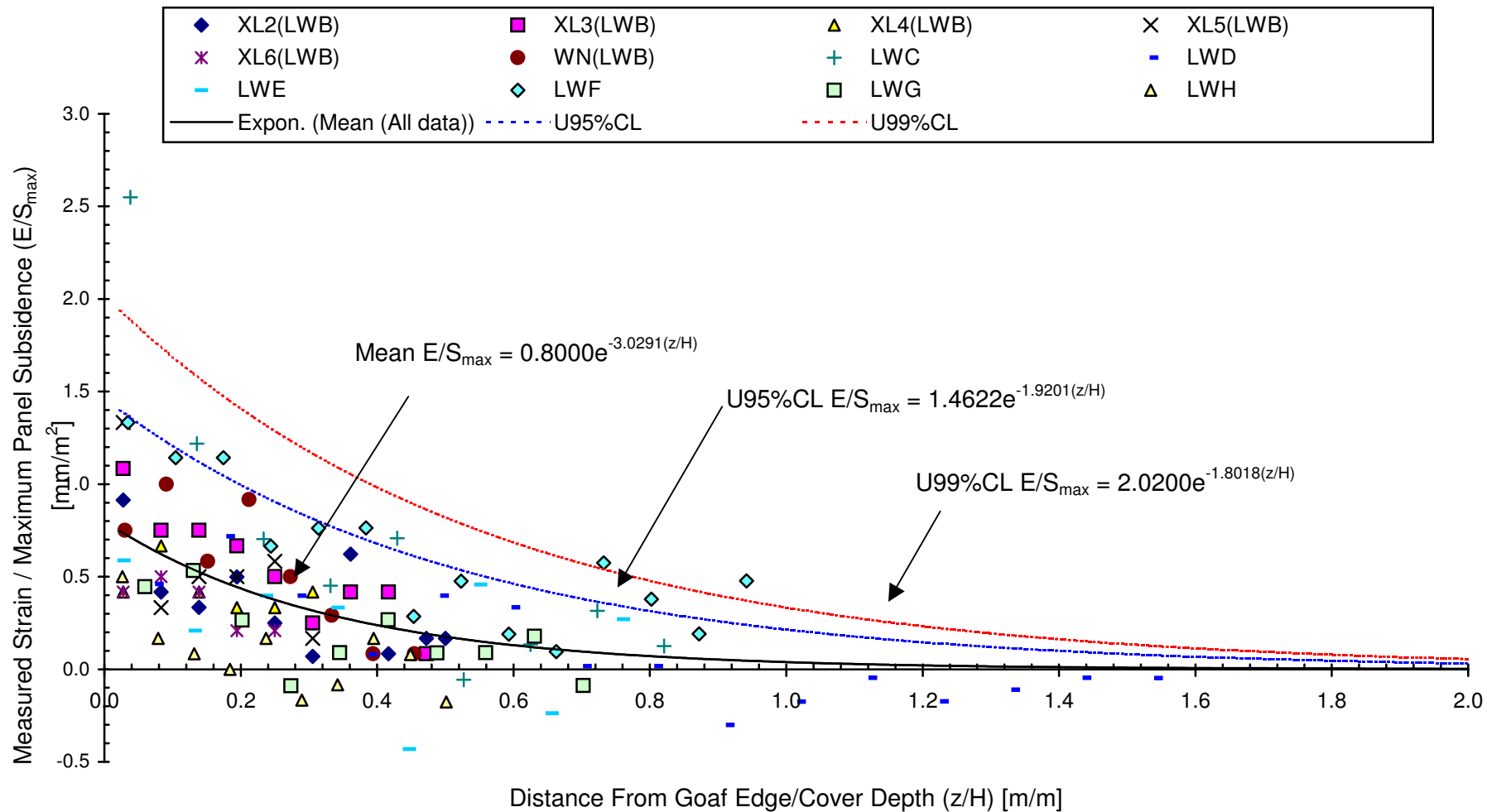
	Engineer:	S.Ditton	Client:	DgS, 2007	
	Drawn:	S.Ditton	Title:	Empirical far-field displacement prediction model using cumulative steel tape measurements from longwall sides and normalised to maximum panel subsidence	
	Date:	22.05.07	Scale:	NTS	Figure No:
	Ditton Geotechnical Services Pty Ltd				A47



	Engineer:	S.Ditton	Client:	DgS, 2007	
	Drawn:	S.Ditton	Title:	Combined empirical far-field displacement prediction models for longwall panel sides, ends and corners.	
	Date:	22.05.07	Scale:	NTS	Figure No: A48
	Ditton Geotechnical Services Pty Ltd				



	Engineer:	S.Ditton	Client:	DgS, 2007	
	Drawn:	S.Ditton			
	Date:	22.05.07	Title:	Example of Map-3D Elastic Boundary Element Model Far-Field Displacement Contours Around a Complex Pillar Extraction Mining Layout	
	Ditton Geotechnical Services Pty Ltd		Scale:	NTS	Figure No:



	Engineer:	S.Ditton	Client:	DgS, 2007	
	Drawn:	S.Ditton	Title:	Empirical far-field strain prediction model using cumulative steel tape measurements from longwall sides and normalised to maximum panel subsidence	
	Date:	22.05.07	Scale:	NTS	Figure No:
	Ditton Geotechnical Services Pty Ltd				A50